Spectroscopic Studies on Cytochrome P450 11-Beta-Hydroxylase and Model Compounds

By

Normand J. Cloutier

Submitted to the Department of Chemistry in Partial Fulfillment of the Requirements for the Degree of

DOCTOR OF PHILOSOPHY
in Biological Chemistry

at the

Massachusetts Institute of Technology
February 1996

Signature of Author _____
Department of Chemistry
November 10, 1995

Certified by _____
William H. Orme-Johnson
Professor of Chemistry
Thesis Supervisor

Accepted by _____
Dietmar Seyferth
Chairman, Departmental Committee on Graduate Students

This doctoral thesis has been examined by a Committee of the Department of Chemistry as follows:

Professor John M. Essigmann _____ Chairman

Professor William H. Orme-Johnson _____ Thesis Advisor

Professor Peter T. Lansbury _____

Professor James R. Williamson _____

Spectroscopic Studies on Cytochrome P450 11-Beta-Hydroxylase and Model Compounds

By

NORMAND J. CLOUTIER

Submitted to the Department of Chemistry on November 10, 1995
in partial fulfillment of the requirements for the degree of
Doctor of Philosophy in Biological Chemistry

ABSTRACT

The partial synthesis of deuterated versions of corticosterone was performed. The C-3 and C-20 carbonyls of corticosterone were protected by forming ethylene glycol-derived ketals. This was followed by the protection of the C-21 hydroxy group with tert-butyldiphenyl silyl chloride, after which the C-11 beta-hydroxy group was oxidized to the ketone with a pyridine-chromic acid reagent. The C-21 silyl ether was then deprotected. Deuteriums were then incorporated, into the 11-keto steroid, at what are believed to be positions C-9 and C-12: (1) one compound with the C-9 and C-12 positions perdeuterated; (2) another with only one deuterium at the beta position of C-12; (3) and a third compound with deuteriums at C-9 and the alpha position of C-12. All non-deuterated intermediates have been characterized by NMR, IR, and MS. MS spectra of the deuterated steroids were consistent with the expected products.

Purifications of adrenodoxin, adrenodoxin reductase, and cytochrome P450 11β-hydroxylase (all from bovine adrenal glands) were performed. Preparation of pure 11β-hydroxylase relied on the use of an adrenodoxin-Sepharose affinity matrix, resulting in a specific activity of 8.3 nmol of the P450 chromophore per mg of protein; this was free of contaminating cytochrome P450 cholesterol side chain cleavage enzyme. Each of these purified proteins gave single bands on silver-stained SDS PAGE gels.

Three-pulse electron spin echo envelope modulation (ESEEM) studies on ^{14}N and ^{15}N isotopically labeled bis (imidazole) and bis (ethyl thioglycolate) heme model compounds were performed. All measurements were conducted at g=2.25 (2900 Gauss, microwave frequency of 9.14 GHz) and a 250 nsec delay between the first and second pulses. A relatively unperturbed ^{15}N-derived larmor frequency modulation at 1.27 MHz (from a sample containing ^{15}N in both its porphyrin and imidazole ligands) was assigned to the axial imidazole. An Apple Macintosh computer program was written that converts 20 bit integer (Nicolet 1180E computer) ESEEM time-domain data to ASCII format. This program also allows the visualization of the data and manipulation of data points, on Apple Macintosh computers.

Extended x-ray absorption fine structure (EXAFS) experiments (measured in fluorescence mode) were performed on bovine cytochrome P450 11β-hydroxylase (with either 11-deoxycorticosterone or metyrapone, bound in the active site) and heme model compounds. Multiple data sets were acquired for each sample, using an energy-resolving 13-element Canberra x-ray fluorescence detector. The dead time for each detector element was determined, after which data from the multiple scans were added. Distinguishable backgrounds from the 13 different detector elements were found, dictating that future data analysis involve 13 separate background removals before all the data (for any one sample) can be accurately summed. Detector artifacts were found to be responsible for the low distance peaks found in previously reported EXAFS studies on the cytochrome P450 side chain cleavage enzyme.

Thesis Supervisor: William H. Orme-Johnson
Title: Professor of Chemistry

DEDICATION

This thesis is dedicated to those who suffer from steroid hormone disorders and for those who are working on helping the situation.

ACKNOWLEDGMENTS

I would like to thank my long-time friends who have stood by me through thick and thin. They are Fred Francis and Lorna Gotzmann. They approach life with the greatest excitement, wonder and determination. I am blessed by their friendship. And a big thank you to Marissa Asta, my best friend for this past year.

My family has been a surprising source of strength for me as well. Although they are all very independent, I have never failed to feel their respect and compassion. I would especially like to thank my brother Marc who has helped me through many personal crises and whom I consider a model human being. I am also very grateful for my parents' support and for their constant faith in me.

My lab mates have made my stay at MIT both more educational and colorful. David Wright earns a gold star in my book for his efforts at organizing us into a team. I am indebted to Jeremy Selengut for his help in getting me started in organic synthesis and for his helpful scientific criticisms; he is both a valued colleague and trusted friend. Patti Christie's friendship, straightforwardness and excellent experimental advice has also helped me 'stay on track'. My XAFS experiments in May of 1995 would not have been possible without the help of Rob Pollock. I am also indebted to the stewardship that I received from Emily Miao and Andrew Kolodziej. I would also like to thank Chun Zuo for taking the time to show me how to operate the Orme-Johnson electron spin echo machine. A great deal of the work described in this thesis was also made far easier with the enthusiastic and focused help of undergraduate students Kurt Snyder and Lisa VanDermark.

I would like to thank all those from other institutes whom I have learned invaluable information from. They are Israel Hanukoglu from the Weizmann Institute and Richard Magliozzo, Jack Peisach, and Mark Chance from the Albert Einstein College of Medicine.

My thanks also go the support staff of the MIT chemistry headquarters. In the final months of thesis preparation, they always treated me with the greatest amount of respect. Prof. Jamie Williamson has my vote for the next departmental chair because of his friendliness, accessibility, and for his efforts on my behalf.

Finally, I would like to thank my thesis advisor, Prof. William (Bill) H. Orme-Johnson, for accepting me into his lab and encouraging my intellectual development. Bill often gave me the benefit of his experience, but always let met do things my own way.

Table of Contents

CHAPTER 1

Placing Cytochrome $P450_{11\beta}$ in Context

Mammalian biosynthesis of steroid hormones relies heavily on the activities of cytochromes P450, membrane-bound enzymes which catalyze most of the oxidations in this pathway. With few exceptions, steroidogenesis can be completely described as a series of cytochrome P450 enzyme reactions (see **Figure 1.1**). Steroid hormones are essential in maintaining many vital systems in mammals; they are found in deficit (e.g. congenital adrenal hyperplasia, Addison's disease, and in certain immune deficiencies [1]) or excess (Cushing's syndrome and Conn's syndrome [2]) in many human ailments. Designing effective treatments for these pathologies requires an understanding of both the physiological systems controlling steroidogenesis and the cytochrome P450 enzymes themselves, which perform most of the actual chemical reactions.

Specific human disorders center on the resulting products (or lack thereof), arising from the enzyme cytochrome P450 11β-hydroxylase ($P450_{11\beta}$). Since it is usually easier to inhibit an enzyme, rather than activate it, the main goal in studying $P450_{11\beta}$ is to design effective inhibitors; however, the ability to activate it would be beneficial as well. Targeting $P450_{11\beta}$ in these illnesses is complicated by the fact that it plays a role in excesses of both glucocorticoids (Cushing's syndrome) and in mineralocorticoids (Conn's syndrome) [2]. Although it is possible to inhibit the hormonal activation of some enzymes, in some ailments steroid overproduction is insensitive to this level of control. For example, hypertension can often be treated by trying to lower levels of angiotensin-II, which activates $P450_{aldo}$ - a form of $P450_{11\beta}$ which makes aldosterone; however, there are conditions of elevated $P450_{aldo}$ activity which are not affected by angiotensin-II. In such cases, the ability to inhibit the $P450_{aldo}$ itself offers the ability to directly limit aldosterone formation. The goal of the work described in this thesis is to add to both the understanding of $P450_{11\beta}$ (and $P450_{aldo}$) and the complex activities which are catalyzed by cytochrome P450 proteins in general. This introduction will attempt to place $P450_{11\beta}$ in context - both chemically, (when compared to other P450 enzymes) and functionally (with respect to steroid hormone synthesis overall).

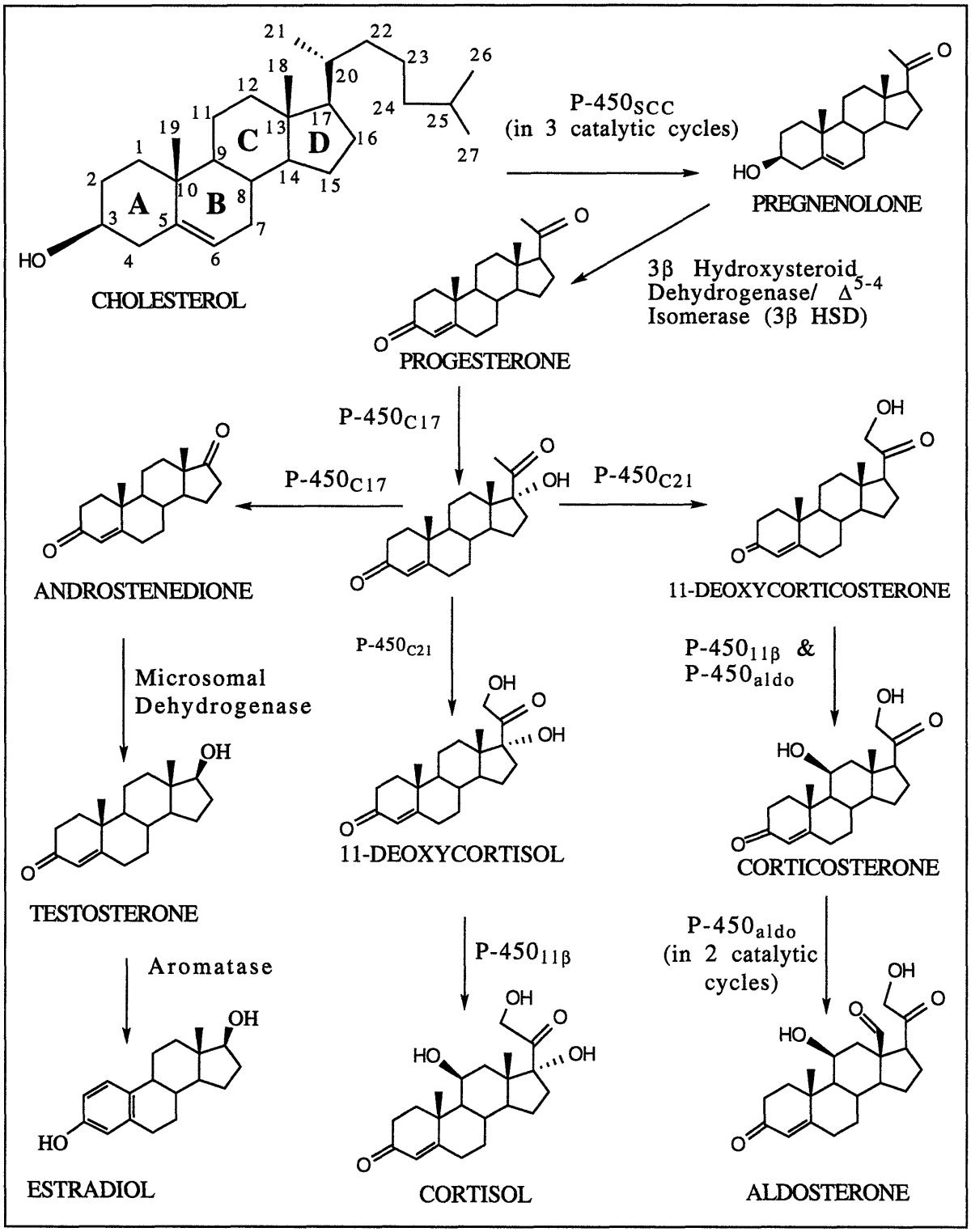

Figure 1.1: The biosynthesis of three categories of mammalian steroid hormones, all originating from cholesterol. The three branches, from left to right, give rise to the sex steroids, the glucocorticoids, and the mineralocorticoids. The numbers and letters on cholesterol refer to the labeling of the carbons and the rings.

1.1. P450 Chemical Mechanism

Issues concerning the chemical mechanism of P450 enzymes have been pursued in studies on each of the enzymes mentioned in **Figure 1.1**, as well as on other cytochromes P450. For instance, studies on cytochrome P450 *d*-camphor hydroxylase ($P450_{cam}$) from the bacteria *Pseudomonas putida* have provided significant mechanistic and structural information. Studying bacterial P450 enzymes carries the advantage that they are not membrane bound and can easily be purified and stabilized. In addition, mammalian livers contain P450 enzymes (possessing a wide range of substrate acceptance) whose function is to oxidize organic toxins, making them more water soluble - thus facilitating their removal from the body; these enzymes were among the first mammalian P450 enzymes purified and their study has yielded a great deal of mechanistic information.

Cytochrome P450 proteins owe their name to the fact that they, when reduced with sodium dithionite and incubated with carbon monoxide, give rise to an optical absorption maximum at 450 nm, relative to an identical sample lacking carbon monoxide - the prefix 'P' representing the word 'pigment'. They fall into a class of enzymes called mixed function oxygenases, or monooxygenases. Monooxygenases oxidize organic substrates using molecular oxygen, leaving one oxygen atom on the organic product, while reducing the other oxygen to form water. The most common reaction catalyzed by P450 enzymes is the hydroxylation of unactivated carbons on alkanes (see **Figure 1.2**). Apart from an organic substrate and oxygen, this reaction requires reducing equivalents, provided by NADPH, which are usually delivered to the P450 enzyme via one or two electron transfer protein(s).

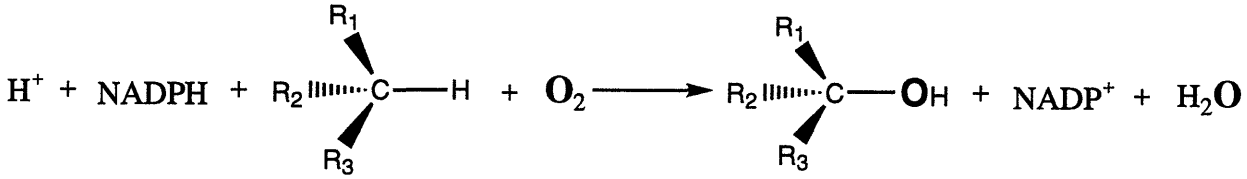

Figure 1.2: The stoichiometry of aliphatic hydroxylation by P450 enzymes.

It is common knowledge that some hydrocarbons, once heated or ignited in the presence of oxygen, are readily flammable; however, the controlled oxidation of unactivated alkanes, by molecular oxygen, is considered a difficult chemical reaction. This difficulty lies in the fact that ground state oxygen exists in a triplet spin state, whereas an aliphatic carbon is found in a singlet spin state. This reaction therefore requires either a significant input of energy - to activate the reagents into compatible spin states - or a catalyst to mediate the reaction. Cytochrome P450 enzymes are capable of mediating this mechanistic impasse, utilizing the organometallic cofactor heme, iron porphyrin, (see **Figure 1.3**).

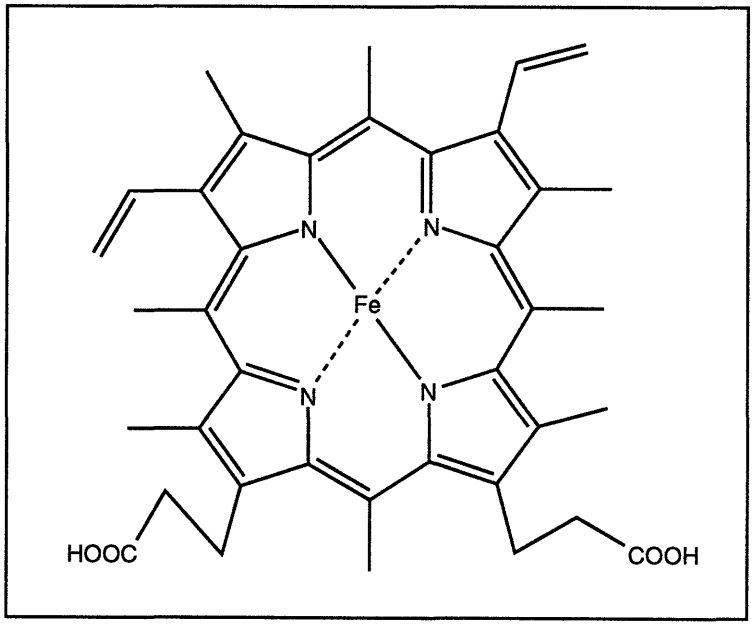

Figure 1.3: The structure of heme, iron protoporphyrin IX.

Cytochrome P450's heme (when the iron is in the ferrous, 2+, state) is capable of binding molecular oxygen in the same way as hemoglobin and myoglobin. In fact, the EPR spectrum of oxy-ferrous $P450_{cam}$:substrate complex (generated by X-irradiation of the oxy-ferric complex) resembles that of oxy-ferrous hemoglobin and myoglobin (generated in the same way) [3]. However, an oxy-ferrous complex of substrate-bound $P450_{scc}$ was shown to decay to the ferric substrate-bound $P450_{scc}$ [4], releasing superoxide. Nevertheless, what distinguishes P450 enzymes (from hemoglobin and myoglobin) is their ability to accept another electron - giving rise to the chemistry described in **Figure 1.2**.

This unique cytochrome P450 chemistry has motivated a great deal of study on heme systems in general. The major chemical difference between P450 enzymes and the globins is the identity of the heme axial ligand, projecting from the interior of the protein (referred to as the proximal ligand). The proximal axial ligand for hemoglobin and myoglobin is histidine, whereas cysteine occupies this position in P450 enzymes. From the examination of a thiolate-tethered heme model compound, the protein's unique spectroscopic characteristics have been attributed to this key ligand [5]; cysteinate ligation is also believed to be mostly responsible for P450's chemical properties [6, 7]. Factors arising from the polarity and structure of the active site appears to carry the largest remaining influence in P450 catalysis [6].

The catalytic cycle of cytochrome P450 enzymes has been discussed at great lengths in other sources [6, 8-13]. **Figure 1.4** summarizes what is now the accepted model of hydroxylation of alkanes by cytochromes P450. The ferric resting state (state A) exists in a predominantly low spin state with either water or hydroxide as the distal heme axial ligand (i.e. the position closest to the surface of the protein). When this form of the enzyme binds its substrate, the active site experiences a dehydration, which includes the displacement of the water (or hydroxide) ligand from the heme. The spin state of the iron then changes to predominantly high spin at the same time as the iron's redox potential shifts in the positive direction, making it more easily reducible (state B). If the enzyme is then reduced by one electron (delivered by its companion electron transfer protein), it can achieve state C which can then readily bind O_2, giving rise to state D (the oxy-ferrous state). (State B can also be immediately converted to state F by the addition of peroxides or various single-oxygen atom donors; this non-physiological pathway is known as the peroxide shunt.) Further reduction of the state D, by a single electron gives rise to state E. State E can also be momentarily detected by combining a ferrous substrate-bound P450 enzyme with superoxide [14]. State E quickly decomposes into a postulated state F which is believed to be the hydroxylating species.

The existence and nature of state F has been debated for some time now. The present consensus is that it is the *bona fide* oxidizing agent for P450 enzymes - at least where hydroxylations are concerned. The fact that single-atom oxygen donors - such as peroxides, iodosobenzene, and amine oxides - can cause $P450_{cam}$ to catalyze hydroxylations, without the need for oxygen or reducing equivalents [6, 13, 15-17] (the peroxide shunt) supports the model that the hydroxylating species requires only a single oxygen on the iron atom. Chloroperoxidase (a heme enzyme which also has a cysteine proximal ligand) and horseradish peroxidase (an imidazole-ligated heme protein) - both capable of cleaving the O-O of O_2 - have been found to possess $[FeO]^{3+}$ and $[FeO]^{2+}$ heme intermediates (referred to as compounds I and II, respectively; see **Figure 1.5**) in their catalytic cycles [6]. EXAFS studies of two horseradish peroxidase samples, prepared in the compound I and II states, have confirmed short Fe-O bond distances (~1.63 Å), consistent with the structures shown in **Figure 1.5** [6]. Rapid scan absorption spectroscopy of *m*-chloroperbenzoate-treated $P450_{cam}$ also revealed many intermediates - one of which was indistinguishable from compound I [18]. Since chloroperoxidase catalyzes some of the same kind of reactions as cytochromes P450 [6], it's believed that state F is identical to compound I. In addition, synthetic model I compounds are also able to catalyze oxygen transfer reactions [13].

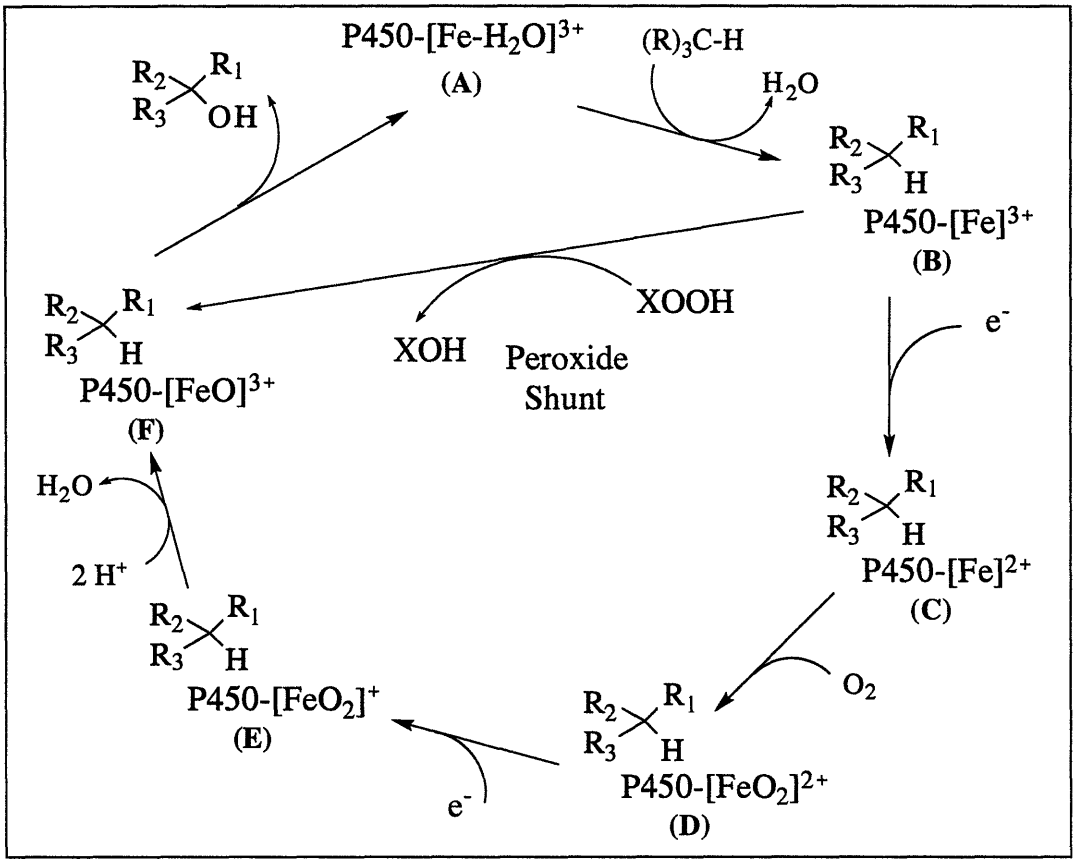

Figure 1.4: The catalytic cycle of cytochrome P450 hydroxylating enzymes.

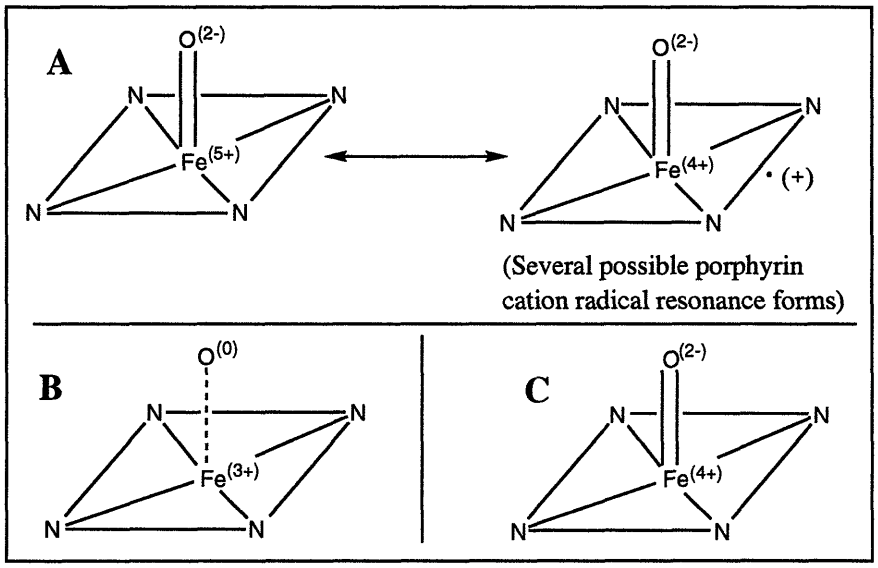

Figure 1.5: (A) The resonance forms of compound I, stipulating a doubly bonded dative ligation of oxygen to the iron. (B) A functional model of compound I, demonstrating that it is the equivalent of a ferric heme, stabilizing an oxygen with a zero charge. (C) One of the resonance forms of Compound II, a one-electron reduced version of compound I. The values in parenthesis are the formal charges.

The sequence of events leading from state F back to the resting state (A) is presently known as the oxygen rebound mechanism [13]. It is illustrated in **Figure 1.6**. It states that the iron-oxo species of state F (termed an oxenoid moiety [19]) first abstracts a hydrogen atom from a carbon on the alkane, creating a carbon radical and a hydroxide radical (which is bound to the iron porphyrin). These two radicals can then recombine to form the alcohol.

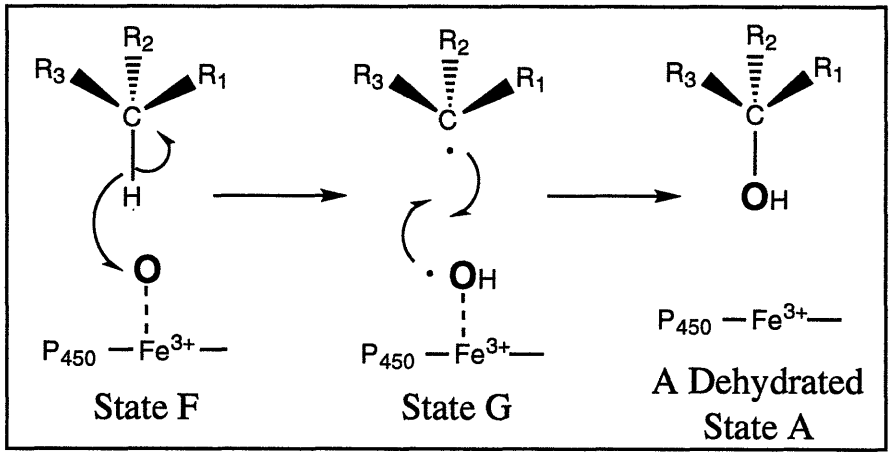

Figure 1.6: The oxygen rebound mechanism. States F and A are the same states depicted on **Figure 1.4**. An additional state (G) is postulated in this mechanism.

Although the oxygen rebound mechanism is well accepted as the mode of operation in hydroxylation reactions, it does not explain all P450 reactions. For instance, the cleavage of some carbon-carbon bonds in certain P450 enzymes is believed to proceed via a Baeyer-Villiger type of oxidation which supports an iron-peroxy species in the final chemistry. This type of mechanism has been proposed in mechanisms of aromatase ($P450_{arom}$) [20-22], lanosterol 14α-demethylase ($P450_{14DM}$) [23] and in the C17,20 lyase activity of $P450_{c17}$ [24, 25]. This mechanism is illustrated in **Figure 1.7**. Whether a protonated state E (as shown in **Figure 1.7**) or a state F (as shown in **Figure 1.6**) becomes the initiating oxidizing species may be related to the P450 enzyme's stabilization of one state over another or to the proximity of the carbonyl when State E is reached.

Proton leakage into a P450 active site (perhaps in state E of **Figure 1.4**) may be related to the commonly seen side product, hydrogen peroxide. Loida and Sligar have reported, from work done on $P450_{cam}$ mutants, that H_2O_2 production is related

to the level of hydration of the the active site [12]. Swinney and Mak proposed that the initiating iron-peroxy species (at the top of **Figure 1.7**) is most likely deprotonated when it attacks the carbonyl carbon and that protonation of this species favors its decomposition into water and the oxenoid moiety [25]. Interaction of certain substrates with oxygenated heme may also cause a preference toward one mechanistic path over another. The ability of 2(3)-t-butyl-4-hydroxyanisol to enhance the production of the hydrogen peroxide side product from $P450_{cam}$ may be an example of such a situation [26]. The normal catalytic cycle of P450 enzymes has also been proposed to be subverted by the actions of 'pseudosubstrates' which: bind to P450 enzymes, allow electrons to be accepted and oxygen to bind, and cause oxygen-derived free-radical damage of these proteins [27].

In the consideration of the effect of substrates on the chemical mechanism of P450 enzymes, one must not forget that the electron transfer protein, which delivers reducing equivalents, is also a substrate. In the case of $P450_{c17}$, it has been found that the concentration of P450 reductase (the companion electron transfer protein) is found to influence whether the enzyme catalyzes a C-17 α-hydroxylation or a C-17,20 lyase activity [28, 29]. Cytochrome b5, which is also capable of delivering electrons to $P450_{c17}$, has also been found to increase the lyase activity, relative to the hydroxylase activity [29, 30]. In addition, a fusion protein of P450 reductase and $P450_{c17}$ was found have a six-fold higher level of lyase activity when cytochrome b5 was added while reconstituting activity [31]. The proven influence of these electron transfer proteins on $P450_{c17}$ is suggestive that the 2Fe-2S ferredoxin, which delivers electrons to the mitochondrial P450 enzymes, may also play a role in determining the chemistry of substrate oxidation.

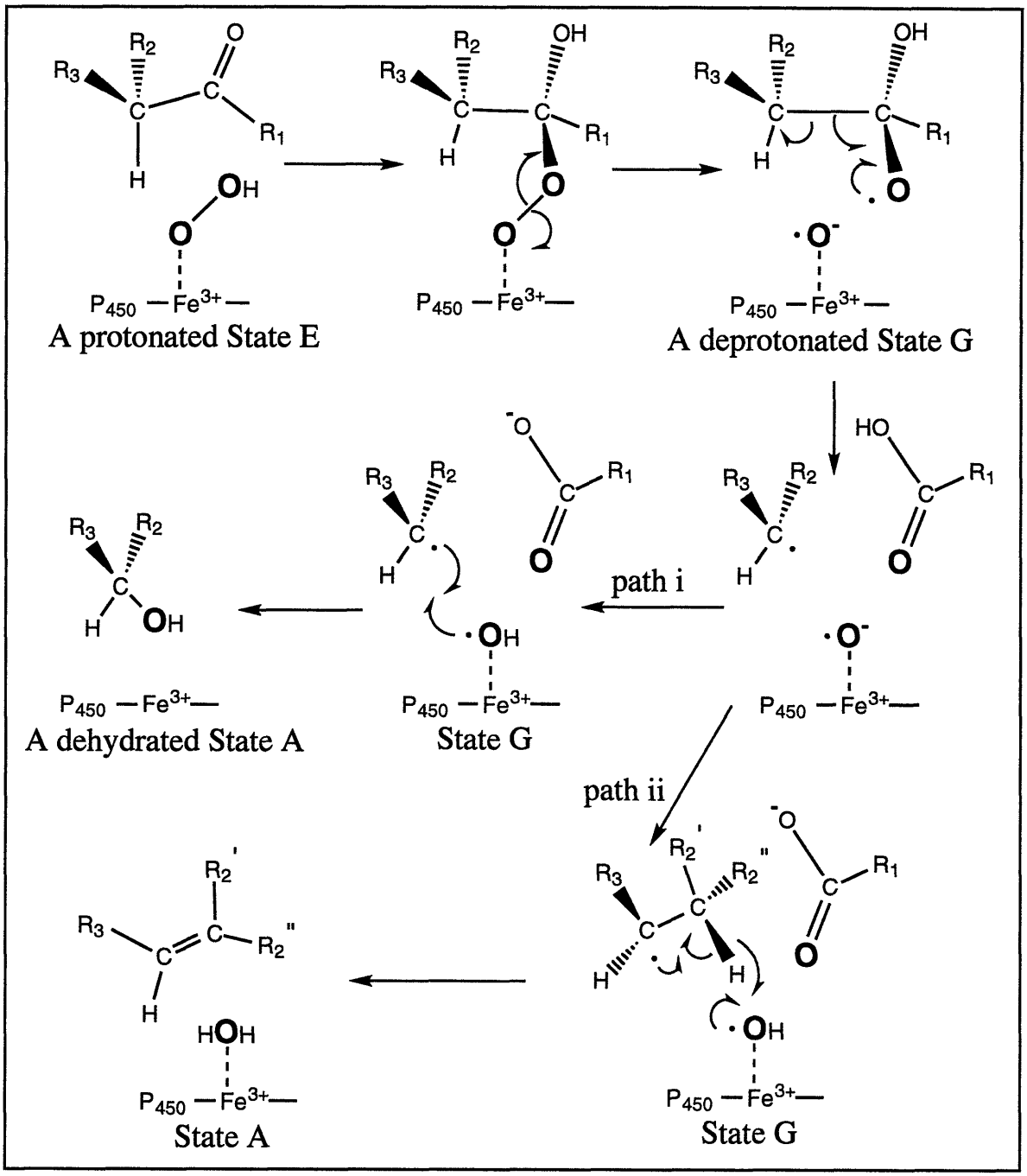

Figure 1.7: Proposed mechanism of carbon-carbon bond cleavage by P450 enzymes when a carbonyl group is present on the substrate. This figure is adapted from [24].

A factor which may influence eukaryotic P450 enzymes is the effect of the lipid composition of membranes holding these proteins. For example, the polychlorinated biphenyl compound Aroclor 1254 lowers the rate of $P450_{c21}$ and $P450_{c17}$ by altering the fluidity of the membranes; however, this compound has no effect on the rate of these enzymes if they are prepared free of membranes [32].

Another example of the role of membranes is that lipids high in cardiolipin (see **Figure 1.8**) stimulate the activity of $P450_{scc}$ [33] - yet they inhibit $P450_{11\beta}$ [34]. Since substrates are delivered to membrane-bound P450 proteins via the lipid bilayer, the lipid composition could also affect the availability of the substrate to the enzyme. One example, suggestive of this mode of control, is the fact that cholesterol sulfate (a good substrate for $P450_{scc}$) binds unproductively to this enzyme at high concentrations; this inhibitory mode of cholesterol sulfate binding is prevented by phospholipids [35].

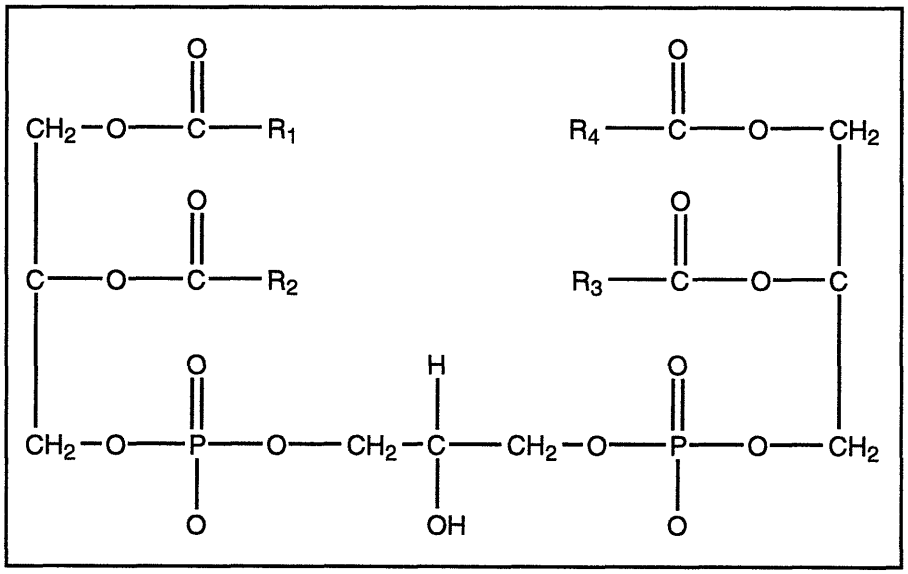

Figure 1.8: Cardiolipin: A dimer of two phosphatidic acid molecules, bridged at their phosphate head groups by an intervening glycerol moiety.

Apart from the lipid composition of membranes, interaction of P450 enzymes with other membrane-bound proteins (even other cytochromes P450) may play a role in controlling P450 activity. Since different P450 proteins (in the same membrane) all receive their reducing equivalents from the same electron transfer companion protein, the activity of one enzyme may be dependent on the state of other membrane-sharing P450 enzymes. Where $P450_{c21}$ and $P450_{c17}$ are present in the same membrane, it has been shown in inhibition studies on $P450_{c21}$ (with the addition of specific antibodies), that there is no direct competition for reduced P450 reductase (their common electron transfer companion protein) [29]. In the case of the two mitochondrial P450 enzymes $P450_{scc}$ and $P450_{11\beta}$, the affinity of

corticosterone for $P450_{11\beta}$ was significantly decreased when $P450_{scc}$ was present in the same membranes [36]. Both of these situations suggest that membrane-bound P450 enzymes have some 'awareness' of the presence of other enzymes in the same membrane.

1.2. Structural Studies On P450 Enzymes

1.2.1. Crystallographic Studies

Much of what we know about the structure (as well as the mechanism) of cytochrome P450 enzymes comes from work performed on $P450_{cam}$. As mentioned above, it is a bacterial protein and not membrane-bound. This enzyme was the first P450 to be purified [37, 38] and the first to be crystallized [39]. Its crystal structure has been determined in many ferric forms: camphor-bound [39, 40], substrate-free [41], metyrapone-bound [42], phenylimidazole-bound [42], norcamphor-bound [43], adamantanone-bound [43], phenyl-bound [44], camphane-bound [45], adamantane-bound [45], and thiocamphor-bound [45]. The crystal structure of only one ferrous form of $P450_{cam}$ has been determined to date, that of carbon monoxide- and camphor-bound ferrous $P450_{cam}$ [46]. The crystal structure of the $P450_{cam}$ Thr252Ala mutant (known to 'uncouple' electron transfer and camphor hydroxylation, producing hydrogen peroxide and water) has also been determined [47]. Information from all of these crystal structures, along with biochemical characterization of $P450_{cam}$ mutants, are helping to reveal more details of P450 chemistry in general.

The crystal structures of other bacterial P450 enzymes have also recently been reported. These are $P450_{terp}$ [48] and $P450_{BM3}$ [49]. $P450_{terp}$ (found in *P. putida* as well) is similar to $P450_{cam}$ in the sense that it requires two electron transfer proteins - a flavoprotein and an iron sulfur protein (ferredoxin) - to mediate the delivery of reducing equivalents from NADH; such enzymes are labeled as class I P450 proteins. These are similar to mitochondrial P450 enzymes which also require a flavoprotein and a ferredoxin. Class II P450 proteins are found in the endoplasmic reticulum; they require only one electron transfer protein (P450 reductase) which contains both a flavin adenine dinucleotide (FAD) and a flavin mononucleotide (FMN) cofactor.

$P450_{BM3}$ (found in *Bacillus megaterium*) is unique because it is a single component monooxygenase system [50]; it does not require any electron transfer proteins. $P450_{BM3}$ is able to accept reducing equivalents directly from NADH. However, $P450_{BM3}$ is considered to be a class II P450 protein since it has 2 separate domains - a P450 reductase and a heme monooxgenase domain [50, 51]. The availability of the structure of $P450_{cam}$ has been used to make models of eukaryotic P450 enzymes [52-56]. The availability of the $P450_{terp}$ and $P450_{BM3}$ structures will aid in such work. However, since it is assumed that such comparisons (using bacterial class I P450 proteins) is more suited for modeling mitochondrial P450 enzymes, the newly available $P450_{BM3}$ structure may now help make more accurate models of microsomal (class II) cytochromes P450.

In the study of mammalian P450 enzymes, one ideally wants a crystal structure of a membrane-bound P450. Unfortunately, no such structure has yet been reported. In fact, there have been very few reported crystal structures of membrane proteins in general. The main problem is that membrane proteins, due to their lipophilic nature, are not easily crystallizable. In the hope of making $P450_{scc}$ more crystallizable, Iwamoto *et al.* [57] treated this enzyme with pyridoxal phosphate (PLP) and trapped the PLP-$P450_{scc}$ imines with $NaBH_4$. From this derivatized protein, they were able to form crystals. Unfortunately, the optical absorption spectrum of this crystallized protein did not match that which is known from the native enzyme. However, a partial crystal structure for $P450_{scc}$ may yet be possible. Chashchin *et al.* [58] have demonstrated that limited trypsinolysis of $P450_{scc}$ yields two fragments which can reconstitute activity when incubated together - thus demonstrating the domain structure of this enzyme. If one of these fragments is less lipophilic than the original $P450_{scc}$, it could conceivably be more crystallizable than the holoprotein. In principle, such an approach could be applied to any other P450 protein which demonstrates independently folded domains. Furthermore, if the fragments are small enough, Nuclear Magnetic Resonance (NMR) could also be used to determine their solution structures.

1.2.2. Non-Crystallographic Studies

The lack of crystals for any membrane-bound P450 enzymes has not impeded all efforts of obtaining structural information on these proteins. Spectroscopic techniques, such as NMR, Electron Spin Echo Envelope Modulation (ESEEM), and Extended X-ray Absorption Fine Structure (EXAFS) spectroscopies have been able to (at least) offer local structural information. NMR studies on the relaxation of protons were able to determine the closest point of approach of water molecules to the heme iron of $P450_{scc}$, when bound with different steroids [59]. ESEEM studies with $P450_{scc}$, complexed with deuterated steroids have been able to give iron-deuterium distances [55, 60]. EXAFS studies with 22(*R*) aminocholesterol and 22(*S*) thiacholesterol-S-oxide were able to give still more iron-steroid distances [55]. With the concerted application of all the local distance information (available from various spectroscopies), along with possible domain structural determinations, it may be feasible to model mammalian P450 on presently known P450 structures to obtain 'best guess' structures.

1.3. Two Classes of Cytochromes P450

P450 enzymes require electron transfer companion proteins since they can only accept one electron at a time, yet NADPH is a two-electron donor. These electron transfer proteins offer the ability to accept the complete hydride from NADPH while delivering the electrons singly to the P450. Mammalian P450 enzymes come in two classes - mitochondrial (class I) and microsomal (class II; found in the endoplasmic reticulum). Each class has a different means of acquiring their reducing equivalents.

1.3.1. Class I Mammalian P450 Enzymes

Mitochondrial P450 enzymes acquire their electrons (from NADPH) through the mediation of a 2Fe-2S ferredoxin (named adrenodoxin (Adx), when obtained from adrenocortical tissue) and an FAD-containing oxidoreductase (called adrenodoxin reductase (AdR), when obtained from the same source as adrenodoxin) (see **Figure 1.9A**). Additionally, since mitochondria do not produce NADPH

through the normal course of the Krebs cycle, these enzymes are dependent of the action of (at least) three different sources for this reductant: (1) $NADP^+$-linked malic dehydrogenase, (2) $NADP^+$-linked isocitrate dehydrogenase, and (3) energy-linked transhydrogenation of $NADP^+$ by NADH [61].

The current model for electron transfer from adrenodoxin reductase to class I cytochromes P450 invokes what is known as the adrenodoxin 'shuttle mechanism' [62] (see **Figure 1.9A**). This mechanism is described by the following sequence of events: (1) NADPH binds to oxidized adrenodoxin reductase (AdR), reducing its FAD cofactor to $FADH_2$; (2) oxidized adrenodoxin (Adx) then binds to the reduced AdR (if it was not already bound to the oxidized AdR, before its reduction by NADPH) and acquires one electron, leaving the AdR flavin cofactor in the semiquinone state. (3) reduced Adx, having a 20-fold lower affinity for AdR [63], then dissociates; (4) the reduced Adx, having an elevated affinity for the substrate-bound class I P450 enzyme, then binds to the cytochrome and reduces it; (5) the resulting oxidized Adx, having a 2-fold lower affinity for reduced P450 [63], dissociates from the cytochrome and cycles back to another fully reduced AdR or an AdR in the semiquinone state - to be reduced yet again. The net result is the stepwise reduction the P450, concurrent with the stepwise oxidation of reduced AdR.

There are three class I cytochromes P450 in the adrenal cortex and two in the kidney. In the adrenal cortex, these are $P450_{scc}$, $P450_{11\beta}$, and $P450_{aldo}$ - the latter two having very similar activities and might not even be present together in the same mitochondrion. The activities of these enzymes are shown in **Figure 1.1**. $P450_{scc}$ is the only class I enzyme in all other steroidogenic tissues (except for the brain which also has $P450_{11\beta}$ [64]). In the kidney, the class I enzymes are $P450_{D1\alpha}$ (25-hydroxyvitamin D_3 1α-hydroxylase) and $P450_{D24}$ (1α,25-dihydroxyvitamin D_3 24-hydroxylase). Although slightly different versions of the 2Fe-2S ferredoxin have been found in adrenocortical and kidney tissues, these ferredoxins can substitute for one another when reconstituting *in vitro* class I P450 activity.

1.3.2. Class II Mammalian P450 Enzymes

Microsomal P450 enzymes acquire their NADPH-stored reducing equivalents through the intermediary P450 reductase, a protein containing both an FAD as well as an FMN cofactor (see **Figure 1.9B**). P450 reductase - by itself - is sufficient in delivering both electrons for microsomal P450 catalysis.

However, P450 reductase may not hold a complete monopoly on the source of all electrons. The first electron, delivered to the P450, must come from P450 reductase, but it has been proposed that reduced cytochrome b5 (also found in the endoplasmic reticular membrane) may be able to deliver the second electron [65, 66]. The addition of moderate amounts of oxidized cytochrome b5 to reconstituted P450 reductase/cytochrome P450 systems often leads to a stimulation of P450 activity, whereas large amounts lead to suppression of activity [65]; this suppression is believed to be caused by interference with P450 reductase-binding to cytochrome P450 [65]. The stimulation was found to reach a maximum when one equivalent of cytochrome b5 (relative to cytochrome P450) is used [67]. Such information is suggestive that b5 may act as an allosteric modifier of cytochrome P450 and/or acts as a second conduit of electron transfer from P450 reductase to the P450 enzyme. In fact, a proposal has been raised that cytochrome b5, when bound to the P450 enzyme, may allow the reductase to deliver both electrons to the b5-P450 complex in a single interaction [68]. Apart from this stimulation of activity, cytochrome b5 is believed to also play a role in controlling the dual activities of $P450_{c17}$ (see sections **1.3.2** and **1.4.2.4**).

There are three class II steroidogenic P450 enzymes in mammals. These are $P450_{c21}$, $P450_{c17}$, $P450_{arom}$; their activities are shown in **Figure 1.1**. $P450_{c17}$ and $P450_{arom}$, like $P450_{scc}$ and $P450_{11\beta}$, both have multiple activities. Interestingly, $P450_{c21}$ is unique in that it is the only steroidogenic P450 enzyme to have only one activity - the C-21 hydroxylation of either pregnenolone or progesterone.

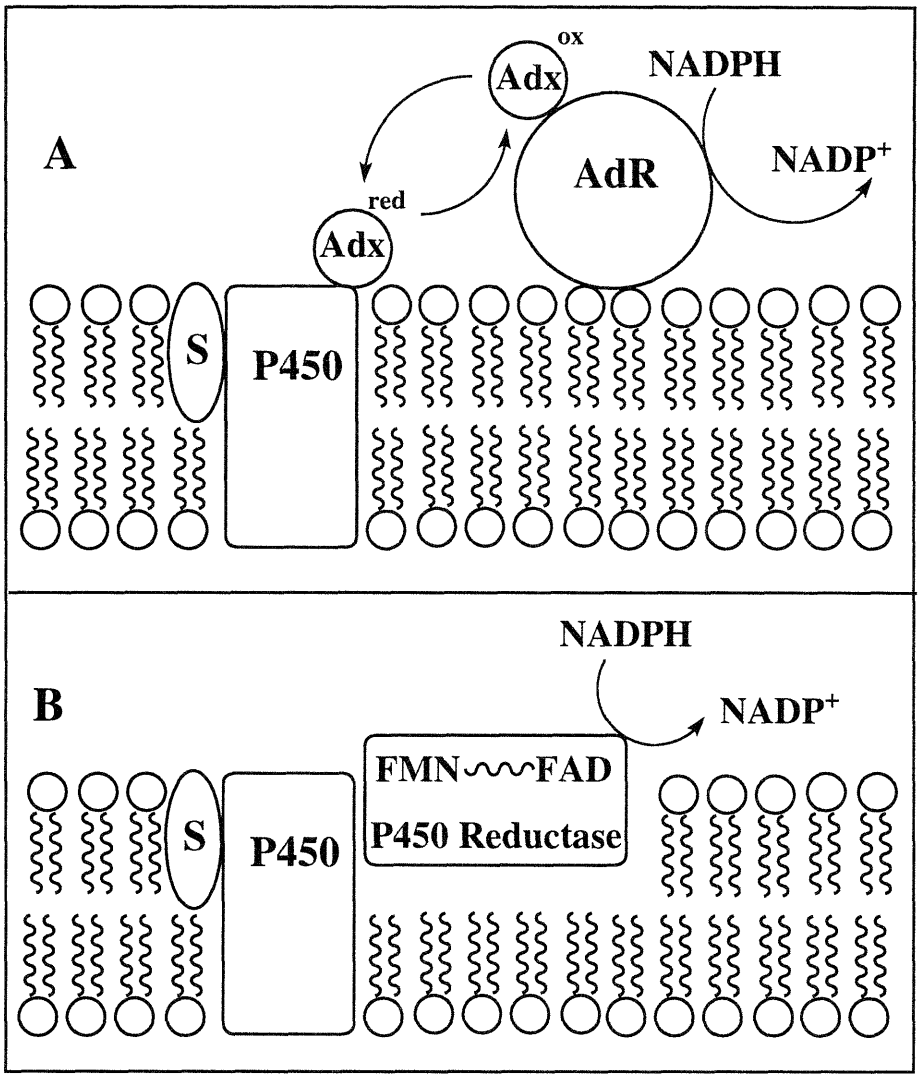

Figure 1.9: The current models for electron transfer from NADPH to the membrane-bound P450 enzyme in (A) the mitochondrion and (B) the endoplasmic reticulum. Abbreviations are 'S' for substrate, 'Adx' for adrenodoxin, and 'AdR' for adrenodoxin reductase; all others are described in the text.

1.3.3. Similarities Between the Two Classes of Mammalian P450 Enzymes

Even though microsomal and mitochondrial P450 enzymes utilize different electron transfer proteins, some degree of cross-reactivity has been reported. For example, cytochrome b5 was found to bind to $P450_{scc}$ with a K_d of 0.28 μM; crosslinking, followed by limited proteolysis revealed that the interaction was at both hydrophobic and hydrophilic regions of $P450_{scc}$ [69]. Additionally, when a reconstituted $P450_{scc}$ system was supplemented with cytochrome b5, an enhancement of P450 activity was observed [70]. Cytochrome b5 was also found to

protect $P450_{scc}$ from being phosphorylated by protein kinase C. [71]. Another example is that adrenodoxin reductase has been reported to have a stimulatory effect on both $P450_{c21}$ and on the 17α-hydroxylase activity of $P450_{c17}$ [72]. Although cytochrome b5 has been reported in mitochondria from liver [73], it was found in the outer mitochondrial membrane; this fact makes it unlikely that it is involved in the *in vivo* actions of class I cytochromes P450.

1.4. Steroidogenesis

All known steroid hormones are derived from cholesterol (shown at the top left of **Figure 1.1**) which by itself plays a role in influencing the fluidity of cellular membranes [74]. Apart from its role in membranes, cholesterol can be degraded to bile acids which act as detergents in the small intestine - aiding in the solubilization of ingested lipids [75]. Rearrangement of the steroid nucleus of 7-dehydrocholesterol is also involved in Vitamin D (cholecalciferol) production [76], which has an essential role in the absorption and mobilization of calcium in mammals [77]. Alternatively, cholesterol can be transformed into steroid hormones.

Once cholesterol is processed by the cytochrome P450 side chain cleavage enzyme ($P450_{scc}$), its product (pregnenolone, see **Figure 1.1**) becomes committed to the production of steroid hormones. $P450_{scc}$ also controls the rate limiting step of steroidogenesis [78]. $P450_{scc}$ is perhaps the most studied of all mammalian steroidogenic P450 enzymes. That fact arises from the pivotal role that it plays and also because it is one of most stable mammalian enzymes in its class. Since all mammalian P450 enzymes are membrane-bound proteins, they have proven difficult to both purify and stabilize for mechanistic and structural studies. From pregnenolone onwards, steroidogenesis branches off into different directions, leading to hormones that regulate specific systems of the body. Apart from the medicinally useful knowledge gained in $P450_{scc}$ studies, the endocrinological challenge has long been to build on what can be learned from stable P450 proteins in order to understand all P450 enzymes. The prize, from such an endeavor, would be the ability to medicinally regulate the production of either the mineralocorticoids, the glucocorticoids, or the sex steroids (the androgens and the estrogens).

The obvious starting place, in devising a medicinal strategy is to understand how the normal organism controls these pathways and to learn about what is similar and different about each of the enzymes involved. From a close examination of **Figure 1.1**, it becomes apparent that one cannot make a simple list of P450 enzymes which influence the production of mutually exclusive categories of hormones. Cytochrome P450 17α hydroxylase/C17,20 lyase ($P450_{c17}$, which can hydroxylate the C-17 α-position, as well as cleave the carbon-carbon bond connecting C-17 to C-20, of steroids) is required for the production of the sex steroids as well as the glucocorticoids. In addition, P450 21-hydroxylase ($P450_{c21}$) is involved in the production of both glucocorticoids and mineralocorticoids. Finally, P450 11β-hydroxylase (which exists in two forms, $P450_{11\beta}$, which can hydroxylate at both the C-11 and C-18 positions of the steroid, and $P450_{aldo}$, which has the same activities as $P450_{11\beta}$ but can also synthesize aldosterone) is required in the biosynthesis of both glucocorticoids and mineralocorticoids. This intertwining of different enzymes in different pathways - which are all specifically regulated by the body - has introduced issues ranging from similar isozymes (differentially regulated or differentially post-translationally modified) to regulated sequestration of substrates from enzymes.

In addition to the lack of correspondence of individual cytochromes P450 with different biosynthetic pathways, some of these enzymes have multiple activities which are differentially regulated. The regulated chemical flexibility of $P450_{c17}$, $P450_{11\beta}$, and $P450_{aldo}$ suggests the presence of either covalent (through phosphorylation, glycosylation, or some other post-translational modification) or non-covalent (i.e. allostery) alteration of these proteins. The modes of control available to the organism is further increased when one considers the fact that these enzymes are found in membranes whose lipid (or proteinaceous) composition can be controlled. Regulated access of the organic substrate and/or molecular oxygen, to the active site, may also be involved in the modulation of activity. The requirement of electron transfer companion proteins, add yet another dimension to control the activity of these enzymes.

1.4.1. Description and Localization of Steroidogenic Cytochromes P450

Mammalian steroidogenic P450 enzymes are found in a variety of tissue cells - some of which specialize in the production of certain classes of hormones. Cholesterol side chain cleavage enzyme ($P450_{scc}$) is found in the adrenal cortex [63], testis [63], ovary [63], corpus luteum [79], and brain [64]. 11β-Hydroxylase ($P450_{11\beta}$) is found in the brain [64] and in both the inner (*zonae reticularis-fasciculata*) and outer (*zona glomerulosa*) regions of the adrenal cortex [63]. Aldosterone synthase ($P450_{aldo}$) is found only in the *glomerulosa* portion of the adrenal cortex [63]. 21-Hydroxylase is found in all regions of the adrenal cortex [63]. 17α-Hydroxylase/17,20 lyase ($P450_{c17}$) is found in the adrenal cortex [63], testis [63], and corpus luteum [80]. Aromatase ($P450_{arom}$) is found in the ovary [63], placenta [63], corpus luteum [81], adipose [82], and brain [82]. Since the production of any steroid hormone hinges on the presence and activity of $P450_{scc}$, the regulation of any portion of steroidogenesis is related to the regulation of this key enzyme.

1.4.2. Physiological Regulation of Steroidogenesis

1.4.2.1. Hormonal Regulation

1.4.2.1.1. Adrenocorticotrophic Hormone (ACTH)

Many P450 enzymes (but predominantly $P450_{scc}$) are stimulated and largely maintained by signals from the brain, or the placenta (in a pregnant woman), to the tissue involved. The brain signals are peptides, released from the anterior lobe of the pituitary gland: adrenocorticotropic hormone (ACTH), luteinizing hormone (LH), and follicle stimulating hormone (FSH) [83]. The signal from the placenta is human chorionic gonadotropin (hCG). ACTH affects a variety of processes in the adrenal cortex. LH and FSH regulate the growth and function of the gonads and are thus grouped in the category of gonadotropins, along with hCG; however, hCG's specific function is to maintain the corpus luteum during pregnancy [83]. Overall, the functions of LH, FSH, and hCG are similar to that of ACTH, except that they affect different tissues. Since this thesis is concerned primarily with the synthesis of corticosteroids, only ACTH's function will be described further.

Specific effects of ACTH include: stimulation of the transcription of the genes for $P450_{scc}$, $P450_{11\beta}$, $P450_{c21}$, $P450_{c17}$, and adrenodoxin [84]; stabilization of $P450_{scc}$ mRNA [84]; and the mobilization of cholesterol from lipid droplets in the cytoplasm to the inner mitochondrial membrane [63]. Cortisol secretion into the bloodstream, resulting from ACTH stimulation of adrenal cortex, eventually comes in contact with the pituitary gland, causing a down regulation of ACTH. Any pathology which inhibits cortisol production, siphons cortisol onward to form still other steroids, or renders the pituitary insensitive to cortisol, effects some subversion of this feedback mechanism. The result of such a disorder is the excessive stimulation of the adrenal cortex (caused by the effects of continually secreted ACTH), giving rise to an hyperplasia. The synthetic corticosteroid dexamethasone (which binds to glucocorticoid receptors ten and five times more strongly than cortisol and corticosterone, respectively [85]) is capable of replacing cortisol in this feedback mechanism. One of the uses of dexamethasone has therefore been to test individuals (who suffer from the effects of corticosteroid overproduction) for an aberrant feedback control system [2]. When this control system is not operative, treatment often necessitates the approach of directly inhibiting the P450 enzyme(s) involved.

Many of the ACTH's functions are enacted by cAMP (cyclic AMP, a second messenger) within the affected cells. However, cAMP may not be the sole second messenger for ACTH, since treatment of cultured adrenocortical cells with cAMP analogs do not exactly mimic the effects of ACTH [86]. Nevertheless, the role of cAMP is essential. There is an absolute requirement for cAMP in the transcription of P450s [87]. cAMP, itself, also activates different classes of protein kinases. cAMP is known to effect transcription of genes in certain operons by way of binding to transcription initiators [88]; however, in adrenocortical cells, cAMP is known to activate the synthesis of short-lived protein factors which mediate increases in transcription of specific genes [89]. In the case of cAMP-dependent transcription of the adrenodoxin gene, however, it has been shown (albeit, in cultured choriocarcinoma cells) that protein synthesis is not required [78]. cAMP-dependent protein synthesis has also been linked with the mobilization of cholesterol to the

inner mitochondrial membrane [90]. Intracellular cholesterol movement also appears to be dependent on GTP hydrolysis and on Ca^{2+} levels [91].

Protein kinases (PKs) also play a complex role in the regulation of P450 activity. Some cAMP-dependent PKs have been linked with gene transcription [92-94]. The activation of PK-dependent transcriptional regulation can also be controlled by factors apart from cAMP; for example, high extracellular potassium concentrations have been found to stimulate PK-dependent induction of $P450_{aldo}$ [93]. A cAMP-dependent PK is also known to activate cholesterol esterase, which hydrolyzes cholesterol esters to free cholesterol [63]. The fact that PKs are known to activate (or deactivate) enzymes via phosphorylation raises the possibility that this form of covalent modification of P450 enzymes (or their electron transfer proteins) may also be able to regulate P450 activity (see section **1.4.2.2**)

1.4.2.1.2. Angiotensin II

The other significant hormonal regulation of the adrenal cortex is caused by the peptide angiotensin II (A-II). Production of A-II results from the coordinated actions of many separate bodily tissues - heart, kidney, lung, and adrenal cortex (see **Figure 1.10**). The purpose of this whole response system is to do any (or all) of the following: (1) control the loss of sodium, (2) cause the loss of potassium, and (3) restore blood pressure. When the sodium/potassium levels and blood pressure become normal, the production of angiotensin II ceases. This hormone stimulates, either primarily (e.g. bovine [95]) or uniquely (e.g. rat [96]), the *zona glomerulosa* of the cortex, stimulating the production of proteins required for aldosterone synthesis: $P450_{scc}$ [97, 98], 3β-hydroxysteroid dehydrogenase [98]; adrenodoxin [97, 98], $P450_{c21}$ [98], and (especially) $P450_{aldo}$ [97-101].

The actions of A-II, as with ACTH, are enacted through the efforts of second messengers. A-II gives rise to a rapid and transient increase in cAMP levels [102]. Cellular intake of Ca^{2+} has been shown to be required in aldosterone synthesis since the administration of calcium channel antagonists (verapamil and nifedipine) suppress A-II's effects [103]. In spite of treatment with verapamil, A-II-dependent increases of free intracellular levels Ca^{2+} has been reported [96], suggesting a direct

role of Ca^{2+} in mediating the effects of A-II [96]. However, in turkey adrenocortical cells, elevations in intracellular Ca^{2+} concentration and aldosterone production were dissociable events and effected by different A-II receptors [104]. Larger increases in the *glomerulosa* (over the *fasciculata*) of intracellular levels of inositol phosphates has also been shown to result from A-II treatment [105].

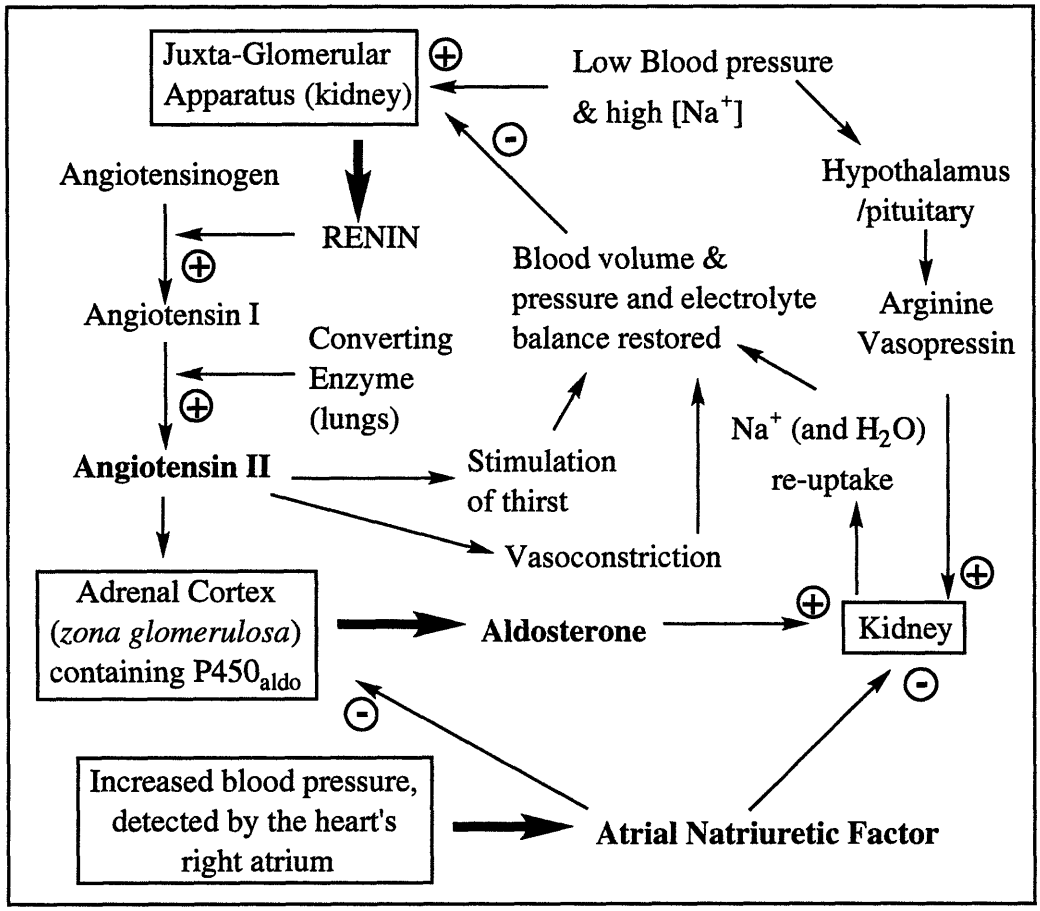

Figure 1.10: Some of the major systems which regulate blood pressure in humans. This figure was adapted from reference [106]. The plus and minus signs refer to stimulation and suppression, respectively.

Apart from effecting an increase in the proteins contributing to aldosterone synthesis, A-II is believed to also lower the level of proteins which divert steroid intermediates toward non-mineralocorticoids. For example, regions of the promoter for the $P450_{c17}$ gene have been shown to contain sequences which suppress transcription when activated by the Ca^{2+}/protein kinase C system, used by A-II [107].

1.4.2.2. Regulation by Post Translational Modification

1.4.2.2.1 Protein phosphorylation

The discovery of protein kinase C's (*in vitro*) ability to phosphorylate $P450_{D1\alpha}$ [108] (25-hydroxyvitamin D_3 1α-hydroxylase, found in the kidney [63]), $P450_{scc}$ [71], and $P450_{11\beta}$ [109] suggests that this may also be a means of regulating P450 activity. cAMP-dependent PKs have been found to phosphorylate both renodoxin (the mitochondrial ferredoxin in the kidney) and adrenodoxin [110, 111]. Phosphorylation of adrenodoxin was found to lower its K_m in both $P450_{scc}$ and $P450_{11\beta}$ reactions [110]. In addition, parathyroid-dependent stimulation of $P450_{D1\alpha}$ activity is accompanied by the dephosphorylation of phosphorylated renodoxin [112, 113]; *in vitro* studies showed that phosphorylated renodoxin significantly inhibits $P450_{D1\alpha}$ [112]. Protein kinase C is also known to phosphorylate the Atrial Natriuretic Factor (ANF) receptor [114] which, when bound with ANF, affect cellular events leading to the production of corticosterone [114] as well as the secretion of aldosterone [115].

1.4.2.2.2. Protein Glycosylation

Protein glycosylation may also be involved in the regulation of steroidogenesis. Both $P450_{scc}$ [116] and adrenodoxin reductase [116, 117] have been reported to be glycoproteins. Since these reports, the glycosylation of $P450_{scc}$ has been put in question. In the case of $P450_{scc}$, it was originally reported that neuraminidase (an enzyme which removes sialic acid residues from glycosylated proteins) treatment of $P450_{scc}$ and/or adrenodoxin reductase abolishes cholesterol side chain cleavage [116]. Subsequently, Tsubaki *et al.* reported that carbohydrate-specific stains could not show that $P450_{scc}$ was glycosylated [118]. In addition, expression of the cDNA for $P450_{scc}$ in *E. coli* (which is not believed to glycosylate proteins) produced a protein - when reconstituted with purified adrenodoxin and adrenodoxin reductase - that could catalyze cholesterol side chain cleavage activity [119, 120]. *E. coli* expression of adrenodoxin [121] and adrenodoxin reductase [122] also produced an active protein - suppressing suspicions that these too might be glycosylated.

Therefore, the glycosylation of adrenodoxin reductase - originally reported to have a composition of 2% (w/w) carbohydrate [117] - is questionable.

1.4.2.2.3. Limited Protein Hydrolysis

The partial hydrolysis of P450 proteins (and/or their electron transfer proteins) is yet another means that steroidogenesis may be controlled. In purification of three separable, but equally active, forms of $P450_{scc}$, Tsubaki *et al.* found that one of these was missing its original N-terminal amino acid residue [118]; such an alteration, however benign toward side chain cleavage activity, could conceivably cause a different interaction with $P450_{11\beta}$, (sharing the same membrane) and/or cause a difference in the strength of competition (between $P450_{scc}$ and $P450_{11\beta}$) for reduced adrenodoxin.

Adrenodoxin has also been reported to be active in differentially (C-terminal) truncated forms. In the original report of the amino acid sequence of adrenodoxin [123], it lacked many C-terminal amino acids that were found when its mRNA was translated in vitro [124] and which were found coded for in its sequenced cDNA gene [125]. The lack of certain amino acids at the C-terminus has also been demonstrated to enhance adrenodoxin's effectiveness as an electron transfer agent [121, 126]. Trypsinolysis of purified adrenodoxin produced a protein lacking the C-terminal amino acid residues 116-128; this smaller version was found to have a 3.8-fold and 3.5-fold lower K_m (compared to normal adrenodoxin) when reconstituted in $P450_{scc}$ and $P450_{11\beta}$ catalyzed reactions, respectively [126]. In addition, the spectral association constant between the truncated adrenodoxin and $P450_{scc}$ was also found to increase 1.5-fold [126]. Removal of adrenodoxin residues 116-128, however, was not found to significantly affect its interaction with adrenodoxin reductase [126].

Similar C-terminal deletion studies on adrenodoxin were also performed using deletion mutants of an adrenodoxin cDNA, expressed in E. coli [121]. Uhlmann *et al.* reported that adrenodoxin may be truncated (at the C-terminal) as far back as amino acid 115 without much effect [121]. Shortening the protein this much did not significantly affect its EPR or absorption spectrum, nor did it affect its ability to accept electrons from adrenodoxin reductase [121]. However, deletion

mutants 4-114 (having only amino acid residue numbers 4 through 114) and 4-109 demonstrated an change in their EPR and CD, compared to normal adrenodoxin [121]. Deletion of a unique proline at position 108 (in making mutant 4-107) abolished its EPR spectrum [121]. The 4-108 and 4-114 mutants were also found to accelerate the first electron transfer to $P450_{11\beta}$ 4.5-fold, but not for $P450_{scc}$.

1.4.2.3. Neuronal Regulation

The release of adrenocortical steroids (and possibly their production) is also under some neuronal control. Neural stimulation, performed on whole pig adrenal glands (with their attached nerve cells still intact) effected an increase in cortisol and aldosterone release [127]. This increase was attributed to the local release of vasoactive intestinal peptide (VIP) [127], which is known to stimulate the secretion of aldosterone and corticosterone [128]. Studies performed on whole frog adrenal cells demonstrated that calcitonin gene-related peptide (CGRP), released by nearby nerve cells, stimulates corticosterone and aldosterone secretion [129].

Different neurotransmitters have also been found to have specific effects on corticosteroid production and/or release. In frogs, adrenal chromaffin cells have been shown to be capable of secreting serotonin which stimulates the production of both corticosterone and aldosterone [130]. Conversely, dopamine has been shown to inhibit both the A-II-dependent rise in intracellular cAMP [102] and A-II-stimulated secretion of aldosterone [131, 132]. The neurotransmitter nitric oxide has also recently been proposed as a possible regulator of P450 activities since it was found to inhibit P450 activity *in vitro* [133].

1.4.2.4. Redox Regulation

The regulation of the dual activities of $P450_{c17}$ (17α-hydroxylase and 17,20 lyase) appears to be effected by the level of P450 reductase and cytochrome b5 present in the environment of this enzyme. As stated in section **1.4.2.4**, the higher the level of these two electron transfer proteins, the higher the ratio of $P450_{c17}$'s lyase activity over its 17α-hydroxylase activity. This control over the direction of catalysis could be the main fashion by which the organism regulates these activities. The fact that

adrenal cortical tissue is 3.5-fold lower in P450 reductase activity, compared to the testis, could account for the higher content of androgens, produced by the latter tissue [28].

Regulation based on the levels of P450 redox partners present may also be involved in the control of 11β-hydroxylation and aldosterone synthesis activities. 11β-Hydroxylation of steroids occurs in all regions of the adrenal cortex (the *zonae reticularis-fasciculata* and the *zona glomerulosa*), but aldosterone is made uniquely in the *glomerulosa*. Bovine *glomerulosa* mitochondria (when compared to *reticularis-fasciculata* mitochondria) have considerably more of semidehydroascorbate reductase [134, 135] and NADH-cytochrome C reductase [134] - both of which contribute to malate-dependent NADPH formation. If the formation of aldosterone requires an altered level of coupling with adrenodoxin and/or a higher level of reducing potential, then the form of activity control apparent in $P450_{c17}$ may also be operative in $P450_{aldo}$.

Antioxidants such as β-carotene and ascorbate may also serve a protective function toward P450 enzymes. As mentioned in section **1.1**, the oxyferrous form of P450 enzymes can decay to ferric forms with concomitant production of superoxide. Superoxide may then initiate P450 chemical modification - leading to inactivation. In the corpus luteum (whose name means 'yellow body'), its high concentration of the yellow pigment β-carotene was found to be (at least one of the factors) responsible for inhibition of endogenous $P450_{scc}$:adrenodoxin covalent crosslinking - destroying side chain cleavage activity [136] This crosslinking was oxygen-dependent and inhibited by the $P450_{scc}$ inhibitor aminoglutethimide [136]. Ascorbate could not replace the function of β-carotene in these cells [136]. However, ascorbate was also found to play a similar protective role toward $P450_{11\beta}$ in cultured adrenocortical cells [137].

1.4.3. A Closer Look at $P450_{scc}$

Due to the fact that $P450_{scc}$ is found in the same mitochondrial membranes as $P450_{11\beta}$, and also reliant on adrenodoxin for its reducing equivalents, it is worthwhile to review some key features about this enzyme. Both $P450_{scc}$ [138, 139] and $P450_{11\beta}$ [140] are found in the inner mitochondrial membrane; they can also be localized in the same mitochondrion [141]. In addition to their possible *in vivo* associations, $P450_{11\beta}$ and $P450_{scc}$ have significant sequence homologies in certain stretches of their amino acid sequence [55, 142]. Therefore, some structural information acquired for $P450_{scc}$ may be potentially transferable to $P450_{11\beta}$.

1.4.3.1. $P450_{scc}$ Catalyzed Reactions

$P450_{scc}$ catalyzes the conversion of cholesterol to pregnenolone by way of three cycles of oxygen- and NADPH-dependent oxidations (see **Figure 1.11**). Since its catalytic intermediates are not released by the enzyme, the first hydroxylation commits the enzyme to the formation of pregnenolone. Not surprisingly, the first hydroxylation is the rate limiting reaction [143]. The two hydroxylations of cholesterol to 20(*S*),22(*R*)-dihydroxycholesterol (with the intermediate 22(*R*)-hydroxycholesterol) are believed to proceed by way of the accepted P450 hydroxylation cycle (see **Figure 1.4**). However, the nature of the oxidative glycol cleavage from 20(*S*),22(*R*)-dihydroxycholesterol to pregnenolone remains undetermined. The possibility of a third hydroxylation, followed by rearrangement appears unlikely due to the retention of the 22(*S*) hydrogen of 20(*S*),22(*R*)-dihydroxycholesterol in the product of isocapraldehyde [9]. In addition, Takemoto *et al.* found little or no incorporation of oxygen into pregnenolone via $P450_{scc}$ catalysis of the glycol cleavage reaction [144]. However, it should be noted that these experiments did not establish the quantitative lower bound of detectability for oxygen incorporation.

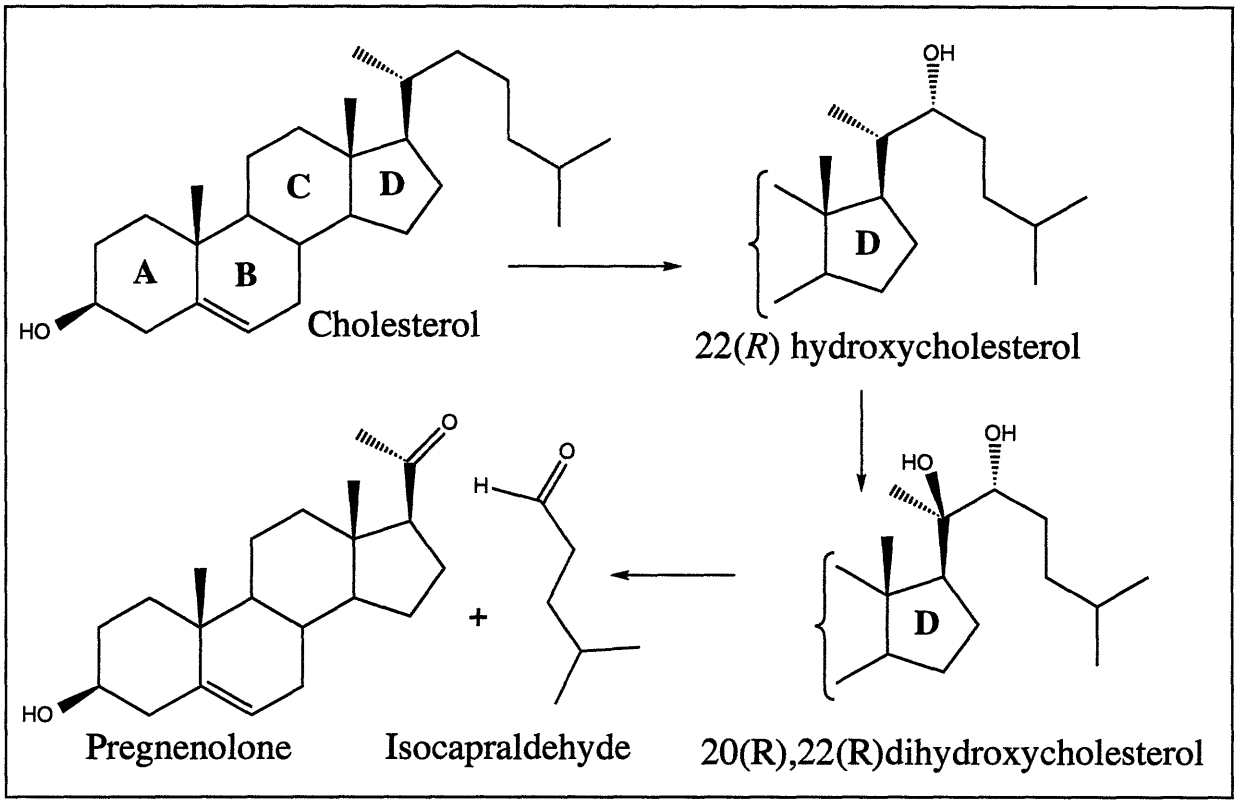

Figure 1.11: The conversion of cholesterol to pregnenolone, catalyzed by $P450_{scc}$.

Ortiz de Montellano has proposed a heterolytic and a homolytic mechanism in which an oxenoid moiety could cause this glycol cleavage reaction (see **Figure 1.12**) [9]. Either one of these mechanisms (paths i and ii of **Figure 1.12**) initially requires the oxenoid moiety to homolytically break a hydrogen-oxygen bond on one of the hydroxyls. This is noteworthy since an oxygen-hydrogen bond is approximately 12 kcal/mol stronger than a carbon-hydrogen bond [145]. If P450 enzymes are capable of generating substrate-bound hydroxyl radicals, this would offer precedence for hydroxyl-radical mediated hydrogen migration proposed, in this introduction, for the final steps in aldosterone formation (see section **1.5.5.3**).

The glycol cleavage is distinct from the first two oxidations of cholesterol, from the perspective of the protein's overall conformation. There is resonance Raman [146] and EPR evidence [147] that there is a significant conformational change in the side chain of cholesterol between the last two oxidations. This conformational change is facilitated by the binding of reduced Adx [147].

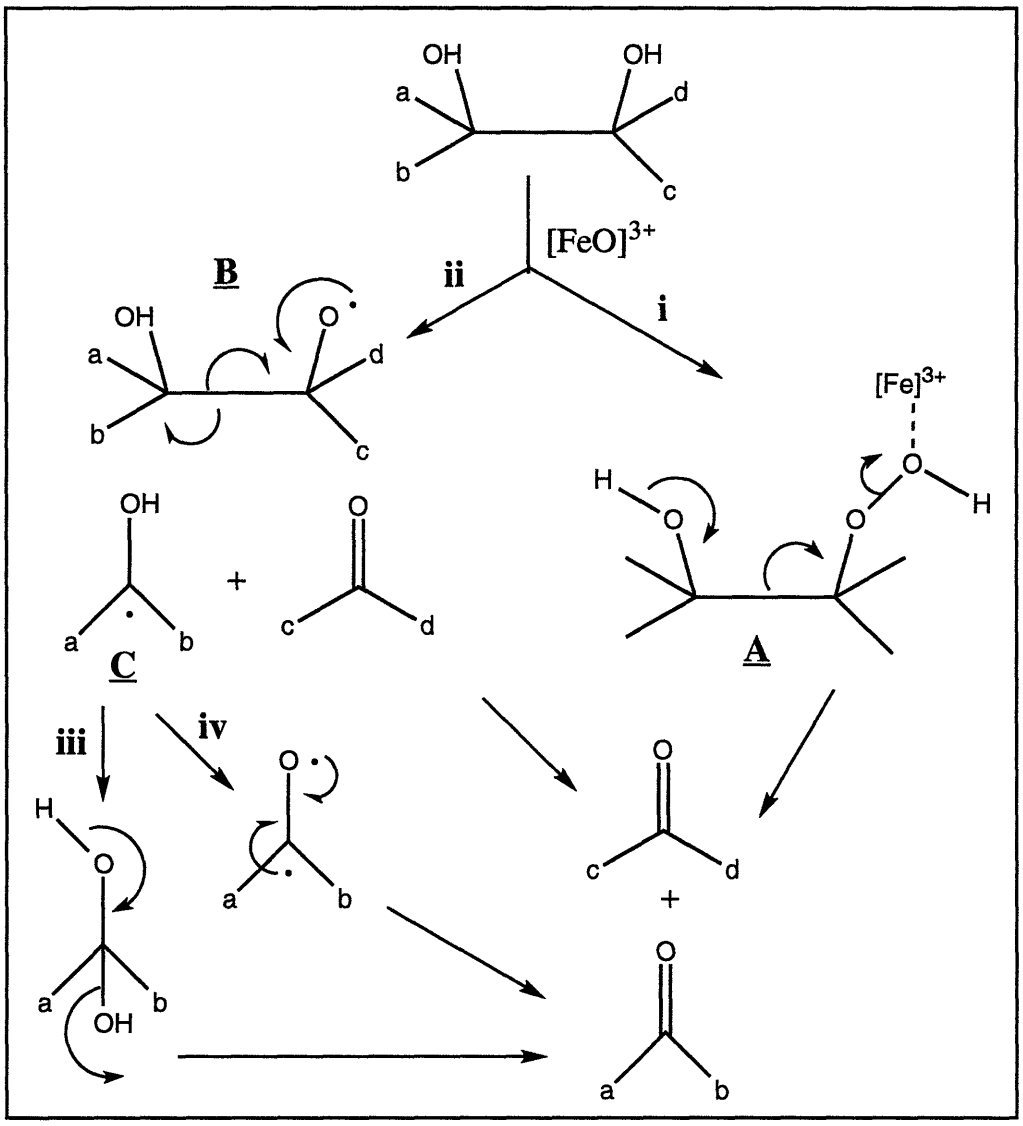

Figure 1.12: Proposed mechanisms for P450-catalyzed glycol cleavage [9]. Both pathways are initiated by hydrogen abstraction from a substrate hydroxyl. Pathway i: This is followed by a recombination of the substrate hydroxyl radical with the iron-bound hydroxyl radical, forming an alkyl peroxide (**A**), which can coordinate to the iron. The iron then acts as a Lewis acid, catalyzing the heterolytic cleavage of the carbon-carbon bond. Pathway ii: The initially formed hydroxyl radical (**B**) rearranges, giving rise to a carbonyl and a carbon-based radical on the remaining alcohol (**C**). Compound **C** then either recombines with the iron-bound hydroxyl radical to form a gem diol (path iii) which dehydrates to form a carbonyl; alternatively, **C** somehow loses a hydrogen atom (path iv) and directly forms a carbonyl.

1.4.3.2. Importation Into the Mitochondrion and Proteolytic Processing

$P450_{scc}$ and $P450_{11\beta}$ appear to share a common means of importation, from the cytoplasm, into the mitochondrion. A synthetic peptide corresponding to the first 15 amino acid residues of $P450_{scc}$ was effective at inhibiting the importation of precursor (pre-) forms of $P450_{scc}$, $P450_{11\beta}$, adrenodoxin, and malate dehydrogenase [148]. In studies performed on isolated mitochondria from corpus luteum (a tissue which does not express $P450_{11\beta}$ activity), it was found that pre-$P450_{11\beta}$ was effectively imported and processed into its mature size by removal of its N-terminal extension peptide [149]. Therefore, this import process appears to be common in different cell types. In fact, pre-$P450_{scc}$ was also found to be successfully incorporated in isolated soybean cotyledon mitochondria [150]. Nonetheless, this import system is not universal since pre-$P450_{11\beta}$ [149] and pre-$P450_{scc}$ [151] could not be imported into isolated heart mitochondria.

The process of P450-binding to mitochondrial membranes may be distinct from that of importation, since it was reported that hydrophobic peptides (containing either lysine or arginine at specific positions) inhibited both pre-adrenodoxin and pre-$P450_{scc}$ incorporation, but did not affect pre-$P450_{scc}$'s ability to bind to the mitochondrial surface [152]. In addition, these peptides were found to not affect the membrane's fluidity [152]. The specific function of P450 extension peptides may be related to the proposal that some mitochondrial signal sequences may aid in the fusion of both the inner and outer mitochondrial membranes, which may be required for P450 importation [153]. It is interesting to note that cardiolipin (which, by it structural nature (see **Figure 1.8**), could facilitate membrane fusion) appears to be involved in $P450_{scc}$'s ability to bind to membranes [154].

The following series of facts leads to a compelling hypothesis for mechanism of importation of pre-$P450_{scc}$. Cardiolipin-containing liposomes are able to fuse more easily when $P450_{scc}$ is present [155]. Cardiolipin is known to be a positive effector for cholesterol binding to $P450_{scc}$ [33, 62]. Cardiolipin is also known to strongly associate with membrane-bound $P450_{scc}$ [156]. Therefore, it seems plausible that pre-$P450_{scc}$ binding to the outer mitochondrial membrane may cause a

clustering of cardiolipin molecules, facilitating membrane fusion, which may be required for subsequent incorporation into the inner membrane.

If $P450_{scc}$ and $P450_{11\beta}$ do indeed share a common mitochondrial import mechanism, then the incorporation of specific information from $P450_{11\beta}$ studies may provide more details on this mutual process. A peptide corresponding to the first 45 amino acid residues of $P450_{11\beta}$ was found to be incorporated into mitochondria in a fashion independent of extramitochondrial ATP [157]. This import was found to not require mitochondrial surface proteins [157]. However, $P450_{11\beta}$ was found to be imported via a potential-dependent pathway and reliant upon protein components on the outer surface of the inner mitochondrial membrane [157].

Note that mitochondrial importation and cleavage of a protein precursor's N-terminal sequence need not be coupled. For instance, Omura and coworkers found that a partially purified rat liver mitochondrial protease was capable of processing pre-$P450_{scc}$ and pre-$P450_{11\beta}$, but not pre-adrenodoxin [151]. That laboratory also found that a partially purified mitochondrial metalloprotease (from either rat liver or bovine adrenal cortex), which processes precursor forms of adrenodoxin and malate dehydrogenase to their mature lengths, had no effect on pre-$P450_{scc}$ and pre-$P450_{11\beta}$ [158]. Subsequently, however, that same laboratory reported that a more highly purified sample of the rat protease was indeed cable of processing all four of these proteins - however, with different levels of efficiency [159]. Therefore, at present, there seems to be a preponderance of evidence that the proteolytic maturation process of P450 proteins is different from that of other mitochondrial proteins.

1.4.3.3. $P450_{scc}$'s Membrane Topology

1.4.3.3.1. $P450_{scc}$'s Orientation in the Membrane

In evaluating the membrane topology of $P450_{scc}$, it was found that the enzyme is a transmembrane protein. As mentioned in section **1.2.1**, trypsin can cleave $P450_{scc}$ into two fragments (F1 and F2) which (when combined) still catalyze the side chain cleavage of cholesterol. In the trypsinolysis of $P450_{scc}$, it was found that its

trypsin site is on the matrix side of the inner mitochondrial membrane [160]. In addition, specific (polyclonal) antibodies for $P450_{scc}$ were used to demonstrate that $P450_{scc}$ has regions exposed on both sides of the membrane [161]. The fraction of $P450_{scc}$ residing within the bilayer, however, may be small. Results from rotational diffusion studies and the absence of any intramembrane particles (examined by freeze-fracturing) suggest it to be weakly penetrating into the membrane and to have large parts exposed to the aqueous interior of the mitochondrial matrix [156].

1.4.3.3.2. $P450_{scc}$'s Interaction With Adrenodoxin

The binding of adrenodoxin to $P450_{scc}$ (and presumably to $P450_{11\beta}$ as well) causes several important effects on the cytochrome. At least in cases of where a high concentration of cholesterol sulfate is used, Adx inhibits unproductive binding of this substrate to $P450_{scc}$ [35]. As mentioned in section **1.4.3.1**, Adx facilitates a conformational change in $P450_{scc}$, which appears to be necessary for its glycol cleavage reaction. Optical absorption measurements of reduced $P450_{scc}$-phenyl isocyanide complexes have shown that, upon Adx binding, Adx causes a conformational change around the ferrous heme.

The interaction between Adx and $P450_{scc}$ is known to be coordinated via ionic interactions since the K_d for Adx:$P450_{scc}$ complexation and Adx's K_m in $P450_{scc}$ catalyzed reactions increase exponentially with ionic strength [162]. Chemical crosslinking of Adx:$P450_{scc}$ ionic structures [163] and site-directed mutagenesis [120, 164, 165] have helped to point out some of the residues involved in the docking of these two proteins. The resulting generalization is that Adx (a highly acidic protein) appears to associate with positively charged patches on class I cytochromes P450.

Modification of $P450_{scc}$ with pyridoxal phosphate (PLP) and $NaBH_4$ led to an inhibition of side chain cleavage activity [166]. This modification was protected by adding excess Adx. It is interesting to note that PLP modification of $P450_{scc}$ increased cholesterol's affinity towards $P450_{scc}$ [166]. The region of attachment of PLP (lys 377 or lys 381) maps to a peptide region which is highly homologous to $P450_{11\beta}$ [166]. In site-directed mutagenesis studies on the $P450_{scc}$ gene, replacement of either of these lysine residues significantly raised the K_d for Adx binding (150-600 fold, depending

on the mutation) without changing the spectral properties of the enzyme or its ability to catalyze its reaction [120]. Upon crosslinking Adx and $P450_{scc}$ with a carbodiimide reagent (and characterization of the complex), it was found that binding occurred in the regions of Leu88-Trp108 and Leu368-Trp417 of $P450_{scc}$ [163, 167] In site-directed mutagenesis studies on an *E. coli* expressed cDNA for Adx, tyrosine-86 (believed to be required for electron delivery from its 2Fe-2S cluster to the P450) was mutated to phenylalanine, serine, and leucine [164]; this raised its K_m (as much as 4-fold) for mitochondrial P450 enzymes, but affected $P450_{scc}$ and $P450_{11\beta}$ catalyzed reactions differently [164].

1.4.3.3.3. Possible Existence of an AdR:Adx:P450 Complex During Catalysis

Since the transfer of electrons from $FADH_2$ (on AdR) to $P450_{scc}$ via Adx offers many opportunities for autoxidation, the concept of an *in vivo* ternary complex of these proteins - efficiently transferring electrons - is an appealing one. However, in several kinetic studies with reconstituted mixtures of adrenodoxin reductase, adrenodoxin, and $P450_{scc}$, the formation of a ternary complex does not appear to be required for activity. Activity titrations with AdR demonstrate that active complexes of AdR:Adx:P450 are not needed for $P450_{scc}$ catalysis in vesicle-reconstituted system [168]. In addition, crosslinking only Adx and $P450_{scc}$ (using a carbodiimide reagent), produced a complex which cannot be reduced by NADPH and AdR [163, 167].

Nevertheless, some evidence in favor of the ternary complex has also been reported. Evidence has been found for AdR:Adx:$P450_{scc}$ complex formation by crosslinking studies. Turko *et al.* argue that these proteins form a ternary complex in solution and have shown that treating a mixture of them with N-succinimidyl-6-(4'-azido-2'-nitrophenylamino)-hexanoate gives rise to a complex of 114 kdal [169]. Shkumatov *et al.* found, using second derivative difference spectroscopy (in the median UV-region) that an Adx-induced $P450_{scc}$ conformational change increased when AdR was added [170].

From measuring the decay of absorption anisotropy (after photolysis of the carbonyl-heme) of adrenocortical mitochondria, it was found that membrane-bound

P450s become increasingly more mobile as the level of cholesterol becomes depleted [171]. The authors of this study propose that the less mobile version of $P450_{scc}$ (which is known to bind more strongly to Adx, when it is bound with cholesterol) is complexed with adrenodoxin as well as AdR [171]. This immobilization was found to be salt dependent [172]. Adx by itself, helped immobilize the P450 molecules but AdR (alone) did not [172]. However, if Adx and AdR were added together, this resulted in a decreased mobility [172]. Since Adx binds more tightly to $P450_{scc}$ when the cytochrome is bound with cholesterol (and the Adx-$P450_{scc}$ complex is known to be held together by ionic interactions), these studies argue that Adx, AdR, and mitochondrial P450 enzymes are capable of forming transient tertiary complexes [171, 172]. Ohta *et al.* also point out that such a ternary complex need not be 1:1:1, but may include multiple adrenodoxin molecules [171], since it is known that Adx's binding site for AdR and $P450_{scc}$ overlap [165]. However, these studies were complicated by the fact that $P450_{scc}$ and $P450_{11\beta}$ may have been sharing the same membranes. Therefore, higher order levels of complexation could also have been taking place with the electron transfer proteins as well as the two different P450 enzymes.

1.5. Background on $P450_{11\beta}$ and $P450_{aldo}$

1.5.1. History of these two proteins

$P450_{11\beta}$ and $P450_{aldo}$ are responsible for the last steps in the formation of glucocorticoids and mineralocorticoids. The glucocorticoids corticosterone and cortisol are known be made by $P450_{11\beta}$ from 11-deoxycorticosterone (DOC) and 11-deoxycortisol, respectively. The mineralocorticoid aldosterone is made from DOC in three P450-dependent reactions (see **Figure 1.13**). In all mammals examined to date, it has been found that only the outer regions of the adrenal cortex (the *zona glomerulosa*) is capable of making aldosterone [173]; however, all regions (the *glomerulosa* and the *zonae reticularis* and *fasciculata*) are capable of making corticosterone and cortisol [61].

The sequence of events and even the identity of the intermediates in aldosterone formation are an issue of some controversy. The overall result is that DOC needs to be hydroxylated at the β-position of C-11 and its C-18 methyl group must be oxidized to the level of an aldehyde. Since corticosterone, 18-hydroxy-DOC, and 18-hydroxycorticosterone are all naturally occurring corticosteroids, these have long been assigned as intermediates in the aldosterone biosynthetic reactions. Since $P450_{11\beta}$ is known to make corticosterone, one of the steps was initially assigned to this enzyme. The remaining activities - the hydroxylation of C-18 and the oxidation of the 18-hydroxy group to aldehyde - are often referred to as corticosterone methyl oxidase I (CMO-I) and corticosterone methyl oxidase II (CMO-II), respectively [174]. CMO-I was presumed to be catalyzed by a specific 18-hydroxylase P450 enzyme. Since both 18-hydroxy-DOC and 18-hydroxycorticosterone are known to exist in mammals, it was put forward that there may exist one (or two) 18-hydroxylase(s) which can act on both (or either) DOC and (or) corticosterone. The report that a DOC 18-hydroxylase co-purified with $P450_{11\beta}$, led to the suspicion that $P450_{11\beta}$ could catalyze both the 11β- and 18-hydroxylations of DOC. This was confirmed when the pairs (or sometimes more than two) of cDNAs (from different species) for $P450_{11\beta}$ were expressed in COS cells and were found to have both of these activities. In most species, only one of these cDNA clones (from the same source) was found capable of making aldosterone. These results have led to the conclusion that there exist two similar enzymes in the adrenal cortex which can both synthesize corticosterone ($P450_{11\beta}$), with only one of them capable of making aldosterone ($P450_{aldo}$). The fact that all known bovine [175] and porcine [176] $P450_{11\beta}$ enzymes can also make aldosterone suggests that in some species, $P450_{11\beta}$ and $P450_{aldo}$ have distinguishable catalytic properties only in intact mitochondria.

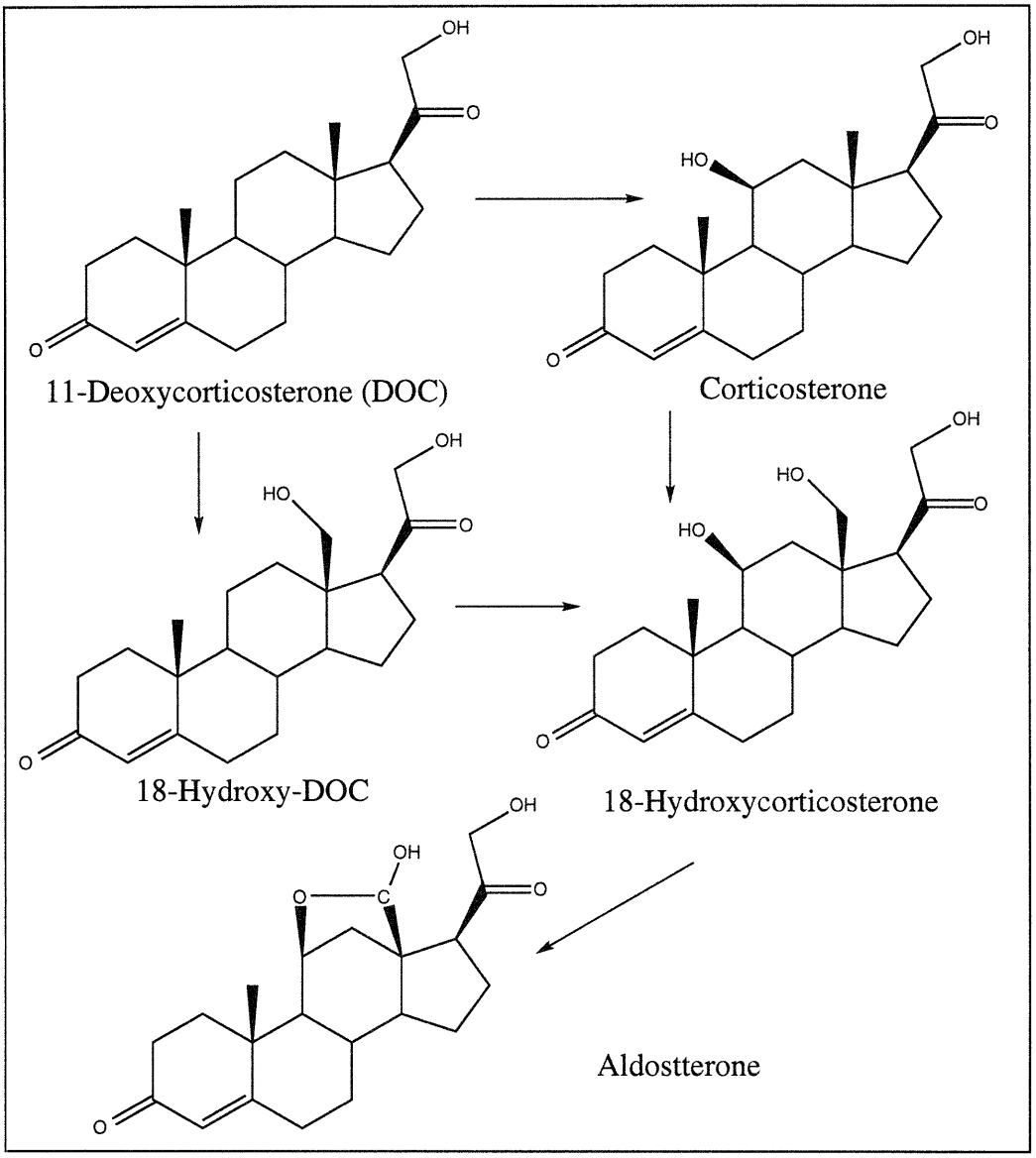

Figure 1.13: Two pathways from 11-deoxycorticosterone (DOC) to aldosterone, catalyzed by $P450_{aldo}$. The preferred path appears to be that which goes through corticosterone first.

Examination of the primary sequence for $P450_{11\beta}$ and $P450_{aldo}$ reveals a homology of 93% in humans [177], 86% in mouse [178], and 88% in rats [179]. Although, there are clearly separate genes for $P450_{11\beta}$ and $P450_{aldo}$, the only two different $P450_{11\beta}$ cDNA clones isolated from bovine are both able to synthesize aldosterone from deoxycorticosterone. Calf fasciculata primary cell cultures (unlike their glomerular counterparts) are unable to synthesize aldosterone; however, when

incubated in the presence of the certain additives (the antioxidants butylated hydroxyanisol and selenous acid, the radioprotectant DMSO, and the P450 inhibitor metyrapone), these cells acquire the ability to produce aldosterone [95]. In intact bovine and porcine adrenocortical mitochondria, only those from the *glomerulosa* can make aldosterone; however, upon solubilization (with the detergent cholate), mitochondria from all adrenocortical zones were able to make aldosterone to the same extent [180]. Two different $P450_{11\beta}$ proteins (48.5 kdal and 49.5 kdal) have been shown to exist in bovine adrenal cortex - both of which, when purified, can make aldosterone [175]. In the porcine case, only one protein has yet been purified (46 kdal) which was shown to be able to make aldosterone [176]. This 'liberation' of aldosterone synthase activity, from $P450_{11\beta}$, however, is not seen in the purified human [181], rat [182, 183] or mouse [178] versions. So far two different cDNAs for bovine $P450_{11\beta}$ have been cloned and expressed in COS cells - both of which have shown aldosterone synthase activity [95]; however, one produces aldosterone more effectively than the other [184]. Since two separate $P450_{aldo}$ enzymes have been characterized - with no limited $P450_{11\beta}$ (i.e. incapable of making aldosterone) yet identified - it seems reasonable to assert that there exists some *in vivo* inhibition of either or both of the two known $P450_{11\beta}$ proteins in bovine (and porcine [173]) mitochondria. This inhibition may arise by way of allosteric modification of one of the components in the P450 reaction (the P450, adrenodoxin, or adrenodoxin reductase) or in the controlled availability of reducing equivalents.

1.5.2. How $P450_{11\beta}$ and $P450_{aldo}$ Proteins are Regulated

1.5.2.1. Hormonal Regulation

ACTH's mechanism of control of $P450_{11\beta}$ is the same as that described earlier for its control of all of adrenocortical steroidogenesis (see section **1.4.2.1.1**). Since cortisol is the major physiological downregulator for pituitary secretion of ACTH [2], it is clear that ACTH's major goal is to stimulate cortisol production. Although the ACTH-regulated $P450_{11\beta}$ produces corticosterone, the additional transformations

required to make aldosterone (catalyzed by $P450_{aldo}$) are regulated by angiotensin II (A-II). Therefore, of the two human chromosomal genes CYP11B1 and CYP11B2 (coding for $P450_{11\beta}$ and $P450_{aldo}$, respectively), the first is under the control of ACTH-dependent events and the latter is regulated by the effects of A-II [173].

The major physiological function of cortisol and corticosterone is to regulate sugar metabolism in the body; aldosterone serves the function of controlling blood pressure. However, both cortisol and aldosterone effectively bind to the mineralocorticoid receptor [185]. This is resolved by the fact that cortisol may be transformed into cortisone, by 11β-hydroxysteroid dehydrogenase, which has very little affinity for this receptor [185]. Regulation towards hypertension can therefore manifest itself in the control of 11β-hydroxysteroid dehydrogenase [186].

1.5.2.2. Possible Regulation By Interaction with Other Proteins

1.5.2.2.1. Interaction with $P450_{scc}$

Since $P450_{scc}$ and $P450_{11\beta}$ levels, in adrenocortical mitochondria, are roughly the same [187], their ability to regulate each other through direct interaction has been studied. In liposomal studies performed on bovine $P450_{11\beta}$ and $P450_{scc}$, Ikusiro *et al.* [188] reported that these proteins form a 1:1 complex. $P450_{scc}$ was found to stimulate the 11β-hydroxylase and 18-hydroxylase activities of $P450_{11\beta}$, but suppressed the production of 18-hydroxycorticosterone and aldosterone [188]. In addition, when anti-$P450_{scc}$ IgG was added to bovine adrenocortical inner mitochondrial membranes from the *zonae reticularis-fasciculata*, it was found to stimulate the production of aldosterone [188]. However, no increase in aldosterone synthesis was found when mitochondria from the *zona glomerulosa* was treated in the same way [188]. Interestingly, $P450_{11\beta}$ was also found to stimulate the side chain cleavage activity of $P450_{scc}$ [188]. Further evidence toward an allosteric effect of $P450_{scc}$ on $P450_{11\beta}$ has been provided by Kominami *et al.* who reported that the binding of corticosterone for liposomal $P450_{11\beta}$ was much lower when $P450_{scc}$ was also present [36].

1.5.2.2.2 Interaction With Adrenodoxin

Since both $P450_{scc}$ and $P450_{11\beta}$ require adrenodoxin to deliver their reducing equivalents, there would seem to be a natural competition for this protein. It has been shown that reduced Adx has a roughly three-fold greater preference for $P450_{scc}$ than for $P450_{11\beta}$ [187]. A decreased access to reduced adrenodoxin would definitely decrease the total activity of $P450_{11\beta}$. The lower effective concentration of reduced adrenodoxin may also affect the type of reactions catalyzed by $P450_{11\beta}$ in the same way that the level of P450 reductase affects the ratio of lyase to 17α-hydroxylase activities of $P450_{c17}$. It would be beneficial to examine the proportion of different products formed, based on different concentrations of reduced adrenodoxin; such a study (to the best of the author's knowledge) has not yet been performed.

1.5.2.2.3. Interaction With Other Proteins Or Small Molecules

As mentioned in section **1.4.2.1.2**, one of the effects of angiotensin II stimulation of aldosterone synthesis involves some action by Ca^{2+} ions. Apart from a direct role of Ca^{2+} on $P450_{11\beta}$, Ca^{2+} may also bind to other proteins which may then directly interact with $P450_{11\beta}$. A Ca^{2+}-dependent role for calmodulin has been suggested for the control of $P450_{11\beta}$ [189]. Ohnishi *et al.* have reported that bovine adrenocortical calmodulin (in the presence of Ca^{2+}) - when added to $P450_{11\beta}$-reconstituted systems - increases the rate of production of 18-hydroxycorticosterone but decreases the rate of aldosterone synthesis [189]. This interaction was found to be separate from that of adrenodoxin with $P450_{11\beta}$ [189].

Cytochrome c reductase may also play a role in favoring aldosterone formation. Cytochrome c reductase (found between the inner and outer membranes) is much more active in bovine adrenocortical mitochondria from the *glomerulosa* than from the fasciculata [134]. It is plausible that the extra reduced cytochrome c reductase (in addition to its normal function of reducing cytochrome

c) may be able to effect a reduction of $P450_{11\beta}$ from the intermembrane space side of the inner mitochondrion; alternatively, it could reduce yet another species which may somehow deliver reducing equivalents to $P450_{11\beta}$.

Ascorbate appears to play a role in the function of $P450_{11\beta}$ and $P450_{aldo}$. P450 enzymes are known to produce both superoxide and hydrogen peroxide when electron transfer and substrate oxidation become uncoupled - either through a mutation [12] or when catalytically stimulated with a pseudosubstrate [190] (which may even be a product of one of its reactions [27]). This uncoupling (or electron leakage) is also found to occur in the normal course of action of endogenous P450 enzymes. Rapoport *et al.* reported that corticosterone stimulated this electron leakage in $P450_{11\beta}$, whereas pregnenolone had no such added effect for $P450_{scc}$ [191]. A protective role of ascorbate for $P450_{11\beta}$, in pseudosubstrate-mediated loss of activity, was reported by Hornsby *et al.* in studies on cultured bovine adrenocortical cells [137]. The concentration of semidehydroascorbate reductase (the enzyme which restores the semi-reduced form of ascorbate to its fully reduced form) is present in bovine adrenocortical *glomerular* mitochondria at more than twice the levels of mitochondria from the *fasciculata* [135]. This fact, along with their demonstration that added ascorbate and NADH stimulate aldosterone synthesis, led Yanagibashi *et al.* to propose that ascorbate may provide a source of reducing equivalents, specific for aldosterone formation [135].

1.5.2.3. Interaction With Lipids

Since the bulk of the $P450_{11\beta}$ and $P450_{aldo}$ proteins are associated with membrane, it is not surprising that the composition of this environment also affects the properties of these proteins. The ratio of the production of aldosterone over the production of 18-hydroxycorticosterone (by purified bovine $P450_{11\beta}$) increases from 0.2 to 0.5 when neutral lipids are added to the reconstituted system [192]. The amount of both of these steroids increased (7-fold for aldosterone and 3-fold for 18-hydroxycorticosterone) when these neutral lipids were added [192].

$P450_{11\beta}$ appears to have a preference for phospholipids containing fatty acids which contain no double bonds [34]. The use of phospholipids with unsaturated fatty acids causes a significant decrease in V_{max}, but only a moderate increase in K_m [34]. Inhibition by cardiolipin, however, results in significant changes in V_{max} (decrease) and K_m for deoxycorticosterone (increase) [34].

1.5.3. Additional Products made by $P450_{11\beta}$ and $P450_{aldo}$

Apart from the glucocorticoids cortisol and corticosterone and the mineralocorticoid aldosterone, $P450_{11\beta}$ and $P450_{aldo}$ are able to make other steroids of unknown physiological value. As already mentioned, $P450_{11\beta}$ and $P450_{aldo}$ can synthesize 18-hydroxy-DOC. This steroid could be of value as intermediate in aldosterone synthesis. The fact that 18-hydroxy-DOC is found sequestered in the cell membrane of the *zona glomerulosa* supports the claim that its major role is one of an intermediate [193, 194]. In the case of 18-hydroxycorticosterone, it may also simply serve as an intermediate in aldosterone formation. However, it has also been reported that 18-hydroxycorticosterone may spontaneously and reversibly convert into less polar forms and derivatives, some of which appear to promote hydrogen transport in renal tubuli [195].

Apart from arguable intermediates in aldosterone formation, $P450_{11\beta}$ and $P450_{aldo}$ have also been either implicated or directly shown to be capable of making steroids of still unknown function. Additional reported $P450_{11\beta}$-derived steroids are: 6β-hydroxy-DOC [196], the $\Delta^{6\text{-}7}$ version of androstenedione [196], 18-hydroxycortisol [197], 18-oxocortisol [197], cortisone [198], 19-oxoandrostenedione [198], 18,19-dihydroxycorticosterone [199], 19-hydroxy-DOC [184, 200], 19-hydroxycorticosterone [201], 18,19-dihydroxy-DOC, 11β-hydroxyandrostenedione [202], 19-hydroxyandrostenedione [202], 19-norandrostenedione [203], 11β-hydroxy-19-norandrostenedione [204], 18-hydroxy-19-norandrostenedione [204], 6β-hydroxynorandrostenedione [204], and estrone [203, 205, 206].

1.5.3.1. $P450_{11\beta}$-Catalyzed oxidations at C-6

Mochizuki *et al.* [196] reported that $P450_{11\beta}$ is capable of: transforming DOC to 6β-hydroxy-DOC and performing 6-desaturase activity on androstenedione. However, this report gives no description of the purity of their enzyme. If $P450_{11\beta}$ was in fact responsible for these reactions, then it may imply another mode of substrate binding in the active site of this enzyme.

1.5.3.2. $P450_{aldo}$-Catalyzed Formation of 18-Hydroxycortisol and 18-Oxocortisol

Calf adrenocortical preparations from the *zona glomerulosa* were used to show the formation of 18-hydroxycortisol and 18-oxocortisol [197]. Their formation was (competitively) inhibited by metyrapone [197] (a relatively specific inhibitor for $P450_{11\beta}$ [190, 207]). Corticosterone inhibited cortisol to 18-hydroxycortisol and 18-oxocortisol transformations with a K_i very close to the K_m for corticosterone in aldosterone formation [197]. From this, the authors conclude that the same enzyme which makes aldosterone is also making both 18-hydroxycortisol and 18-oxocortisol [197]. In studying the regulation of 18-oxocortisol production in normal human indivi-duals, it was found to be differentially regulated by either or both the ACTH and renin-angiotensin system, depending on the individual [208]. In another study on normal individuals, Yamakita *et al.* reported that 18-hydroxycortisol and 18-oxocortisol production is more dependent on ACTH regulation and less on the renin-angiotensin system than aldosterone production [209]. In studying the formation of 18-hydroxycortisol in rats, it was found that it could be made from either 11-deoxycortisol or cortisol in the *glomerulosa,* but could only be made from 11-deoxycortisol (and not cortisol) in the *fasciculata-reticularis* [210]. These results are informative about the possible different modes of cortisol binding in rat $P450_{11\beta}$ and $P450_{aldo}$. Since the $P450_{11\beta}$- (in the inner zones) catalyzed reaction must have proceeded by first forming 18-hydoxy-11-deoxycortisol, this means either that this inter-mediate can bind more favorably than cortisol or that once cortisol is formed,

the enzyme is incapable of hydroxylating the C-18 position. $P450_{aldo}$ (in the *glomerulosa*), however, seems to be able to both bind cortisol and catalyze its 18-hydroxylation.

Although 18-hydroxycortisol is found in patients with primary aldosteronism, it has very little effectiveness as either a glucocorticoid or mineralocorticoid [211]. Even though 18-oxocortisol is found in some patients with glucocorticoid-suppressible aldosteronism [212], it has also been shown to be poor as either a glucocorticoid or mineralocorticoid [213].

1.5.3.3. $P450_{11\beta}$-Catalyzed Hydroxysteroid Dehydrogenase Activity

The ability of $P450_{11\beta}$ to make cortisone form cortisol and 19-oxoandrostenedione from 19-hydroxyandrostenedione assigns it a hydroxysteroid dehydrogenase activity [198]. Such an activity can be accounted for by a direct oxidation of hydroxy oxygen of the substrate or as the formation of a gem diol which spontaneously dehydrates to the carbonyl. The gem diol intermediate is believable in a 19-oxidase activity, but not as easily acceptable for an 11-oxidase activity. Presumably, β-hydroxylation at the C-11 position (by $P450_{11\beta}$) occurs because the heme is positioned on the β face (see **Figure 1.18**) of the steroid. In order to perform a second hydroxylation at this position, the 11β-hydroxysteroid would either have to epimerize at the C-11 position or bind in a completely different fashion. It therefore, seems more reasonable that $P450_{11\beta}$ is capable of directly oxidizing an 11β-steroidal-hydroxyl group. While the physiological role of 19-oxygenated steroids is unknown, the ability to make cortisone would enable $P450_{11\beta}$ to reduce the levels of cortisol in the body. Since cortisol (unlike cortisone) can also bind to the mineralocorticoid receptor [185], this would implicate some role for $P450_{11\beta}$ in the lowering of blood pressure.

1.5.3.4. $P450_{11\beta}$-Catalyzed 19-Hydroxylation

19-Hydroxylation of various steroids [184, 199-201] should not be surprising since the C-11 position is very close in space to the C-18 and C-19 positions. Since purified bovine $P450_{11\beta}$ has been shown to hydroxylate DOC to both corticosterone and 18-hydroxy-DOC with a ratio of 6:1 [202], it appears that the heme center is positioned closer to the C-11 carbon, when DOC is bound. This positioning of the heme relative to substrate may: (1) change when different steroids are bound, (2) be different in individual isozymes of $P450_{11\beta}$, or (3) alter, if the protein is induced into a certain conformation. The effect of different steroids in seen between the facility by which $P450_{11\beta}$ performs a 19-hydroxylation on androstenedione versus DOC. One fourth of the $P450_{11\beta}$ hydroxylations on androstenedione occur at C-19 [202], whereas approximately two percent of $P450_{11\beta}$ hydroxylations of DOC occur at the C-19 locus [200]. In terms of differences in isozymes, it was shown by Nonaka *et al.* that although rat $P450_{11\beta}$ could occasionally transform DOC into 19-hydroxy-DOC, no detectable 19-hydroxy-DOC was found when using rat $P450_{aldo}$ [200]. Additionally, it is known that corticosterone and 19-hydroxycorticosterone are produced in nearly equal amounts in gerbils [201]. On studies using solubilized gerbil adrenal mitochondria, Drummond *et al.* showed that 19-hydroxycorticosterone formation was inhibited by a polyclonal antibody against bovine $P450_{11\beta}$ and by metyrapone [201]; in addition, they found that application of these inhibiting agents caused a parallel decline in both 11β- and 19-hydroxylations. The possibility of induced conformational changes in $P450_{11\beta}$, which may cause a change in product distribution, remains to be demonstrated but is plausible - considering the ability of some (still undetermined) component of bovine fasciculata mitochondria which inhibits aldosterone formation [173].

1.5.3.5. $P450_{11\beta}$-Catalyzed 10-Demethylase and Aromatase Activity

$P450_{11\beta}$'s demonstrated 10-demethylase (in the formation of 19-norandrostenedione [203]) and aromatase (in the formation of estrone [203, 205, 206]) demonstrates still more catalytic versatility. $P450_{11\beta}$ can form either 19-norandrostenedione [203] or estrone [203, 205, 206] from 19-oxoandrostenedione. The formation of a 19-nor steroid could arise from the spontaneous (or perhaps enzyme-assisted) activities decarboxylation of the C-19 carboxylic acid, which is a vinylogous β-keto acid. Estrone formation could result from a Baeyer-Villiger type of oxidation as described in **Figure 1.7**. If the mechanism of **Figure 1.7** is operative in $P450_{11\beta}$-catalyzed estrone formation, it would imply that this enzyme may be capable of stabilizing an iron-peroxy oxidizing species in its catalytic cycle. The existence of this rarely considered species may play some role in the differentiation of $P450_{11\beta}$ and $P450_{aldo}$ activities.

1.5.4. Inhibitors of $P450_{11\beta}$ and $P450_{aldo}$

1.5.4.1. Reversible Inhibitors

Reversible binding to P450 proteins is loosely grouped into two categories - those that cause a type-I or a type II spectral shift. A type-I shift is normally caused by a substrate (but could also be effected by inhibitors), which favors a recruitment of the resting state ferric heme protein to the electronic high spin state. Conversely, a type-II binder is named for causing a shift toward the low spin state. In general, a type-II spectral shift is indicative of an amino ligation to the ferric heme.

The most successful example of a reversible (type-II) inhibitor for $P450_{11\beta}$ and $P450_{aldo}$ is the compound metyrapone (see **Figure 1.14**). Although metyrapone shows some degree of binding to most P450 enzymes, it has a particularly strong affinity for $P450_{11\beta}$ and $P450_{aldo}$. This preference for metyrapone is often used to selectively suppress the activity (or cause a spectral change [207]) of $P450_{11\beta}$ [201, 214], when present in the same mixture as $P450_{scc}$; it exhibits a K_i in the range of 0.1-0.2 μM for $P450_{11\beta}$-catalyzed reactions, whereas its K_i for $P450_{scc}$ is 160 μM [202]. With the

goal of determining what factors make this simple compound an effective $P450_{11\beta}$ inhibitor, Tobes *et al.* reported the inhibition properties of different metyrapone analogs toward $P450_{11\beta}$ and $P450_{scc}$ [215]. These analogs each had the same structural skeleton, but substituted a phenyl ring for one of either or both of the metyrapone pyridyl rings. The result was that there is an absolute requirement for the B-pyridyl ring, and less need for the A-pyridyl ring, in the inhibition of both $P450_{11\beta}$ and $P450_{scc}$ [215]; for all of these analogs, inhibition was also greatest toward $P450_{11\beta}$.

Aminoglutethimide (see **Figure 1.14**), although displaying some degree of inhibition for $P450_{11\beta}$, has a stronger affinity towards $P450_{scc}$ [216]. This offers the reverse effects of metyrapone, when studying a two-component system of $P450_{scc}$ and $P450_{11\beta}$.

Imidazole-containing compounds have also been successful $P450_{11\beta}$ inhibitors. Ketoconazole, clotrimazole, and micoanzole (normally agents used to treat fungal infections) and etomidate (an anesthetic) (see **Figure 1.14**) are known to inhibit $P450_{11\beta}$ [216-220]. Inhibition by the anti-fungal agents affects P450 enzymes of all pathways [216]. However etomidate appears to be more specific - inhibiting $P450_{11\beta}$ and $P450_{scc}$ effectively, while not affecting $P450_{C21}$ [216]. Like metyrapone, it has a stronger preference for $P450_{11\beta}$, over $P450_{scc}$ [218].

Spironolactone (an aldosterone antagonist for the mineralocorticoid receptor) is also known to bind to $P450_{11\beta}$, albeit at high levels [216]. $P450_{11\beta}$ is even capable of hydroxylating spironolactone at the β-position of C-11 [221], leaving the enzyme unharmed.

1.5.4.2. Mechanism-Based Inhibitors

At present, there are no fully characterized mechanism-based inhibitors for $P450_{11\beta}$. There have only been reports of compounds which exhibit adrenocortical cytotoxic activities, once activated by $P450_{11\beta}$. Examples of these are 7-hydroxymethyl-12-methylbenz(a)anthracene [190], 7,12-dimethylbenz(a)anthracene

[190], 3-methylsulphonyl-2,2-bis (4-chlorophenyl)-1,1-dichloroethene [214], and 18-ethynyl-deoxycorticosterone (18-E-DOC) [222] (see **Figure 1.14**). The first two are claimed to act as pseudosubstrates for $P450_{11\beta}$ - causing the enzyme to produce peroxides and superoxide [190], which are known to destroy P450 enzymes. The third compound was reported to irreversibly bind within adrenal mitochondria; this permanent binding was inhibited by the inhibitor metyrapone, implicating $P450_{11\beta}$ as the activating species [214]. It is not certain whether 18-E-DOC requires activation or not, for its inhibition of aldosterone formation. In studies performed on calf adrenal *zona glomerulosa* cells, it was found that pre-incubation of the cells with 18-E-DOC (followed by washing for 5 minutes) caused a 75% inhibition of aldosterone formation [222]. After 24 hours of washing, 50% of aldosterone synthesis capabilities returned [222]. Even lacking information on the any required activation of 18-E-DOC, it seems likely that it might indeed be a mechanism-based inhibitor. Its structure is reminiscent of the steroid, 19-acetylenic androstenedione which is known to be a mechanism-based inhibitor for $P450_{arom}$. Future studies are required to bear this out.

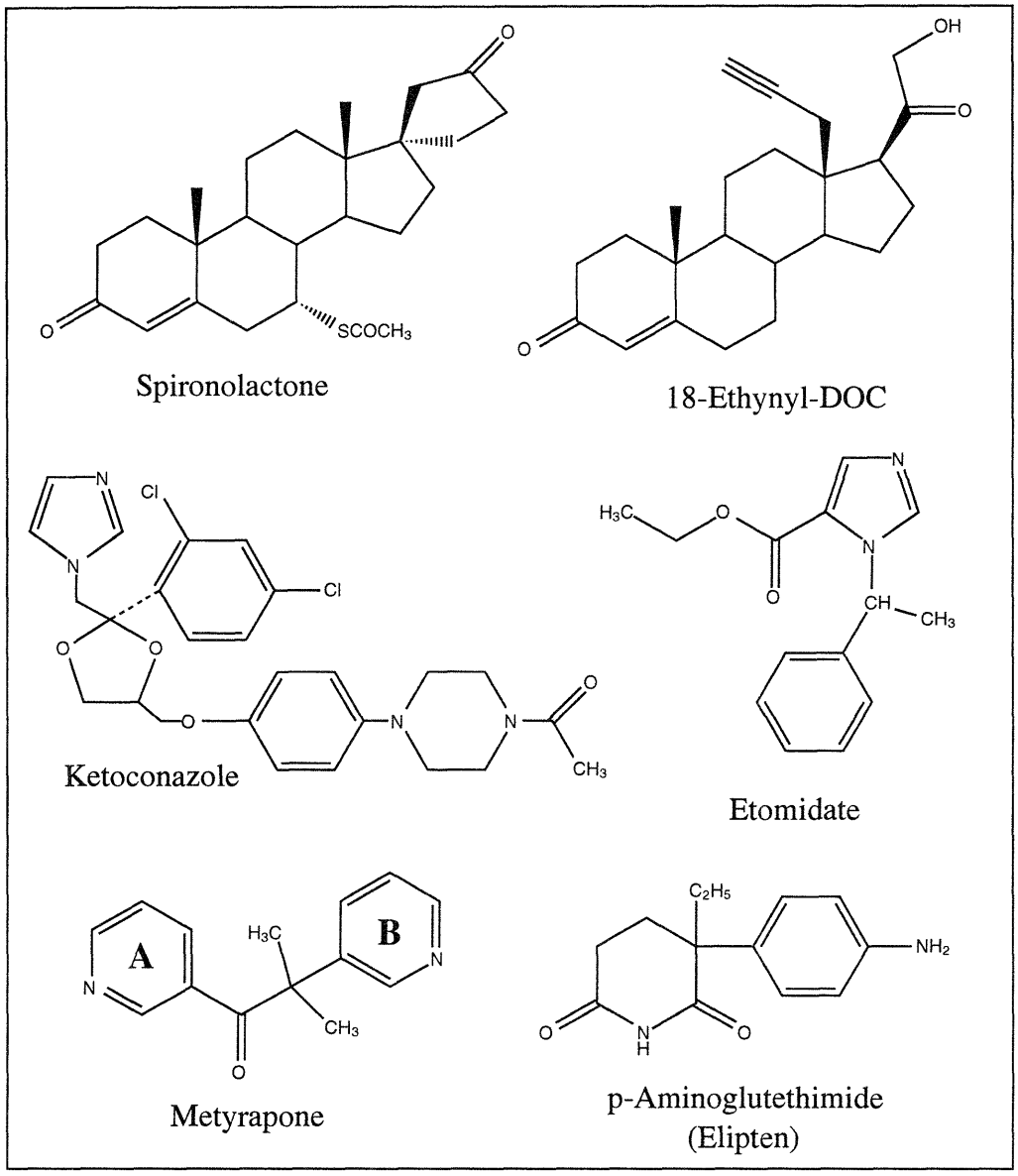

Figure 1.14: Examples of a few $P450_{11\beta}$ inhibitors.

1.5.5. $P450_{11\beta}$ Chemical Mechanism

1.5.5.1. The Identification of Intermediates

Ordinarily metabolic pathways involve the sequential production of intermediates. This is not the case in the production of aldosterone, which can be made by two pathways (**Figure 1.13**) [61]. A dual pathway is also seen in the production of 17α-hydroxyprogesterone (see **Figure 1.15**) [223].

The two routes to 17α-Hydroxyprogesterone are made possible due to the versatility of both 3β-hydroxysteroid dehydrogenase/isomerase (3βHSD) and $P450_{c17}$.

3βHSD can act on either pregnenolone or 17α-hydroxypregnenolone and $P450_{c17}$ can perform a 17α-hydroxylation on either pregnenolone or progesterone [223].

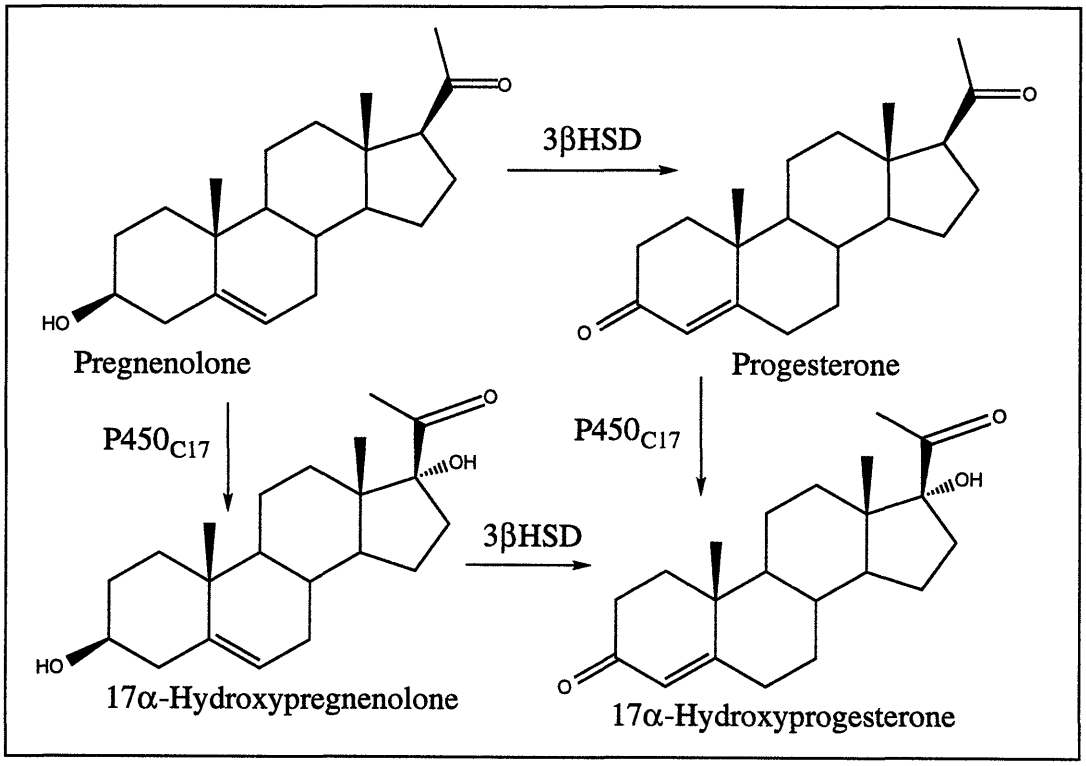

Figure 1.15: Two pathways to get from pregnenolone to 17α-hydroxyprogesterone. 17α-hydroxyprogesterone can then be directed into the synthesis of the sex steroids or into 11-deoxycortisol (see **Figure 1.1**).

Although the production of aldosterone from DOC has been found possible by a single $P450_{aldo}$, there appears be two valid sequences of events that can occur (see **Figure 1.13**). $P450_{aldo}$ can make aldosterone from either DOC, corticosterone, 18-hydroxy-DOC, or 18-hydroxycorticosterone. The acceptance of all of these substrates is consistent with the production of a common intermediate. Since 18-hydroxycorticosterone is also made by $P450_{aldo}$ [224], this would appear to be that intermediate. However, when the cDNA for $P450_{aldo}$ was expressed in COS-7 cells, it was found that administration of 18-hydroxy-DOC or 18-hydroxycorticosterone could not form aldosterone [200]; these same cells, however, could make aldosterone from either DOC or corticosterone [200]. The immediate suspicion that administration of 18-hydroxyDOC and 18-hydroxycorticosterone may not have been able to cross the membrane of these cells is seemingly resolved by the fact that the same report was able to detect outward diffusion of both of these steroid intermediates when DOC and corticosterone (respectively) were used as substrates [200]. However, Lantos *et al.* report that 18-hydroxycorticosterone exists in many forms in solution, some of which are less polar than others [195] (see **Figure 1.16**). If $P450_{11\beta}$ forms 18-hydroxycorticosterone in a relatively non-polar form, it may diffuse across the membrane and spontaneously (or as a result of the extraction process) transform into a more polar and less membrane-diffusible form. These forms are found to be rapidly interconvertible at low pH [195]. If the immediate vicinity of the cytosolic side of the inner mitochondrial membrane is substantially acidic (as it perhaps should be, due to the Mitchel chemi-osmotic hypothesis), then the $P450_{11\beta}$ enzyme may be able to utilize a preferred version of 18-hydroxycorticosterone, from this pool of interconverting species. Alternatively, $P450_{11\beta}$ may directly produce a single form of 18-hydroxycorticosterone; it may only be when examining these steroids (after extraction from the reconstituted mixture) that the analytical methods recruit this steroid to a form different from than in the native mitochondria (or even from that diffused out from the cell. Such a scenario would make 18-hydroxycorticosterone appear as a false intermediate in the synthesis of aldosterone in rats.

Another explanation for the rat data may be that $P450_{aldo}$ prefers to make aldosterone from DOC, without releasing any intermediates [224]. This situation is reminiscent of $P450_{scc}$ which is known to make pregnenolone from cholesterol via two tightly held intermediates 22(*R*)-hydroxycholesterol and 20(*R*),22(*R*)-dihydroxycholesterol. However, as was found for $P450_{scc}$, these intermediates have much lower dissociation constants for the enzyme than does cholesterol [225]. This does not appear to be the case for bovine $P450_{aldo}$ [224].

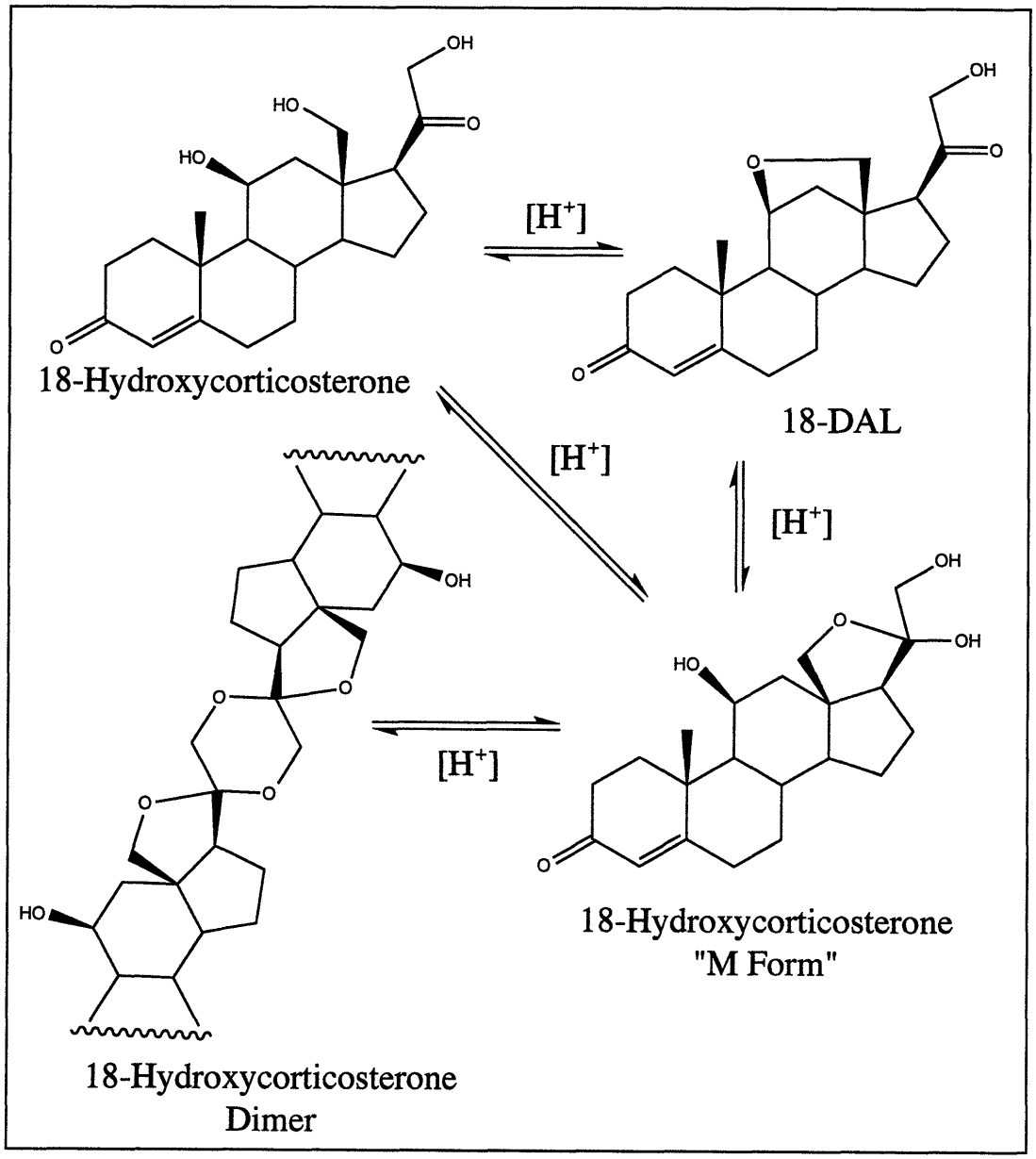

Figure 1.16: Different possible forms of '18-hydroxycorticosterone', known to interconvert under acid conditions [195]. 18-DAL stands for 21-hydroxy-11β,18-oxido-4-prenene-3,20-dione [195].

Ikushiro *et al.* reported that when bovine $P450_{aldo}$ is reconstituted into liposomes, it was found to produce aldosterone (from DOC) with very little release of the intermediates corticosterone, 18-hydroxy-DOC, and 18-hydroxycorticosterone [224]. These intermediates were also found to be poorer substrates than DOC [224]; the rates of aldosterone formation from corticosterone and 18-hydroxycorticosterone were 70% and 30% (respectively) of the rate measured when DOC itself was used [224]. In addition, when radioactive DOC was added to the liposomal $P450_{aldo}$, the addition of non-radioactive corticosterone, 18-DOC, and 18-hydroxycorticosterone did not significantly dilute out the radioactivity from the produced aldosterone [224].

From the rat data along with the experiments done on bovine liposomal $P450_{aldo}$, the validity of (at least) 18-hydroxycorticosterone, as an intermediate, is in question.

The identity of a key intermediate in aldosterone biosynthesis appears to have been determined by Lantos *et al.* [195]. Having discovered that 18-hydroxycorticosterone is able to interconvert into different forms (see Figure 1.16), they measured the rate of aldosterone synthesis with different forms of this steroid. They eventually found that the steroid 18-DAL (21-hydroxy-11β,18-oxido-4-pregnene-3,20-dione) was a much more favorable substrate than the 11β-hydroxy,18-hydroxy form of 18-hydroxycorticosterone. From their data, they proposed the reaction sequence shown in **Figure 1.17**.

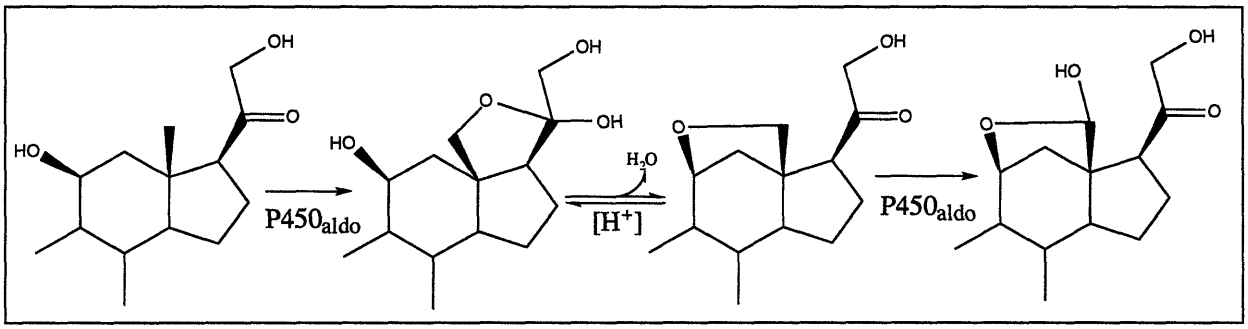

Figure 1.17: Reaction sequence from corticosterone to aldosterone. This figure was adapted from Lantos *et al.* [195].

1.5.5.2. The first oxidation by $P450_{11\beta}$ or $P450_{aldo}$

The first hydroxylation of DOC to either corticosterone or 18-hydroxy-DOC is well described by the common P450 hydroxylation mechanism depicted in **Figure 1.6**. The fact that both the 11β-hydroxylated and 18-hydroxylated versions of DOC are both made may reflect the crowded substrate β-face (see **Figure 1.18**) that $P450_{11\beta}$ must contend with. In terms of the 6:1 ratio of 11β to 18-hydroxylation of DOC, this may reflect the positioning of the heme with respect to the substrate and/or the stability of the substrate based radicals; the secondary carbon radical intermediate at C-11 would be more stable than the primary radical at C-18.

1.5.5.3. The second oxidation by $P450_{aldo}$

1.5.5.3.1. Hydroxylation at the Remaining (C-11 or C-18) Unhydroxylated Carbon

If the β-face of the steroid is indeed crowded, then a second hydroxylation could conceivably cause a space problem for the enzyme. Accommodation for a dihydroxysteroid could be one of the advantages that $P450_{aldo}$ has over $P450_{11\beta}$. If the reaction sequence described by Lantos *et al.* is at work, the newly formed 18-hydroxycorticosterone would then have to convert into 18-DAL before the last oxidation can occur. Lantos *et al.* describe this conversion as taking place on the acidic interior side of the inner mitochondrial membrane. If this area is sufficiently acidic, then it would appear to be a valid means by which 18-DAL could form. However, if we are to include the information from experiments on bovine $P450_{11\beta}$ reconstituted within liposomes (with no proton gradient), we need another means to make the putative essential 18-DAL intermediate. $P450_{aldo}$ may yet prove capable of catalyzing this conversion itself.

1.5.5.3.2 Direct Formation of 18-DAL

From this collection of facts, the following questions surface. Could 18-DAL be formed directly within the active site of $P450_{aldo}$? Can 18-DAL be made directly from either corticosterone or 18-hydroxy-DOC, without adding a second hydroxy group on an already crowded face of the steroid? **Figure 1.18**, **Figure 1.19**, and

Figure 1.20 describe how 18-DAL could be directly made from either corticosterone or 18-hydroxy-DOC.

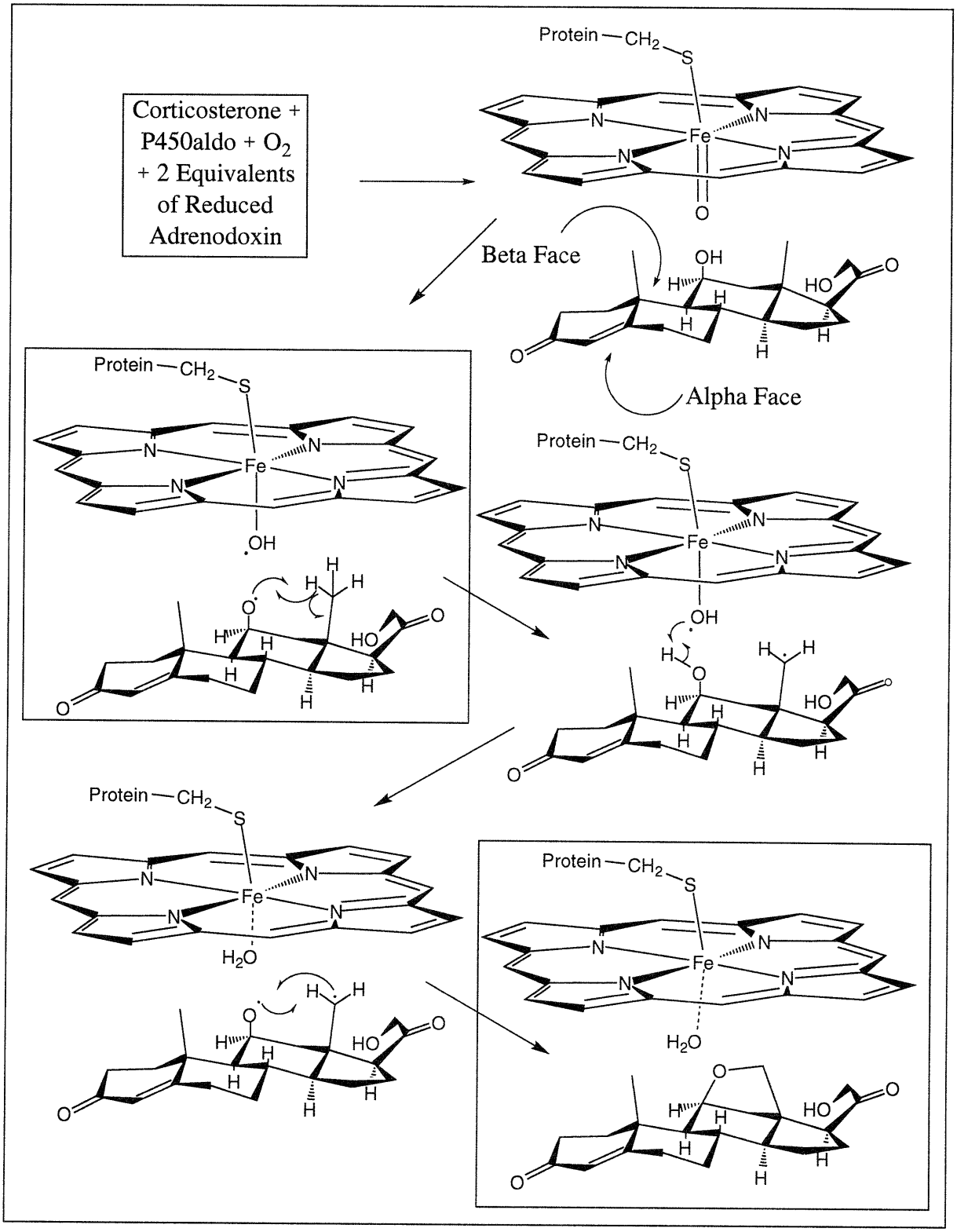

Figure 1.18: The radical-mediated formation of 18-DAL, from corticosterone.

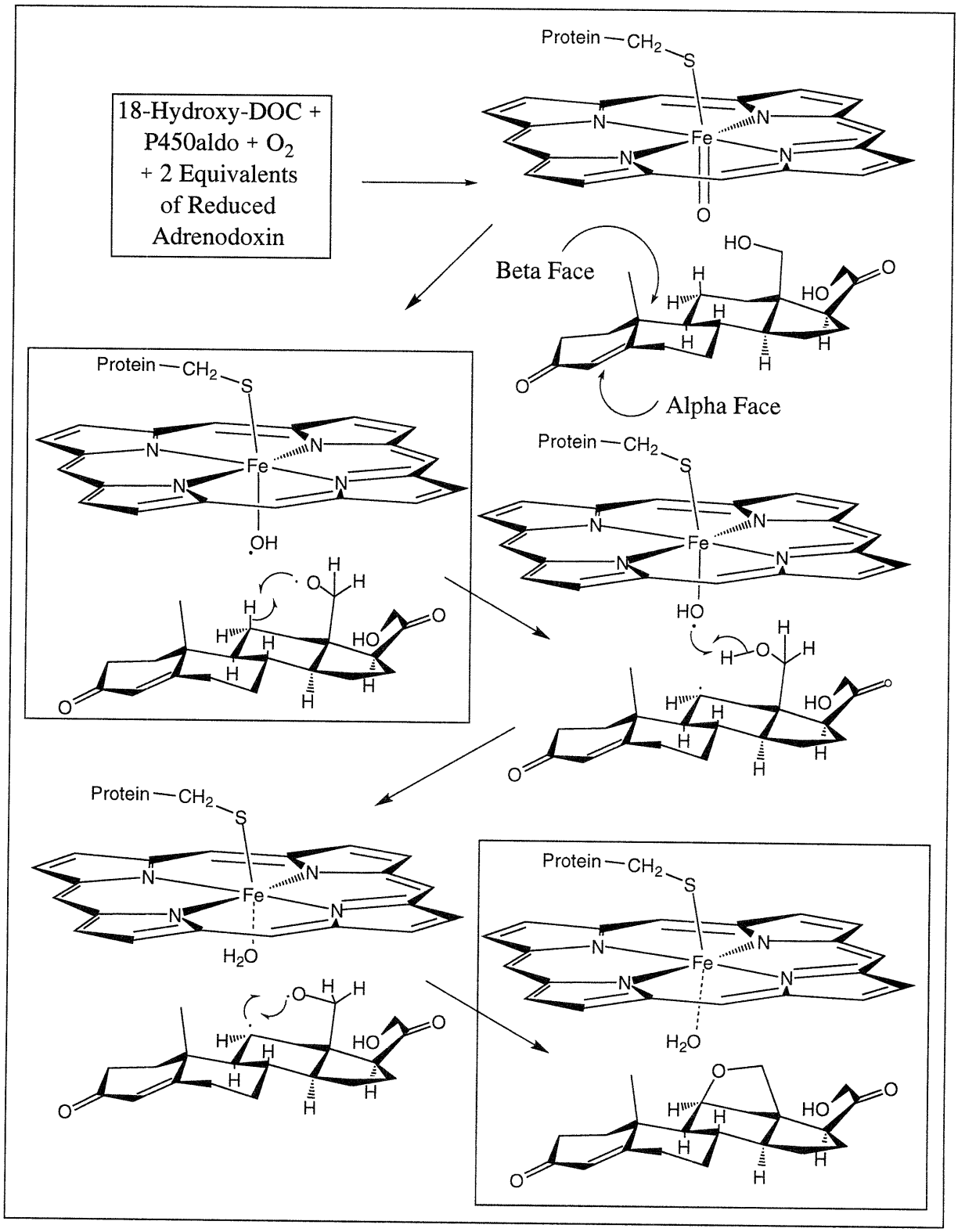

Figure 1.9: The radical-mediated formation of 18-DAL, from 18-hydroxy-DOC.

1.5.5.3.2.1. Radical-Mediated Formation of 18-DAL

The key feature in these radical-mediated direct syntheses of 18-DAL (**Figures 1.18** and **1.19**) is the initial abstraction of a hydrogen atom from a hydroxyl oxygen, by the oxenoid moiety. Although this step does not appear to have great deal of precedence in known cytochrome P450 chemistry, it is implied in some situations. In the glycol cleavage reaction of $P450_{scc}$, there has not yet been any evidence of a third hydroxylation that might initiate the C-20 to C-22 bond lysis. In fact, the two most prominent suggested mechanisms involve an initial step requiring the abstraction of a hydrogen atom from a substrate hydroxyl group [9]. In addition, $P450_{11\beta}$ was shown capable of oxidizing cortisol to cortisone, entailing the formation of carbonyl at C-11 from an 11β-hydroxy group [198]. If the oxidizing agent in this reaction involves the heme cofactor, then it seems that it could only form the gem diol if it first epimerized the 11β-hydroxy group to an 11α-hydroxyl or if the steroid would bind in an 'upside down' manner, relative to its normal mode of binding. Without these extra conditions, $P450_{11\beta}$ could only form the C-11 carbonyl by abstracting a hydrogen for the 11β-hydroxyl. Since the oxenoid moiety has proven itself as a radical initiator, it is plausible that an 11-oxidase activity could manifest itself in a homolytic fashion on $P450_{11\beta}$. Assuming this property of $P450_{11\beta}$, and knowing that $P450_{aldo}$ is highly homologous to it, the initial steps described in **Figures 1.18** and **1.19** appear reasonable.

Once we allow the possibility of having an oxygen centered radical, we now can explore what other reactions are possible beyond this point. It is well known that radical-initiated hydrogen atom migrations are readily possible when the transition state forms a six-member ring, in a chair conformation [226, 227]. In the case of corticosterone- or 18-hydroxy-DOC-derived alkoxy radicals, the rigid nature of the steroid itself, forces an almost perfect 6-member chair transition state. Therefore, the 1,5 hydrogen transfer, proposed in **Figures 1.18** and **1.19** is well precedented.

Beyond the 1,5 hydrogen transfer the mechanisms on **Figures 1.18** and **1.19** require the removal of another hydroxyl hydrogen atom. Formation of this second

alkoxy radical would conceivably lead to a rapid recombination with either the C-18 or C-11 carbon-based radical, forming 18-DAL directly from either corticosterone (see **Figure 1.18**) or 18-hydroxy-DOC (see **Figure 1.19**), respectively.

1.5.5.3.2.2. Heterolytic-Type Formation of 18-DAL

If 18-DAL is formed without leaving the active site of $P450_{11\beta}$ - and if 18-hydroxycorticosterone is not a valid intermediate - 18-DAL could conceivably be arrived at via a C-ring olefin intermediate. Two pathways for this alternative are given in **Figure 1.20**. The formation of such an intermediate would be another way of not crowding the active site. The major shortcoming to this proposed route for 18-DAL formation is that it is not accessible to the substrate 18-hydroxy-DOC. If this pathway is operative in $P450_{11\beta}$, the question which arises is where might the C-ring olefin reside? Considering a report by Sih in 1969 that 9,11-dehydrocortexolone (the $\Delta^{9\text{-}11}$ version of 11-deoxycortisol) was converted to the epoxide by $P450_{11\beta}$ [228], this argues against **path i** of **Figure 1.20**. This is due to the fact that epoxides are not known to be intermediates in aldosterone synthesis along with the assumptions that 11-deoxycortisol is known to make 18-oxocortisol (presumably by the same pathway as DOC is transformed to aldosterone). However, if the $\Delta^{9\text{-}11}$ version of corticosterone did form, it would probably result in the wash out of the C-9 hydrogen of corticosterone (see Figure 1.20) as well as the 11β-hydroxy oxygen; these could be confirmed with isotope studies.

Evidence for the existence of a $\Delta^{11\text{-}12}$ olefinic intermediate could also be found in isotope wash out experiments. Pathway **ii** of **Figure 1.20** may cause the wash out of hydrogen atoms at the C-12 position. This pathway also involves the loss of the 11β-hydroxyl oxygen of corticosterone. Turnover studies with deuterated steroid/protonated water or simply with $^{18}O_2$ would answer these questions. Such experiments would address whether or not this compound is a chemically competent intermediate in aldosterone formation.

1.5.5.4. The third oxidation by $P450_{aldo}$

Since Lantos *et al.* have shown that 18-DAL is the most probable penultimate intermediate in aldosterone formation, the final oxidation appears straightforward [195]. Once 18-DAL binds in the active site of $P450_{aldo}$, it may bind in such a way as to deliver the C-18 methylene closer to the heme. In addition, the C-18 methylene can now stabilize a radical more easily, due to the presence of oxido oxygen that it shares with C-11.

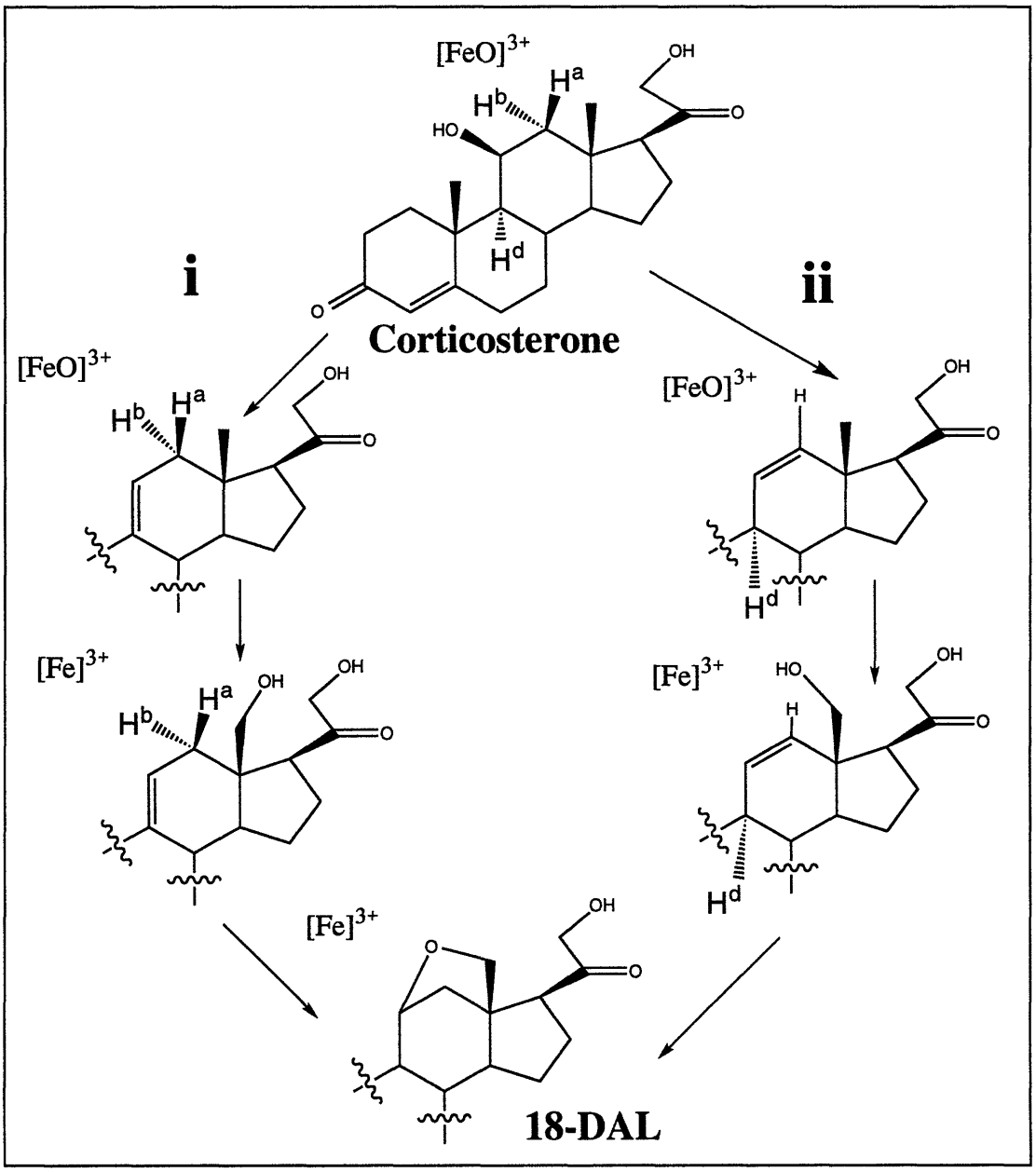

Figure 1.20: The direct formation of 18-DAL via the formation of one of either two C-ring olefins.

18-DAL may not only be a sensible chemical intermediate; it also appears to play a complementary and sometimes antagonistic role (*in vivo*), when compared to aldosterone [195]. Lantos, *et al.* point out that sodium retention by the kidneys, effected by the aldosterone signal, compromises the body's ability to get rid of acid [195]. 18-DAL, by competing with aldosterone for the mineralocorticoid receptor, may be a key hormone in regulating the loss of H^+ in the urine. When $P450_{aldo}$ converts 18-DAL into aldosterone, it not only increases the concentration of aldosterone, but it also decreases the concentration of perhaps its key competitor for the mineralocorticoid receptor. This would potentially make the last step of aldosterone a point of control (which may go wrong in some pathologies), which additional mitochondrial factors could modulate in some way. It is interesting to note that there are individuals who produce sufficient amounts of 18-hydroxycorticosterone to make aldosterone, but lack the ability to carry through the additional step to make aldosterone [229]. This suggests that the final step (hydroxylation of 18-DAL) perhaps proceeds by yet a different mechanism.

1.5.6. Known Structural Information on $P450_{11\beta}$ and $P450_{aldo}$

Compared to $P450_{scc}$, very little structural information has been reported on cytochrome $P450_{11\beta}$. This fact is linked to its instability when removed from mitochondrial membranes. It has always been easier to allow the contaminating $P450_{11\beta}$ (in $P450_{scc}$ preparations) to deactivate, leaving only one type I P450 form as the active species. Another factor involved in the relative neglect of $P450_{11\beta}$ concerns the fact that its multiple activities implied that one could not remove it from its 'contaminating activities'. The expression of cDNA clones for $P450_{11\beta}$ and $P450_{aldo}$ [178, 179, 230-232] has convinced investigators of the catalytic capabilities of this single enzyme. The increasing trend of studying mammalian P450 enzymes in liposomes may also bring needed attention back to this important enzyme.

Nevertheless, knowledge gained in the study of other P450 proteins will help us to better understand $P450_{11\beta}$. Both steroidogenesis in general and cytochrome P450 proteins in particular have common themes which can be carried over to less

explored pathways and enzymes. The availability of several crystal structures on $P450_{cam}$ [39-47, 233] as well as the structures of $P450_{terp}$ [48] and $P450_{BM3}$ [49], has enabled sequence alignment studies, associating sections of mammalian P450 proteins with well defined domains. The NMR solution structures of putidaredoxin [234-237] will presumably soon reveal the binding mode of this protein with $P450_{cam}$. This will have a direct benefit to type I P450 enzymes. Even though putidaredoxin and adrenodoxin are not interchangeable in the respective catalytic cycles of mitochondrial and bacterial type I P450 enzymes, it may still lead to generalizable modes of electron transfer between ferredoxins and cytochromes P450.

The studies on adrenodoxin and $P450_{scc}$ will also benefit $P450_{11\beta}$ research. Even though $P450_{scc}$ is the preferred acceptor of reducing equivalents from adrenodoxin [187], $P450_{11\beta}$ still gets its electrons from this electron transfer protein and may bind in similar ways.

1.5.6.1. $P450_{11\beta}$ is Mostly Membrane-Integrated

Lombardo *et al.* reported that trypsin treatment of liposome-integrated $P450_{11\beta}$ left a 34 kdal peptide component still in the membrane [109]. This membrane-bound fragment was found to still hold onto the heme [109]. Although $P450_{11\beta}$ has been shown to be capable of phosphorylation at a serine, by a cAMP-dependent protein kinase, the identity of this residue remains uncertain due to its instability while subjecting it to mild proteolytic digestion. [109].

1.5.6.2. Spectroscopic Information

In EPR [207, 238] and Resonance Raman studies [238], it was found that the low spin forms of $P450_{11\beta}$ and $P450_{scc}$ are similar, but that their high spin forms differ.

1.5.6.3. Mutations Known to Alter Activity

In mammals, $P450_{11\beta}$ is made from the transcription of a gene designated as CYP11B1, whereas $P450_{aldo}$ is a product the CYP11B2 gene. These genes have been isolated and characterized in human[231, 232], rat [200, 230], and mouse [178]. In the case of bovine, both of the isolated genes give rise to proteins with *in vitro* aldosterone synthase activity; therefore, the designation of one of these as the CYP11B2 remains undecided.

In humans these genes are 95% identical in the coding regions and give rise to proteins which are 93% identical (in terms of amino acids) [177]. There are known mutations which affect the activity of the final gene product. An arginine-448 to histidine mutation was found responsible for 11β-hydroxylase deficiency in some human subjects, with congenital adrenal hyperplasia [239]. The mutation of Val386 to Ala (in the CYP11B2 gene) causes CMO II deficiencies [240]. Unequal crossing over between the CYP11B1 and CYP11B2 genes gave to a form of glucocorticoid-suppressible hyperaldosteronism [241]. In one group of individuals, the following mutations in the CYP11B2 gave rise to these effects (compared to wild type): R181W lowered 18-hydroxylase activity and eliminated 18-oxidase activity and V386A gave rise to small but consistent reduction in 18-hydroxycorticosterone formation [174, 242]. A mutation in CYP11B1 (in yet another group), where Arg448 was changed to histidine, gave rise to a deficiency in $P450_{11\beta}$ activity [174, 243]; this mutation is believed to be in the heme binding region [243].

Mutations which might provide insight on the mechanism of $P450_{11\beta}$ and $P450_{aldo}$ have also been noted in other species. The amino acid changes Phe66 to Leu and Ser126 to Pro was found to extinguish all cortisol and aldosterone synthesis activities from bovine $P450_{11\beta}$ [244]. The cDNA sequence for $P450_{11\beta}$ from salt-resistant normotensive (DR) rats (lacking normal levels of aldosterone) possessed five amino acid changes compared to the wild type; these were Arg127 to Cys, Val351 to Ala, Val381 to Leu, Ile384 to Leu, and Val443 to Met [245]. The rate of 18-hydroxylation to 11β-hydroxylation, of DOC, was 0.58 for wild type and 0.23 for the $P450_{11\beta}$-DR-expressed COS-7 cells.

1.5.6.4. Molecular Modeling

Lacking a crystal structure of $P450_{11\beta}$, molecular modeling offers an important tool in building an emerging model for this protein. Since its reported crystal structure in 1985 [39], $P450_{cam}$ has long been the model that all other P450 proteins have been compared to. Three-dimensional models of the highly homologous herbicide-inducible bacterial proteins $P450_{SU1}$ and $P450_{SU2}$ (from *Streptomyces griseolus*) have been obtained by aligning them with the known structure of $P450_{cam}$ [246].

The known structure of $P450_{BM3}$ has also been reported to have been used in the modeling of a mammalian P450 enzyme. Ruan *et al.* generated a three-dimensional model of the human protein P450 thromboxane synthase [51]. Although information for both $P450_{cam}$ and $P450_{BM3}$ were used to obtain their derived structures, the authors mention that $P450_{BM3}$ was a more suitable template.

The less homologous, but still related, P450 enzymes from mammals have also benefited from $P450_{cam}$'s known structure. Sequence alignments among many of the sequenced mammalian P450 enzymes, with each other and with $P450_{cam}$, have been reported [55, 247-249]. Alignment of the predicted secondary structures of these mammalian P450 proteins with $P450_{cam}$ has also been done [55, 249-251]. So far this kind of study has led to complete three-dimensional predicted structures for P450 nifedipine oxidase [53], P450 debrisoquine 4-hydroxylase [54], and $P450_{scc}$ [56].

The prediction of protein structures from information gained of crystallized (and similar) proteins, however, is still an emerging technique. It is a process with many steps, with sometimes diverging choices at each stage. Braatz *et al.* have commented that their models of $P450_{SU1}$ and $P450_{SU2}$ changed depending on choices made during primary and secondary structural alignments as well as during refinement [246]. They mentioned that some regions of the active sites (of the aligned structures) are highly dependent on different choices made during energy minimization [246]. Such concerns encourage using additional spectroscopic and structural information - already known about the protein in question - to constrain the different structures that molecular modeling generates.

Since eukaryotic P450 enzymes are longer in sequence than $P450_{cam}$, alignment methods inevitably generate gaps. Some of the stretches of unhomologous amino acids have been proposed to be related to the fact that the eukaryotic P450 proteins must bind to membranes, where $P450_{cam}$ does not. However, this dual phase in which eukaryotic P450 proteins exist, is not accounted for in the modeling work reported at present.

In an effort to avoid the problems of modeling membrane P450 proteins with soluble $P450_{cam}$, Joardar constrained his modeled structures of some mammalian steroidogenic P450 enzymes ($P450_{C17}$, $P450_{C21}$, $P450_{scc}$, and $P450_{11\beta}$) to areas of the heme binding site and the presumed substrate binding site [55]. Amino acid residues in the initial $P450_{cam}$ structure were replaced with 'aligned' amino acids from the mammalian P450 protein in question; this was performed only in the ($P450_{cam}$-designated) regions of helices I and L and in the sequence connecting them. No sequence gaps were introduced. Once these substitutions were made, the mutated structures were energy minimized. For the $P450_{scc}$ structure, Joardar incorporated known distances between heme iron and substrate (acquired from EXAFS and ESEEM experiments), along with a docked substrate, before performing the final energy minimization [55]. Although complete structures of the mammalian enzymes were not obtained in this method, they introduced fewer perturbations into the pre-minimized structure and may offer more meaningful representations of the derived active site structures.

The $P450_{11\beta}$ structure, obtained by Joardar [55], would be a good place to begin in mapping out its active site. The goal of the work presented in this thesis is to add to the spectroscopically-obtained structural information on $P450_{11\beta}$. As more information obtained from mutation results, mechanistic studies, and (experimentally-obtained) structural work is incorporated into a modeled structure of $P450_{11\beta}$, we will hopefully come to be better understand this intriguing enzyme.

References

1. Vinson, G.P., Whitehouse, B., and Hinson, J., *Disorders of Adrenal Cortex II: Hypofunction and Inborn Error in Biosynthesis*, in *The Adrenal Cortex*, M.E. Hadley, Editor. 1992, Prentice Hall: Englewood Cliffs, New Jersey. p. 225-243.
2. Vinson, G.P., Whitehouse, B., and Hinson, J., *Disorders of Adrenal Cortex I: Hyperfunction*, in *The Adrenal Cortex*, M.E. Hadley, Editor. 1992, Prentice Hall: Englewood Cliffs, New Jersey. p. 196-224.
3. Davydov, R., Kapple, R., Hüttermann, J., and Peterson, J.A., *EPR-spectrocopy of reduced oxyferrous-P450$_{cam}$.* FEBS Letters, 1991. **295**: p. 113-115.
4. Kashem, M.A. and Dunford, H.B., *The formation and decay of the oxyferrous complex of beef adrenocortical cytochrome P-450scc. Rapid-scan and stopped-flow studies.* Biochem Cell Biol, 1987. **65**(5): p. 486-492.
5. Collman, J.P. and Groh, S.E., *"Mercaptan-Tail" Porphyrins: Synthetic Analogues for the Active Site of Cytochrome P-450.* Journal of the American Chemical Society, 1982. **104**: p. 1391-1403.
6. Dawson, J.H., *Probing structure-function relations in heme-containing oxygenases and peroxidases.* Science, 1988. **240**(4851): p. 433-439.
7. Liu, H.I., Sono, M., Kadkhodayan, S., Hager, L.P., Hedman, B., Hodgson, K.O., and Dawson, J.H., *X-ray Absorption Near Edge Studies of Cytochrome P450cam, chloroperoxidase, and myoglobin: Direct evidence for the electron releasing character of a cysteine thiolate proximal ligand.* Journal of Biological Chemistry, 1995. **270**(18): p. 10544-10550.
8. Guengerich, F.P. and MacDonald, T.L., *Mechanisms of cytochrome P-450 catalysis.* FASEB, 1990. **4**: p. 2453-2459.
9. Ortiz de Montellano, P., *Oxygen Activation and Transfer*, in *Cytochrome P-450: Structure and Mechanism and Biochemistry*, P. Ortiz de Montellano, Editor. 1986, Plenum Press: New York. p. 217-272.
10. Poulos, T.L. and Raag, R., *Cytochrome P450cam: crystallography, oxygen activation, and electron transfer.* Faseb J, 1992. **6**(2): p. 674-679.
11. Guengerich, F.P., *Enzymatic Oxidation of Xenobiotic Chemicals.* Crit. Rev. Biochem. Mol. Biol., 1990. **25**(2): p. 97-148.
12. Loida, P.J. and Sligar, S.G., *Molecular Recognition in Cytochrome P-450: Mechanism for the Control of Uncoupling Reactions.* Biochemistry, 1993. **32**(43): p. 11530-11538.
13. McMurry, T.J. and Groves, J.T., *Metalloporphyrin Models for Cytochrome P-450*, in *Cytochrome P-450: Structure and Mechanism and Biochemistry*, P. Ortiz de Montellano, Editor. 1986, Plenum Press: New York. p. 1-28.
14. Kobayashi, K., Iwamoto, T., and Honda, K., *Spectral intermediate in the reaction of ferrous cytochrome P450cam with superoxide anion.* Biochem Biophys Res Commun, 1994. **201**(3): p. 1348-1355.
15. Hrycay, E.G., Gustafsson, J.-A., Ingelman-Sundberg, M., and Ernster, L., *Sodium periodate, sodium chlorite, and organic hydroperoxides as hydroxylating agents in hepatic microsomal steroid hydroxylation reactions by cytochrome P-450.* FEBS Letters, 1975. **56**: p. 161-165.
16. Hrycay, E.G., Gustafsson, J., Ingelman-Sundber, M., and Ernster, L., *Sodium periodate, sodium chlorite, organic hydroperoxides, and H2O2 as hydroxylating agents in steroid hydroxylation reactions catalyzed by partially purified cytochrome P-450.* Biochem. Biophys. Res. Commun., 1975. **66**: p. 209-216.
17. Lichtenberger, F., Nastainczyk, W., and Ullrich, V., *Cytochrome P-450 as an oxene transferase.* Biochem. Biophys. Res. Commun., 1976. **70**: p. 939-946.
18. Egawa, T., Shimada, H., and Ishimura, Y., *Evidence for compound I formation in the reaction of cytochrome P450cam with m-chloroperbenzoic acid.* Biochem. Biophys. Res. Commun., 1994. **201**(3): p. 1464-1469.

19. Lippard, S.J. and Berg, J.M., *Atom- and Group-Transfer Chemistry*, in *Principles of Bioinorganic Chemistry*. 1994, University Science Books: Mill Valley, California. p. 283-347.
20. Akhtar, M., Njar, V.C.O., and Wright, J.N., *Mechanistic Studies on Aromatase and Related C-C Bond Cleaving P-450 Enzymes.* Journal of Steroid Biochemistry and Molecular Biology, 1993. **44**: p. 375-387.
21. Akhtar, M., Corina, D., Miller, S., Shydadehi, A.Z., and Wright, J.N., *Mechanism of the Acyl-Carbon Cleavage and Related Reaction Catalyzed by Multifunctional P-450s: Studies on Cytochrome P-450$_{17\alpha}$* Biochemistry, 1994. **33**: p. 4410-4418.
22. Korzekwa, K.R., Trager, W.F., Mancewicz, J., and Osawa, Y., *Studies on the Mechanism of Aromatase and Other Cytochrome P450 Mediated Deformylation Reactions.* Journal of Steroid Biochemistry and Molecular Biology, 1993. **44**: p. 367-373.
23. Fischer, R.T., Trzaskos, J.M., Magolda, R.L., Ko, S.S., Brosz, C.S., and Larsen, B., *Lanosterol 14α-Methyl Demethylase. Isolation and Characterization of the Third Metabolically Generated Oxidative Demethylation Intermediate.* J. Biol. Chem., 1991. **266**(10): p. 6124-6132.
24. Corina, D.L., Miller, S.L., Wright, J.N., and Akhtar, M., *The mechanism of cytochrome P-450 dependent C-C bond cleavage: studies on 17α-hydroxylase-17,20-lyase.* Journal of the Chemical Society Chemical Communications, 1991(11): p. 782-783.
25. Swinney, D.C. and Mak, A.Y., *Androgen Formation by Cytochrome P450 CYP17. Solvent Isotope Effect and pL Studies Suggest a Role for Protons in the Regulation of Oxene versus Peroxide Chemistry.* Biochemistry, 1994. **33**: p. 2185-2190.
26. Gettings, S.D., Brewer, C.B., Pierce, W.M., Jr., Peterson, J.A., Rodrigues, A.D., and Prough, R.A., *Enhanced decomposition of oxyferrous cytochrome P450CIA1 (P450cam) by the chemopreventive agent 3-t-butyl-4-hydroxyanisole.* Arch Biochem Biophys, 1990. **276**(2): p. 500-509.
27. Quinn, P.G. and Payne, A.H., *Steroid product-induced, oxygen-mediated damage of microsomal cytochrome P-450 enzymes in Leydig cell cultures. Relationship to desensitization.* J Biol Chem, 1985. **260**(4): p. 2092-2099.
28. Hall, P.F., *Cytochrome P-450 C$_{21scc}$: One enzyme with two actions: hydroxylase and lyase.* Journal of Steroid Biochemistry, 1991. **40**(4-6): p. 527-532.
29. Yanagibashi, K. and Hall, P.F., *Role of electron transport in the regulation of the lyase activity of C21 side-chain cleavage P-450 from porcine adrenal and testicular microsomes.* J Biol Chem, 1986. **261**(18): p. 8429-8433.
30. Sakai, Y., Yanase, T., Hara, T., Takayanagi, R., Haji, M., and Nawata, H., *Mechanism of abnormal production of adrenal androgens in patients with adrenocortical adenomas and carcinomas.* J Clin Endocrinol Metab, 1994. **78**(1): p. 36-40.
31. Shet, M.S., Fisher, C.W., Arlotto, M.P., Shackleton, C.H., Holmans, P.L., Martin-Wixtrom, C.A., Saeki, Y., and Estabrook, R.W., *Purification and enzymatic properties of a recombinant fusion protein expressed in Escherichia coli containing the domains of bovine P450 17A and rat NADPH-P450 reductase.* Arch Biochem Biophys, 1994. **311**(2): p. 402-417.
32. Goldman, D. and Yawetz, A., *The interference of aroclor 1254 with progesterone metabolism in guinea pig adrenal and testes microsomes.* J Biochem Toxicol, 1990. **5**(2): p. 99-107.
33. Tuckey, R.C. and Stevenson, P.M., *Purification and analysis of phospholipids in the inner mitochondrial membrane fraction of bovine corpus luteum, and properties of cytochrome P-450scc incorporated into vesicles prepared from these phospholipids.* Eur J Biochem, 1985. **148**(2): p. 379-384.
34. Seybert, D.W., *Lipid Regulation of Bovine Cytochrome P450$_{11\beta}$ Activity.* Archives of Biochemistry and Biophysics, 1990. **279**: p. 188-194.
35. Greenfield, N.J., Parsons, R., Welsh, M., and Gerolimatos, B., *The side-chain cleavage of cholesterol sulfate--II. The effect of phospholipids on the oxidation of the sterol sulfate by inner mitochondrial membranes and by a reconstituted cholesterol desmolase system.* Biochemistry, 1985. **24**(11): p. 2768-2772.

36. Kominami, S., Harada, D., and Takemori, S., *Regulation mechanism of the catalytic activity of bovine adrenal cytochrome P-450(11)beta.* Biochim Biophys Acta, 1994. **1192**(2): p. 234-240.
37. Sharrock, M., Debrunner, P.G., Schulz, C., Lipscomb, J.D., Marshall, V., and Gunsalus, I.C., Biochim. Biophys. Acta, 1976. **420**: p. 8-26.
38. Lange, R., Hui Bon Hoa, G., Debey, P., and Gunsalus, I.C., Eur. J. Biochem., 1977. **77**: p. 479-485.
39. Poulos, T.L., Finzel, B.C., Gunsalus, I.C., Wagner, G.C., and Kraut, J., *The 2.6-crystal structure of Pseudomonas putida cytochrome P-450.* Journal of Biological Chemistry, 1985. **260**: p. 16122-16130.
40. Poulos, T.L., Finzel, B.C., and Howard, A.J., *High-resolution crystal structure of cytochrome P450cam.* Journal of Molecular Biology, 1987. **195**: p. 687.
41. Poulos, T.L., Finzel, B.C., and Howard, A.J., *Crystal structure of substrate-free Pseudomonas putida cytochrome P-450.* Biochemistry, 1986. **25**(18): p. 5314-5322.
42. Poulos, T.L. and Howard, A.J., *Crystal structures of metyrapone- and phenylimidazole-inhibited complexes of cytochrome P-450cam.* Biochemistry, 1987. **26**(25): p. 8165-8174.
43. Raag, R. and Poulos, T.L., *The structural basis for substrate-induced changes in redox potential and spin equilibrium in cytochrome P-450CAM.* Biochemistry, 1989. **28**(2): p. 917-922.
44. Raag, R., Swanson, B.A., Poulos, T.L., and Ortiz de Montellano, P.R., *Formation, crystal structure, and rearrangement of a cytochrome P-450cam iron-phenyl complex.* Biochemistry, 1990. **29**(35): p. 8119-8126.
45. Raag, R. and Poulos, T.L., *Crystal structures of cytochrome P-450$_{CAM}$ complexed with camphane, thiocamphor, and adamantane: factors controlling P-450 substrate hydroxylation.* Biochemistry, 1991. **30**(10): p. 2674-2684.
46. Raag, R. and Poulos, T.L., *Crystal structure of the carbon monoxide-substrate-cytochrome P-450CAM ternary complex.* Biochemistry, 1989. **28**(19): p. 7586-7592.
47. Raag, R., Martinis, S.A., Sligar, S.G., and Poulos, T.L., *Crystal structure of the cytochrome P-450CAM active site mutant Thr252Ala.* Biochemistry, 1991. **30**(48): p. 11420-11429.
48. Hasemann, C.A., Ravichandran, K.G., Peterson, J.A., and Deisenhofer, J., *Crystal structure and refinement of cytochrome P450terp at 2.3 A resolution.* J Mol Biol, 1994. **236**(4): p. 1169-1185.
49. Ravichandran, K.G., Boddupalli, S.S., Haemann, C.A., Peterson, J.A., and Deisenhofer, J., *Crystal Structure of Hemoprotein Domain of P450BM-3, a Prototype for Microsomal P450's.* Science, 1993. **261**: p. 731-736.
50. Fulco, A.J., *P450BM-3 and other inducible bacterial P450 cytochromes: biochemistry and regulation.* Annu Rev Pharmacol Toxicol, 1991: p. 177-203.
51. Ruan, K.H., Milfeld, K., Kulmacz, R.J., and Wu, K.K., *Comparison of the construction of a 3-D model for human thromboxane synthase using P450cam and BM-3 as templates: implications for the substrate binding pocket.* Protein Eng, 1994. **7**(11): p. 1345-1351.
52. Buczko, E., Koh, Y.C., Miyagawa, Y., and Dufau, M.L., *The rat 17 alpha-hydroxylase-17,20-desmolase (CYP17) active site: computerized homology modeling and site directed mutagenesis.* J Steroid Biochem Mol Biol, 1995. **52**(3): p. 209-218.
53. Ferenczy, G.G. and Morris, G.M., *The active site of cytochrome P-450 nifedipine oxidase: a model-building study.* J. Mol. Graphics, 1989. **7**: p. 206-211.
54. Islam, S.A., Wolf, C.R., Lennard, M.S., and Sternberg, M.J.E., *A three-dimensional molecular template for substrates of human cytochrome P450 involved in debrisoquine 4-hydroxyaltion.* Carcinogenesis, 1991. **12**(12): p. 2211-2219.
55. Joardar, S., *Mapping the Active Sites of Steroidogenic Cytochromes P-450*, in *Chemistry.* 1993, M.I.T.: Cambridge. p. 197.
56. Vijayakumar, S. and Salerno, J.C., *Molecular modeling of the 3-D structure of cytochrome P-450scc.* Biochim Biophys Acta, 1992. **1160**(3): p. 281-286.
57. Iwamoto, Y., Tsubaki, M., Hiwatahi, A., and Ichikawa, Y., *Crystallization of cytochrome P-450$_{scc}$ from bovine adrenocortical mitochondria.* FEBS Letters, 1988. **233**(1): p. 31-36.

58. Chashchin, V.L., Vasilevsky, V.I., Shkumatov, V.M., Lapko, V.N., Adamovich, T.B., Berikbaeva, T.M., and Akhrem, A.A., *The domain structure of the cholesterol side-chain cleavage cytochrome P-450 from bovine adrenocortical mitochondria. Localization of haem group and domains in the polypeptide chain.* Biochim. Biophys. Acta, 1984. **791**: p. 375-383.
59. Jacobs, R.E., Singh, J., and Vickery, L.E., *NMR studies of cytochrome P-450$_{scc}$. Effects of steroid binding on water proton access to the active site of the ferric enzyme.* Biochem., 1987. **26**(14): p. 4541-4545.
60. Groh, S.E., Nagahisa, A., Tan, S.L., and Orme-Johnson, W.H., *Electron spin echo modulation demonstrates P-450$_{scc}$ complexation.* J. Am. Chem. Soc., 1983. **105**: p. 7445-7446.
61. Vinson, G.P., Whitehouse, B., and Hinson, J., *Nature, Biosynthesis, and Metabolism of the Adrenocortical Secretion*, in *The Adrenal Cortex*, M.E. Hadley, Editor. 1992, Prentice Hall: Englewood Cliffs, New Jersey. p. 34-64.
62. Lambeth, J.D., Seybert, D.W., Lancaster, J.R.J., Salerno, J.C., and Kamin, H., *Steroidogenic electron transport in adrenal cortex mitochondria.* Molecular and Cellular Biochemistry, 1982. **45**: p. 13-31.
63. Jefcoate, C.R., *Cytochrome P-450 Enzymes in Sterol Biosynthesis and Metabolism*, in *Cytochrome P-450: Structure and Mechanism and Biochemistry*, P. Ortiz de Montellano, Editor. 1986, Plenum Press: New York. p. 387-428.
64. Ohnishi, J., Fukuoka, H., Nishii, Y., Nakano, M., and Ichikawa, Y., *Cytochrome P-450-linked monooxygenase systems of bovine brain mitochondria and microsomes.* Int J Biochem, 1990. **22**(10): p. 1139-1145.
65. Kominami, S., Ogawa, N., Morimune, R., De-Ying, H., and Takemori, S., *The role of cytochrome b5 in adrenal microsomal steroidogenesis.* J Steroid Biochem Mol Biol, 1992. **42**(1): p. 57-64.
66. Peterson, J.A. and Prough, R.A., *Cytochrome P-450 Reductase and Cytochrome b5 in Cytochrome P-450 Catalysis*, in *Cytochrome P-450: Structure and Mechanism and Biochemistry*, P. Ortiz de Montellano, Editor. 1986, Plenum Press: New York. p. 89-117.
67. Halvorson, M., Greenway, D., Eberhart, D., Fitzgerald, K., and Parkinson, A., *Reconstitution of testosterone oxidation by purified rat cytochrome P450p (IIIA1).* Arch Biochem Biophys, 1990. **277**(1): p. 166-180.
68. Schenkman, J.B., Voznesensky, A.I., and Jansson, I., *Influence of ionic strength on the P450 monooxygenase reaction and role of cytochrome b5 in the process.* Arch Biochem Biophys, 1994. **314**(1): p. 234-241.
69. Usanov, S.A., Chashchin, V.L., and Akhrem, A.A., *Interaction of cholesterol-hydroxylating cytochrome P-450 with cytochrome b_5.* Biochemstry USSR, 1989. **54**(3): p. 364-376.
70. Usanov, S.A. and Chashchin, V.L., *Interaction of cytochrome P-450scc with cytochrome b5.* FEBS Lett, 1991. **278**(2): p. 279-282.
71. Lobanov, N.A., Khensei, K., Usanov, S.A., and Atstsi, A., *[Phosphorylation of cytochrome P-450SCC by protein kinase C. The protective effect of adrenodoxin and cytochrome b5]. Fosforilirovanie tsitokhroma P-450SCC proteinkinazoi C. Zashchitnyi effekt adrenodoksina i tsitokhorma b5.* Biokhimiia, 1993. **58**(10): p. 1529-1537.
72. Guzov, V.M., Zel'ko, I.N., Chernogolov, A.A., and Usanov, S.A., *[Interrelationship of microsomal and mitochondrial systems for hydroxylating steroids from cattle adrenal cortex: effect of highly-purified components of the mitochondrial monoxygenase system on hydroxylation of steroids by microsomes]. Bzaimootnosheniia mikrosomal'nykh i mitokhondrial'nykh sistem gidroxsilirovaniia steroidov kory nadpochechnikov byka: vliianie vysokoochishchennykh komponentov mitokhondrial'noi monooksigenaznoi sistemy na gidroksilirovanie steroidov mikrosomami.* Biokhimiia, 1993. **58**(11): p. 1761-1770.
73. Lemberg, R. and Barret, J., *Cytochromes b*, in *Cytochromes*. 1973, Academic Press: London and New York. p. 58-121.
74. Zubay, G.L., *Biological Membranes: Structure and Assembly*, in *Biochemistry*. 1983, Addison-Wesley: Reading, Massachusetts. p. 573-619.

75. Zubay, G.L., *Metabolism of Steroids and Lipoproteins*, in *Biochemistry*. 1983, Addison-Wesley: Reading, Massachusetts. p. 545-571.
76. Zubay, G.L., *Hormone Action*, in *Biochemistry*. 1983, Addison-Wesley: Reading, Massachusetts. p. 1103-1145.
77. Moffett, D.F., Moffett, S.B., and Schauf, C.L., *Control of Body Fluid, Electrolyte, and Acid-base Balance*, in *Human Physiology. Foundations & Frontiers*, R.J. Callanan, Editor. 1993, Mosby-Year Book, Inc.: St. Louis, Missouri. p. 562-587.
78. Ritvos, O. and Voutilainen, R., *Regulation of the cholesterol side-chain cleavage cytochrome P-450 and adrenodoxin mRNAs in cultured choriocarcinoma cells.* Mol Cell Endocrinol, 1992. **84**(3): p. 195-202.
79. Hanukoglu, I. and Hanukoglu, Z., *Stoichiometry of mitochondrial cytochromes P-450, adrenodoxin and adrenodoxin reductase in adrenal cortex and corpus luteum. Implications for membrane organization and gene regulation.* Eur J Biochem, 1986. **157**(1): p. 27-31.
80. Hedin, L., Rodgers, R.J., Simpson, E.R., and Richards, J.S., *Changes in content of cytochrome P450(17)alpha, cytochrome P450scc, and 3-hydroxy-3-methylglutaryl CoA reductase in developing rat ovarian follicles and corpora lutea: correlation with theca cell steroidogenesis.* Biol Reprod, 1987. **37**(1): p. 211-223.
81. Hickey, G.J., Oonk, R.B., Hall, P.F., and Richards, J.S., *Aromatase Cytochrome P450 and Cholesterol Side-Chain Cleavage Cytochrome P450 in Corpora Lutea of Pregnant Rats: Diverse Regulation by Peptide and Steroid Hormones.* Endrocrinology, 1989. **125**: p. 1673-1682.
82. Simpson, E.R., Mahendroo, M.S., Means, G.D., Kilgore, M.W., Jo Corbin, C., and Mendelson, C.R., *Tissue-Specific Promoters Regulate Aromatase Cytochrome P450 Expression.* Journal of Steroid Biochemistry and Molecular Biology, 1993. **44**: p. 321-330.
83. Moffett, D.F., Moffett, S.B., and Schauf, C.L., *Homeostatic Control: Neural and Endocrine Control Mechanisms*, in *Human Physiology. Foundations & Frontiers*, R.J. Callanan, Editor. 1993, Mosby-Year Book, Inc.: St. Louis, Missouri. p. 96-135.
84. Boggaram, V., John, M.E., Simpson, E.R., and Waterman, M.R., *Effect of ACTH on the stability of mRNAs encoding bovine adrenocortical P-450$_{scc}$, P450$_{11\beta}$, P-450$_{17\alpha}$ P-450$_{C21}$ and adrenodoxin.* Biochemical and Biophysical Research Communications, 1989. **160**: p. 1227-1232.
85. Vinson, G.P., Whitehouse, B., and Hinson, J., *Effect of Corticosteroids*, in *The Adrenal Cortex*, M.E. Hadley, Editor. 1992, Prentice Hall: Englewood Cliffs, New Jersey. p. 140-195.
86. Hanukoglu, I., Feuchtwanger, R., and Hanukoglu, A., *Mechanism of corticotropin and cAMP induction of mitochondrial cytochrome P450 system enzymes in adrenal cortex cells.* J. Biol. Chem., 1990. **265**: p. 20602-20608.
87. Waterman, M.R. and Simpson, E.R., *Regulation of the biosynthesis of cytochromes P-450 involved in steroid hormone synthesis.* Clin Chim Acta, 1986. **160**(3): p. 255-263.
88. Lewin, B., *A Panoply of Operons: The Lactose Paradigm and Others*, in *Genes*. 1987, John Wiley & Sons: New York. p. 219-247.
89. John, M.E., John, M.C., Boggaram, V., Simpson, E.R., and Waterman, M.R., *Transcriptional regulation of steroid hydroxylase genes by corticotropin.* Endocrinology, 1986. **119**(1): p. 323-330.
90. Stevens, V.L., Xu, T., and Lambeth, J.D., *Cholesterol trafficking in steroidogenic cells. Reversible cycloheximide-dependent accumulation of cholesterol in a pre-steroidogenic pool.* Eur J Biochem, 1993. **216**(2): p. 557-563.
91. Kowluru, R., Yamazaki, T., McNamara, B.C., and Jefcoate, C.R., *Metabolism of exogenous cholesterol by rat adrenal mitochondria is stimulated equally by physiological levels of free Ca2+ and by GTP.* Mol Cell Endocrinol, 1995. **107**(2): p. 181-188.
92. Momoi, K., Waterman, M.R., Simpson, E.R., and Zanger, U.M., *3',5'-Cyclic Adenosine Monophosphate-Dependent Transcription of the CYP11A (Cholesterol Side Chain Cleavage Cytochrome P450) Gene Involves a DNA Response Element Containing a Putative Binding Site for Transciption Factor Sp1.* Molecular Endocrinology, 1992. **6**: p. 1682-1690.
93. Pushkarev, V.M. and Mikosha, A.S., *The participation of cAMP and protein kinase C in the regulation of aldosterone biosynthesis by potassium.* Biomed Sci, 1991. **2**(2): p. 135-139.

94. Parker, K.L., Chaplin, D.D., Wong, M., Seidman, J.G., and Schimmer, B.P., *Molecular analysis of 21-hydroxylase gene expression in mouse adrenal cells.* Endocr Res, 1986. **12**(4): p. 409-427.
95. Chavarri, M.R., Yamakita, N., Chious, S., and Gomez-Sanchez, C.E., *Calf Adrenocortical Fasciculata Cells Secrete Aldosterone When Placed in Primary Culture.* Journal of Steroid Biochemistry and Molecular Biology, 1993. **45**: p. 493-500.
96. Ogishima, T., Suzuki, H., Hata, J., Mitani, F., and Ishimura, Y., *Zone-specific expression of aldosterone synthase cytochrome P-450 and cytochrome P-45011 beta in rat adrenal cortex: histochemical basis for the functional zonation.* Endocrinology, 1992. **130**(5): p. 2971-2977.
97. Tremblay, A. and Lehoux, J.G., *Influence of captopril on adrenal cytochrome P-450s and adrenodoxin expression in high potassium or low sodium intake.* J Steroid Biochem Mol Biol, 1992. **41**(3-8): p. 799-808.
98. Tremblay, A. and LeHoux, J.G., *Transcriptional activation of adrenocortical steroidogenic genes by high potassium or low sodium intake.* FEBS Lett, 1993. **317**(3): p. 211-215.
99. Holland, O.B., Mathis, J.M., Bird, I.M., and Rainey, W.E., *Angiotensin increases aldosterone synthase mRNA levels in human NCI-H295 cells.* Mol Cell Endocrinol, 1993. **94**(2): p. R9-13.
100. Malee, M.P. and Mellon, S.H., *Zone-specific regulation of two messenger RNAs for P450c11 in the adrenals of pregnant and nonpregnant rats.* Proc Natl Acad Sci U S A, 1991. **88**(11): p. 4731-4735.
101. Sander, M., Ganten, D., and Mellon, S.H., *Role of adrenal renin in the regulation of adrenal steroidogenesis by corticotropin.* Proc Natl Acad Sci U S A, 1994. **91**(1): p. 148-152.
102. Missale, C., Memo, M., Liberini, P., and Spano, P., *Dopamine selectively inhibits angiotensin II-induced aldosterone secretion by interacting with D-2 receptors.* J Pharmacol Exp Ther, 1988. **246**(3): p. 1137-1143.
103. Freed, M.I., Rastegar, A., and Bia, M.J., *Effects of calcium channel blockers on potassium homeostasis.* Yale J Biol Med, 1991. **64**(2): p. 177-186.
104. Kocsis, J.F., Schimmel, R.J., McIlroy, P.J., and Carsia, R.V., *Dissociation of increases in intracellular calcium and aldosterone production induced by angiotensin II (AII): evidence for regulation by distinct AII receptor subtypes or isomorphs.* Endocrinology, 1995. **136**(4): p. 1626-1634.
105. Roskelley, C.D., Baimbridge, K.G., Leung, P.C., and Auersperg, N., *Divergent differentiation of rat adrenocortical cells is associated with an interruption of angiotensin II-mediated signal transduction.* Mol Cell Endocrinol, 1992. **89**(1-2): p. 79-89.
106. Vinson, G.P., Whitehouse, B., and Hinson, J., *Physiological and Cellular Aspects of the Control of Adrenocortical Hormone Secretion*, in *The Adrenal Cortex*, M.E. Hadley, Editor. 1992, Prentice Hall: Englewood Cliffs, New Jersey. p. 65-139.
107. Moore, C.C.D. and Miller, W.L., *The role of transcriptional regulation in steroid hormone biosynthesis.* Journal of Steroid Biochemistry, 1991. **40**: p. 517-525.
108. Ghazarian, J.G. and Yanda, D.M., *Inhibition of 25-hydroxyvitamin D 1 alpha-hydroxylase by renal mitochondrial protein kinase-catalyzed phosphorylation.* Biochem Biophys Res Commun, 1985. **132**(3): p. 1095-1102.
109. Lombardo, A., Laine, M., Defaye, G., Monnier, N., Guidicelli, C., and Chambaz, E.M., *Molecular organization (topography) of cytochrome P-450(11)beta in mitochondrial membrane and phospholipid vesicles as studied by trypsinolysis.* Biochim Biophys Acta, 1986. **863**(1): p. 71-81.
110. Monnier, N., Defaye, G., and Chambaz, E.M., *Phosphorylation of bovine adrenodoxin. Structural study and enzymatic activity.* J Biol Chem, 1987. **262**(31): p. 15246-15250.
111. Mandel, M.L., Moorthy, B., and Ghazarian, J.G., *Reciprocal post-translational regulation of renal 1 alpha- and 24-hydroxylases of 25-hydroxyvitamin D3 by phosphorylation of ferredoxin. mRNA-directed cell-free synthesis and immunoisolation of ferredoxin.* Biochem J, 1990. **266**(2): p. 385-392.

112. Nemani, R., Ghazarian, J.G., Moorthy, B., Wongsurawat, N., Strong, R., and Armbrecht, H.J., *Phosphorylation of ferredoxin and regulation of renal mitochondrial 25-hydroxyvitamin D-1 alpha-hydroxylase activity in vitro.* J Biol Chem, 1989. **264**(26): p. 15361-15366.
113. Siegel, N., Wongsurawat, N., and Armbrecht, H.J., *Parathyroid hormone stimulates dephosphorylation of the renoredoxin component of the 25-hydroxyvitamin D3-1 alpha-hydroxylase from rat renal cortex.* Bioorg Khim, 1986. **12**(9): p. 1286-1289.
114. Jaiswal, R.K., Jaiswal, N., and Sharma, R.K., *Negative regulation of atrial natriuretic factor receptor coupled membrane guanylate cyclase by phorbol ester. Potential protein kinase C regulation of cyclic GMP signal in isolated adrenocortical carcinoma cells of rat.* FEBS Lett, 1988. **227**(1): p. 47-50.
115. Rosenberg, J., Pines, M., and Hurwitz, S., *Regulation of aldosterone secretion by avian adrenocortical cells.* J Endocrinol, 1988. **118**(3): p. 447-453.
116. Ichikawa, Y. and Hiwatashi, A., *The role of the sugar regions of components of the cytochrome P-450-linked mixed-function oxidase (monooxygenase) system of bovine adrenocortical mitochondria.* Biochim. Biophys. Acta, 1982. **705**: p. 82-91.
117. Chu, J.-W. and Kimura, T., *Studies on adrenal steroid hydroxylases.* J. Biol. Chem., 1973. **248**(6): p. 2089-2094.
118. Tsubaki, M., Ohkubo, H., Tsuneoka, Y., Tomita, S., Hiwatashi, A., and Ichikawa, Y., *Existence of multiple forms of cytochrome P-450$_{scc}$ purified from bovine adrenocortical mitochondria.* Biochimica et Biophysica Acta, 1987. **914**: p. 246-258.
119. Wada, A., Mathew, P.A., Barnes, H.J., Sanders, D., Estabrook, R.W., and Waterman, M.R., *Expression of functional bovine cholesterol side chain cleavage cytochrome P450 (P450scc) in Escherichia coli.* Archives of Biochemistry and Biophysics, 1991. **290**: p. 376-380.
120. Wada, A. and Waterman, M.R., *Identification by site-directed mutagenesis of two lysine residues in cholesterol side chain cleavage cytochrome P450 that are essential for adrenodoxin binding.* J Biol Chem, 1992. **267**(32): p. 22877-22882.
121. Uhlmann, H., Kraft, R., and Bernhardt, R., *C-terminal region of adrenodoxin affects its structural integrity and determines differences in its electron transfer function to cytochrome P-450.* J Biol Chem, 1994. **269**(36): p. 22557-22564.
122. Brandt, M.E. and Vickery, L.E., *Charge pair interactions stabilizing ferredoxin-ferredoxin reductase complexes. Identification by complementary site-specific mutations.* J Biol Chem, 1993. **268**(23): p. 17126-17130.
123. Tanaka, M., Haniu, M., and Yasunobu, K.T., *The amino acid sequence of bovine adrenodoxin.* J. Biol. Chem., 1973. **248**(4): p. 1141-1157.
124. Nabi, N. and Omura, T., *In vitro synthesis of adrenodoxin and adrenodoxin reductase: Existence of a putative large precursor form of adrenodoxin.* Biochem. Biophys. Res. Comm., 1980. **97**(2): p. 680-686.
125. Okamura, T., John, M.E., Zuber, M.X., Simpson, E.R., and Waterman, M.R., *Molecular cloning and amino acid sequence of the precursor form of bovine adrenodoxin: evidence for a previously unidentified COOH-terminal peptide.* Proc. Natl. Acad. Sci. USA, 1985. **82**(17): p. 5705-5709.
126. Cupp, J.R. and Vickery, L.E., *Adrenodoxin with a COOH-terminal deletion (des 116-128) exhibits enhanced activity.* Journal of Biological Chemistry, 1989. **264**: p. 1602-1607.
127. Ehrhart-Bornstein, M., Bornstein, S.R., Scherbaum, W.A., Pfeiffer, E.F., and Holst, J.J., *Role of the vasoactive intestinal peptide in a neuroendocrine regulation of the adrenal cortex.* Neuroendocrinology, 1991. **54**(6): p. 623-628.
128. Cunningham, L.A. and Holzwarth, M.A., *Vasoactive intestinal peptide stimulates adrenal aldosterone and corticosterone secretion.* Endocrinology, 1988. **122**(5): p. 2090-2097.
129. Esneu, M., Delarue, C., Remy-Jouet, I., Manzardo, E., Fasolo, A., Fournier, A., Saint-Pierre, S., Conlon, J.M., and Vaudry, H., *Localization, identification, and action of calcitonin gene-related peptide in the frog adrenal gland.* Endocrinology, 1994. **135**(1): p. 423-430.

130. Delarue, C., Lefebvre, H., Idres, S., Leboulenger, F., Homo-Delarche, G., Lihrmann, I., Feuilloley, M., and Vaudry, H., *Serotonin stimulates corticosteroid secretion by frog adrenocortical tissue in vitro.* J Steroid Biochem, 1988. **29**(5): p. 519-525.
131. Stern, N., Tuck, M., Ozaki, L., and Krall, J.F., *Dopaminergic binding and inhibitory effect in the bovine adrenal zona glomerulosa.* Hypertension, 1986. **8**(3): p. 203-210.
132. Yanase, T., Nawata, H., Higuchi, K., Kato, K., and Ibayashi, H., *[The effects of metoclopramide and dopamine on aldosterone secretion in cultured adrenocortical adenoma cells and adjacent non-adenoma cells from patients with primary aldosteronism].* Nippon Naibunpi Gakkai Zasshi, 1985. **61**(6): p. 631-641.
133. Wink, D.A., Osawa, Y., Darbyshire, J.F., Jones, C.R., Eshenaur, S.C., and Nims, R.W., *Inhibition of cytochromes P450 by nitric oxide and a nitric oxide-releasing agent.* Arch Biochem Biophys, 1993. **300**(1): p. 115-123.
134. Hall, P.F., Yanagibashi, K., and Kobayashi, Y., *Synthesis of aldosterone by mitochondria and homogeneous 11 beta-hydroxylase from beef and pig.* Endocr Res, 1991. **17**(1-2): p. 135-149.
135. Yanagibashi, K., Kobayashi, Y., and Hall, P.F., *Ascorbate as a source of reducing equivalents for the synthesis of aldosterone.* Biochem Biophys Res Commun, 1990. **170**(3): p. 1256-1262.
136. Young, F.M., Luderer, W.B., and Rodgers, R.J., *The antioxidant beta-carotene prevents covalent cross-linking between cholesterol side-chain cleavage cytochrome P450 and its electron donor, adrenodoxin, in bovine luteal cells.* Mol Cell Endocrinol, 1995. **109**(1): p. 113-118.
137. Hornsby, P.J., Harris, S.E., and Aldern, K.A., *The role of ascorbic acid in the function of the adrenal cortex: studies in adrenocortical cells in culture.* Endocrinology, 1985. **117**(3): p. 1264-1271.
138. della-Cioppa, G., Muffly, K.E., Yanagibashi, K., and Hall, P.F., *Preparation and characterization of submitochondrial fractions from adrenal cells.* Mol Cell Endocrinol, 1986. **48**(2-3): p. 111-120.
139. della-Cioppa, G., Muffly, K.E., Yanagibashi, K., and Hall, P.F., *Preparation and characterization of submitochondrial fractions from adrenal cells.* Mol Endocrinol, 1988. **2**(6): p. 499-506.
140. Ishimura, K., Yoshinaga, T., Fujita, H., Sugano, S., Okamoto, M., and Yamano, T., *Light and electron microscopic immunohistochemistry on the localization of cytochrome P-450 of the side chain cleavage system and of cytochrome P-450 of 11 beta-hydroxylase in the bovine adrenal cortical cells.* Arch Histol Jpn, 1985. **48**(5): p. 541-546.
141. Geuze, H.J., Slot, J.W., Yanagibashi, K., McCracken, J.A., Schwartz, A.L., and Hall, P.F., *Immunogold cytochemistry of cytochromes P-450 in porcine adrenal cortex. Two enzymes (side-chain cleavage and 11 beta-hydroxylase) are co-localized in the same mitochondria.* Histochemistry, 1987. **86**(6): p. 551-557.
142. Morohashi, K., Yoshioka, H., Gotoh, O., Okada, Y., Yamamoto, K., Miyata, T., Sogawa, K., Fujii-Kuriyama, Y., and Omura, T., *Molecular cloning and nucleotide sequence of DNA of mitochondrial cytochrome P-450(11β) of bovine adrenal cortex.* J. Biochem., 1987. **102**(3): p. 559-568.
143. Tuckey, R.C. and Cameron, K.J., *Catalytic properties of cytochrome P-450scc purified from the human placenta: comparison to bovine cytochrome P-450scc.* Biochim Biophys Acta, 1993. **1163**(2): p. 185-194.
144. Takemoto, C., Nakano, H., Sato, H., and Tamaoki, B.-I., *Fate of Molecular Oxygen Required by Endocrine Enzymes for the Side Chain Cleavage of Cholesterol.* Biochimica et Biophysica Acta, 1968. **152**: p. 749-757.
145. Kemp, D.S. and Vellaccio, F., *The Stability of Organic Molecules*, in *Organic Chemistry.* 1980, Worth Publishers, Inc.: New York. p. 1053-1082.
146. Tsubaki, M., Hiwatashi, A., and Ichikawa, Y., *Effects of cholesterol analogues and inhibitors on the heme moiety of cytochrome P-450$_{SCC}$: a resonance Raman study.* Biochem., 1987. **26**: p. 4535-4540.

147. Tsubaki, M., Hiwatashi, A., Ichikawa, Y., Fujimoto, Y., Ikekawa, N., and Hori, H., *Electron paramagnetic resonance study of ferrous cytochrome P-450scc-nitric oxide complexes: effects of 20(R),22(R)-dihydroxycholesterol and reduced adrenodoxin.* Biochem., 1988. **27**: p. 4856-4862.
148. Furuya, S., Okada, M., Ito, A., Aoyagi, H., Kanmera, T., Kato, T., Sagara, Y., Horiuchi, T., and Omura, T., *Synthetic partial extension peptides of P-450(SCC) and adrenodoxin precursors: effects on the import of mitochondrial enzyme precursors.* Biokhimiia, 1987. **52**(10): p. 1717-1725.
149. Matocha, M.F. and Waterman, M.R., *Import and processing of P-450SCC and P-450(11) beta precursors by corpus luteal mitochondria: a processing pathway recognizing homologous and heterologous precursors.* Arch Biochem Biophys, 1986. **250**(2): p. 456-460.
150. Luzikov, V.N., Novikova, L.A., Whelan, J., Hugosson, M., and Glaser, E., *Import of the mammalian cytochrome P450 (scc) precursor into plant mitochondria.* Biochem Biophys Res Commun, 1994. **199**(1): p. 33-36.
151. Ogishima, T., Okada, Y., and Omura, T., *Import and processing of the precursor of cytochrome P-450(SCC) by bovine adrenal cortex mitochondria.* J Biochem (Tokyo), 1985. **98**(3): p. 781-791.
152. Ito, A., Ogishima, T., Ou, W., Omura, T., Aoyagi, H., Lee, S., Mihara, H., and Izumiya, N., *Effects of synthetic model peptides resembling the extension peptides of mitochondrial enzyme precursors on import of the precursors into mitochondria.* J Biochem (Tokyo), 1985. **98**(6): p. 1571-1582.
153. Leenhouts, J.M., Torok, Z., Demel, R.A., de Gier, J., and de Kruijff, B., *The full length of a mitochondrial presequence is required for efficient monolayer insertion and interbilayer contact formation.* Mol Membr Biol, 1994. **11**(3): p. 159-164.
154. Ou, W.J., Ito, A., Umeda, M., Inoue, K., and Omura, T., *Specific binding of mitochondrial protein precursors to liposomes containing cardiolipin.* Biokhimiia, 1988. **53**(11): p. 1810-1816.
155. Schwarz, D., Richter, W., Kruger, V., Chernogolov, A., Usanov, S., and Stier, A., *Direct visualization of a cardiolipin-dependent cytochrome P450scc-induced vesicle aggregation.* J Struct Biol, 1994. **113**(3): p. 207-215.
156. Schwarz, D., Kruger, V., Chernogolov, A.A., Usanov, S.A., and Stier, A., *Rotation of cytochrome P450SCC (CYP11A1) in proteoliposomes studied by delayed fluorescence depolarization.* Biochem Biophys Res Commun, 1993. **195**(2): p. 889-896.
157. Furuya, S., Mihara, K., Aimoto, S., and Omura, T., *Cytosolic and mitochondrial surface factor-independent import of a synthetic peptide into mitochondria.* Embo J, 1991. **10**(7): p. 1759-1766.
158. Kumamoto, T., Ito, A., and Omura, T., *Characterization of a mitochondrial matrix protease catalyzing the processing of adrenodoxin precursor.* Ukr Biokhim Zh, 1988. **60**(2): p. 26-30.
159. Ou, W.J., Ito, A., Okazaki, H., and Omura, T., *Purification and characterization of a processing protease from rat liver mitochondria.* Biokhimiia, 1989. **54**(7): p. 1206-1216.
160. Usanov, S.A., Chernogolov, A.A., and Chashchin, V.L., *Inhibitory domain-specific antibodies to cytochrome P-450$_{scc}$.* FEBS Letters, 1989. **255**: p. 125-128.
161. Usanov, S.A., Chernogolov, A.A., and Chashchin, V.L., *[Immunochemical study of cholesterol-hydroxylating cytochrome P-450. Topology of the peptide chain of the heme protein in the phospholipid membrane]. Immunokhimicheskoe issledovanie kholesteringidroksiliruiushchego tsitokhroma P-450. Topologiia polipeptidnoi tsepi gemoproteida v fosfolipidnoi membrane.* Biokhimiia, 1989. **54**(6): p. 916-925.
162. Hanukoglu, I., Spitsberg, V., Bumpus, J.A., Dus, K.M., and Jefcoate, C.R., *Adrenal mitochondrial cytochrome P-450scc. Cholesterol and adrenodoxin interactions at equilibrium and during turnover.* J. Biol. Chem., 1981. **256**(9): p. 4321-4328.
163. Turko, I.V., Adamovich, T.B., Kirillova, N.M., Usanov, S.A., and Chashchin, V.L., *Cross-linking studies of the cholesterol hydroxylation system from bovine adrenocortical mitochondria.* Seikagaku, 1989. **61**(1): p. 26-29.

164. Beckert, V., Dettmer, R., and Bernhardt, R., *Mutations of tyrosine 82 in bovine adrenodoxin that affect binding to cytochromes P45011A1 and P45011B1 but not electron transfer.* J Biol Chem, 1994. **269**(4): p. 2568-2573.
165. Coghlan, V.M. and Vickery, L.E., *Site-specific mutations in human ferredoxin that affect binding to ferredoxin reductase and cytochrome P450scc.* J Biol Chem, 1991. **266**(28): p. 18606-18612.
166. Tsubaki, M., Iwamoto, Y., Hiwatashi, A., and Ichikawa, Y., *Inhibition of electron transfer from adrenodoxin to cytochrome P-450$_{SCC}$ by chemical modification with pyridoxal 5'-phosphate: identification of adrenodoxin-binding site of cytochrome P-450$_{SCC}$.* Biochem., 1989. **28**: p. 6899-6907.
167. Turko, I.V., Adamovich, T.B., Kirillova, N.M., Usanov, S.A., and Chashchin, V.L., *[A covalently linked complex of cytochrome P-450 with adrenodoxin. Localization of the adrenodoxin binding site of cytochrome P-450]. Kovalentno sshityi kompleks tsitokhroma P-450 s adrenodoksinom. Lokalizatsiia adrenodoksinsviayvaiushchego uchastka tsitokhroma P-450.* Biokhimiia, 1988. **53**(12): p. 1962-1971.
168. Seybert, D.W., Lancaster, J.R., Jr., Lambeth, J.D., and Kamin, H., *Participation of the membrane in the side chain cleavage of cholesterol. Reconstitution of cytochrome P-450$_{SCC}$ into phospholipid vesicles.* J. Biol. Chem., 1979. **254**(23): p. 12088-12098.
169. Turko, I.V., Usanov, S.A., Akhrem, A.A., and Chashchin, V.L., *[Mechanism of electron transport in the cholesterol-hydroxylating system of adrenal cortex mitochondria: a triple complex of adrenodoxin reductase, adrenodoxin and cytochrome P-450]. Mekhanizm elektronnogo transporta v kholesteringidroksiliruiushchei sisteme mitokhondrii kory nadpochechnikov: troinoi kompleks adrenodoksinreduktazy, adrenodoksina i tsitokhroma P-450.* Biokhimiia, 1988. **53**(8): p. 1352-1356.
170. Shkumatov, V.M., Smettan, G., Ristau, O., Rein, H., Ruckpaul, K., Chaschin, V.L., and Akhrem, A.A., *Quantitation of interaction between cytochrome P-450scc and adrenodoxin--analysis in the median UV-region by second derivative spectroscopy.* J Biol Chem, 1988. **263**(31): p. 16195-16201.
171. Ohta, Y., MItani, F., Ishimura, Y., Yanagibashi, K., Kawamura, M., and Kawato, S., *Conversion of cholesterol to pregnenolone mobilizes cytochrome P-450 in the inner membrane of adrenocortical mitochondria: protein rotation study.* J. Biochem., 1990. **107**(1): p. 97-104.
172. Ohta, Y., Yanagibashi, K., Hara, T., Kawamura, M., and Kawato, S., *Protein rotation study of cytochrome P-450 in submitochondrial particles: effect of KCl and intermolecular interactions with redox partners.* J Biochem (Tokyo), 1991. **109**(4): p. 594-599.
173. Muller, J., *Aldosterone: the minority hormone of the adrenal cortex.* Steroids, 1995. **60**(1): p. 2-9.
174. Rösler, A. and White, P.C., *Mutations in Human 11§-Hydroxyalse Genes: 11§-Hydroxylase Defficiency in Jews of Morocco and Corticosterone Methyl-Oxidase II Deficiency in Jews of Iran.* Journal of Steroid Biochemistry and Molecular Biology, 1993. **45**: p. 99-106.
175. Ogishima, T., Mitani, F., and Ishimura, Y., *Isolation of two distinct cytochromes P-450$_{11\beta}$ with aldosterone synthase activity from bovine adrenocortical mitochondria.* Journal of Biochemistry (Tokyo), 1989. **105**: p. 497-499.
176. Yanagibashi, K., Shackleton, C.H.L., and Hall, P.F., *Conversion of 11-deoxycorticosterone and corticosterone to aldosterone by cytochrome P-450 11β-/18-hydroxylase from porcine adrenal.* Journal of Steroid Biochemistry, 1988. **29**: p. 665-675.
177. Mornet, E., Dupont, J., Vitek, A., and White, P.C., *Characterization of two genes encoding human steroid 11β-hydroxylase (P-450$_{11\beta}$).* J. Biol. Chem., 1989. **264**(35): p. 20961-20967.
178. Domalik, L.J., Chaplin, D.D., Kirkman, M.S., Wu, R.C., Liu, W.W., Howard, T.A., Seldin, M.F., and Parker, K.L., *Different isozymes of mouse 11 beta-hydroxylase produce mineralocorticoids and glucocorticoids.* Mol Endocrinol, 1991. **5**(12): p. 1853-1861.

179. Nomura, R., Morohashi, I., Kirita, S., Nonaka, Y., Okamoto, M., Nawata, H., and Omura, T., *Three Forms of Rat CYP11B Genes: 11β-Hydroxylase Gene, Aldosterone Synthase Gene, and a Novel Gene.* Journal of Biochemistry (Tokyo), 1993. **113**: p. 144-152.
180. Ohnishi, T., Wada, A., Lauber, M., Yamano, T., and Okamoto, M., *Aldosterone biosynthesis in mitochondria of isolated zones of adrenal cortex.* Journal of Steroid Biochemistry, 1988. **31**: p. 73-81.
181. Ogishima, T., Shibata, H., Shimada, H., Mitani, F., Suzuki, H., Saruta, T., and Ishimura, Y., *Aldosterone synthase cytochrome P-450 expressed in the adrenals of patients with primary aldosteronism.* J Biol Chem, 1991. **266**(17): p. 10731-10734.
182. Lauber, M., Sugano, S., Ohnishi, T., Okamoto, M., and Müller, J., *Aldosterone biosynthesis and cytochrome P-450$_{11\beta}$: evidence for two different forms of the enzyme in rats.* J. steroid Biochem., 1987. **26**(6): p. 693-698.
183. Ogishima, T., Mitani, F., and Ishimura, Y., *Isolation of aldosterone synthase cytochrome P-450 from zona glomerulosa mitochondria of rat adrenal cortex.* J. Biol. Chem., 1989. **264**(19): p. 10935-10938.
184. Morohashi, K., Nonaka, Y., Kirita, S., Hatano, O., Takakusu, A., Okamoto, M., and Omura, T., *Enzymatic activities of P-450(11β)s expressed by two cDNAs in COS-7 cells.* J. Biochem., 1990. **107**: p. 635-640.
185. White, P.C., Pascoe, L., Curnow, K.M., Tannin, G., and Rösler, A., *Molecular Biology of 11β-Hydroxylase and 11β-Hydroxysteroid Dehydrogenase Enzymes.* Journal of Steroid Biochemistry and Molecular Biology, 1992. **43**: p. 827-835.
186. Whorwood, C.B., Ricketts, M.L., and Stewart, P.M., *Regulation of sodium-potassium adenosine triphosphate subunit gene expression by corticosteroids and 11 beta-hydroxysteroid dehydrogenase activity.* Endocrinology, 1994. **135**(3): p. 901-910.
187. Yamazaki, T., McNamara, B.C., and Jefcoate, C.R., *Competition for electron transfer between cytochromes P450scc and P45011 beta in rat adrenal mitochondria.* Mol Cell Endocrinol, 1993. **95**(1-2): p. 1-11.
188. Ikushiro, S., Kominami, S., and Takemori, S., *Adrenal P-450$_{scc}$ Modulates Activity of P-450$_{11\beta}$ in Liposomal and Mitchondrial Membranes. Implication of P-450$_{scc}$ in Zone Specificity of Aldosterone Biosynthesis in Bovine Adrenal.* Journal of Biological Chemistry, 1992. **267**(3): p. 1464-1469.
189. Ohnishi, T., Wada, A., Nonaka, Y., Sugiyama, T., Yamano, T., and Okamoto, M., *Effect of calmodulin on aldosterone synthesis by a cytochrome P-450$_{11\beta}$-reconstituted system from bovine adrenocortical mitochondria.* J. Biochem., 1986. **100**(4): p. 1065-1076.
190. Hallberg, E. and Rydstrom, J., *Toxicity of 7,12-dimethylbenz[a]anthracene and 7-hydroxymethyl-12-methylbenz[a]anthracene and its prevention in cultured rat adrenal cells. Evidence for a peroxidative mechanism of action.* Toxicology, 1987. **47**(3): p. 259-275.
191. Rapoport, R., Sklan, D., and Hanukoglu, I., *Electron leakage from the adrenal cortex mitochondrial P450scc and P450c11 systems: NADPH and steroid dependence.* Arch Biochem Biophys, 1995. **317**(2): p. 412-416.
192. Ohnishi, T., Wada, A., Nonaka, Y., Okamoto, M., and Yamano, T., *Effect of phospholipid on aldosterone biosynthesis by a cytochrome P-450$_{11\beta}$-reconstituted system.* Biochem. Int., 1984. **9**(6): p. 715-723.
193. Laird, S.M., Vinson, G.P., and Whitehous, B.J., *Steroid sequestration within the rat adrenal zona glomerulosa.* J. Endocr., 1988. **117**: p. 191-196.
194. Vinson, G.P. and Whitehouse, B.J., *The biosynthesis and secretion of aldosterone by the rat adrenal zona glomerulosa, and the significance of the compartmental arrangement of steroids.* Acta Endocr., 1973. **72**: p. 746-752.
195. Lantos, C.P., Damasco, M.C., Aragones, A., Ceballos, N.R., Burton, G., and Cozza, E.N., *Versatile steroid molecules at the end of the aldosterone pathway.* J Steroid Biochem, 1987. **27**(4-6): p. 791-800.

196. Mochizuki, H., Suhara, K., and Katagiri, M., *Steroid 6 beta-hydroxylase and 6-desaturase reactions catalyzed by adrenocortical mitochondrial P-450.* J Steroid Biochem Mol Biol, 1992. **42**(1): p. 95-101.
197. Cozza, E.N., Chavarri, M.R., Foecking, M.F., and Gomez-Sanchez, C.E., *Synthesis of 18-hydroxycortisol and 18-oxocortisol in bovine adrenal zona glomerulosa mitochondria.* Proc Soc Exp Biol Med, 1993. **203**(3): p. 317-322.
198. Suhara, K., Takeda, K., and Katagiri, M., *P-450$_{11\beta}$-dependent conversion of cortisol to cortisone, and 19-hydroxyandrostenedione to 19-oxoandrostenedione.* Biochem. Biophys. Res. Comm., 1986. **136**(1): p. 369-375.
199. Fujii, S., Momoi, K., Okamoto, M., Yamano, T., Okada, T., and Terasawa, T., *18,19-Dihydroxydeoxycorticosterone, a new metabolite produced from 18-hydroxydeoxycorticosterone by cytochrome P-450$_{11\beta}$. Chemical synthesis and structural analysis by ^{1}H NMR.* Biochemistry, 1984. **23**(12): p. 2558-2564.
200. Nonaka, Y. and Okamoto, M., *Functional expression of the cDNAs encoding rat 11β-hydroxylase [cytochrome P450(11β)] and aldosterone synthase [cytochrome P450(11β, aldo)].* European Journal of Biochemistry, 1991. **202**(3): p. 897-902.
201. Drummond, T.D., Mason, J.I., and McCarthy, J.L., *Gerbil Adrenal 11§- and 19-Hydroxylating Activities Respond similarly to Inhibitory or Stimulatory Agents: Two Activities of a Single Enzyme.* Journal of Steroid Biochemistry, 1988. **29**: p. 641-648.
202. Sato, H., Ashida, N., Sujara, K., Itagaki, E., Takemori, S., and Katagiri, M., *Properties of an adrenal cytochrome P-450 (P-450$_{11\beta}$) for hydroxylations of corticosteroids.* Arch. Biochem. Biophys., 1978. **190**(1): p. 307-314.
203. Suhara, K., Ohashi, K., Takahashi, K., and Katagiri, M., *Aromatase and nonaromatizing 10-demethylase activity of adrenal cortex mitochondrial P-450$_{11\beta}$.* Arch. Biochem. Biophys., 1988. **267**(1): p. 31-37.
204. Suhara, K., Yamamoto, M., and Katagiri, M., *Hydroxylation of 19-norandrostenedione by adrenal cortex mitochondrial P-450(11)beta.* Biokhimiia, 1990. **55**(4): p. 665-673.
205. Suhara, K., Ohashi, K., Takeda, K., and Katagiri, M., *P-450$_{11\beta}$-dependent conversion of adrogen to estrogen the aromatase reaction.* Biochem. Biophys. Res. Comm., 1986. **140**(2): p. 530-535.
206. Suhara, K., Ohashi, K., Takeda, K., and Katagiri, M., *P-450(11beta)-dependent conversion of androgen to estrogen, the aromatase reaction.* Eur J Biochem, 1987. **164**(1): p. 21-25.
207. Jefcoate, C.R., Orme-Johnson, W.H., and Beinert, H., *Cytochrome P-450 of Bovine Adrenal Mitochondria. Ligand Binding to two Forms Resolved by EPR Spectroscopy.* The Journal of Biological Chemistry, 1976. **251**: p. 3706-3715.
208. Gomez-Sanchez, C.E., Zager, P.G., Foecking, M.F., Holland, O.B., and Ganguly, A., *18-Oxocortisol: Effect of Dexamethasone, ACTH and Sodium Restriction.* Journal of Steroid Biochemistry, 1989. **32**: p. 409-412.
209. Yamakita, N., Gomez-Sanchez, C.E., T., M., Yoshida, H., Miyazaki, S., Yasuda, K., and Nakai, T., *Regulation of 18-Oxocortisol and 18-Hydroxycortisol by the Renin-Angiotensin System and ACTH in Man.* Journal of Steroid Biochemistry and Molecular Biology, 1993. **46**: p. 395-399.
210. Gomez-Sanchez, C.E., Foecking, M.F., Shackleton, C.H.L., Chavarri, M.R., and Gomez-Sanchez, E.P., *18-Hydroxy-11-Deoxycortisol: A New Steroid Isolated From Incubations of the Adrenal With 11-Deoxycortisol.* Journal of Steroid Biochemistry, 1987. **26**: p. 105-111.
211. Gomez-Sanchez, E.P., Gomez-Sanchez, C.E., Smith, J.S., Ferris, M.W., and Foecking, M., *Receptor Binding and Biological Activity of 18-Hydroxycortisol.* Endrocrinology, 1984. **115**: p. 462-466.

212. Gomez-Sanchez, C.E., Montgomery, M., Ganguly, A., Holland, O.B., Gomez-Sanchez, E.P., C.E., G., and Weinberger, M.H., *Elevated Urinary Excretion of 18-Oxocortisol in Glucocorticoid-Suppressible Aldosteronism.* Journal of Clinical Endocrinology and Metabolism, 1984. **59**: p. 1022-1024.
213. Gomez-Sanchez, C.E., Gomez-Sanchez, E.P., Smith, J.S., Ferris, M.W., and Foecking, M.F., *Receptor Binding and Biological Activity of 18-Oxocortisol.* Endrocrinology, 1985. **116**: p. 6-10.
214. Jonsson, C.J. and Lund, B.O., *In vitro bioactivation of the environmental pollutant 3-methylsulphonyl-2, 2-bis(4-chlorophenyl)-1,1-dichloroethene in the human adrenal gland.* Toxicol Lett, 1994. **71**(2): p. 169-175.
215. Tobes, M.C., Hays, S.J., Gildersleeve, D.L., Wieland, D.M., and Beierwaltes, W.H., *Adrenal cortical 11 beta-hydroxylase and side-chain cleavage enzymes. Requirement for the A- or B-pyridyl ring in metyrapone for inhibition.* J Steroid Biochem, 1985. **22**(1): p. 103-110.
216. Vinson, G.P., Whitehouse, B., and Hinson, J., *Inhibitors of Corticoid Biosynthesis*, in *The Adrenal Cortex*, M.E. Hadley, Editor. 1992, Prentice Hall: Englewood Cliffs, New Jersey. p. 265-280.
217. Couch, R.M., Muller, J., Perry, Y.S., and Winter, J.S., *Kinetic analysis of inhibition of human adrenal steroidogenesis by ketoconazole.* J Clin Endocrinol Metab, 1987. **65**(3): p. 551-554.
218. De Coster, R., Beerens, D., Haelterman, C., and Wouters, L., *Effects of etomidate on cortisol biosynthesis in isolated guinea-pig adrenal cells: comparison with metyrapone.* J Endocrinol Invest, 1985. **8**(3): p. 199-202.
219. Schuster, I., *The interaction of representative members from two classes of antimycotics--the azoles and the allylamines--with cytochromes P-450 in steroidogenic tissues and liver.* Xenobiotica, 1985. **15**(6): p. 529-546.
220. Wada, A., Ohnishi, T., Nonaka, Y., and Okamoto, M., *Inhibition of bovine adrenocortical mitochondrial cytochrome P-450$_{11\beta}$-mediated reactions by imidazole derivatives and mineralocorticord analogs.* Journal of Steroid Biochemistry, 1988. **31**(5): p. 803-808.
221. Flowers, N.L., Sherry, J.H., O'Donnell, J.P., and Colby, H.D., *Adrenal mitochondrial metabolism of spironolactone. Absence of metabolic activation.* Biochem Pharmacol, 1988. **37**(8): p. 1591-1595.
222. Yamakita, N., Chiou, S., and Gomez-Sanchez, C.E., *Inhibition of Aldosterone Biosynthesis by 18-Ethynyl-Deoxycorticosterone.* Endrocrinology, 1991. **129**: p. 2361-2366.
223. Waterman, M.R., John, M.E., and Simpson, E.R., *Regulation of Synthesis and Activity of Cytochrome P-450 Enzymes in Physiological Pathways*, in *Cytochrome P-450: Structure and Mechanism and Biochemistry*, P. Ortiz de Montellano, Editor. 1986, Plenum Press: New York. p. 345-386.
224. Ikushiro, S., Kominami, S., and Takemori, S., *Adrenal cytochrome P-45011 beta-proteoliposomes catalyzing aldosterone synthesis: preparation and characterization.* Biochim Biophys Acta, 1989. **984**(1): p. 50-56.
225. Orme-Johnson, N.R., Light, D.R., White-Stevens, R.W., and Orme-Johnson, W.H., *Steroid binding properties of beef adrenal cortical cytochrome P-450 which catalyzes the coversion of cholesterol into pregnenolone.* Journal of Biological Chemistry, 1979. **254**: p. 2103-2111.
226. Barton, D.H.R. and Parekh, S.I., *Half a Century of Free Radical Chemistry*, ed. L.A.R. di Brozolo. 1993, New York: Cambridge University Press. 164.
227. Heusler, K. and Kalvoda, J., *Intramolecular free-radical reactions.* 1964. **3**: p. 525-596.
228. Sih, C.J., *Enzymatic Mechanism Of Steroid Hydroxylation. Reduced nicotinamide-adenine dinucleotide phosphate serves two distinct roles in hydroxlyation.* Science, 1969. **163**: p. 1297-1300.
229. Rösler, A., Rabinowitz, D., Theodor, R., Ramirez, L.C., and Ulick, S., *The Nature of the Defect in a Salt-Wasting Disorder in Jews of Iran.* Journal of Clinical Endocrinology and Metabolism, 1977. **44**: p. 279-291.

230. Imai, M., Shimada, H., Okada, Y., Matsushima-Hibiya, Y., Ogishima, T., and Ishimura, Y., *Molecular cloning of a cDNA encoding aldosterone synthase cytochrome P-450 in rat adrenal cortex.* FEBS Letters, 1990. **263**: p. 299-302.
231. Kawamoto, T., Mitsuuchi, Y., Toda, K., Miyahara, K., Yokoyama, Y., Nakao, K., Hosoda, K., Yamamoto, Y., Imura, H., and Shizuta, Y., *Cloning of cDNA and genomic DNA for human cytochrome P-450$_{11\beta}$.* FEBS Letters, 1990. **269**: p. 345-349.
232. Kawamoto, T., Mitsuuchi, Y., Ohnishi, T., Ichikawa, Y., Yokoyama, Y., Sumimoto, H., Toda, K., Miyahara, K., Kuribayashi, I., Nakao, K., Hosoda, K., Yamamoto, Y., Imura, H., and Shizuta, Y., *Cloning and expression of a cDNA for human cytochrome P-450$_{aldo}$ as related to primary aldosteronism.* Biochemical and Biophysical Research Communications, 1990. **173**(1): p. 309-316.
233. Raag, R., Li, H., Jones, B.C., and Poulos, T.L., *Inhibitor-induced conformational change in cytochrome P-450CAM.* Biochemistry, 1993. **32**(17): p. 4571-4578.
234. Pochapsky, T.C. and Ye, X.M., *1H NMR identification of a beta-sheet structure and description of folding topology in putidaredoxin.* Biochemistry, 1991. **30**(16): p. 3850-3856.
235. Ye, X.M., Pochapsky, T.C., and Pochapsky, S.S., *1H NMR sequential assignments and identification of secondary structural elements in oxidized putidaredoxin, an electron-transfer protein from Pseudomonas.* Biochemistry, 1992. **31**(7): p. 1961-1968.
236. Pochapsky, T.C., Ratnaswamy, g., and Petera, A., *Redox-Dependent ^{1}H NMR Spectral Features and Tertiary Structural Constraints on the C-Terminal Region of Putidaredoxin.* Biochemistry, 1994. **33**(21): p. 6433-6441.
237. Pochapsky, T.C., Ye, M.X., Ratnaswamy, G., and Lyons, T.A., *An NMR-Derived Model for the Solution Structure of Oxidized Putidaredoxin, a 2-Fe, 2-S Ferredoxin from Pseudomonas.* Biochemistry, 1994. **33**(21): p. 6424-6432.
238. Tsubaki, M., Ichikawa, Y., Fujimoto, Y., Yu, N.-T., and Hori, H., *Active site of bovine adrenocortical cytochrome P-450$_{11\beta}$ studied by resonance Raman and electron paramagnetic resonance spectroscopies: distinction from cytochrome P-450$_{scc}$.* Biochem., 1990. **29**: p. 8805-8812.
239. Curnow, K.M., Slutsker, L., Vitek, J., Cole, T., Speiser, P.W., New, M.I., White, P.C., and Pascoe, L., *Mutations in the CYP11B1 gene causing congenital adrenal hyperplasia and hypertension cluster in exons 6, 7, and 8.* Proceedings of the National Academy of Sciences USA, 1993. **90**: p. 4552-4556.
240. Mitsuuchi, Y., Kawamoto, T., Rösler, A., Naiki, Y., Miyahara, K., Toda, K., Kuribayashi, I., Orii, T., Yasuda, K., Miura, K., Nakao, K., Imura, H., Ulick, S., and Shizuta, Y., *Congenitally defective aldosterone biosynthesis in humans: the involvement of point mutations of the P-450C$_{18}$ gene (CYP11B2) in CMO II deficient patients.* Biochemical and Biophysical Research Communications, 1992. **182**: p. 974-979.
241. Miyahara, K., Kawamoto, T., Mitsuuchi, Y., Toda, K., Imura, H., Gordon, R.D., and Shizuta, Y., *The chimeric gene linked to glucocorticoid-suppressible hyperaldosteronism encodes a fused P-450 protein possessing aldosterone synthase activity.* Biochem Biophys Res Commun, 1992. **189**(2): p. 885-891.
242. Pascoe, L., Curnow, K.M., Slutsker, L., Rösler, A., and White, P.C., *Mutations in the human CYP11B2 (aldosterone synthase) gene causing corticosterone methyloxidase II deficiency.* Proceedings of the National Academy of Sciences USA, 1992. **89**: p. 4996-5000.
243. White, P.C., Dupont, J., New, M.I., Leiberman, E., Hochberg, z., and Rösler, A., *A Mutation in CYP11B1 (Arg-448->His) Associated with Steroid 11β-Hydroxylase Deficiency in Jew of Moroccan Origin.* Journal of Clinical Investigations, 1991. **87**: p. 1664-1667.
244. Mathew, P.A., Mason, J.I., Trant, J.M., Sanders, D., and Waterman, M.R., *Amino acid substitutions Phe^{66}-->Leu and Ser^{126}-->Pro abolish cortisol and aldosterone synthesis by bovine cytochrome P450$_{11\beta}$.* J. Biol. Chem., 1990. **265**(33): p. 20228-20233.

245. Matsukawa, N., Nonaka, Y., Higaki, J., Nagano, M., Mikami, H., Ogihara, T., and Okamoto, M., *Dahl's Salt-resistant Normotensive Rat has Mutations in Cytochrome P450(11β), but the Salt-sensitive Hypertensive Rat Does Not.* Journal of Biological Chemistry, 1993. **268**: p. 9117-9121.
246. Braatz, J.A., Bass, M.B., and Ornstein, R.L., *An evaluation of molecular models of the cytochrome P450 Streptomyces griseolus enzymes P450SU1 and P450SU2.* J Comput Aided Mol Des, 1994. **8**(5): p. 607-622.
247. Kalb, V.F. and Loper, J.C., *Proteins from eight eukaryotic cytochrome P-450 families share a segmented region of sequence similarity.* Proc. Natl. Acad. Sci. USA, 1988. **85**: p. 7221-7225.
248. Nelson, D.R. and Strobel, H.W., *Evolution of cytochrome P-450 proteins [published erratum appears in Mol Biol Evol 1988 Mar;5(2):199].* Mol Biol Evol, 1987. **4**(6): p. 572-593.
249. Ouzounis, C.A. and Melvin, W.T., *Primary and secondary structural patterns in eukaryotic cytochrome P-450 families correspond to structures of the helix-rich domain of Pseudomonas putida cytochrome P-450cam. Indications for a similar overall topology.* Eur J Biochem, 1991. **198**(2): p. 307-315.
250. Edwards, R.J., Murray, B.P., Boobis, A.R., and Davies, D.S., *Identification and location of α-helices in mammalian cytochromes P450.* Biochemistry, 1989. **28**(9): p. 3762-3770.
251. Nelson, D.R. and Strobel, H.W., *Secondary structure prediction of 52 membrane-bound cytochromes P450 shows a strong structural similarity to P450cam.* Biochemistry, 1989. **28**(2): p. 656-660.

CHAPTER 2

Synthesis of Deuterated Versions of Corticosterone

2.1. Uses of Corticosterone Analogs

Corticosterone is the product of 11β-hydroxylation of 11-deoxy-corticosterone by cytochrome P450 11β-hydroxylase ($P450_{11\beta}$) as well as aldosterone synthase ($P450_{aldo}$). It is one of the glucocorticoid hormones and also an intermediate in the biosynthetic pathway leading to aldosterone. On occasion, $P450_{11\beta}$ is able to hydroxylate corticosterone once more at the C-18 position, forming 18-hydroxycorticosterone [1]. Cytochrome $P450_{aldo}$ (aldosterone synthase) is able to use corticosterone, as a substrate, to make aldosterone (see Chapter 1). Since corticosterone is able to bind to both $P450_{11\beta}$ and $P450_{aldo}$, it can serve as a structural probe for both of these enzymes. Spectroscopically determined iron-corticosterone distances may then offer valuable information on any structural differences in the active sites of these related enzymes.

2.1.1 The Requirements of ESEEM and EXAFS Spectroscopies

Iron-steroid distances have been successfully determined by Groh *et al.* [2] and Joardar [3], for the case of cholesterol side chain cleavage enzyme ($P450_{scc}$). Both of these reports utilized the technique of electron spin echo envelope modulation (ESEEM); Joardar also used extended x-ray absorption fine structure (EXAFS) spectroscopy [3]. Both of these techniques benefit enormously from substrates which exhibit some degree of covalency toward the heme iron.

ESEEM benefits from ligands that are able to induce a low spin in the paramagnetic heme iron. Since ESEEM directly benefits from long paramagnetic relaxation times, low spin complexes (indicative of low spin-orbit coupling) allow data to be collected at longer times; this allows more modulations to be observed which have a direct effect on the resolution of the frequency domain spectrum. Groh et al. [2] capitalized on this when utilizing the (deuterated version of the) low spin inducing [4] 22(*R*)-hydroxy-cholesterol. Joardar's sulfoxide probe was also a low spin inducer [3, 5].

Apart from the benefit added from low spin complexes, ESEEM studies have the absolute requirement of a detectable nuclear spin in the structural probe. The

preferred nuclear spin in such experiments is deuterium. The specific replacement of a hydrogen, from the P450-binding probe, with a deuterium allows one to use spectra from both the protonated and deuterated P450:probe complexes to pull out the specific spin echo modulation arising from the deuterium. Fitting the experimental data to simulations then provides the iron-deuterium distance [6]. Additionally, electron spin echo spectrometers can be specifically tuned to measure deuterium modulations, without any background proton modulations [7].

In the case of EXAFS, a bond between the iron and the substrate helps to diminish the Debye-Waller damping term in the equations used when transforming the raw data into structural information [8]. Joardar's two EXAFS probes (22(*R*)-aminocholesterol and 20(*S*),22(*R*)-22-thiacholesterol-S-oxide) demonstrated good iron coordination from EPR studies [3] - which contributed to a more favorable EXAFS structural determination than would otherwise be the case. EXAFS also benefits from the incorporation of large atoms into the substrate; this advantage was also exploited by Joardar, in the utilization of a sulfur-containing cholesterol analog as a structural probe [3].

2.1.2. Desired Properties in Corticosterone Analogs as $P450_{11\beta}$ Probes

If one wishes to use corticosterone analogs as structural probes for ESEEM and EXAFS studies of $P450_{11\beta}$, the spectroscopic requirements (mentioned above) must be examined. The fact that corticosterone is known to bind only weakly to detergent-solubilized $P450_{11\beta}$ [9], and that it does not completely recruit $P450_{11\beta}$ to the low spin state [10], argues that it may not be the ideal probe for these spectroscopies. However, corticosterone's affinity for liposomal-bound $P450_{11\beta}$ is substantially better [9]. In addition, it is still capable of a 60 to 70% low spin inducement [10]. Therefore, under the proper conditions, corticosterone meets the binding properties of both spectroscopies.

Corticosterone is also ideally set up for a relatively straightforward specific incorporation of deuteriums. With a properly protected version of this steroid, its 11β-hydroxy group can be oxidized to a carbonyl, after which it then has

exchangeable protons (α to the carbonyl atom). This chapter describes the synthesis of the 11-keto version of corticosterone (see **Figure 2.1**). In addition, the incorporation of deuteriums in the C-9 and C-12 positions is described. The deuterated steroids, synthesized in this work, still require further spectroscopic (NMR) evidence before the deuteriums can be assigned to specific carbons.

2.2 Materials

Corticosterone (**1**) was purchased from Merck Sharpe & Dome. *p*-Toluenesulfonic acid and *tert*-Butyldiphenylchlorosilane were obtained from Fluka. All other reagents and solvents were of the highest grade available and used without further purification, unless noted otherwise.

2.3 Methods

All spectra of samples were acquired at MIT, using the chemistry department's NMR, FTIR, and MS instruments and the Orme-Johnson Hewlett Packard diode-array uv-vis spectrophotometer. All NMR samples were prepared in deuterochloroform with tetramethylsilane as an internal standard. NMR spectra were acquired on either the XL-series or Unity 300 MHz Varian spectrometers or on a Brüker 250 MHz spectrometer. Mass spectra were taken using a Finnegan System quadrupole mass spectrometer in electron ionization mode. Infrared samples were prepared by dissolving them in methylene chloride and allowing them to dry as thin films on NaCl plates. FTIR spectra were obtained from a Perkin Elmer 1600 spectrometer.

Purification of reaction products was performed using silica gel chromatography. The first stages of chromatography were generally performed on a Florisil (60-100 mesh; Fisher Scientific) preparatory size flash column. Finer purifications were then performed on a Chromatotron system (Harrison Research; Palo Alto, California).

2.4. Protection of the C-3 and C-20 Carbonyls of Corticosterone

The protection of the C-3 and C-20 carbonyls of corticosterone utilized the strategy of forming cyclic ketals, with ethylene glycol. This was achieved in a single step (see step a of **Figure 2.1**). This reaction was performed several times; a description of an average synthesis follows. One equivalent of corticosterone (**1**) and 30 equivalents of anhydrous ethylene glycol were refluxed in benzene (420 mL for every 5 grams of **1**) with a catalytic amount (0.02 equivalents) of *p*-toluenesulfonic acid. The removal of water, by means of a Dean-Stark apparatus, effected the formation of the first ketal [absorbing in the long uv (as does corticosterone), with a molecular ion peak, by MS, of 390; the 5.668 ppm NMR signal of C-4 vinyl proton still present; strong IR C=O stretch at 1657.8 cm^{-1} still present; this corresponds to the C-20 ketal] and then the other, giving the final product **2** (non-absorbing in the long uv). The reaction was monitored by silica gel TLC in a solvent mixture of ethyl acetate:hexane (6:1) - the C-20 mono-protected compound traveling slower than **1**, but **2** traveling slightly faster than **1**. The total reaction time was generally 8 hours.

The reaction was then quenched with the addition of a saturated $NaHCO_3$ aqueous solution (400 mL for a 5 g reaction with **1**), followed by a work up. The lower aqueous layer was removed using a separatory funnel. The organic layer was then treated with another $NaHCO_3$ wash (200 mL for a 5 g reaction with **1**), followed by removal of the aqueous layer once again. The organic layer was then dried over anhydrous sodium sulfate, after which it was evaporated down to an oil (rotary evaporator, over a ~60°C water bath). This oil was then dissolved in ethyl acetate:hexane (1:1) and applied to a flash column (5 X 40 cm; column material Florisil), equilibrated with the same solvent system. The column was eluted in three stages, using different solvent proportions of ethyl acetate:hexane: 1:1, 3:1, and then 6:1. The best fractions were then pooled and further purified on a Chromatotron plate, using two stages of elution with ethyl acetate:hexane - first with a 6:1 solvent

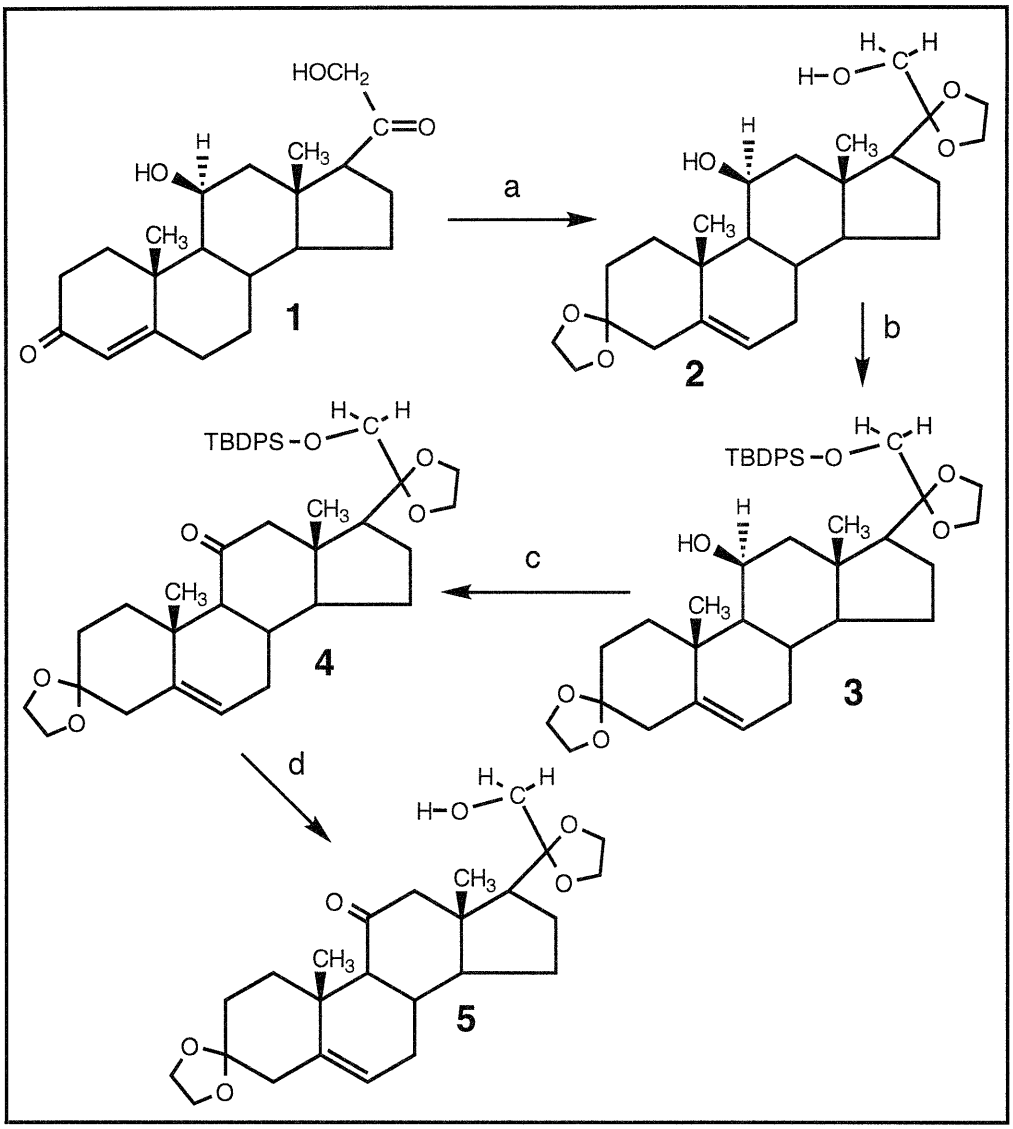

Figure 2.1: Synthesis of the 11-keto version of the C-3 and C-20 protected corticosterone. (a) 30-fold excess of anhydrous ethylene glycol, catalytic amount of *p*-toluenesulfonic acid, benzene, reflux under anhydrous conditions with the additional removal of water; (b) *tert*-butyldiphenyl-chlorosilane, 5 eq. of imidazole (base), methylene chloride:DMF (4:1.3), room temperature; (c) 5 eq. of CrO_3, 12 eq. of pyridine, methylene chloride, room temperature; (d) *tert*-butylammonium fluoride, THF, room temperature.

mixture, followed by a 12:1 mixture. IR (cm^{-1}): 3488.0 (s, O-H stretch), 2941.1 and 2891.5 (s, aliphatic C-H stretches), no C=O stretch seen. ^1H NMR (ppm): 5.234 (t, J=2.25 Hz, C-6 vinyl proton). MS showed a molecular ion peak of 434.

2.5. Protection of the C-21 Hydroxyl Group

The protection the C-21 hydroxy group was performed using the silating reagent *tert*-butyldiphenyl silyl chloride [11] (see step b of **Figure 2.1**). This reagent was chosen due to its bulkiness - which was expected to selectively protect the C-21 primary, over the C-11 secondary, hydroxyl group. The eventual C-21 silyl ether was also expected to be stable to the conditions used for the subsequent oxidation of the C-11 hydroxy to the ketone.

The initial steroid (**2**) (1.97×10^{-2} moles) was combined with 530 mL of methylene chloride:DMF (4:1.3) and imidazole base (0.101 moles). Once, the steroid dissolved, the *tert*-butyldiphenyl silyl chloride (2.36×10^{-2} moles) liquid was added. The reaction was stirred at room temperature, under a water condenser and drying tube. The reaction was monitored by silica gel TLC in a solvent mixture of ethyl acetate:hexane (6:1) - with compound **3**, traveling the fastest.

The reaction was stopped (after 10 hours) with the addition of 500 mL of saturated aqueous solution of $NaCO_3$. The mixture was placed in a separatory funnel, after which the lower organic layer was recovered. The aqueous phase was extracted with 200 mL of ether; the upper organic layer, from this separation, was added to the first organic layer. The pooled organic layers were then dried over anhydrous sodium sulfate, filtered, and evaporated to dryness. The evaporation was performed using a high vacuum rotary evaporator over warm (~60°C) water. Compound **3** was purified from a Florisil column, using a solvent system of ethyl acetate:hexane (6:1). Pure fractions from this column were used in subsequent reactions; less pure fractions were purified further using a Chromatotron. A uv absorbance spectrum of **3** demonstrated the presence of the protecting group; its extinction coefficient at 264 nm was estimated at 0.79 $cm^{-1}g^{-1}L$. IR (cm^{-1}): 3509.9 (a diminished O-H band, compared to **2**), 3067.9 and 3048.5 (w, aromatic C-H stretch), 2932.5 and 2892.8 (s, aliphatic C-H stretches), 1111.5 (s, Si-O-C band). ^1H NMR (ppm): 7.67 (m, possible ortho protons of the phenyl rings), 7.36 (m, possible meta and para protons of the phenyl rings), 5.227 (C-6 vinyl proton). MS: molecular ion peak at 673.

2.6. Formation of the C-11 Carbonyl

The 11-ketosteroid was formed using the reagent dipyridine-chromium(VI) oxide [12, 13] (see step c of **Figure 2.1**). Chromium trioxide (0.106 moles), pyridine (0.211 moles) and methylene chloride (500 mL) were combined and stirred at room temperature for 20 minutes. This resulted in the development of a maroon color. The steroid reactant (**3**) (1.76X 10^{-2} moles) was then added. The mixture was stirred at room temperature and the reaction monitored by silica gel TLC [solvent mixture ethyl acetate:hexane (6:1)] - the fasted moving spot corresponding to the desired product.

The reaction was quenched with the addition of 500 mL of a saturated aqueous solution of $NaHCO_3$. After the organic layer was recovered, the aqueous layer was back- extracted three times with methylene chloride. The pooled organic layer was washed with $NaHCO_3$ once more. This new aqueous layer was then back-extracted with methylene chloride, as before, and pooled with the organic layer. The recovered organic solution was evaporated down to an oil, using a rotary evaporator. The oil was then dissolved in ~30 mL of methylene chloride and filtered to remove particulate material. The brown solution was then twice passed through minimal amounts of silica (eluting with methylene chloride), making the solution less dark. This was evaporated down to an oil once more, after which it was purified on a Florisil flash column, using a solvent system of ethyl acetate:hexaxe (6:1). IR (cm^{-1}): 1759.4 (s, C=O stretch). MS showed a molecular ion peak of 670.

2.7. Removal of the C-21 Silyl Group

Before the incorporation of deuteriums into the target 11-keto steroid, the C-21 silyl group was removed (see step d of **Figure 2.1**). Compound **4** (1.56 X 10^{-2} moles) was dissolved in ~200 mL of THF, in a small vial. Tetrabutyl ammonium fluoride (3.13 X 10^{-2} moles) was then added to the solution. The mixture was stirred at room temperature and stopped after five hours.

The reaction was quenched with saturated aqueous $NaHCO_3$. After recovering the organic layer, the aqueous layer was back-extracted three times with

diethyl ether and pooled with the first organic layer. This new organic layer was then washed with distilled water. After removal of the aqueous phase, the organic layer was evaporated to dryness. The product was then recrystallized by heating it in ethyl acetate and a small amount of hexane; upon cooling crystals formed. IR (cm^{-1}): 3501.4 (s, O-H stretch), no aromatic C-H stretch visible, 2930.3 (s, C-H stretch) 1696.4 (s, C=O stretch). ^1H NMR: no aromatic protons detected. MS showed a molecular ion peak of 432.

2.8 Perdeuteration of C-9 and C-12 of Compound 5

Exchange of the protons on the carbons (which are) α to the C-11 keto carbon of **5**, was performed using sodium deuteroxide in deuterated methanol. Compound **5** (2.77 X 10-3 moles) was combined with NaOD (6.85 X 10^{-2} moles, dissolved in 7.0 mL of D_2O) and deuterated methanol (60 mL). This mixture was refluxed for 4 days, under a water condenser connected to a drying tube. Cooling then gave rise to crystals which were analyzed by MS. The perdeuterated- (at carbons 9 and 12) compound **5** is designated as compound **6** (molecular weight 436.27 g/mole, when the C-21 hydroxyl is deuterated). MS demonstrated a steroid with the parent ion peak of 436 g/mole. Further verification of these positions of deuteration (by NMR) has yet to be performed.

2.9. Deuteration of Compound 5 at the C-9 and C-12α Positions

The α face of the steroid is more accessible and axial protons (on α carbons) are more acidic [14]. As a result, the exchange of the C-9 and C-12α protons was achieved under similar conditions, described in section 2.8, with the exception that the reaction was refluxed for less time. Compound **5** (1.79 X 10-3 moles) was combined with NaOD (4.41 X 10-2 moles) and 60 mL of deuterated methanol and refluxed for four hours. The mixture was then cooled, forming crystals. The 9-deutero,12α-deutero version of compound **5** is designated as compound **7** (molecular weight of 435.26 g/mole when the C-21 hydroxyl is deuterated).

MS demonstrated a parent ion peak of 435 g/mole. Further verification of these positions of deuteration (by NMR) has yet to be performed.

2.10. Back-protonation of Compound 6, Making 12β-Deutero Compound 5

Back-protonation of the (C-9 and C-12) perdeuterated steroid **6** was achieved utilizing similar conditions as was used to make compound **6** itself. Compound **6** (4.59×10^{-4} moles) was combined with NaOH (0.035 moles) and ~100 mL of 70% methanol (in H_2O). This was heated to reflux conditions. Refluxing was continued for 65 minutes, after which the mixture was allowed to cool. The 12β-deutero-compound **5** is designated as compound **8** (molecular weight 433.26 g/mole, when the C-21 hydroxyl is protonated). MS demonstrated a steroid with the parent ion peak of 433 g/mole. Further verification of 12β-position of deuteration of compound **8** (by NMR) has yet to be performed.

References

1. Ohnishi, T., Wada, A., Lauber, M., Yamano, T., and Okamoto, M., *Aldosterone biosynthesis in mitochondria of isolated zones of adrenal cortex.* Journal of Steroid Biochemistry, 1988. **31**: p. 73-81.
2. Groh, S.E., Nagahisa, A., Tan, S.L., and Orme-Johnson, W.H., *Electron Spin Echo Modulation Demonstrates P-450$_{scc}$ Complexation.* J. Am. Chem. Soc., 1983. **105**: p. 7445-7446.
3. Joardar, S., *Mapping the Active Sites of Steroidogenic Cytochromes P-450*, in *Chemistry.* 1993, M.I.T.: Cambridge. p. 197.
4. Orme-Johnson, N.R., Light, D.R., White-Stevens, R.W., and Orme-Johnson, W.H., *Steroid binding properties of beef adrenal cortical cytochrome P-450 which catalyzes the coversion of cholesterol into pregnenolone.* Journal of Biological Chemistry, 1979. **254**: p. 2103-2111.
5. Miao, E., Joardar, S., Zuo, C., Cloutier, N.J., Nagahisa, A., Byon, C., Wilson, S.R., and Orme-Johnson, W.H., *Cytochrome P-450scc-Mediated Oxidation of (20S)-22-Thiacholesterol: Characterization of Mechanism-Based Inhibiton.* Biochemistry, 1995. **34**(26): p. 8415-8421.
6. Mims, W.B., Davis, J.L., and Peisach, J., *The Exchange of Hydrogen Ions and of Water Molecules near the Active Site of Cytochrome c.* Journal of Magnetic Resonance, 1990. **86**: p. 273-292.
7. Kevan, L., *Modulation of Electron Spin-Echo Decay*, in *Time Domain Electron Spin Resonance*, L. Kevan and R.N. Schwartz, Editors. 1979, Wiley: New York. p. 279-341.
8. Teo, B.K., *EXAFS: Basic Principles and Data Analysis.* Inorganic Chemistry Concepts. Vol. 9. 1986, Berlin: Springer-Verlag. 349.
9. Kominami, S., Harada, D., and Takemori, S., *Regulation mechanism of the catalytic activity of bovine adrenal cytochrome P-450(11)beta.* Biochim Biophys Acta, 1994. **1192**(2): p. 234-240.
10. Martsev, S.P., Bespalov, I.A., Chashchin, V.L., and Akhrem, A.A., *[Spectrophotometric study of cytochrome P-450 (11 beta) interaction with physiological effectors]. Spektrofotometricheskoe izuchenie vzaimodeistviia tsitokhroma P-450 (11 beta) s fiziologicheskimi effektorami.* Biokhimiia, 1985. **50**(5): p. 707-724.
11. Hanessian, S. and Lavallee, P., *The preparation and synthetic utility of tert-butyldiphenylsilyl ethers.* 1975. **53**: p. 2975-2977.
12. Collins, J.C., Hess, W.W., and Frank, F.J., *Dipyridine-Chromium(VI) Oxide Oxidation of Alcohols in Dichloromethane.* Tetrahedron Letters, 1968(30): p. 3363-3366.
13. Ratcliffe, R. and Rodehorst, R., *Improved Procedure for Oxidations with the Chromium Trioxide-Pyridine Complex.* J. Org. Chem., 1970. **35**(11): p. 4000-4002.
14. Corey, E.J. and Sneen, R.A., *Stereoelectronic Control in Enolization-Ketonization Reactions.* J. Am. Chem. Soc., 1956. **78**: p. 6269-6278.

CHAPTER 3

Purification of Proteins

Spectroscopic and mechanistic studies of cytochrome P450 11β hydroxylase ($P450_{11\beta}$) requires this P450 enzyme itself and its two electron transfer companion proteins - adrenodoxin (Adx) and adrenodoxin reductase (AdR). All of these proteins are found in the adrenal cortex of mammals. The proteins described in this thesis are from bovine. Conveniently, these adrenal glands can be obtained from beef slaughter houses. Since all of the desired proteins are found in the outer tissue (the cortex) of the gland, an immediate purification can be achieved by dissecting out the inner medullar tissue (which is lighter in color than the cortex). Once the cortex is isolated, the soluble (and highly acidic) Adx can be significantly purified from this homogenated tissue, using an ion exchange resin as a first step. However, since $P450_{11\beta}$ and AdR lack as strong a distinction from other cellular proteins, it is necessary to first isolate the mitochondria, where they are all found.

3.1. Materials and Methods

3.1.1. Materials

Bovine adrenal glands were obtained within 24 hours of slaughtering from Green Bay Dressed Beef (Green Bay, Wisconsin); these glands arrived on wet ice and were never frozen. Protease inhibitors were obtained from Boehringer Mannheim. Cyanogen bromide-activated Sepharose 4B was obtained either from Pharmacia LKB or from Sigma Chemical Company. Octyl-Sepharose 4B, 2'5' ADP-Sepharose 4B, and mono-Q ion exchange columns was acquired from Pharmacia. Nicotinamide adenine dinucleotide phosphate (in the oxidized form) was purchased from Sigma Chemical Company. Ethanolamine was purchased from Aldrich. Bovine serum albumin was obtained from Sigma Chemical Company.

3.1.2. Methods

All uv-vis absorption spectra were acquired on a Hewlett Packard diode array spectrophotometer. Sodium dodecyl sulfate polyacrylamide gel electrophoresis (SDS PAGE) was performed on a Pharmacia Phastgel™ system, using homogeneous 20% acrylamide gels, and stained using silver nitrate-based staining procedures. Mono-Q column chromatography was performed on a Pharmacia FPLC automated

chromatography unit. Quantitation of Adx solutions were made based on a 414 nm extinction coefficient of 10^4 $M^{-1}cm^{-1}$ [1] and an assumed molecular weight of 14.2 kdal (this is the molecular weight of an C-terminal-intact version of Adx). Quantitation of AdR solutions were based on a 450 nm extinction coefficient of 11.3 X 10^3 $M^{-1}cm^{-1}$ and an assumed molecular weight of 52.5 kdal [2]. Protein assays of Adx and AdR employed either the Coomassie blue-based Bio-Rad Protein Reagent or the Lowry method [3], using bovine serum albumin as a standard. Protein assays of cytochrome $P450_{11\beta}$ were based on a so-called modified Lowry method [4], also using bovine serum albumin as a standard. P450 content was determined by the carbon monoxide binding assay [5].

3.2. Isolation of Bovine Adrenocortical Mitochondria (BACM)

Isolation of the bovine adrenocortical mitochondria (BACM) is performed according the method of Omura *et al.* [6] (See **Figure 3.1**). All steps are performed at 5 °C, unless otherwise noted. Once the medulla has been removed, the cortex is homogenized in a buffer of 0.25 M sucrose and 10 mM Potassium phosphate (pH 7.4, 4°C) using a blender (approximately 2 liters for every 2.5 kg of cortical tissue). The resulting homogenate is centrifuged at 2,200 RPM in a Sorval (Dupont Instruments) centrifuge (using a GSA rotor) for 10 minutes. The supernatant is decanted through cheese cloth, after which the pellets are resuspended with 70% of the original volume of buffer used for the original homogenization. This resuspended pellet is then homogenized again - the resulting homogenate centrifuged as before). The supernatant from this centrifugation is decanted through cheese cloth as well, pooling it with the first supernatant. The pellet is discarded.

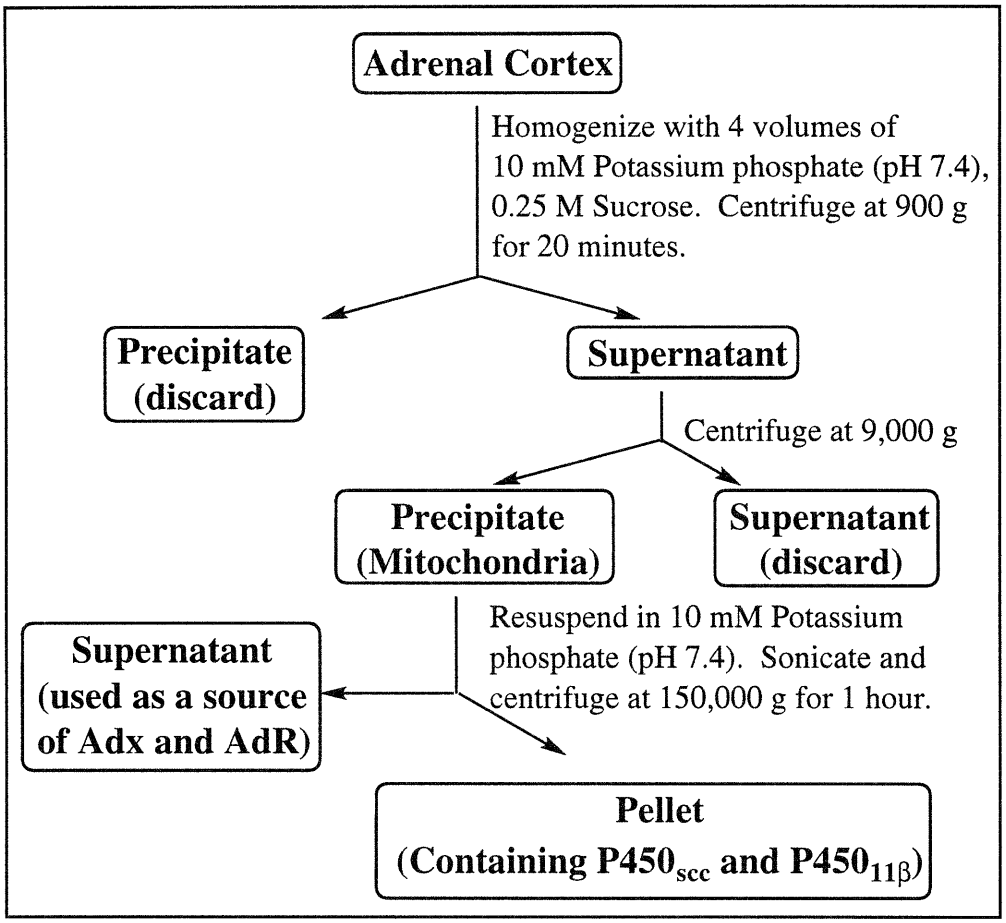

Figure 3.1: The general breakdown of the process of isolating either the soluble interior mitochondrial proteins (Adx and AdR) or the membrane-bound mitochondrial P450 proteins.

The pooled supernatants are further centrifuged at 10,000 RPM (same rotor and centrifuged as before) for 30 minutes. The supernatant is discarded. The pellet contains the adrenocortical mitochondria - predominantly unbroken.

3.3. Isolation of BACM Membranes

The isolated bovine adrenocortical mitochondria are predominantly intact. Disruption of these organelles allows the soluble Adx and AdR proteins to be separated from the membrane-bound $P450_{11\beta}$ and $P450_{scc}$ proteins.

Disruption of the BACM was performed using sonication. BACM was resuspended in 10 mM potassium phosphate (7.4) (~1 liter for every 2 kg of original cortex material). This homogenate was then sonicated in ~100 mL aliquots in an ice-

chilled metal beaker (3 times 20 seconds, duty cycle of 60%, allowing for cooling on ice between sonications), using a Sonics & Materials Vibra Cell; the sonicator probe had the dimensions of 1.9 cm X 6.5 cm.

The sonicated mixture was then centrifuged at high speed to pellet the membranes. Centrifugation was performed using a Beckman ultracentrifuge at 28,000 RPM for 1 hour (type 30 rotor, 4°C). The resulting supernatant contained the Adx and AdR proteins. The pellet contained the P450 membrane proteins.

3.4. Purification of the Specific Proteins

3.4.1. Purification of Adrenodoxin

Due to the fact that adrenodoxin (Adx) is highly acidic and that it is found in high concentrations in the adrenal cortex, it can be directly purified from whole adrenocortical tissue, without further isolation of the mitochondria. Since Adx has been isolated with some degree of heterogeneity at its C-terminal [7] (differential C-terminal truncation), it is possible that endogenous proteases partially degrade this protein upon normal isolation. As a result of this observation, the standard methods of purification of adrenodoxin [8, 9] were revised with the use of protease inhibitor-supplemented buffers, in the early stages of the purification

After the excision of the medulla, the adrenocortical tissue was sliced into smaller sizes and immediately frozen in liquid nitrogen. The frozen tissue (1 kg) was then ground to a powder in liquid nitrogen, using a blender. The frozen powder was then allowed to thaw in 1.75 liters of low salt detergent buffer, containing protease inhibitors (10 mM Tris•HCl (pH 7.5), 10 mM KCl, 0.5% Tween 20, 0.1 mM PMSF, 0.5 μg/mL leupeptin, and 0.7 μg/mL pepstatin).

The cellular debris was removed. The thawed homogenate was centrifuged at 4,300 RPM (Sorval centrifuge, GSA rotor) for 20 minutes. The supernatant was decanted through cheese cloth and saved; the pellet was then extracted with 1 liter of the same buffer, blended again, and centrifuged as above. The supernatants from both centrifugations were pooled and combined with 170 mL of settled DE-52 (equilibrated 10 mM Tris•HCl (pH 7.5), 10 mM KCl, 0.5% Tween 20). The mixture was then mechanically stirred (by propeller, making sure that this not shear the DE-

52 into smaller particles) for 4 hours. The mixture was then centrifuged at 10,000 RPM (Sorval centrifuge, GSA rotor) for 20 minutes. The supernatant was then discarded. The pellet was then resuspended two more times in low salt detergent buffer (10 mM Tris•HCl (pH 7.5), 10 mM KCl, 0.5% Tween 20), centrifuging and discarding the supernatants each time. The pellet was extracted three times with medium salt buffer (10 mM Tris•HCl (pH 7.5), 330 mM KCl) - centrifuging at 10,000 RPM for 30 minutes and saving the supernatants each time. A higher salt concentration could be used (and effects a better elution of Adx from the DE-52), but interferes with the solubility of ammonium sulfate in the next purification step and may also elute a sizable amount of unwanted nucleic acids from the DE-52.

Ammonium sulfate is useful in concentrating Adx solutions. Since Adx is highly soluble, it precipitates only when the concentration of ammonium sulfate is quite high.

Per 100 mL of the DE-52-eluted Adx solution, 29.1 g of ammonium sulfate was slowly added; this rendered the solution 50% saturated in ammonium sulfate. Minimal amounts of 6 M ammonium hydroxide was added to maintain the pH at 7.5. This was then centrifuged at 10,000 RPM (Sorval centrifuge, GSA rotor) for 60 minutes, after which the pellet was discarded. The recovered supernatant was then brought to 95% saturation with ammonium sulfate by adding 30.8 g of the salt for every 100 mL of supernatant. This was centrifuged as above after which the supernatant was discarded.

The pellet (from the 50% through 95% ammonium sulfate fractionation) was then dissolved in a minimal amount of low salt buffer (10 mM Tris•HCl (pH 7.5), 100 mM KCl). This was then chromatographed on a Sephadex G-100 (5 cm X ~90 cm), equilibrated with the same low salt buffer. The sample was applied to the bottom of the column and chased with the same low salt buffer, all with an upward flow. The flow rate used was ~20 mL/hour. 10 mL Fractions were collected and those which were brown in color were examined by uv-vis spectroscopy. Fractions giving rise to spectra that resembled the characteristic absorption pattern of Adx (see **Figure 3.2**) were kept.

The G-100 Adx-containing fractions were then pooled and concentrated by either ammonium sulfate precipitation (50%-95% saturated $(NH_4)_2SO_4$ fraction), described above, or by DE-52 adsorption and elution. Concentration by DE-52 was effected by applying the pooled G-100 fractions to a DE-52 column (equilibrated with 10 mM Tris•HCl (pH 7.5), 100 mM KCl). Once all of the Adx was adsorbed onto the top of the column, the brown colored band was removed and placed into a smaller column cylinder. This brown DE-52 column, with a saturated amount of Adx was then eluted with a minimal amount of high salt buffer (10 mM Tris•HCl (pH 7.5), 500 mM KCl).

The concentrated Adx solution was then applied to a Sephadex G-50 column (2.5 cm X ~90 cm), equilibrated with high salt buffer (10 mM Tris•HCl (pH 7.5), 500 mM KCl). As in the case of the G-100 column, the sample was also applied from the bottom and chased with buffer (this time high salt buffer) in the upward flow mode. The column was eluted at a flow rate of ~20 mL/hour; 5 mL fractions were collected. Fractions were analyzed by uv-vis spectroscopy; fractions of similar purity were pooled and reprocessed on the G-50 column until the ratio of the absorbance at 414 nm to that at 280 nm was greater than 0.8. SDS PAGE revealed a single band with a molecular weight of ~13 kdal. A sample of this quality was used to make an Adx-Sepharose affinity column (see section **3.4.2.**).

When adrenodoxin was to be used for XAFS and EPR spectroscopy, it was purified still further using mono-Q ion exchange chromatography (Pharmacia LKB). The electrophoretically pure adrenodoxin (equilibrated in 20 mM Tris•HCl (pH 7.5), 100 mM KCl; **buffer A**) was applied to a mono-Q column (also equilibrated with buffer A). Adx was then eluted with a linear gradient of **buffer A** and **buffer B** (100 mM Tris•HCl (pH 7.5), 500 mM KCl). Fractions with absorbance ratios (414 nm to 280 nm) over 0.9 were achieved with this purification step.

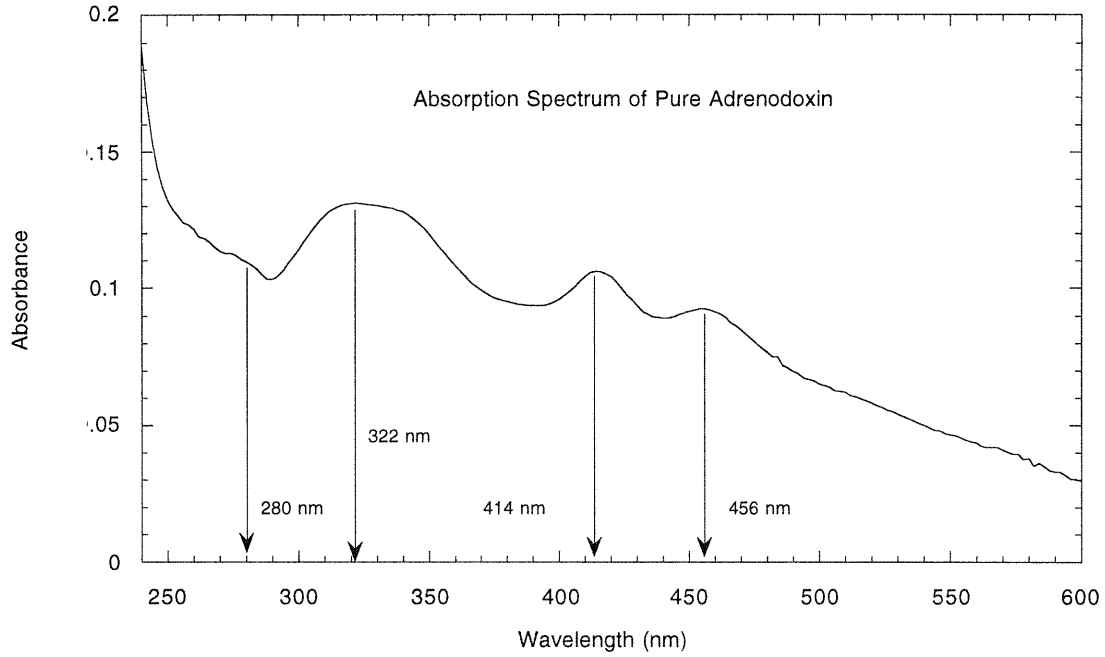

Figure 3.2: The absorption spectrum for pure adrenodoxin. The ratio of the absorbance at 414 nm to 280 nm, for this sample, is 0.97.

3.4.2. The Making of an Adrenodoxin-Sepharose Affinity Matrix

Since AdR and $P450_{11\beta}$ are both able to bind to Adx (see **Figure 1.9A**), an Adx-based affinity column can be used to significantly purify these two proteins. Cyanogen bromide activated Sepharose, commercially available, offers a convenient means of coupling Adx to an insoluble matrix.

Purified Adx was first exchanged with coupling buffer (0.1 M $NaHCO_3$ (pH 8.1), 0.5 NaCl), to remove the Tris buffer used in its purification; tris (being a primary amine) would compete with Adx in coupling to CN-Br-activated Sepharose. This was performed either by passing it through a Sephadex G-15 column (equilibrated with coupling buffer) or by dialyzing it against coupling buffer.

A typical coupling procedure follows: Cyanogen bromide-activated Sepharose 4B was swelled in 1 mM HCl for 30 minutes. This was then filtered through a coarse glass filter funnel. It was then washed 3 times with 20 mL of coupling buffer and then quickly transferred to a 25 mL sample of Adx (~40 mg, in coupling buffer). This mixture was gently shaken at room temperature for 3 hours. The suspension was then filtered to give a brown resin and a clear flow-through solution. The excess

coupling sites on the brown Adx-Sepharose material were blocked with a blocking buffer [1 M ethanolamine in coupling buffer (pH 8.2)] and gently shaken at room temperature for 3 hours. The affinity-matrix was filtered and then washed - first with three times 20 mL of blocking buffer and then three times 20 mL of 1 M potassium phosphate (pH 7.4). This material was then stored at 5 °C.

3.4.3. Purification of Adrenodoxin Reductase

The supernatant from centrifuging the sonicated BACM contains both Adx and AdR. AdR can be separated Adx (as well as purified from other contaminating protein) by ammonium sulfate fractionation, size exclusion chromatography, affinity chromatography, and ion exchange chromatography. In the case of affinity chromatography, 2'5' ADP-Sepharose can be used to selectively bind NADPH-binding proteins; alternatively, Adx-Sepharose can be used to selectively bind AdR.

An AdR purification procedure follows. The BACM supernatant was brought to 30% saturation of ammonium sulfate by adding 16.4 g of $(NH_4)_2SO_4$ for every 100 mL of protein solution. This was then centrifuged at 10,000 RPM (Sorval centrifuge, GSA rotor) for 60 minutes. The pellet was discarded, but the supernatant was then brought to 60% saturation of $(NH_4)_2SO_4$ by adding 18.1 g of $(NH_4)_2SO_4$ for every 100 mL of supernatant. This was then centrifuged as before, after which the pellet was used for further AdR purification; the supernatant was brought to 95% of $(NH_4)_2SO_4$, saturation (23.9 g of $(NH_4)_2SO_4$ per 100 mL of supernatant), after which Adx was purified from it (see section **3.4.1.**).

The AdR $(NH_4)_2SO_4$ fraction was then dialyzed against 10 mM potassium phosphate (pH 7.4), 70 mM KCl. This solution was then centrifuged at 17,000 RPM (Sorval centrifuge, SS-34 rotor) after which it was filtered through a 0.22 μm (Millipore low protein binding) filter. This clarified solution was then applied to an Adx-Sepharose column (equilibrated with 10 mM potassium phosphate (pH 7.4), 70 mM KCl). AdR was then eluted with 10 mM potassium phosphate (pH 7.4), 400 mM KCl.

Adx-Sepharose eluted yellow fractions were pooled and precipitated by bringing the solution up to 60% $(NH_4)_2SO_4$ saturation by adding 36.1 g of $(NH_4)_2SO_4$

per 100 mL of sample. This AdR precipitate was dissolved in a minimal amount of 10 mM potassium phosphate (pH 7.4), 400 mM KCl. This concentrated AdR sample was then purified on Sephadex G-100 column (2.5 cm X 100 cm, equilibrated in 10 mM potassium phosphate (pH 7.4), 400 mM KCl). The sample was applied at the bottom of the column and chased with the 400 mM KCl phosphate buffer, running the column in the upward flow manner at ~20 mL/hour.

The most yellow Sephadex G-100 fractions were then pooled and dialyzed against 10 mM potassium phosphate (pH 7.4). This was then applied to a 2'5' ADP-Sepharose 4B column (equilibrated with same buffer). The AdR-loaded column was washed with 50 mM potassium phosphate (pH 7.4). AdR was then eluted with 50 mM potassium phosphate (pH 7.4), 0.5 mM NADP (sodium salt). SDS PAGE of this sample gave a single band at a molecular weight of ~50 kdal. An absorption spectrum of AdR is given in **Figure 3.3**.

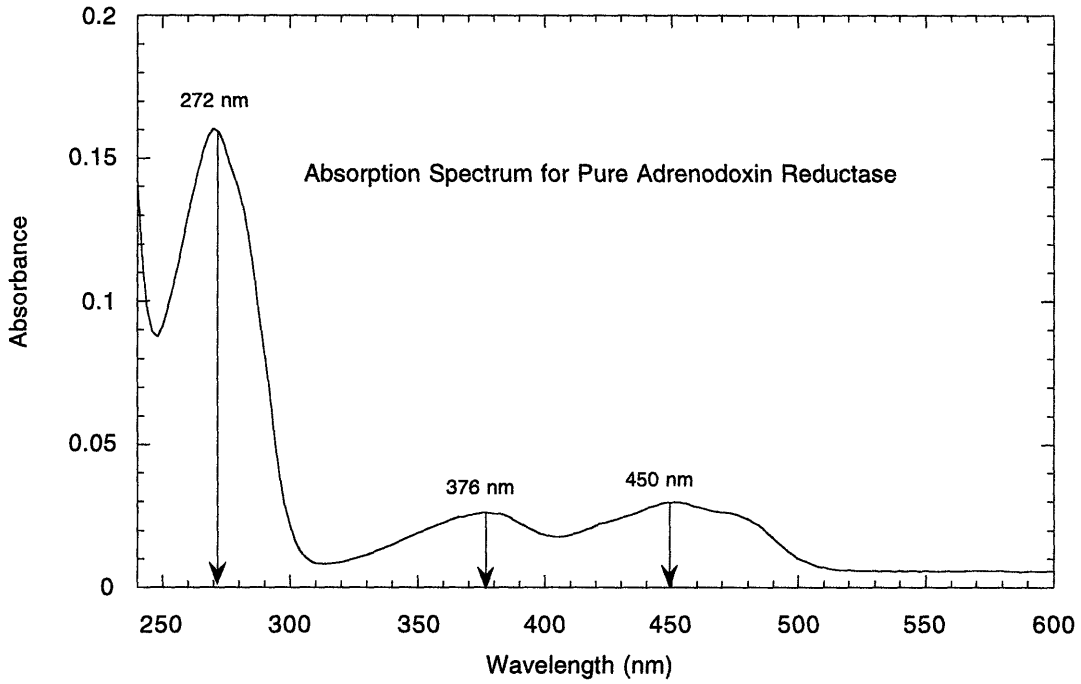

Figure 3.3: The uv-vis absorption spectrum for purified adrenodoxin reductase. The ratio of absorbances at 450 nm to 272 nm is 0.188, for this sample.

3.4.4. Purification of $P450_{11\beta}$

The isolated BACM membranes contain both $P450_{11\beta}$ and $P450_{scc}$. These proteins can be separated based on their differences in solubility. Since $P450_{11\beta}$ is more lipophilic than $P450_{scc}$, it is found predominantly in the 0%-33% $(NH_4)_2SO_4$ fraction, whereas $P450_{scc}$ can be found in the 33%-45% $(NH_4)_2SO_4$ fraction [10-12]. In addition $P450_{11\beta}$ precipitates when it is dialyzed against buffers containing no detergents, whereas $P450_{scc}$ is considerably more soluble. A purification procedure for $P450_{11\beta}$ (based on the method of Tsubaki et al. [13]) is given below.

BACM membranes were homogenized with standard buffer (50 mM potassium phosphate pH 7.4, 0.1 mM dithiothreitol, 0.1 mM EDTA, 20 mM 11-deoxycorticosterone) to a protein concentration of ~20 mg/mL (as determined by a Bio-Rad assay). This mixture was then brought up to 1% (w/v) in sodium cholate, in order to solubilize the proteins. This was then centrifuged at 28,000 RPM (Beckman ultracentrifuge, type 30 rotor) to removed any insoluble material. The supernatant was then brought to 33% saturation with $(NH_4)_2SO_4$ (by adding 18.20 g of $(NH_4)_2SO_4$ per 100 mL of solution). The protein suspension was then centrifuged at 10,000 RPM (Sorval centrifuge, GSA rotor) for 60 minutes. The pellet was then processed further.

The 0%-33% $(NH_4)_2SO_4$ fraction was homogenized in standard buffer and dialyzed against the same buffer. This step allowed contaminating $P450_{scc}$ to dissolve and for $P450_{11\beta}$ to remain in precipitated form. The dialysate suspension was then centrifuged at 10,000 RPM (Sorval centrifuge, GSA rotor) for 60 minutes. The pellet was homogenized with standard buffer containing 1% (w/v) sodium cholate. The protein mixture was centrifuged at 28,000 RPM (Beckman ultracentrifuge, type 30 rotor) to remove any insoluble material. The supernatant was then diluted with standard buffer to render the solution 0.7% (w/v) in sodium cholate. This was then applied to an octyl-Sepharose 4B column, equilibrated with standard buffer containing 0.7% (w/v/) sodium cholate, creating a brown band. After washing the column with the same buffer, the brown band was scooped out and placed into another column cylinder. $P450_{11\beta}$ was then eluted, from the brown octyl-Sepharose

column material, with standard buffer containing 300 mM KCl and 1% (w/v) sodium cholate. Dark colored fractions with absorbance ratios (of 390 nm to 280 nm) greater than 0.2 were pooled.

The pooled octyl-Sepharose-eluted sample was dialyzed against standard buffer. This caused $P450_{11\beta}$ to precipitate. The dialysate-suspension was then centrifuged at 28,000 RPM (Beckman ultracentrifuge, type 30 rotor) for 60 minutes. The pellet was dissolved in 5-fold diluted standard buffer, containing 0.5 % (v/v) Tween 20 and 1% potassium cholate. This was applied to an Adx-Sepharose affinity column (equilibrated with the same buffer). After washing the column with the same buffer, $P450_{11\beta}$ was eluted with standard buffer containing 0.5% (v/v) Tween 20 and 0.2 % (w/v) potassium cholate. The eluted sample (8.3 nmole of P450 per mg of protein) gave a single band on SDS PAGE and gave a $P450_{11\beta}$-specific EPR signal (with no contaminating $P450_{scc}$). This sample was used for EXAFS experiments. Its uv-vis absorption spectrum is given in **Figure 3.4**.

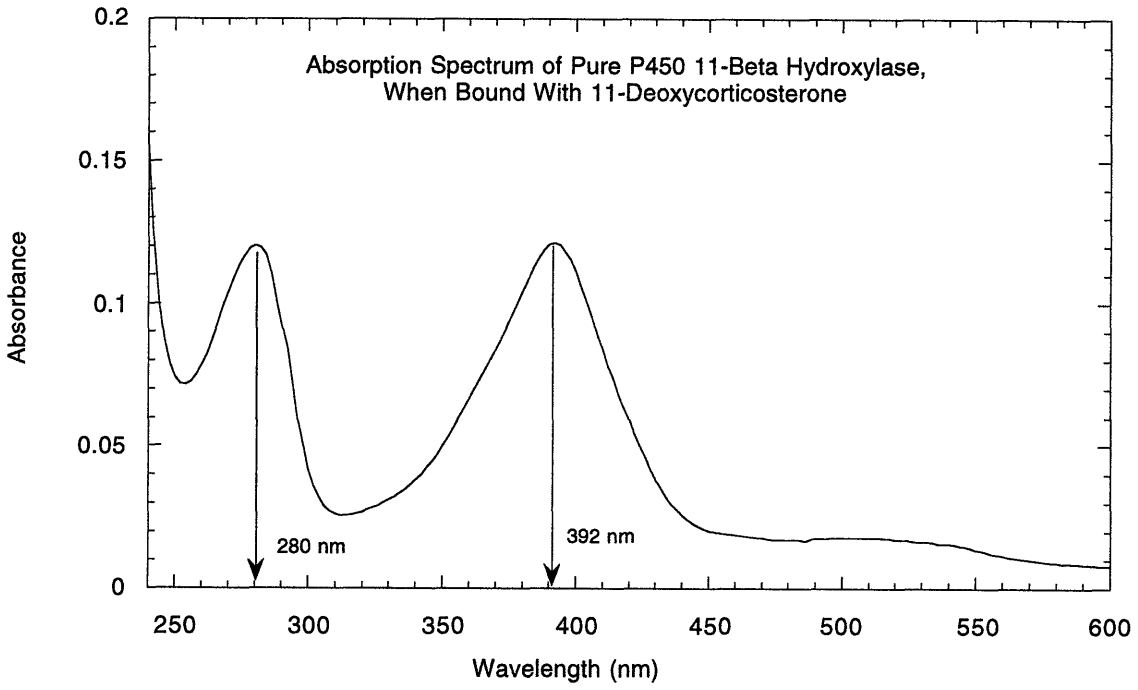

Figure 3.4: The uv-vis absorption spectrum of purified $P450_{11\beta}$, bound with 11-deoxycorticosterone.

References

1. Hiwatashi, A., Ichikawa, Y., Yamano, T., and Maruya, N., *Properties of crystalline reduced nicotinamide adenine dinucleotide phosphate-adrenodoxin reductase from bovine adrenocortical mitochondria. II. Essential histidyl and cysteinyl residues at the NADPH binding site of NADPH-adrenodoxin reductase.* Biochem., 1976. **15**(14): p. 3091-3097.
2. Hiwatashi, A., Ichikawa, Y., Maruya, N., Yamano, T., and Aki, K., *Properties of crystalline reduced nicotinamide adenine dinucleotide phosphate-adrenodoxin reductase from bovine adrenodocortical mitochondria. I. Physicochemical properties of holo- and apo-NADPH-adrenodoxin reductase and interaction between non-heme iron proteins and the reductase.* Biochem., 1976. **15**(14): p. 3082-3090.
3. Lowry, O.H., Rosebrough, N.J., Farr, A.L., and Randall, R.J., *Protein measurement with the Folin phenol reagent.* J. Biol. Chem., 1951. **193**: p. 265-275.
4. Peterson, G.L., *A Simplification of the Protein Assay Method of Lowry et al. Which is More Generally Applicable.* Analytical Bichemistry, 1977. **83**: p. 346-356.
5. Omura, T. and Sato, R., *The Carbon Monoxide-binding Pigment of Liver Microsomes. II. Solubilization, Purification, and Properties.* The Journal of Biological Chemistry, 1964. **239**: p. 2379-2385.
6. Omura, T., Sanders, E., Estabrook, R.W., Cooper, D.Y., and Rosenthal, O., *Isolation from Adrenal Cortex of a Nonheme Iron Protein and a Flavoprotein Functional as a Reduced Triphosphopyridine Nucleotide-Cytochrome P-450 Reductase.* Archives of Biochemistry and Biophysics, 1966. **117**: p. 660-673.
7. Cupp, J.R. and Vickery, L.E., *Adrenodoxin with a COOH-terminal deletion (des 116-128) exhibits enhanced activity.* Journal of Biological Chemistry, 1989. **264**: p. 1602-1607.
8. Lambeth, J.D. and Kamin, H., *Adrenodoxin reductase¥adrenodoxin complex. Flavin to iron-sulfur electron transfer as the rate-limiting step in the NADPH-cytochrome c reductase reaction.* J. Biol. Chem., 1979. **254**(8): p. 2766-2774.
9. Suhara, K., Takemori, S., and Katagiri, M., *Improved purification of bovine adrenal iron-sulfur protein.* Biochim. Biophys. Acta, 1972. **263**: p. 272-278.
10. Hanukoglu, I., Privalle, C.T., and Jefcoate, C.R., *Mechanisms of ionic activation of adrenal mitochondrial cytochromes P-450$_{scc}$ and P-450$_{11\beta}$.* Journal of Biological Chemistry, 1981. **256**: p. 4329-4335.
11. Katagiri, M., Takemori, S., Itagaki, E., Suhara, K., Gomi, T., and Sato, H., *Characterization of Purified Cytochrome P-450$_{scc}$ And P-450$_{11\beta}$ From Bovine Adrenocortical Mitochondria*, in *Iron And Copper Proteins*, K.T. Yasunobu, H.F. Mower, and O. Hayaishi, Editors. 1976, Plenum Press: New York and London. p. 281-289.
12. Suhara, K., Gomi, T., Sato, H., Itagaki, E., Takemori, S., and Katagiri, M., *Purification and immunochemical characterization of the two adrenal cortex mitochondrial cytochrome P-450-Proteins.* Arch. Biochem. Biophys., 1978. **190**(1): p. 290-299.
13. Tsubaki, M., Ichikawa, Y., Fujimoto, Y., Yu, N.-T., and Hori, H., *Active site of bovine adrenocortical cytochrome P-450$_{11\beta}$ studied by resonance Raman and electron paramagnetic resonance spectroscopies: distinction from cytochrome P-450$_{scc}$.* Biochem., 1990. **29**: p. 8805-8812.

CHAPTER 4

EPR and ESEEM Experiments on Heme Model Compounds

4.1. Background and Significance of These Studies

Until the crystal structure of $P450_{cam}$ was determined in 1985 [1], the nature of its heme axial ligands were an issue of some controversy. From spectroscopic studies on model compounds, it was clear that one of the ligands was a thiolate [2-4]. Carbon monoxide, bound to model ferrous (thiolato) hemes reproduced the characteristic 450 nm absorption peak [5]. The remaining axial ligand of $P450_{cam}$ is displaced when substrate binds - causing the ferric heme iron to adopt a five-coordinate structure [3]. Speculation of the displaced ligand's identity ranged from an oxygen [6] (from either water or an endogenous hydroxy side chain from an active site amino acid) to nitrogen [7] (from an active site residue). The crystal structure revealed that ligand to be oxygen from either water or hydroxide. However, Peisach *et al.* [7] reported 'definitive' proof that one of the axial ligands was indeed a nitrogen; they even went so far as to say that it was most likely an imidazole. Evidence for this putative imidazole was acquired using the spectroscopic technique of electron spin echo envelope modulation (ESEEM).

Further ESEEM studies on $P450_{cam}$ were performed by Zuo [8] (in collaboration with Prof. John Dawson of the University of South Carolina). Zuo found no ^{14}N modulations when performing ESEEM studies while exciting g_z transitions. However, when exciting g_y and g_x transitions, Zuo found similar low frequency peaks that Peisach *et al.* [7] reported. Zuo reported that these signals had large Fermi contact terms and suggested that they were caused by porphyrin pyrrole nitrogens.

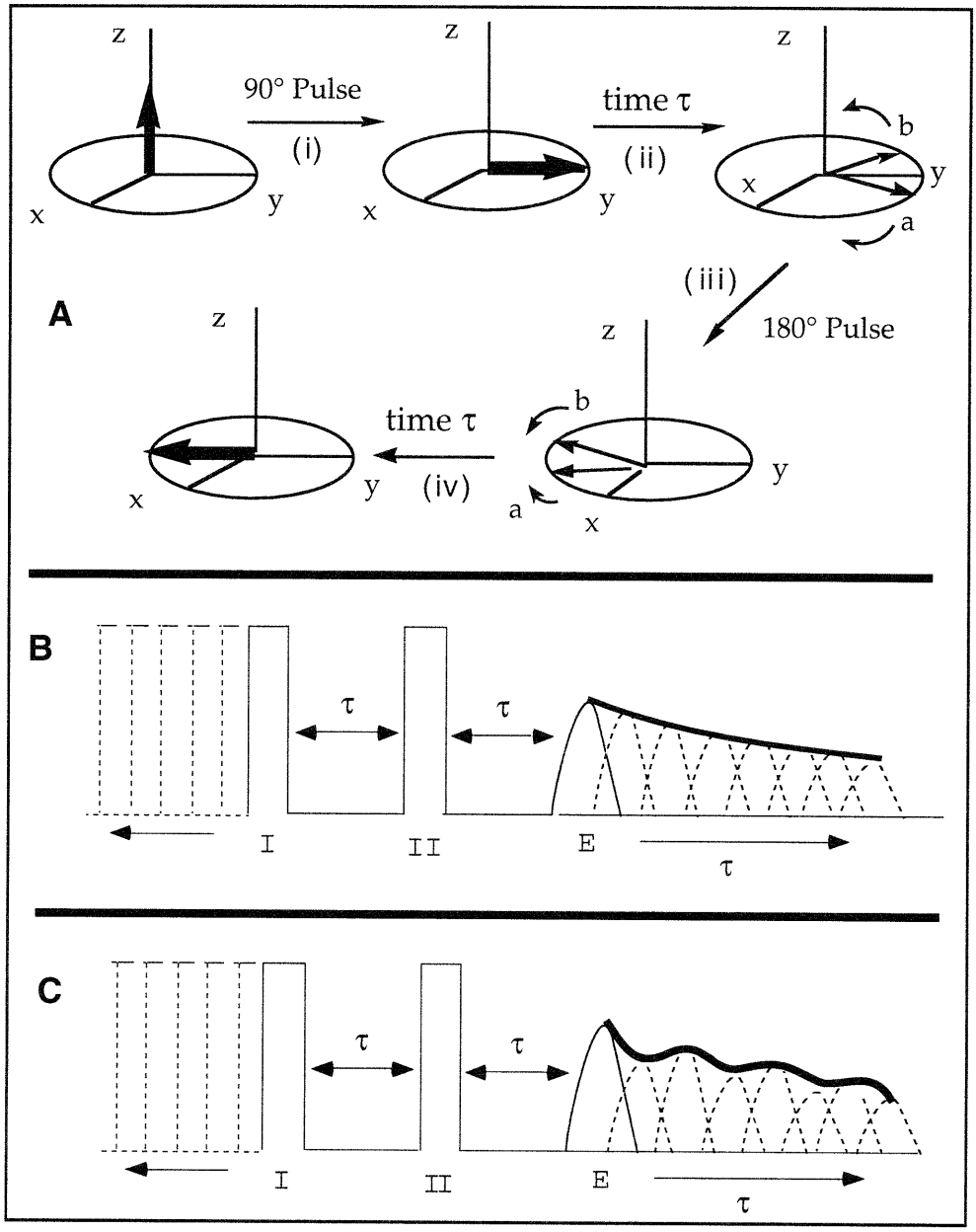

Figure 4.1: **A**. The generation of an electron spin echo, generated by two microwave pulses: (i) the bulk net magnetization is deflected from its orientation along the positive z-axis to the positive y-axis with a 90° pulse, (ii) a period of time τ is permitted to go by, which gives rise to a dephasing of individual spin packets from the bulk, (iii) a 180° pulse causes the y-coordinate to change sign, (iv) after a period of time τ (same value as before) passes, the individual spin packets refocus on the negative y-axis. **B**. Measuring echo amplitudes (for a series of different τ values), of magnetically isolated electron spins, reveals a smoothly decaying function. **C**. The echo amplitude decay has a noticeable modulation when nearby nuclei are close enough to affect the paramagnet's relaxation rate.

4.2. The ESEEM Technique

ESEEM is an ideal technique for measuring the interaction of relatively weakly coupled nuclei to paramagnets ; electron nuclear double resonance (ENDOR) spectroscopy is the complementary technique which is used for studying strongly coupled nuclei. ESEEM and ENDOR, in essence, provide the nuclear magnetic resonance (NMR) spectrum of only nuclei which are interacting with the paramagnetic. Therefore, the paramagnet serves as an "NMR flashlight" within a limited volume around itself. Electron spin echoes are (in a sense) the 'carrier wave' that enables us to observe the nuclear signal.

Electron spin echoes are generated by subjecting a paramagnetic sample to a sequence of microwave pulses (see **Figure 4.1**). Although almost any sequence of multiple pulses can generate spin echoes, echoes created by a 90° and 180° can be explained with the simple vector notation. However, despite their pedagogical simplicity, two-pulse echoes suffer from two limitations: (1) the echo decay envelope diminishes quickly and (2) its modulated decay contains (in addition to the frequencies of the interacting nuclei) the sums and differences of the nuclear frequencies. The rate of decay of two-pulse echoes are a result of the T_2 paramagnetic relaxation time. However, two-pulse echoes have the advantage that they can detect all interacting nuclei; this will be explained below, when describing three-pulse echoes and the experimental results.

The three-pulse method entails a series of three 90° pulses (see **Figure 4.2**), where the spacing between the first and second (τ) is fixed while that between the second and third pulse (T) is varied. Vector diagrams depicting this method of echo generation are complicated and do not easily lend themselves to a visual understanding of what causes the echo. Suffice it to say that the first two echoes (along with its intervening time delay τ) stimulate a population difference in the +z and -z components in the bulk magnetization [9]. The third pulse (which by itself would simply cause a free induction decay of the z component of the bulk magnetization) causes the population difference to manifest itself into an echo at a time τ later. This stimulated population difference has prompted the nick name for

the three-pulse echo as the 'stimulated' echo. If paramagnetics are magnetically isolated, stimulated echo envelopes give rise to a smoothly decaying function, depending on the T_1 relaxation time. But, as in the case of the two-pulse technique, if a nuclear spin interacts with the electron spin, a modulation is observed.

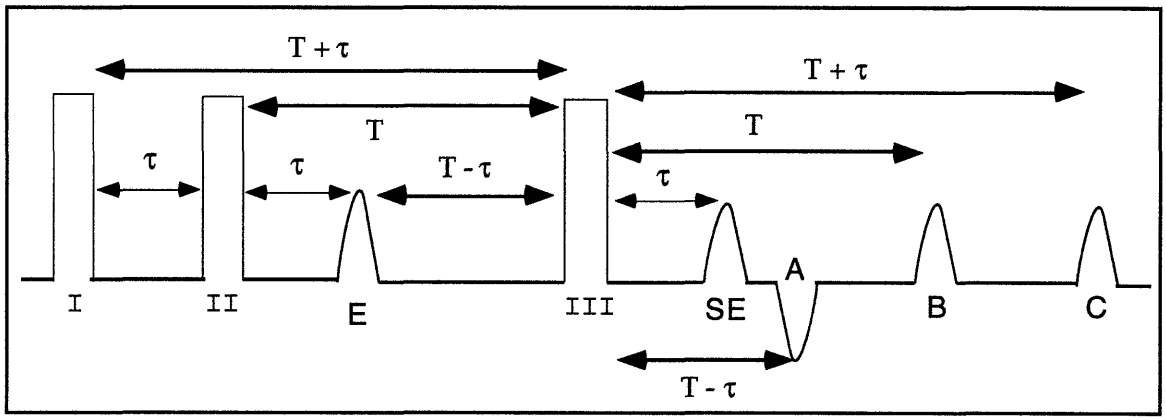

Figure 4.2: Three-pulse sequence for electron spin echo formation. Pulses I and II stimulate the z-polarized population difference; they also give rise to a two-pulse echo (E) at time τ later. Pulse III gives rise to a stimulated echo (SE) at time t later. A series of other unwanted two-pulse echoes are also generated (A, B, and C); these can be eliminated by sampling the data in a repetitive cycle, using specific phases of the applied pulses [10]. Echoes A, B, and C are the two pulse echoes arising from a combination of pulse III with either echo E, pulse II, or pulse I, respectively. This figure was adapted from reference [9].

Three-pulse sequences have a variety of advantages over two-pulse experiments. One can measure decay modulations at longer times; this permits the resolution of low frequency components. It is also possible (with a judicious choice for τ) to suppress specific frequency components. As a result, this method provides a means for two-dimensional spin echo spectroscopy. In addition, this technique gives only the unique nuclear frequencies, without their sums and differences. The durability of the echo decay envelope relates to the fact that the nuclear spins affect the paramagnet's T_1 relaxation time, which is always longer than it T_2 time.

After the echo envelope is acquired, there are some preliminary steps that must be performed on the data before it can be accurately interpreted. The spectrum must usually be either reconstructed at low time points or it must truncated. Additionally, the decaying background must be removed.

The problem arising from low time points of the spectrum result from the spectrometer dead time. Since the instrument pulses high intensity microwave

bursts into the ESEEM cavity, this energy must dissipate before the detectors can observe any refocussed echo. The time required to dissipate the microwaves from the cavity is called the ring down time. One can alter the ring down time by adjusting the impedance-matching of the cavity to the wave guide (connecting it to the amplified microwave source); however, no matter how much this 'bleeding' time is shortened, it will still be large enough to be noticeable on the final spectrum.

Another source of low time artifacts is a result of the choice of spectrometer design and components. In some electron spin echo spectrometers (e.g. the one present in the Orme-Johnson laboratory), the downstream detector is permanently unshielded from cavity. Consequently, when the microwave amplifier pulses the cavity, the detector amplifier (in a sense) gets blinded. This blinding of the detector introduces another factor affecting low acquisition times - the detector 'wake-up' time. This problem has been corrected in some laboratories (e.g. that of Prof. Jack Peisach of Albert Einstein College of Medicine) by the use of a microwave intensity limiter between the cavity and the detector, in tandem with a high speed (timer controlled) switch, between the limiter and the detector. However, the high cost of such components has inhibited their implementation into the Orme-Johnson spectrometer.

Dead time artifacts are dealt with by either reconstructing these data points from the periodicity of the remaining data points [11] or by removing them entirely. Since the technique of dead time reconstruction requires data from the remainder of the spectrum, it adds no new information. The reason why it is performed at all is to be able to perform a cosine fourier transform on the time domain data - without changing the phase of the resulting (complex) frequency-domain version of the data.

If this dead time region is simply removed, one must perform additional manipulations of the data. The remaining ("dead-time-less") data can be left justified , after which the background must be removed - followed with a filling of a sufficient number of zeros at the right of the new shorter spectrum. This zero filling enables one to use the fast fourier transform procedure. Alternatively, the original spectrum can be multiplied by an extended cosine bell window function and zero filled before performing the fourier transform.

The decay background of an ESEEM spectrum needs to be removed before a fourier transform can be performed. The consequence of not doing so is frequency-domain data possessing a significant sloping background; this can hide (especially) low frequency peaks. However, the nature of this background is often more complicated than a simple exponential decay [12]. A high-order polynomial can often be used without adversely affecting the data. However, one should check the fourier transform of the fitted background function to determine whether or not it removes frequency intensity in region of interest.

4.3. Materials and Methods

4.3.1. Materials

Irradiated sucrose was a gift from Dr. Ralph Weber of Brüker. ^{15}N Heme (^{15}N imidazole)$_2$, ^{14}N Heme (^{14}N imidazole)$_2$, ^{15}N Heme (^{14}N imidazole)$_2$, ^{14}N Heme (^{15}N imidazole)$_2$, ^{14}N Heme ($SCH_2COOCH_2CH_3$)$_2$, and ^{15}N Heme ($SCH_2COOCH_2CH_3$)$_2$ were provided by the laboratory of Prof. John Dawson of the University of South Carolina. Horse heart myoglobin was purchased from Sigma Chemical Company.

4.3.2. Methods

EPR spectra were acquired on the MIT Chemistry Department's Brüker ER series X-band CW spectrometer (at 9.44 GHz), using a commercial liquid helium circulating Oxford cryostat. Concentrations of the heme iron for each model compound was determined by spin quantitation [13] using a standard 0.363 mM (low spin) myoglobin azide standard. ESEEM spectra were taken on the home-made electron spin echo spectrometer of the laboratory of prof. W. H. Orme-Johnson. Its design [14, 15] and modifications [8] are described elsewhere. Cryogenic ESEEM temperatures were achieved with cold helium gas by heating liquid helium, forcing it through a transfer line that delivered it to the ESEEM cavity. A calibrated 100 Ω carbon resistor thermocouple (in close proximity with the cavity) was used to determine the temperature of each ESEEM experiment.

The spectrometer is controlled by a program called ANLESE (Argon National Laboratories Electron Spin Echo), running on a Nicolet 1180E computer. This

program was written by Dr. Mike Bowman, by partially modifying an NMR acquisition program. Due to the incompleteness of the program, it was necessary to verify that ANLESE was providing the requested spectra. A discrepancy between the requested spectral width (50 MHz) and that resulting from the actual data (25 MHz) was discovered by using the standard γ-irradiated sucrose (see **Appendix 4.1** of this chapter).

Data files were then downloaded (using the kermit transfer protocol) to an Apple Macintosh (SE) computer, directly wired (via RS232 cable) to the Nicolet computer. Data files (consisting of 20 bit integer numbers) was converted to 32 bit integers with the use of a program given in **Appendix 4.2** of this chapter.

Dead time regions of the acquired spectra were excised. This was followed by fitting the background of each spectra to fifth-order polynomials (performed using Kaleidagraph version 3.0). The "background-removed" spectra were then left justified and a sufficient number of zeros (enough for a fast fourier transform) placed at the far right. Fourier transforms and power spectra were computed using Matlab 4.2d (for the Power Macintosh).

4.4. Results

4.4.1. EPR Spectra

EPR spectra of ^{15}N Heme (^{15}N imidazole)$_2$, ^{14}N Heme (^{14}N imidazole)$_2$, ^{15}N Heme (^{14}N imidazole)$_2$, ^{14}N Heme (^{15}N imidazole)$_2$, ^{14}N Heme ($SCH_2COOCH_2CH_3$)$_2$, and ^{15}N Heme ($SCH_2COOCH_2CH_3$)$_2$ were acquired (see **Figure 4.3** through **Figure 4.8**, respectively). Estimated concentrations of these species is given in **Table 4.1**.

Sample	Concentration (mM)
^{15}N Heme (^{15}N imidazole)$_2$	0.0687
^{14}N Heme (^{14}N imidazole)$_2$	0.143
^{15}N Heme (^{14}N imidazole)$_2$	0.204
^{14}N Heme (^{15}N imidazole)$_2$	0.0889
^{14}N Heme ($SCH_2COOCH_2CH_3$)$_2$	0.0735
^{15}N Heme ($SCH_2COOCH_2CH_3$)$_2$	0.0170

Table 4.1: Concentration of the heme model compounds, determined by spin quantitation, using myoglobin as a standard. The concentrations here depict that of the low spin signal of each sample.

From Figures 4.7, and 4.8, it is apparent that there are some high spin components to these spectra. This has most likely resulted from sample decomposition over time. However, since these high spin components relax much more quickly, they should be relatively silent during ESEEM acquisition. The worst effect of the high spin regions is that they lower the effective concentration of the species giving rise to the ESEEM.

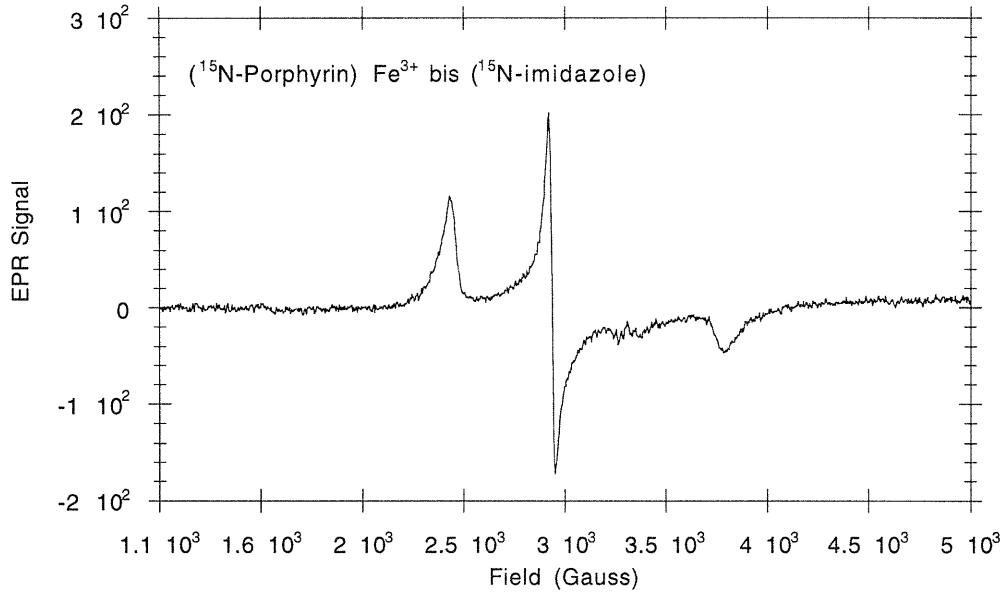

Figure 4.3: CW EPR spectrum of ^{15}N Heme (^{15}N imidazole)$_2$ at 10 K and 9.44 GHz.

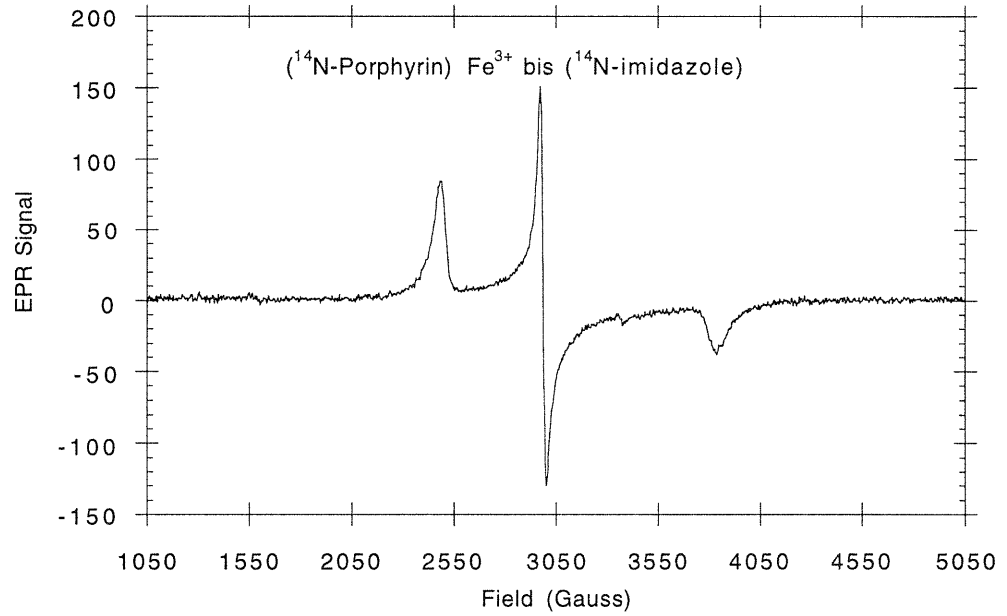

Figure 4.4: CW EPR spectrum of ^{14}N Heme (^{14}N imidazole)$_2$ at 10 K and 9.44 GHz.

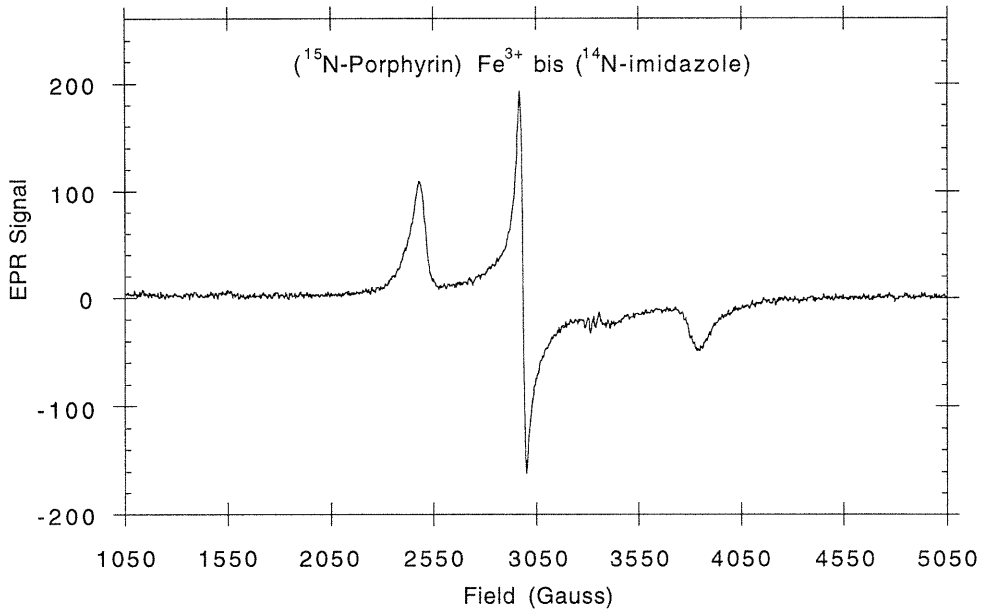

Figure 4.5: CW EPR spectrum of ^{15}N Heme (^{14}N imidazole)$_2$ at 10 K and 9.44 GHz.

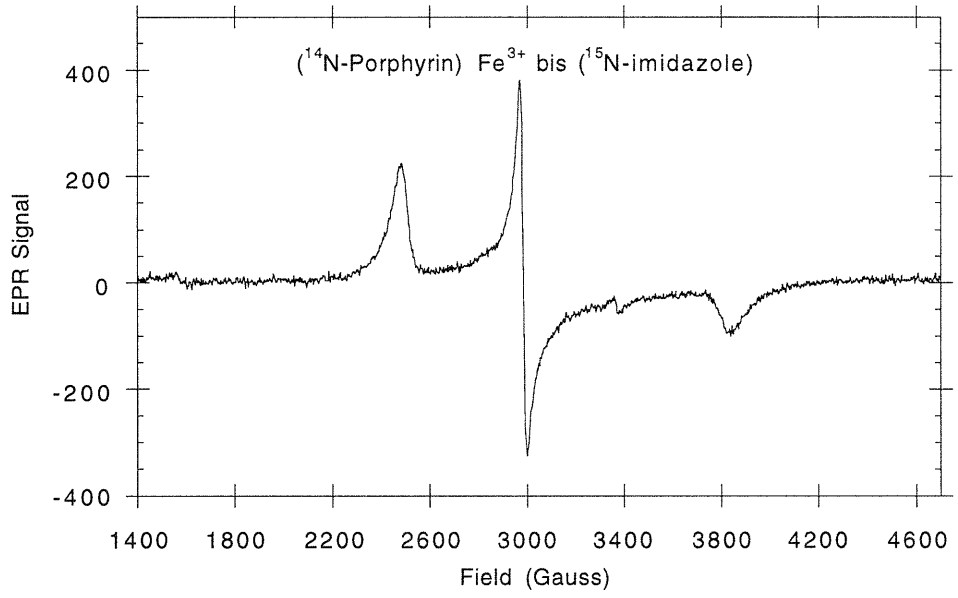

Figure 4.6: CW EPR spectrum of ^{14}N Heme (^{15}N imidazole)$_2$ at 10 K and 9.44 GHz.

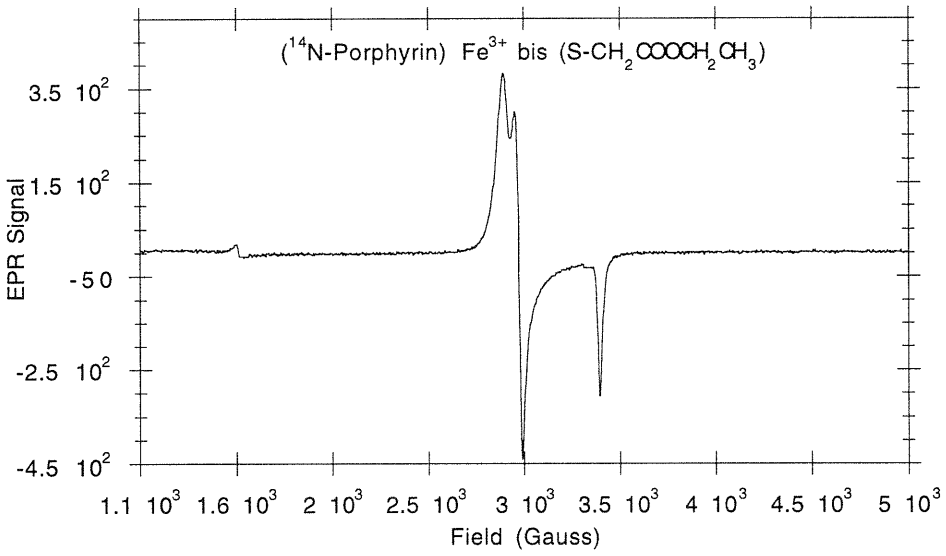

Figure 4.7: CW EPR spectrum of ^{14}N Heme $(SCH_2COOCH_2CH_3)_2$ at 10 K and 9.44 GHz.

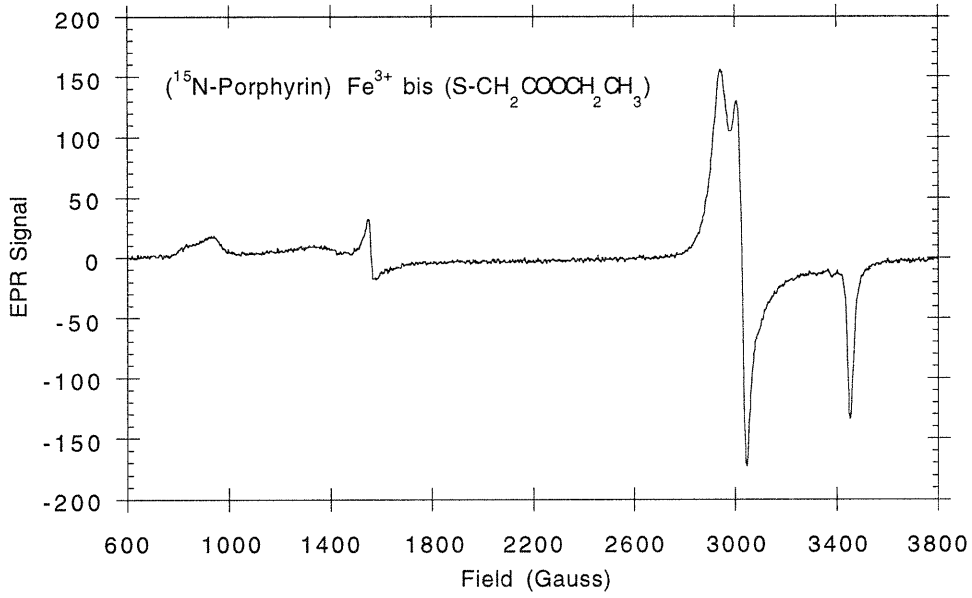

Figure 4.8: CW EPR spectrum of ^{15}N Heme $(SCH_2COOCH_2CH_3)_2$ at 10 K and 9.44 GHz.

4.4.2. The ESEEM Spectra

4.4.2.1. The Time Domain Data

ESEEM data is first acquired in the time domain form. As illustrated on Figure 4.1, the period(s) of modulation in the spin echo decay envelope provides the nuclear frequencies that are modulating the electron spin relaxation. Data was acquired with the three-pulse method in these experiments. As stated above, this procedure benefits from long acquisition times and simplified frequencies of modulation. It also offers the ability to suppress specific frequencies, by choosing an appropriate value for τ. However, this last advantage also reveals a limitation. Since the three-pulse technique is a two-dimensional experiment, certain modulations may inadvertently be passed over due to certain choices of τ.

All of the experiments described in this chapter were performed at a single τ value. Spin echoes were found to be weak in these compounds - even at very low temperatures. Consequently, the τ value which gave the strongest echoes (250 nsec) was used for all acquisitions; all acquired spectra were composites of numerous scans. Another limitation on the number of spectra acquired was the time and expense (in terms of liquid helium). The spectrometer is designed such that only rigid cryogenic transfer lines can deliver the coolant; additionally, there is a geometric constraint in the spectrometer area, limiting the experimenter to shallow liquid helium tanks. This dictated a maximum of 25 liters of liquid helium per spectral series - imposing a four hour limit on an average experiment at 9 K.

Apart from changing the value of τ, it is beneficial to measure ESEEM data at different g values and frequencies. The excitation at different g values effects a selection of (coupled) nuclear spins at specific orientations relative to the paramagnet. The examination of ESEEM at different frequencies (but at the same g value) allows one to solve for many of the components in the spin Hamiltonian that contribute to the ESEEM at a certain g value. All ESEEM spectra described in this chapter were acquired at g=2.25 (2900 Gauss) and a frequency of 9.14 GHz. Note that the times on the x-axes (of **Figures 4.9** through **4.14**) should be twice of what is shown (see **Appendix 4.1** for the explanation).

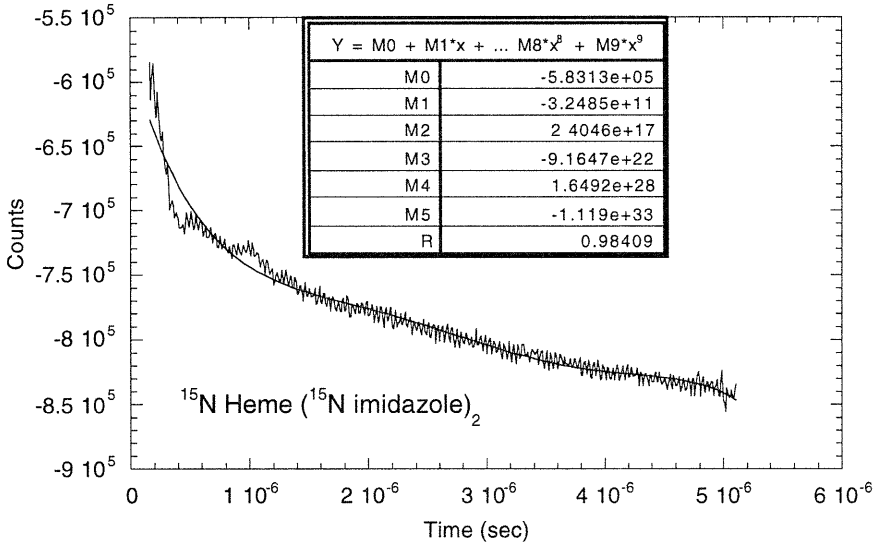

Figure 4.9: ESEEM spectrum of ^{15}N Heme (^{15}N imidazole)$_2$ with its fifth order polynomial background overlaid on top. This spectrum is the summation of 50 acquisitions measured at 8.5 K.

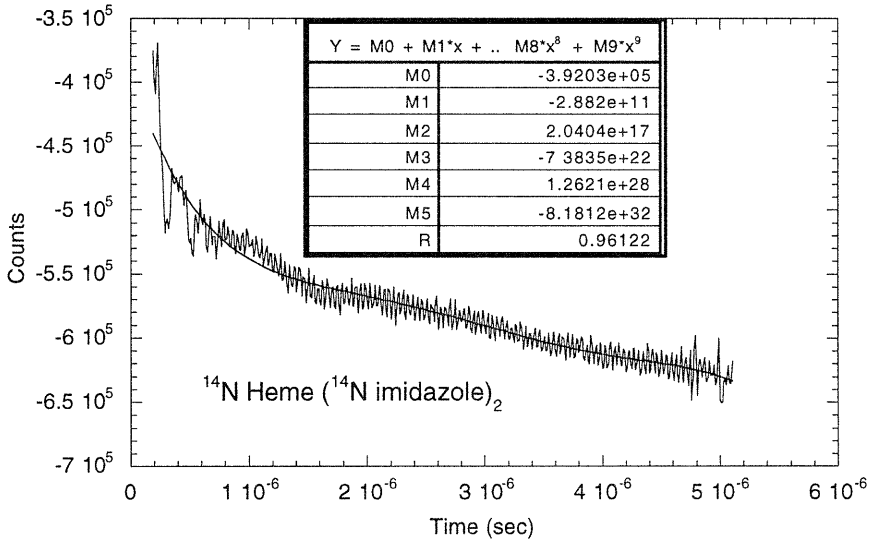

Figure 4.10: ESEEM spectrum of ^{14}N Heme (^{14}N imidazole)$_2$ with its fifth order polynomial background overlaid on top. This spectrum is the summation of 102 acquisitions measured at 8.4 K.

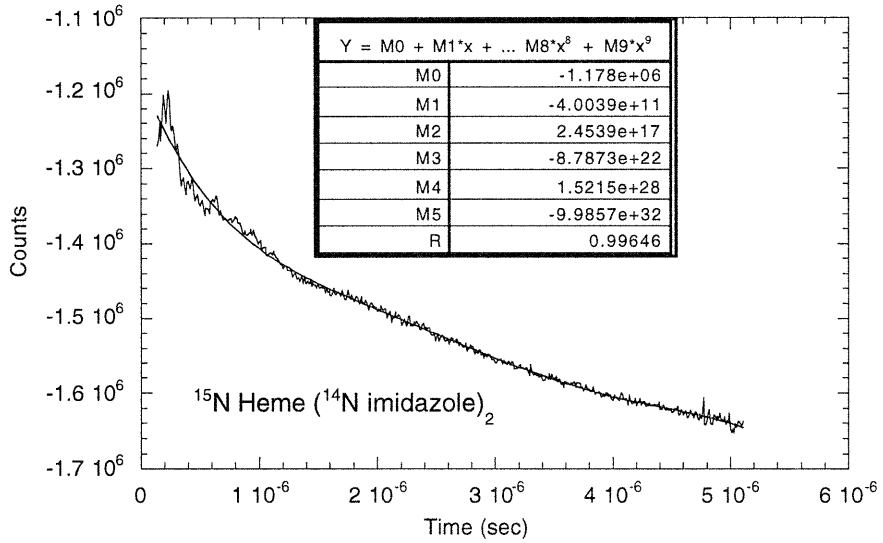

Figure 4.11: ESEEM spectrum of ^{15}N Heme (^{14}N imidazole)$_2$ with its fifth order polynomial background overlaid on top. This spectrum is the summation of 100 acquisitions measured at 8.2 K.

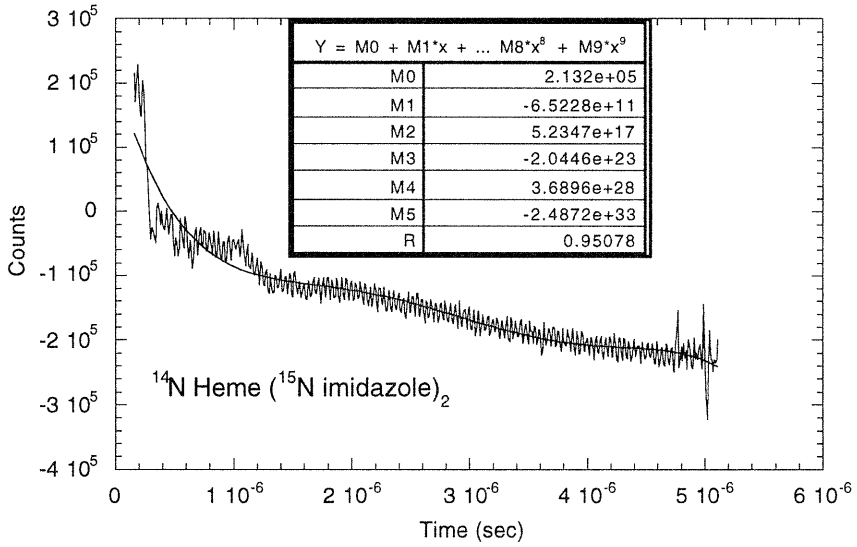

Figure 4.12: ESEEM spectrum of ^{14}N Heme (^{15}N imidazole)$_2$ with its fifth order polynomial background overlaid on top. This spectrum is the summation of 404 acquisitions measured at 8.3 K.

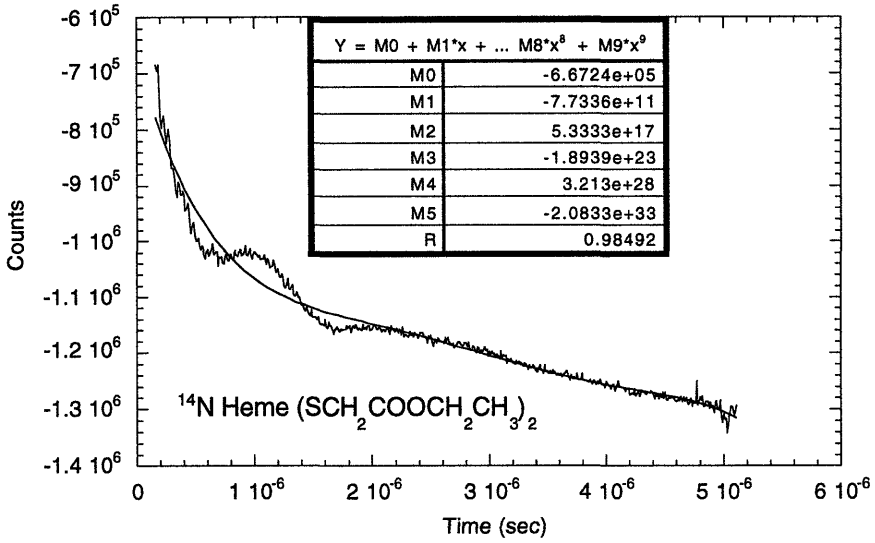

Figure 4.13: ESEEM spectrum of ^{14}N Heme $(SCH_2COOCH_2CH_3)_2$ with its fifth order polynomial background overlaid on top. This spectrum is the summation of 202 acquisitions measured at 7.6 K.

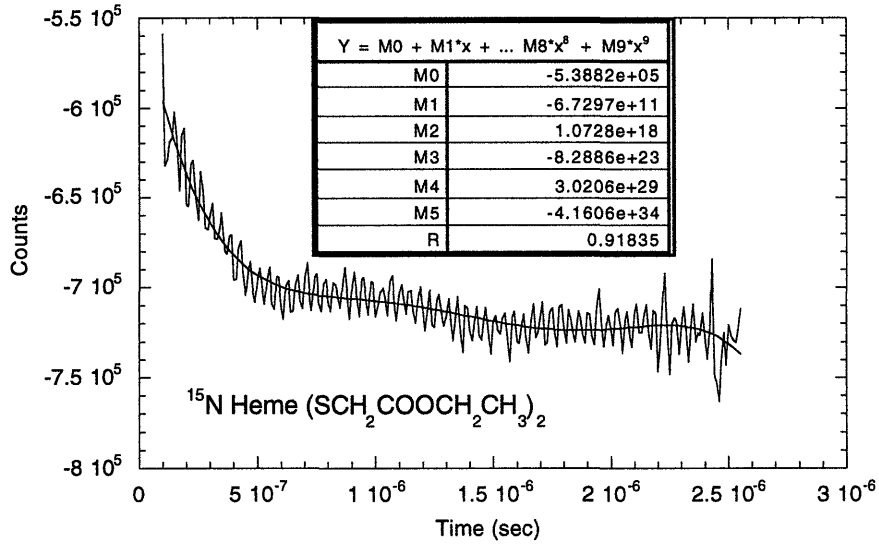

Figure 4.14: ESEEM spectrum of ^{15}N Heme $(SCH_2COOCH_2CH_3)_2$ with its fifth order polynomial background overlaid on top. This spectrum is the summation of 110 acquisitions measured at 8.4 K.

4.4.2.2. The Frequency Domain Data

Solving for the Hamiltonian parameters that give rise to the ESEEM is facilitated if the experimental data is transformed to the frequency domain. The overlay of simulations and experimental data in frequency space allows for a quick evaluation of the goodness of fit by inspection. It also permits one to observe distinct shifts in frequency peaks as conditions are changed.

In the experiments described in this chapter, all spectra were processed in similar ways before performing the fourier transform. Instead of reconstructing the dead time, the data points corresponding to this area were removed, after which the spectra were all fit to fifth order polynomials. The fitted polynomial functions were then subtracted from the spectra. The time domain data points were then left-shifted over to the y-axis. Since the removal of the dead time data points for each sample gave rise to a spectrum lacking the number of points corresponding to a multiple of two (a requirement for the fast fourier transform), each spectrum was zero filled at the right, restoring it to the same number of points that it originally had.

The shifting of the time data points to earlier times resulted in a hiding of spectral information in the imaginary component of the fourier transformed data. This hidden information was retrieved by calculating the modulus squared of the fourier transform. This is called a power spectrum. Therefore, the frequency domain spectra of the heme model compound (shown in **Figure 4.15** through **Figure 4.26**) are power spectra from their respective time domain points.

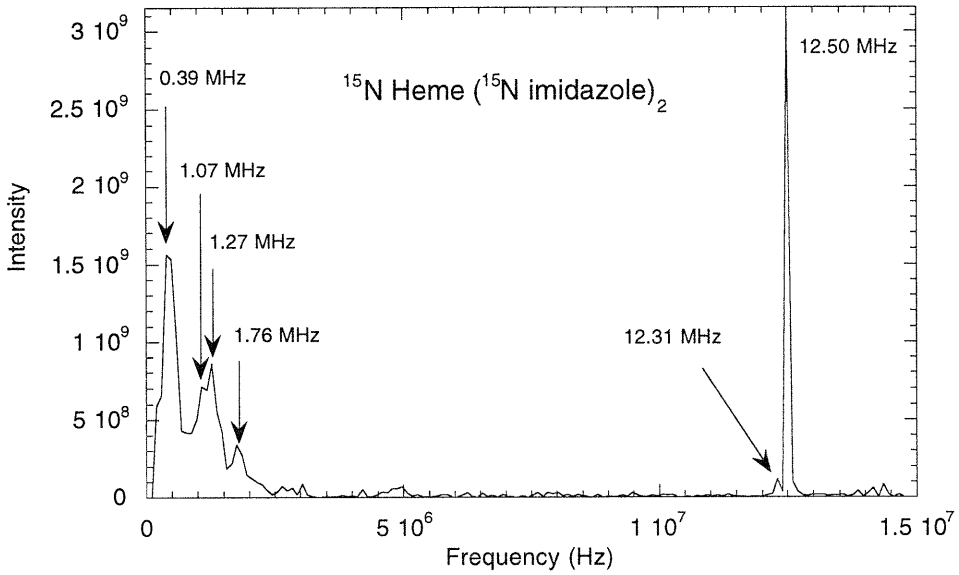

Figure 4.15: Wide ESEEM frequency spectrum of ^{15}N Heme (^{15}N imidazole)$_2$.

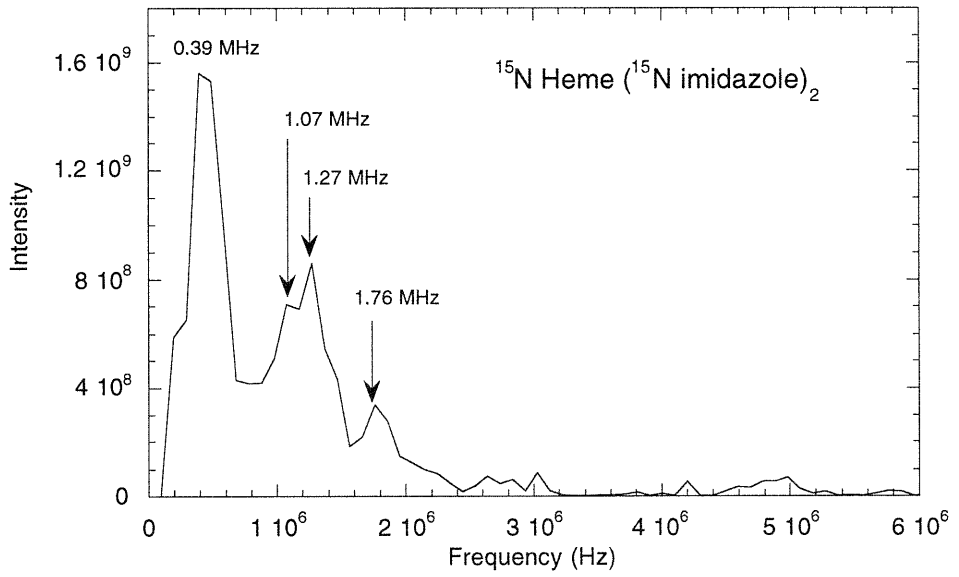

Figure 4.16: Narrow ESEEM spectrum of ^{15}N Heme (^{15}N imidazole)$_2$.

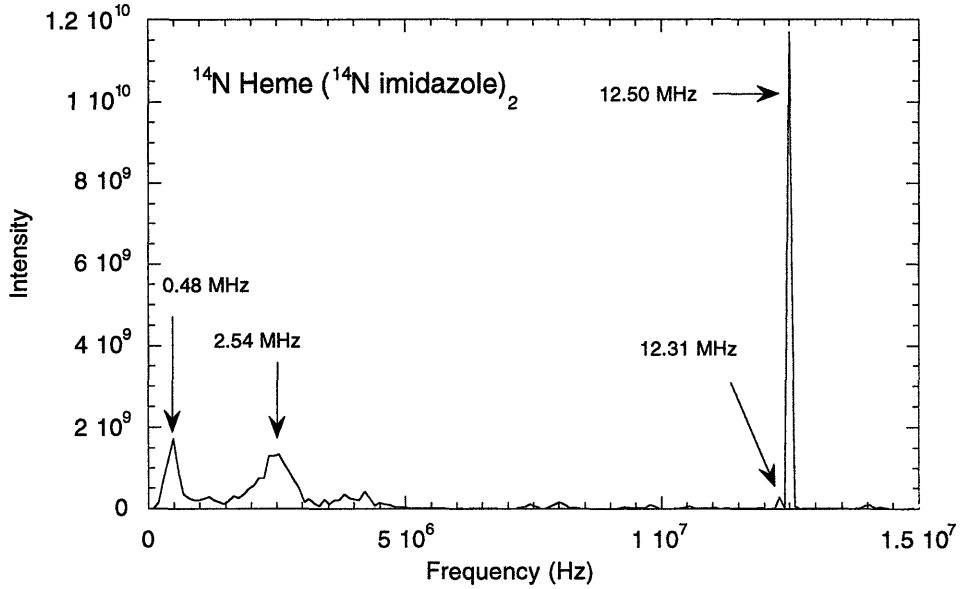

Figure 4.17: Wide ESEEM frequency spectrum of ^{14}N Heme (^{14}N imidazole)$_2$.

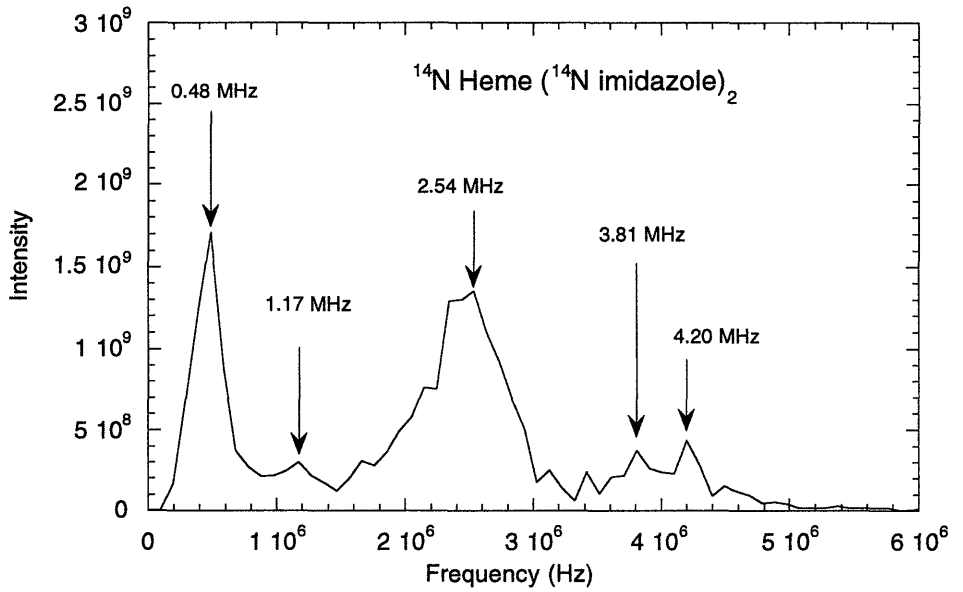

Figure 4.18: Narrow ESEEM spectrum of ^{14}N Heme (^{14}N imidazole)$_2$.

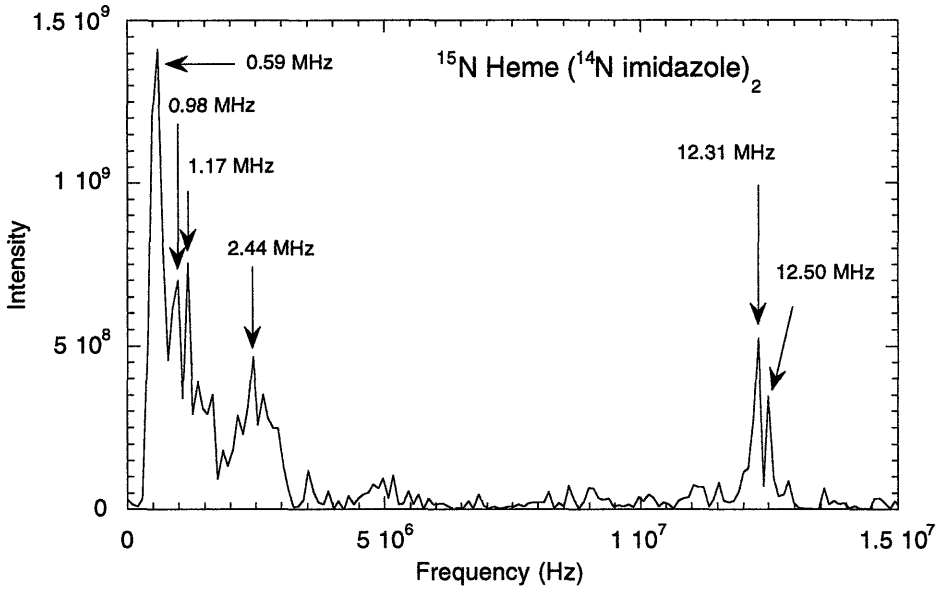

Figure 4.19: Wide ESEEM frequency spectrum of ^{15}N Heme (^{14}N imidazole)$_2$.

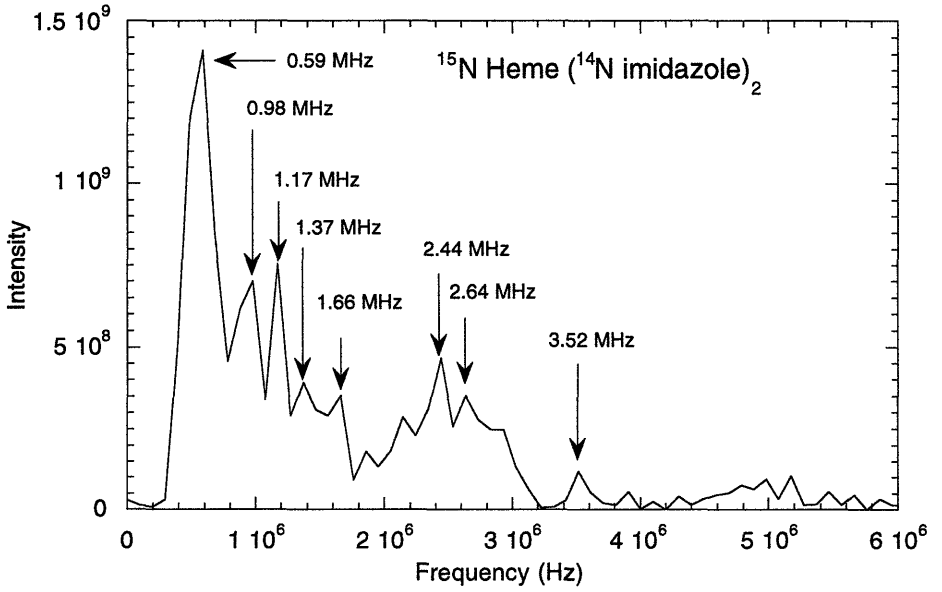

Figure 4.20: Narrow ESEEM spectrum of ^{15}N Heme (^{14}N imidazole)$_2$.

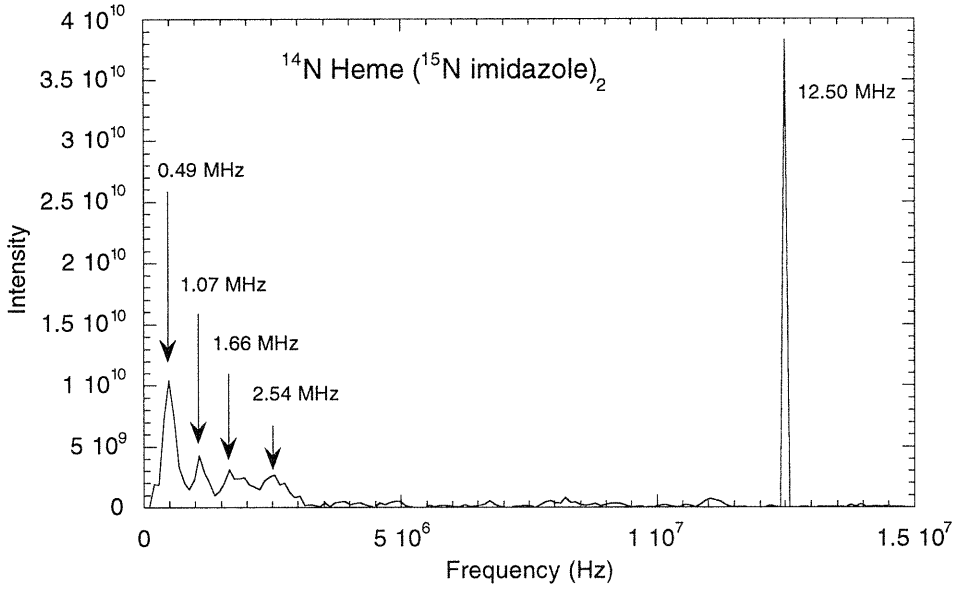

Figure 4.21: Wide ESEEM frequency spectrum of ^{14}N Heme (^{15}N imidazole)$_2$.

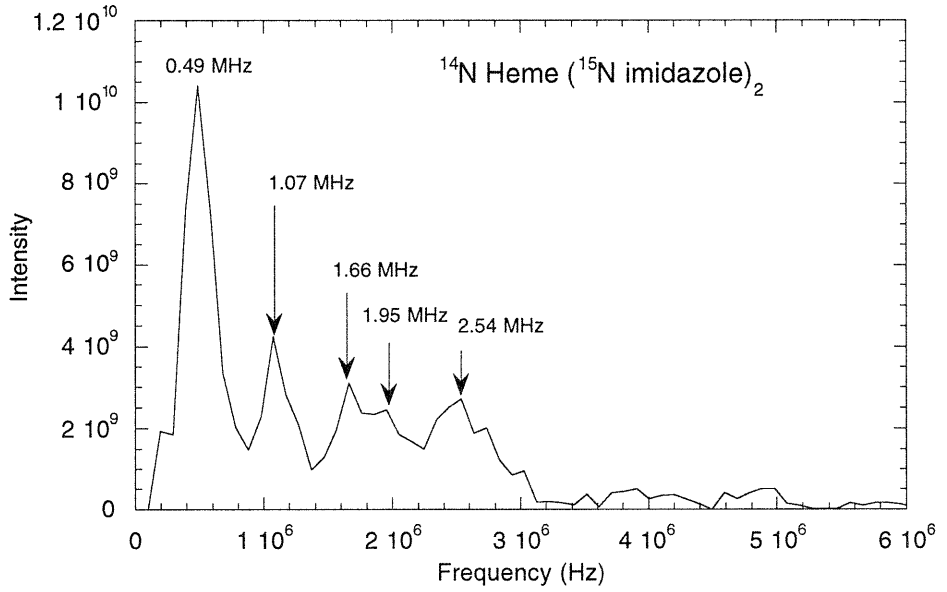

Figure 4.22: Narrow ESEEM spectrum of ^{14}N Heme (^{15}N imidazole)$_2$.

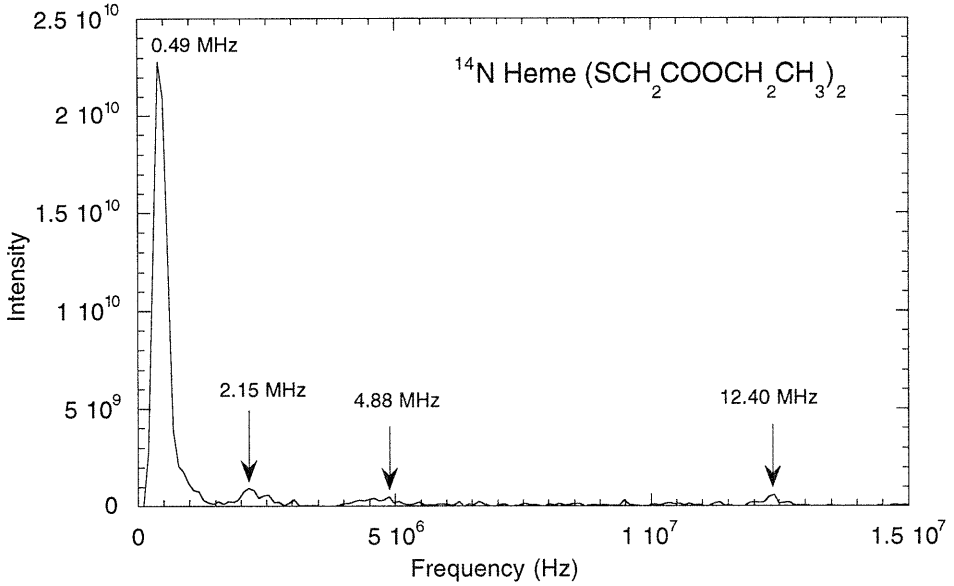

Figure 4.23: ESEEM frequency spectrum of ^{14}N Heme $(SCH_2COOCH_2CH_3)_2$.

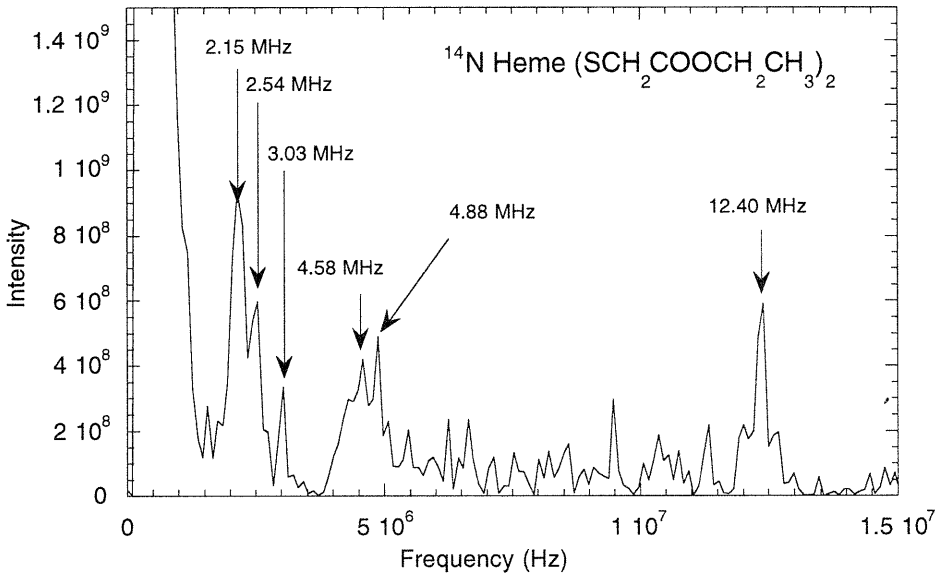

Figure 4.24: ESEEM spectrum (expanded) of ^{14}N Heme $(SCH_2COOCH_2CH_3)_2$.

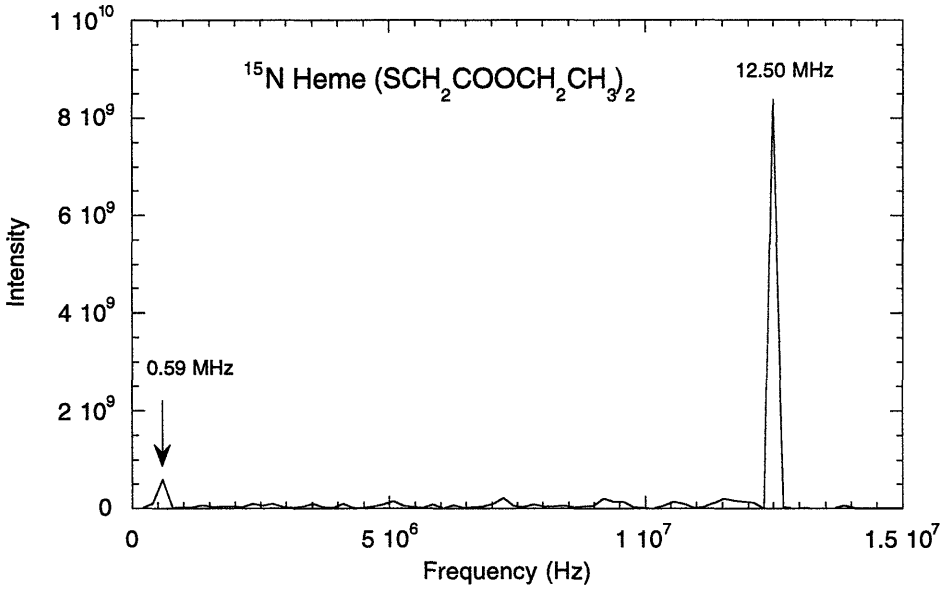

Figure 4.25: Wide ESEEM spectrum of ^{15}N Heme $(SCH_2COOCH_2CH_3)_2$.

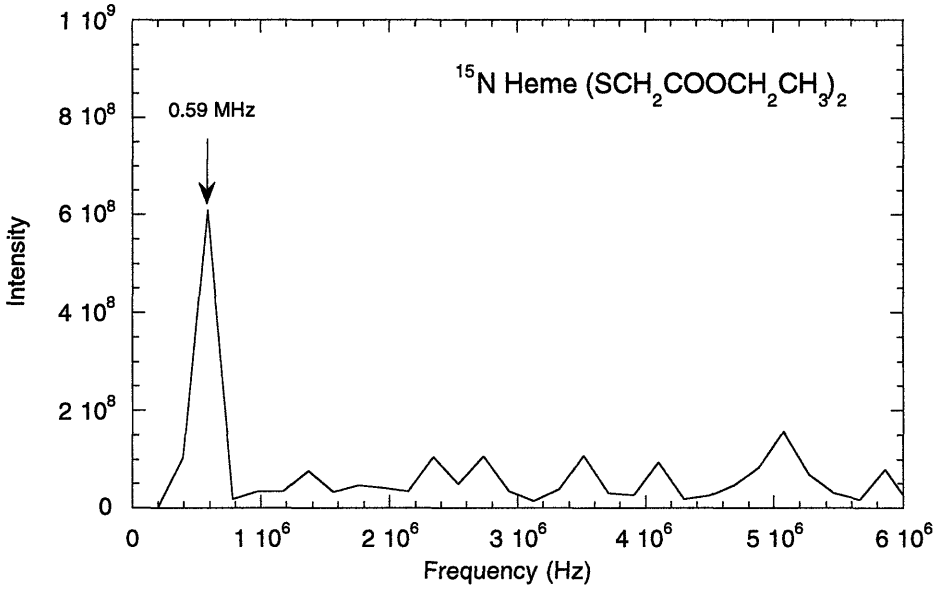

Figure 4.26: Narrow ESEEM spectrum of ^{15}N Heme $(SCH_2COOCH_2CH_3)_2$.

4.5. Discussion

As stated at the beginning of this chapter, the $P450_{cam}$ ESEEM studies 'revealing' imidazole axial coordination [7] did not agree with $P450_{cam}$ crystal structure. This result motivated a collaboration between the laboratories of professors Orme-Johnson and Dawson to design a series of ESEEM experiments that are hoped to assign the individual contributions of the nitrogens from axial imidazole and equatorial porphyrin as well as the effect of thiolate ligation. The six model compounds, provided for the work described in this chapter, serve to address this issue. This chapter summarizes the state of this project to date.

The factors influencing the modulation frequencies of the electron spin echo envelope are: (1) the nuclear larmor frequency, (2) the electron-nuclear hyperfine interaction (***A***), and (3) the nuclear quadrupole interaction. These parameters have been incorporated in derived ESEEM equations, described elsewhere [8, 9, 16-18]. Of all of these factors, the most complex is that of ***A***. This parameter is influenced the by Fermi constant term, the distance between the nucleus and the paramagnet, and the relative orientation of the nuclear-spin and electron-spin natural axes systems. The relative orientation of the nuclear-quadrupolar and electron-spin natural axes systems also plays an influence in the nuclear quadrupole interaction. Suffice it to say, that all of these different parameters can only be uniquely solved for by acquiring ESEEM spectra under a variety of conditions - which (in combination) can 'tease' out the values of each of these components.

Although it is often difficult to see the influence of one of the modulating factors on an ESEEM spectrum, two of them can be directly identified on the data acquired. The larmor frequencies for ^{15}N and ^{14}N (at 2900 Gauss) are 1.25 MHz and 0.88 MHz, respectively. In the frequency domain ESEEM spectrum of ^{15}N Heme (^{15}N imidazole)$_2$ (**Figures 4.15** and **4.16**), one can see a peak (~1.27 MHz) corresponding to the larmor frequency of ^{15}N. The 12.31 MHz signal of **Figures 4.15, 4.17**, and **4.19** and the 12.40 MHz signal of **Figure 4.24** resembles the expected 12.35 MHz larmor frequency of interacting ^{1}H nuclei. Clear identification of the ^{14}N larmor frequency of ^{14}N-containing samples was not possible on the data acquired; however, all ^{14}N Heme-containing samples gave rise to a consistent 0.5 MHz frequency signal (see

Figures 4.18, 4.22, and **4.23**). The lack of a clear ^{14}N larmor frequency peak could be due to the influence of the ^{14}N nuclear quadrupole interaction and/or the masking of this signal by latent low frequency background factors; the Fermi contact term does not appear to be responsible for this lack of 0.88 MHz signal since it did not impede the detection of the ^{15}N larmor frequency of ^{15}N Heme (^{15}N imidazole)$_2$.

Since the ^{15}N Heme (^{15}N imidazole)$_2$ sample gave rise to an ^{15}N larmor frequency signal, the question of whether this arose from the porphyrin or imidazole nitrogens (or both) immediately arises. In principle this could be addressed by examining the ESEEM spectra of ^{15}N Heme (^{14}N imidazole)$_2$, and ^{14}N Heme (^{15}N imidazole)$_2$. However, the interaction of ^{14}N from either the imidazole (see **Figure 4.20**) or the porphyrin (see **Figure 4.22**) gives rise to frequency components which mask out the ^{15}N larmor frequency of the porphyrin or imidazole, respectively. Examination of the ESEEM of ^{15}N Heme ($SCH_2COOCH_2CH_3$)$_2$ (see **Figure 4.26**) reveals the lack of an ^{15}N larmor frequency signal. This may argue for the case that the ^{15}N larmor frequency signal from ^{15}N Heme (^{15}N imidazole)$_2$ arose from the axial imidazoles, but the presence of the thioglycolate axial ligands of ^{15}N Heme ($SCH_2COOCH_2CH_3$)$_2$ may have given rise to an altered the Fermi term of the porphyrin ^{15}N nuclei, which would change their modulation effect. The report by Zuo [8] that $g_{parallel}$ ESEEM experiments of $P450_{cam}$ reveal large nitrogen Fermi terms argues that unperturbed nuclear larmor frequency modulations on electron spin echoes arise most likely from axial ligands. Therefore, from the available data, it appears that the 1.27 MHz signal of **Figure 4.16** is due to the axial imidazole ligands.

^{14}N-derived spectral features could be identified by generating difference spectra with ^{15}N-containing samples. Such an operation would require a common (sample-derived) feature in the corresponding spectra, needed for normalization of the two data sets. Although most spectra have a prominent 12.50 MHz signal, this is believed to arise from the spectrometer itself - since it is also found in a sample of γ-irradiated sucrose (see **Appendix 4.1**). The ^{1}H-derived signal is inappropriate as well since this may reflect the different levels of protonation of the solvents for each

sample (note that bulk nuclei which are distant from the electron spin can create a cumulative modulation effect on the electron spin echo).

The best normalization factor would be the spin echo amplitude at zero time. Unfortunately, the absolute value of the time domain spectra are not accurately transferred when converting the data from the 20-bit Nicolet format to the 32-bit Macintosh format (as can be seen by some negative y-coordinates on the **Figures 4.10** through **4.14**). This artifact is a result of the conversion algorithm used in the program of **Appendix 4.2**. This algorithm was obtain from the laboratory of prof. Larry Kevan (University of Texas) where their ESEEM spectrometer is also controlled by a similar Nicolet computer. This problem can therefore be corrected by running a program on the Nicolet computer itself which would print out the actual integer values of its stored files. The author did not have time to write such a program due to the effort required to learn how to program this unsupported computer system. However, given enough time, this task relatively straightforward for any future analysis.

Although the samples used in the above experiments offer the opportunity of assigning ESEEM influences from all of the different nuclear spins, all of the necessary experiments have not yet been performed. In addition, some of the acquired ESEEM spectra should be acquired again due to the low signal to noise in some of the acquisitions (see **Figures 4.10**, **4.12**, and **4.14**). From the spin quantitation of the paramagnetic centers (see **Table 4.1**), it appears that the low concentration of these samples may be at fault. Therefore, the synthesis of new (more concentrated samples of) model compounds is recommended.

The acquisition of ESEEM at different g values and at different microwave frequencies also remains to be performed before all modulating parameters can be fully assigned. Performing ESEEM studies at different frequencies requires a microwave generator of sufficient band width. The klystron microwave/power source unit, presently installed on the Orme-Johnson spectrometer, has a band width ranging from 8.8 to 9.6 GHz. This range is insufficient; a frequency difference of 2 GHz would be preferable. ESEEM experiments at different frequencies also requires the use of cavities which resonate at each of those frequencies. A Britt-

Klein style cavity [19] would offer this flexibility and would also provide a lower ring down time than the uncoupled EPR cavity used in the experiments described in this chapter; such a cavity could also be used with an insulated liquid helium immersion dewar which would permit data acquisition series which could last longer and could proceed at lower temperatures. Alternatively, these experiments could be performed at another laboratory equipped with such hardware necessities.

References

1. Poulos, T.L., Finzel, B.C., Gunsalus, I.C., Wagner, G.C., and Kraut, J., *The 2.6- crystal structure of Pseudomonas putida cytochrome P-450.* Journal of Biological Chemistry, 1985. **260**: p. 16122-16130.
2. Collman, J.P. and Groh, S.E., *"Mercaptan-Tail" Porphyrins: Synthetic Analogues for the Active Site of Cytochrome P-450.* Journal of the American Chemical Society, 1982. **104**: p. 1391-1403.
3. Dawson, J.H., *Probing structure-function relations in heme-containing oxygenases and peroxidases.* Science, 1988. **240**(4851): p. 433-439.
4. Liu, H.I., Sono, M., Kadkhodayan, S., Hager, L.P., Hedman, B., Hodgson, K.O., and Dawson, J.H., *X-ray Absorption Near Edge Studies of Cytochrome P450cam, chloroperoxidase, and myoglobin: Direct evidence for the electron releasing character of a cysteine thiolate proximal ligand.* Journal of Biological Chemistry, 1995. **270**(18): p. 10544-10550.
5. Collman, J.P., Sorrell, T.N., Dawson, J.H., Trudell, J.R., Bunnenberg, E., and Djerassi, C., Proc. Natl. Acad. Sci, 1976. **73**: p. 6-10.
6. Dawson, J.H., Andersson, L.A., and Sono, M., J. Biol Chem., 1982. **257**: p. 3606-3617.
7. Peisach, J., Mims, W.B., and Davis, J.L., *Studies of the Electron-Nuclear Coupling between Fe(III) and ^{14}N in Cytochrome P-450 and in a Series of Low Spin Heme Compounds.* Journal of Biological Chemistry, 1979. **254**: p. 12379-12389.
8. Zuo, C., *Paradigms of Magnetic Resonance Studies in Catalysis*, in *Chemistry*. 1990, Massachusetts Institute of Technology: Cambridge. p. 196.
9. Mims, W.B. and Peisach, J., *Electron Spin Echo Spectroscopy and the Study of Metalloproteins*, in *Biological Magnetic Resonance*, L.J. Berliner and J. Reuben, Editors. 1981, Plenum Press: New York and London. p. 213-263.
10. Fauth, J.-M., Schweiger, A., Braunschweiler, L., Forrer, J., and Ernst, R.R., *Elimination of Unwanted Echoes and Reduction of Dead time in Three-Pulse Electron Spin-Echo Spectroscopy.* Journal of Magnetic Resonance, 1986. **66**: p. 74-85.
11. Mims, W.B., *Elimination of the Dead-Time Artifact in Electron Spin-Echo Envelope Spectra.* Journal of Magnetic Resonance, 1984. **59**: p. 291-306.
12. Larsen, R.G., Halkides, C.J., RedField, A.G., and Singel, D.J., *Electron Spin-Echo Envelope Modulation Spectroscopy of Mn^{2+}¥GDP Complexes of N-ras p21 with Selective ^{15}N Labeling.* J. Am. Chem. Soc., 1992. **114**: p. 9608-9611.
13. Orme-Johnson, N.R. and Orme-Johnson, W.H., *Detection and quantitation of free cytochrome P-450 and cytochrome P-450 complexes by EPR spectroscopy.* Methods in Enzymology, 1978. **52**: p. 252-257.
14. Tan, S.L., Waugh, J.s., and Orme-Johnson, W.H., *Increased amplitudes of electron spin echoes by phase shifted excitation.* Journal of Chemical Physics, 1984. **81**: p. 576-578.
15. Tan, S.L., *Electron Spin Echo Spectroscopy of Metalloproteins*, in *Chemistry*. 1984, Massachusetts Institute of Technology: Cambridge. p. 126.
16. Dikanov, S.A., Shubin, A.A., and Parmon, V.N., *Modulation Effects in Electron Spin Echo Resulting from Hyperfine Interaction with a Nucleus of an Arbitrary Spin.* Journal of Magnetic Resonance, 1981. **42**: p. 474-487.
17. Flanagan, H.L. and Singel, D.J., *Analysis of ^{14}N ESEEM patterns of randomly oriented solids.* Journal of Chemical Physics, 1987. **87**: p. 5606-5616.
18. Kevan, L., *Modulation of Electron Spin-Echo Decay*, in *Time Domain Electron Spin Resonance*, L. Kevan and R.N. Schwartz, Editors. 1979, Wiley: New York. p. 279-341.
19. Britt, R.D. and Klein, M.P., *A Versatile Loop-Gap Resonator Probe for Low-Temperature Electron Spin-Echo Studies.* Journal of Magnetic Resonance, 1987. **74**: p. 535-540.

Appendix 4.1

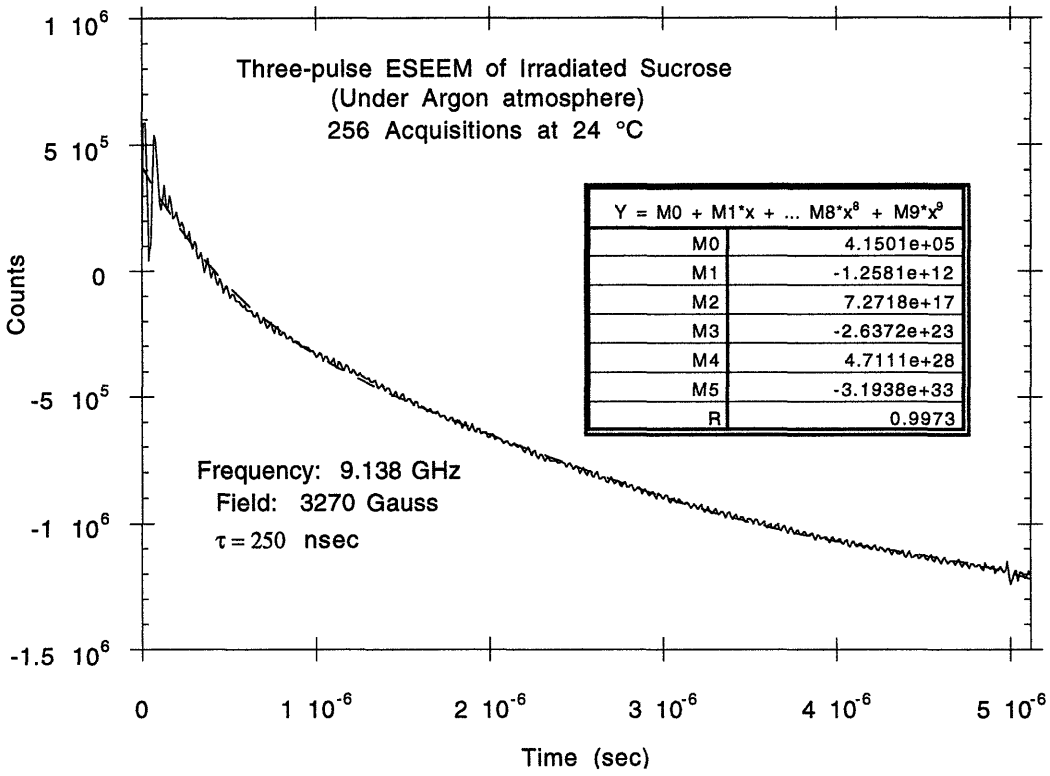

Figure 4.27: Time domain data of γ-irradiate sucrose.

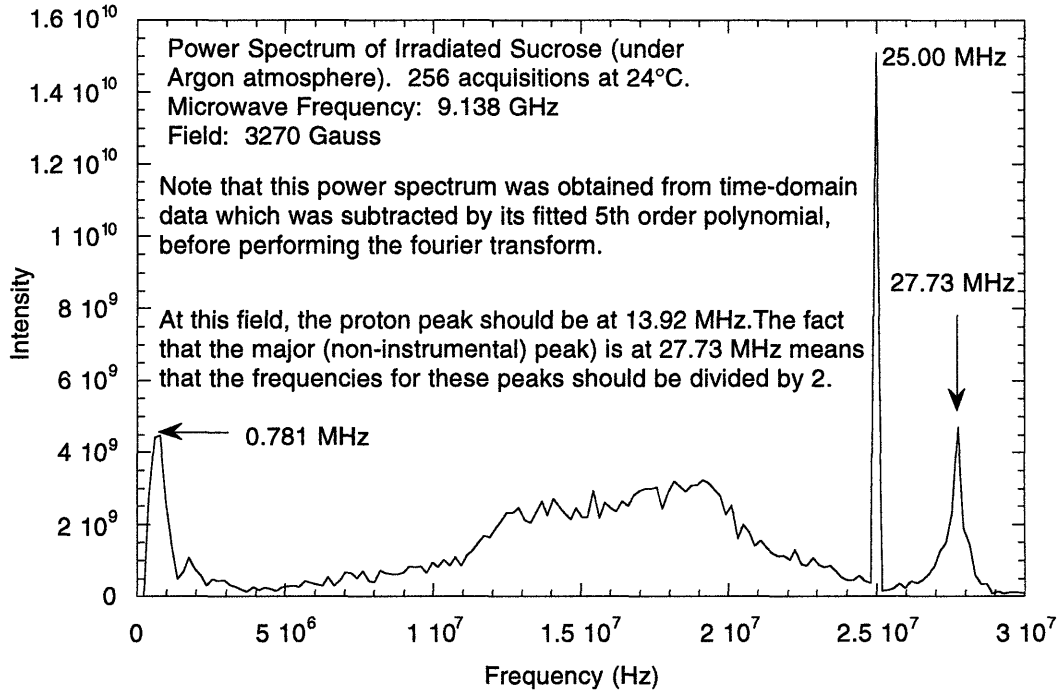

Figure 4.28: Power spectrum of γ-irradiate sucrose.

Appendix 4.2

```
'This program was written by Normand J. Cloutier, for use in manipulating
'ESEEM data acquired on the electron spin echo spectrometer of the
'laboratory of prof. W.H. Orme-Johnson of the MIT chemistry department.
'The present form of this program has bugs in the fourier transform and
'inverse fourier transform routines; other programs should therefore be
'used for these functions.  The language of the program is FutureBASIC (by
'Zedcor, Inc.) which runs on an Apple Macintosh.

'---------------------------- Header -------------------------------
'RESOURCES                              'open the resource file
COMPILE 0, _caseInsensitive                    'optional (might be useful)
'--------------------------- Constants -----------------------------
_no = 0
_yes = 1
_JumpJudger = 800000
_JumpValue = 1048580

'Menu constants

_mFile = 1                              'define the File menu as id 1
_iOpen = 1                              'define the open item as item 1
_iConvert = 2                           'define the Convert item as item 2
_iSaveR = 3                             'define the save Real item as 3
_iSaveC = 4                             'define the save Complex item as 4
_iQuit = 5                              'define the quit item as item 5

_mEdit = 2                              'define the Edit menu as id 2
_iUndo = 1                              'define the Undo item as item 1
_iCut = 3                               'define the Cut item as item 3
_iCopy = 4                              'define the Copy item as item 4
_iPaste = 5                             'define the Paste item as item 5
_iClear = 6                             'define the Clear item as item 6
_iSelectAll = 8                         'define the Select All item as item 8

_mCommands = 3                          'define the Commands menu as id 3
_iMakeReal = 1                          'define the "Delete Imaginary Points" item as 1
_iFourierTransform = 2                  'define the "Fourier Transform" item as item 2
'define the "Inverse Fourier Transform" item as 3
_iInverseFourierTransform = 3
_iFitLongTimes = 4                      'define the "Fit Ending Tail" item as item 4
_iZeroPoints = 5                        'define the "Zero A Spectrum Portion" item as 5
_iAddPortion = 6                        'define the "Append New Values" item as 6
_iSelectRegions = 7                     'define the "Select Regions" item as 7
_iZoom = 8                              'define the "Zoom In" item as item 8
_iExpand = 9                            'define the "Expand Out" item as item 9
```

```
_iFitShortTimes = 10          'define the "Approximate Short Times" item as 10

'------------------------- Globals ----------------------------
DIM plotFlag                    'Flag to indicate if a cross-hair has been drawn
DIM regionsSelected             'Flag to indicate a region has been selected
DIM windowOpen                  'Flag to indicate if a window has been drawn
DIM mousePnt.4                  'Structure to store the coordinates of the cursor

DIM tValue&(10241)              '4 * 10 K of space for time domain values
DIM fValue#(10241)              '8 * 5 K of space for frequency values
DIM xValue#(10241)              '4 * 10 K space for x coordinate data
DIM tempArray#(10241)           'Array to do transforms in

DIM maxTValue&                  'Maximum ordinate in the current time view
DIM minTValue&                  'Minimum ordinate in the current time view
DIM tSpread&                    'Difference in maxTValue& and minTValue&
DIM maxFValue#                  'Maximum ordinate in the current freq. view
DIM minFValue#                  'Minimum ordinate in the current freq. view
DIM fSpread#                    'Difference in maxFValue# and minFValue#
DIM xValueJump                  'skipping factor for index of yCoordinate
DIM tValueJump                  'skipping factor for index of tValue&()
DIM fValueJump                  'skipping factor for index of fValue#()

DIM lowerBoundView              'Data index of lower bound of the current view
DIM upperBoundView              'Data index of the upper bound of the current view
DIM yCoordinate(513)            'array for pixel values of the current plot
DIM xCoordinate#(513)           'array for values of abscissas of current plot
DIM baseYCoordinate             'the pixel ordinate of the x-axis of plot

DIM numOfData&                  'The number of real+imaginary data in the file
DIM numOfPoints&                'The number of data points in the file

DIM dataSpread                  'Number of points used for plot
DIM xInterval#
DIM xCoordSpacInt#

DIM 32 inFileName$              '32 character filename
DIM 32 outFileName$             '32 character filename
DIM 32 curFileName$             '32 character name of current file
DIM 40 xAxis$                   'Label for x-Axis
DIM 40 yAxis$                   'Label for y-Axis
DIM sum1#
DIM sum2#
DIM sum3#
DIM sum4#
DIM slope#
DIM meanX#
```

```
DIM meanY#
DIM yIntercept#
DIM expAmplitude#
DIM pi#
DIM iSign
END GLOBALS

'------------------------- Functions -----------------------------
LOCAL FN fitExponentialDecay
  numOfFittedPoints# = INT((upperBoundView - lowerBoundView)/2 + 1)
  sum1# = 0
  sum2# = 0
  sum3# = 0
  sum4# = 0

  counter = lowerBoundView - 2
  DO
    counter = counter + 2
    tempY# = LOG(tValue&(counter))
    sum1# = sum1# + ( xValue#(counter) * tempY# )
    sum2# = sum2# + xValue#(counter)
    sum3# = sum3# + tempY#
    sum4# = sum4# + xValue#(counter)^2

  UNTIL counter = upperBoundView - 1

  numerator# = sum1# - ((sum2#)*(sum3#)/numOfFittedPoints#)
  denominator# = sum4# - (((sum2#)^2)/numOfFittedPoints#)
  slope# = numerator#/denominator#
  meanX# = sum2#/numOfFittedPoints#
  meanY# = sum3#/numOfFittedPoints#
  yIntercept# = meanY# - ( (slope#) * meanX# )
  expAmplitude# = EXP(yIntercept#)

END FN
```

```
LOCAL FN drawData
'This function plots a graph with a labelled x-axis and draws the graph
'represented by the pixel coordinates stored in array yCoordinate(). If there
'were orinally less data points than the 512 available pixel positions, this
'function only plots the points representing the horizontally scaled graph.
'This sparseness of points is compensated by drawing a line connecting the
'spaced out points.

 windowOpen = _yes
 WINDOW CLOSE #1
 WINDOW #1, curFileName$, (0,0)-(570,355), _docNoGrow
 COORDINATE WINDOW
 CALL MOVETO(33,10)
 CALL LINETO(33,310)
 CALL LINETO(547,310)
 CALL TEXTSIZE(10)
 FOR hTick = 10 TO 500 STEP 10
  LONG IF hTick MOD 50 = 0
    CALL MOVETO(33+hTick,306)
    CALL LINETO(33+hTick,314)
     valueTemp# = INT( (xCoordinate#(hTick) + _
                                          xCoordSpacInt# )/xCoordSpacInt# )
     tickValue& = INT(valueTemp#)

    tickFlag = 0
    numberOfDigits& = 0
    WHILE tickFlag = 0
      numberOfDigits& = numberOfDigits& + 1
      digitTemp& = INT(tickValue&/10)
     IF digitTemp& = 0 THEN tickFlag = 1
      tickValue& = digitTemp&
    WEND

    xTick = (33+hTick) - (numberOfDigits& * 4)
     tick$ = STR$(valueTemp#)
    PRINT% (xTick,324) tick$
  XELSE
    CALL MOVETO(33+hTick,308)
    CALL LINETO(33+hTick,312)
  END IF
 NEXT hTick
 whole$ = xAxis$ + "( X " + STR$(xCoordSpacInt#) + " )"
 PRINT% (250,340) whole$
 counter = 0
 CALL MOVETO (33+counter,yCoordinate(counter+1))
 firstCounter = counter + (2 * xValueJump)
 FOR counter = firstCounter TO 1022 STEP (2 * xValueJump)
```

```
    position = ((counter)/2+1)
    CALL LINETO (33+position,yCoordinate(position))
  NEXT counter
  whole$ = STR$(dataSpread) + " " + "data points"
  EDIT FIELD #1, whole$, (400,40)-(550,50), _statFramed, _leftJust
END FN

LOCAL FN generateY
'This function fills the array yCoordinate() with the correct pixel coordinates
'needed to draw an autoscaled plot between data indexes lowerBoundView
'and upperBoundView by the function drawData

  dataSpread = upperBoundView - lowerBoundView +1
  LONG IF UCASE$(LEFT$(xAxis$,1)) = "T"
     minTValue& = tValue&(lowerBoundView)
     maxTValue& = minTValue&
     FOR counter = lowerBoundView TO upperBoundView-1 STEP 2
       IF minTValue& > tValue&(counter) THEN minTValue& = _

          tValue&(counter)
       IF maxTValue& < tValue&(counter) THEN maxTValue& = _

          tValue&(counter)
    NEXT counter
    tSpread& = maxTValue& - minTValue&
   LONG IF dataSpread < 1024
     xValueJump = (1024/dataSpread)
   XELSE
     xValueJump = 1
   END IF
   LONG IF dataSpread > 1024
     tValueJump = (dataSpread/1024)
   XELSE
     tValueJump = 1
   END IF
   FOR counter = 1 TO 512
     yCoordinate(counter) = 310
   NEXT counter
   tData = lowerBoundView
   FOR counter = 0 TO 1022 STEP 2 * xValueJump
     height = (250 * (tValue&(tData)-minTValue&))/tSpread&
     yCoordinate((counter)/2+1) = 310 - (baseYCoordinate + height)
     tData = tData + (tValueJump * 2)
   NEXT counter

    xCoordInterval# = xValue#(upperBoundView) - xValue#(lowerBoundView)
    numOfViewedPoints = (upperBoundView - lowerBoundView) / 2
```

```
    xCoordSpacInt# = xCoordInterval# / numOfViewedPoints
    baseXCoord# = xValue#(lowerBoundView)
   FOR counter = 0 TO 511
     xCoordinate#(counter + 1) = baseXCoord# + (counter * xCoordSpacInt#)
   NEXT counter

  XELSE
    minFValue# = fValue#(lowerBoundView)
    maxFValue# = minFValue#
    FOR counter = lowerBoundView TO upperBoundView
      IF minFValue# > fValue#(counter) THEN minFValue# = fValue#(counter)
      IF maxFValue# < fValue#(counter) THEN maxFValue# = fValue#(counter)
   NEXT counter

    fSpread# = maxFValue# - minFValue#
   LONG IF dataSpread < 2048
     xValueJump = (2048/dataSpread)
   XELSE
     xValueJump = 1
   END IF
   LONG IF dataSpread > 1024
     fValueJump = (dataSpread/1024)
   XELSE
     fValueJump = 1
   END IF
   FOR counter = 1 TO 512
     yCoordinate(counter) = 310
    NEXT counter
    tData = lowerBoundView
    FOR counter = 0 TO 1022 STEP 2 * xValueJump
      height = (250 * (fValue#(tData)-minFValue#))/fSpread#
     yCoordinate((counter)/2+1) = 310 - (baseYCoordinate + height)
     tData = tData + (fValueJump * 2)
   NEXT counter

    xCoordInterval# = xValue#(upperBoundView/2 + 2) -
xValue#(lowerBoundView)
    numOfViewedPoints = (upperBoundView - lowerBoundView) / 2
    xCoordSpacInt# = xCoordInterval# / numOfViewedPoints
    baseXCoord# = xValue#(lowerBoundView)
   FOR counter = 0 TO 511
     xCoordinate#(counter + 1) = baseXCoord# + (counter * xCoordSpacInt#)
   NEXT counter

  END IF

END FN
```

```
LOCAL FN openFile
'This function opens an ASCII data file, containing values for both the
'abscissa and ordinate values of a data file. It fills up two arrays - an xValue#()
'array and either a tValue&() integer array or an fValue#() double precision
'real array - with both real and imaginary data points. The tValue&() array is
'chosen if the first line data file starts with the character "t" or "T",
'corresponding to x-axis label. If successive data pairs have the same abscissa
'value, then the data file is judged to contain a complex data set and the two
'arrays are filled up with the exact corresponding values found in the data
'file. If successive data pairs have different abscissa values, then the file is
'judged to contain a real data set; this causes the xValue#() array and either
'the tValue&() or fValue#() array to be filled with paired duplicate values
'(i.e. x-1,x-1; x-2,x-2; x-3,x-3;...;x-n,x-n  where n is the number of paired data
'points in the file).

 'Show TEXT files only
  inFileName$=FILES$(_fOpen,"TEXT",,volRefNum%)
 LONG IF LEN(inFileName$)                    'if len=0 then Cancel open
   OPEN "I", 1, inFileName$,,volRefNum%
                          'Note:  volRefNum%=folder of inFileName$
   curFileName$ = inFileName$
  LINE INPUT #1,firstLine$                   'Read in the labels for the axes
  tabPosition = 0
  flag=0
   lenOfLine = LEN(firstLine$)
   WHILE tabPosition <= (lenOfLine - 1) AND flag=0
    tabPosition = tabPosition + 1
    LONG IF MID$(firstLine$,tabPosition,1) = CHR$(9)
     flag = 1
    END IF
   WEND
   xAxis$ = LEFT$(firstLine$,tabPosition-1)
   yAxis$ = RIGHT$(firstLine$,lenOfLine-tabPosition)
  numOfData& = 0
  realFlag = 0
   LONG IF UCASE$(LEFT$(xAxis$,1)) = "T"
    WHILE NOT EOF(1)
      numOfData& = numOfData& + 1
      'read in a line with 2 numbers separated by a TAB
      LINE INPUT #1, aLine$
      tabPosition = 0
     flag=0
      lenOfLine = LEN(aLine$)
      WHILE tabPosition <= (lenOfLine - 1) AND flag=0
       tabPosition = tabPosition + 1
```

```
    LONG IF MID$(aLine$,tabPosition,1) = CHR$(9)
     flag = 1
    END IF
   WEND
   xString$ = LEFT$(aline$,tabPosition-1)
   yString$ = RIGHT$(aLine$,lenOfLine-tabPosition)
   xValue#(numOfData&) = VAL(xString$)
   tValue&(numOfData&) = VAL(yString$)

  LONG IF numOfData& MOD 2 = 0
    LONG IF xValue#(numOfData&) <> lastXValue#
     tempX# = xValue#(numOfData&)
     tempT& = tValue&(numOfData&)
     xValue#(numOfData&) = lastXValue#
     tValue&(numOfData&) = 0
     numOfData& = numOfData& + 1
     xValue#(numOfData&) = tempX#
     tValue&(numOfData&) = tempT&
    realFlag = 1
   END IF
  END IF
   lastXValue# = xValue#(numOfData&)
   lastTValue& = tValue&(numOfData&)

 WEND
 LONG IF realFlag = 1
  numOfData& = numOfData& + 1
  xValue#(numOfData&) = xValue#(numOfData& - 1)
 END IF

 lowerBoundView = 1
 upperBoundView = numOfData&
 FN generateY
XELSE
 WHILE NOT EOF(1)
  numOfData& = numOfData& + 1
  'read in a line with 2 numbers separated by a TAB
  LINE INPUT #1, aLine$
  tabPosition = 0
  flag=0
  lenOfLine = LEN(aLine$)
  WHILE tabPosition <= (lenOfLine - 1) AND flag=0
   tabPosition = tabPosition + 1
   LONG IF MID$(aLine$,tabPosition,1) = CHR$(9)
    flag = 1
   END IF
  WEND
```

```
      xString$ = LEFT$(firsLine$,tabPosition-1)
      yString$ = RIGHT$(firstLine$,lenOfLine-tabPosition)
      xValue#(numOfData&) = VAL(xString$)
      fValue#(numOfData&) = VAL(yString$)

     LONG IF numOfData& MOD 2 = 0
       LONG IF xValue#(numOfData&) <> lastXValue#
        tempX# = xValue#(numOfData&)
        tempF# = fValue#(numOfData&)
        xValue#(numOfData&) = lastXValue#
       fValue#(numOfData&) = 0
       numOfData& = numOfData& + 1
        xValue#(numOfData&) = tempX#
        fValue#(numOfData&) = tempF#
       realFlag = 1
      END IF
     END IF
      lastXValue# = xValue#(numOfData&)
      lastFValue# = fValue#(numOfData&)
    WEND

    LONG IF realFlag = 1
      numOfData& = numOfData& + 1
      xValue#(numOfData&) = xValue#(numOfData& - 1)
    END IF

     lowerBoundView = 1
     upperBoundView = numOfData&/2
    FN generateY
   END IF
   CLOSE #1
    numOfPoints& = numOfData&/2
    xInterval# = xValue#(3) - xValue#(1)
   FN drawData                          'graph out the data in a window
    MENU _mCommands, _iSelectRegions, _enable, "Select Regions"
    MENU _mCommands, _iZoom, _enable, "Zoom In"
    MENU _mCommands, _iMakeReal, _enable, "Delete Imaginary Points"
    MENU _mFile, _iSaveR, _enable, "Save..."
    MENU _mFile, _iSaveC, _enable, "Save Complex..."
    MENU _mCommands, _iFitLongTimes, _enable, "Fit Ending Tail"
    MENU _mCommands, _iZeroPoints, _enable, "Zero A Spectrum Portion"
    MENU _mCommands, _iFitShortTimes, _enable, "Approximate Short Times"
    MENU _mCommands, _iFourierTransform, _enable, "Fourier Transform"
    MENU _mCommands, _iInverseFourierTransform, _enable, "Inverse Fourier
Transform"
  XELSE
   BEEP
```

```
  END IF
END FN


LOCAL FN saveComplexFile                    'saves both the real and imaginary
  LONG IF UCASE$(LEFT$(xAxis$,1)) = "T"  'data points of the current data set
    ext$="-time"
  XELSE
    ext$="-freq"
  END IF
  default$ = inFileName$ + ext$
  outFileName$ = FILES$(_fSave,"Save File As:",default$,volRefNum%)
  DEF OPEN "TEXTTTXT"
  OPEN "O",1,outFileName$,,volRefNum%
  curFileName$ = outFileName$
  PRINT #1, xAxis$ + CHR$(9) + yAxis$
  LONG IF ext$="-time"
    FOR counter = 1 TO numOfData&
      PRINT #1, STR$(xValue#(counter)) + CHR$(9) + STR$(tValue&(counter))
    NEXT counter
  XELSE
    FOR counter = 1 TO numOfData&
      PRINT #1, STR$(xValue#(counter)) + CHR$(9) + STR$(fValue#(counter))
    NEXT counter
  END IF
  CLOSE #1
  CURSOR _arrowCursor
  FN drawData
END FN


LOCAL FN saveRealFile                       'saves only the real data points
  LONG IF UCASE$(LEFT$(xAxis$,1)) = "T"          'of the current data set
    ext$="-time"
  XELSE
    ext$="-freq"
  END IF
  default$ = inFileName$ + ext$
  outFileName$ = FILES$(_fSave,"Save File As:",default$,volRefNum%)
  DEF OPEN "TEXTTTXT"
  OPEN "O",1,outFileName$,,volRefNum%
  curFileName$ = outFileName$
  PRINT #1, xAxis$ + CHR$(9) + yAxis$
  LONG IF ext$="-time"
    FOR counter = 1 TO numOfData& STEP 2
      PRINT #1, STR$(xValue#(counter)) + CHR$(9) + STR$(tValue&(counter))
    NEXT counter
```

```
  XELSE
    FOR counter = 1 TO numOfData& STEP 2
      PRINT #1, STR$(xValue#(counter)) + CHR$(9) + STR$(fValue#(counter))
    NEXT counter
  END IF
  CLOSE #1
   CURSOR _arrowCursor
  FN drawData
END FN

LOCAL FN getXValues                    'Function to fill in xValues array
'This function should be eventually replaced with one which can access this
'parameter from the header information of the KERMITted ANLESE data file,
'being converted.

  INPUT "What is the interval between data points? "; xInterval#
  counter = 0
  factor = 0
  WHILE counter <= numOfData&
    counter = counter + 1
    xValue#(counter) = (factor) * (xInterval#)
    counter = counter + 1
    xValue#(counter) = (factor) * (xInterval#)
   factor = factor + 1
  WEND
END FN


LOCAL FN convert                'Function to read in and convert ANLESE files

'The Nicolet files can be transferred to a Macintosh computer if there is a
'connection from the serial port of the Macintosh to the channel B serial port
'of the Nicolet computer.  Once the Nicolet computer is booted up (with a
'dumb terminal connected to its channel A serial port) under the DEXTER/2
'operating system, and the Macintosh has an "opened connection" (with a
'terminal emulator program such as VersaTermPro) to the Nicolet, the files
'can be transferred using the KERMIT protocol.  The KERMIT protocol on the
'Nicolet is accessed by simply typing the RUN KERMIT command at the
'DEXTER/2 prompt.  The KERMIT protocol on the Macintosh can be accessed
'as described in the manual for the terminal emulator.

  inFileName$=FILES$(_fOpen,"TEXT",,volRefNum%)    'Show TEXT files only
  LONG IF LEN(inFileName$)                  'if len=0 then Cancel open
    OPEN "I", 1, inFileName$,,volRefNum%          'volRefNum%=folder of
inFileName$
    curFileName$ = inFileName$
```

```
'Loop to read in the header information. This will bring the file pointer to
'the location (location 881) of the first byte of the first unconverted ANLESE
'data value. This could not be read in as a huge string of 880 characters since
'there is a limit of 255 for character strings in FutureBASIC.

  FOR counter = 1 TO 88
   READ #1, aLine$;10
  NEXT counter


'The following while loop was adapted from a program written by
'Xinhua Chen and Chris Stenland (when they were part of Dr. Larry Kevan's
'Laboratory at the Department of Chemistry at the University of Houston in
'Houston, Texas 77204-5641. Their original program was written in Microsoft
'QuickBASIC for MS DOS. This original program was emailed to
'Normand Cloutier (from Chris Stenland at stenland&hydrogen.ucsc.edu on
'December 17, 1993.

'This while loop is the algorithm to convert data files acquired from the
'ANLESE program of a Nicolet 1180E or Nicolet 1280 computer. The Nicolet
'computer stores this data in 20-bit integer format. The first part of every data
'file is header information containing parameters used in the ANLESE scan.
'The routine in Chen and Stenland's program to read the comment string of
'this header was found to not work and they made no provision to read any
'of the other parameters in the header part. However, their program correctly
'translates the orginal 20-bit integer data into 32-bit integer data, readable by
'this program and can then be saved in ASCII format.

  numOfData& = 0                    'Reset the number of data values to zero

  WHILE NOT EOF(1)
   READ #1, D$;5
   A& = CVI(LEFT$(D$,4))
   B& = CVI(RIGHT$(D$,4))
   D12& = (A& AND &HFF) * &H1000
   A1& = A& AND &HFFFF0000&
   A1& = A& - A1&
   D3& = (A1& AND &HF000)/&H10
   D4& = (A& AND &HF00)/&H10
   D5& = (A& AND &HF00000&)\&H100000&
   numOfData& = numOfData& + 1
   tValue&(numOfData&) = D12& + D3& + D4& + D5&
   numOfData& = numOfData& + 1
   B1& = (B& AND &HF00) * &H100
   B23& = (B& AND &HFF0000&) / &H100
   B45& = ((B& AND &HFF000000&) / &H1000000&) AND &HFF
   tValue&(numOfData&) = B1& + B23& + B45&
```

```
   WEND
   CLOSE #1
    numOfPoints& = numOfData&/2

   FOR counter& = 3 TO numOfData&
      difference& = tValue&(counter&) - tValue&(counter&-2)
     LONG IF difference& > 0
       LONG IF difference& > _JumpJudger
         tValue&(counter&) = tValue&(counter&) -
(INT(difference&/_JumpJudger)*(_JumpValue))
       END IF
     XELSE
       LONG IF difference& < ((-1)*(_JumpJudger))
         tValue&(counter&) = tValue&(counter&) +
(INT(difference&/_JumpJudger)*(_JumpValue))
       END IF
     END IF
    NEXT counter&

    FN getXValues
    xAxis$ = "Time (sec)"
    yAxis$ = "Counts"

    lowerBoundView = 1
    upperBoundView = numOfData&
   FN generateY
    xInterval# = xValue#(2) - xValue#(1)
   FN drawData
     MENU _mCommands, _iSelectRegions, _enable, "Select Regions"
     MENU _mCommands, _iZoom, _enable, "Zoom In"
     MENU _mCommands, _iMakeReal, _enable, "Delete Imaginary Points"
     MENU _mFile, _iSaveR, _enable, "Save..."
     MENU _mFile, _iSaveC, _enable, "Save Complex..."
     MENU _mCommands, _iFitLongTimes, _enable, "Fit Ending Tail"
     MENU _mCommands, _iZeroPoints, _enable, "Zero A Spectrum Portion"
     MENU _mCommands, _iFitShortTimes, _enable, "Approximate Short Times"
     MENU _mCommands, _iFourierTransform, _enable, "Fourier Transform"
     MENU _mCommands, _iInverseFourierTransform, _enable, "Inverse Fourier
Transform"
  XELSE
    BEEP
  END IF
END FN

LOCAL FN makeReal
  FOR counter=1 TO numOfData& STEP 2
    tvalue&(counter+1) = 0
```

```
  NEXT counter
END FN


LOCAL FN addPortion
END FN


LOCAL FN doDialog
  evnt = DIALOG(0)                    'this returns the event
  id = DIALOG(evnt)                   'this tells us more about the event
  SELECT evnt
  END SELECT
END FN

LOCAL FN selectRegions
  FOR pointsSelected = 1 TO 2
   DO
     LONG IF windowOpen = _yes
      CALL GETMOUSE(mousePnt)
      X = (mousePnt.h)
      Y = (mousePnt.v)
     LONG IF X >= 33 AND Y > = 10
      LONG IF X <= 547 AND Y <= 310

        dataIndex = ((((X-33)/xValueJump)*tValueJump) + 1) * 2 - 2 + _

       lowerBoundView

        xDataValue# = xValue#(dataIndex)
        yDataValue& = ( (tSpread&) * (Y - 310 + baseYCoordinate) / (-250) ) + _

              minTValue&
        xDataValue$ = STR$(xDataValue#)
        yDataValue$ = STR$(yDataValue&)
        whole$ = xDataValue$ + "," + yDataValue$
        EDIT FIELD #1, whole$, (400,40)-(550,50), _statFramed, _leftJust
        CURSOR _crossCursor
       PEN 1,1,1,2,0
       LONG IF plotFlag
        PLOT 33,lastY TO 547,lastY
        PLOT lastX,10 TO lastX,310
       END IF
       PLOT 33,Y TO 547,Y
       PLOT X,10 TO X,310
       plotFlag = 1
       lastX = X
```

```
        lastY = Y
       XELSE
         CURSOR _arrowCursor
        LONG IF plotFlag
         PLOT 33,lastY TO 547,lastY
         PLOT lastX,10 TO lastX,310
         plotFlag = 0
        END IF
        CALL PENNORMAL
       END IF
      XELSE
        CURSOR _arrowCursor
       LONG IF plotFlag
        PLOT 33,lastY TO 547,lastY
        PLOT lastX,10 TO lastX,310
        plotFlag = 0
       END IF
       CALL PENNORMAL
     END IF
    XELSE
      CURSOR _arrowCursor
    END IF
   UNTIL FN BUTTON
   LONG IF pointsSelected = 1
     EDIT FIELD #2, whole$, (400,60)-(550,75), _statFramed, _leftJust
    boundary1 = dataIndex
  XELSE
     EDIT FIELD #3, whole$, (400,80)-(550,95), _statFramed, _leftJust
    boundary2 = dataIndex
  END IF
  DELAY _secQuarter
 NEXT pointsSelected
 CURSOR _arrowCursor
PLOT 33,lastY TO 547,lastY
PLOT lastX,10 TO lastX,310
plotFlag = 0
CALL PENNORMAL
LONG IF boundary1 <> boundary2
  LONG IF boundary 1 < boundary2
    lowerBoundView = boundary1
    upperBoundView = boundary2 + 1
  XELSE
    lowerBoundView = boundary2
    upperBoundView = boundary1 + 1
  END IF
  regionsSelected = _yes
XELSE
```

```
   BEEP
  END IF
END FN


LOCAL FN zoomIn
  FN selectRegions
  FN generateY
  FN drawData
   MENU _mCommands, _iExpand, _enable, "Expand Out"
  regionsSelected = _no
END FN

LOCAL FN ExpandOut
  lowerBoundView = 1
  LONG IF UCASE$(LEFT$(xAxis$,1)) = "T"
    upperBoundView = numOfData&
    FN generateY
  XELSE
    upperBoundView = numOfData&/2
    FN generateY
  END IF
  FN drawData                          'graph out the data in a window
   MENU _mCommands, _iZoom, _enable, "Zoom In"
  MENU _mCommands, _iExpand, _disable, "Expand Out"
END FN

LOCAL FN fitLongTimes
  FN selectRegions
  FN fitExponentialDecay
  FOR counter = (numOfData& + 1) TO (5 * numOfData& - 1) STEP 2
    xValue#(counter) = xValue#(counter - 1) + xInterval#
    xValue#(counter + 1) = xValue#(counter)
    tValue&(counter) = INT( expAmplitude# * EXP(slope# * xValue#(counter)) )
    tValue&(counter + 1) = 0
  NEXT counter
  numOfData& = counter - 1
  numOfPoints& = numOfData&/2
  lowerBoundView = 1
  upperBoundView = numOfData&
  FN expandOut
END FN

LOCAL FN replaceWithZeros
  FOR counter = lowerBoundView TO upperBoundView - 2 STEP 2
    LONG IF UCASE$(LEFT$(xAxis$,1)) = "T"
      tValue&(counter) = 0
```

```
    XELSE
      fValue#(counter) = 0
    END IF
  NEXT counter
END FN

LOCAL FN zeroPoints
  FN selectRegions
  FN replaceWithZeros
  FN expandOut
END FN

LOCAL FN fitShortTimes
  FN selectRegions
  FN replaceWithZeros
  finished = _no
  fCounter = -1
  DO
    fCounter = fCounter + 2
    IF tValue&(fCounter) <> 0 THEN finished = _yes
  UNTIL finished
  lowerBoundView = fCounter
  upperBoundView = lowerBoundView + 61
  FN fitExponentialDecay
  fGoodPoint& = tValue&(fCounter)
  estInitPoint& = INT(expAmplitude#)
  dTime# = xValue#(fCounter)
  finished = _no
  sCounter = -1
  DO
    sCounter = sCounter + 2
    angle# = (pi# * xValue#(sCounter)) / (2 * dTime#)
    loss# = estInitPoint& * SIN(pi# * xValue#(sCounter)) / (2 * dTime#)
    tempGain# = fGoodPoint& * SIN(pi# * xValue#(sCounter)) / (2 * dTime#)
    'tempY# = (estInitPoint&)-(estInitPoint&-fGoodPoint&)*SIN((pi# *
xValue#(sCounter))/(2*dTime#))
    tempY# = (estInitPoint&) - loss# + tempGain#
    tValue&(sCounter) = INT(tempY#)

    IF sCounter = fCounter-2 THEN finished = _yes
  UNTIL finished
  FN expandOut
END FN

LOCAL FN fastFourierTransform
'This subroutine was adapted from pp. 394-395 of _Numerical Recipes_
'(FORTRAN version) by William H. Press, Brian P. Flannery, Saul A.
```

```
'Teukolsky, and William T. Vetterling (1986) published by  Cambridge
'University Press, 818 pages

'This function replaces the contents of the array tempArray#() with its
'discrete Fourier transform (if iSign = 1) or its inverse discrete Fourier
'transform (if iSign = -1).  tempArray#() is a complex array of length
'numOfPoints& - the entries are ordered as (point[1] - real,imaginary;
'point2 - real, imaginary .... point[numOfPoints&] - real,imaginary)
'Therefore, a data set that only had real data entries was padded with
'alternating zeros, so that it can still be treated as a complex array by this
'function.

 LONG IF UCASE$(LEFT$(xAxis$,1)) = "T"
   FOR counter = 1 TO numOfData&
     tempArray#(counter) = tValue&(counter)
   NEXT counter

 XELSE
   FOR counter = 1 TO numOfData&
     tempArray#(counter) = fValue#(counter)
   NEXT counter
 END IF

 firstPointer=1
 FOR secondPointer = 1 TO numOfData& STEP 2
   LONG IF firstPointer > secondPointer
     tempReal# = tempArray#(firstPointer)
     tempImaginary# = tempArray#(firstPointer+1)
     tempArray#(firstPointer) = tempArray#(secondPointer)
     tempArray#(firstPointer+1) = tempArray#(secondPointer+1)
     tempArray#(secondPointer) = tempReal#
     tempArray#(secondPointer+1) = tempImaginary#
   END IF
   mValue = numOfData&/2
   WHILE mValue > 2 AND firstPointer > mValue
     firstPointer = firstPointer-mValue
     mValue = mValue/2
   WEND
   firstPointer = firstPointer + mValue
 NEXT secondPointer
 mMax = 2

 WHILE numOfData& > mMax
   iStep = 2 * mMax
   theta# = (6.28318530717959#)/(iSign*mMax)
   wPr# = (-2#) * (SIN(.5# * theta#)^2)
   wPi# = SIN(theta#)
```

```
  wR# =1#
  wI#=0#
  FOR mValue = 1 TO mMax STEP 2
    FOR secondPointer = mValue TO numOfData& STEP iStep
     firstPointer = secondPointer + mMax
      tempReal# = (wR# * tempArray#(firstPointer)) - (wI# * _
                                    tempArray#(firstPointer+1))
      tempImaginary# = (wR# * tempArray#(firstPointer+1)) + (wI# * _
                                    tempArray#(firstPointer))
      tempArray#(firstPointer) = tempArray#(secondPointer) - tempReal#
      tempArray#(firstPointer+1) = tempArray#(secondPointer+1) - _
                                    tempImaginary#
      tempArray#(secondPointer) = tempArray#(secondPointer) + tempReal#
      tempArray#(secondPointer+1) = tempArray#(secondPointer+1) + _
                                    tempImaginary#
    NEXT secondPointer
    wTemp# = wR#
    wR# = (wR# * wPr#) - (wI# * wPi#) + wR#
    wI# = (wI# * wPr#) + (wTemp# * wPi#) + wI#
   NEXT mValue
   mMax = iStep
  WEND


 LONG IF UCASE$(LEFT$(xAxis$,1)) = "T"
   FOR counter = 1 TO numOfData&
     fValue#(counter) = tempArray#(counter)
   NEXT counter

'Filling up the xValue#() array with the frequency values.  For a description
'of how this algorithm was derived, look at Figure 12.2.2b on p. 394 of
'_Numerical  Recipes_

    'Filling up the xValue#() array with the positive frequency values

   freq# = 0#
   counter = 1

    'this is needed to use numOfPoints& as a real
    tempNumOfPoints# = numOfPoints&

   DO
     xValue#(counter) = freq#

      ' PRINT counter,freq#,xValue#(counter)

     counter = counter + 1
```

```
      xValue#(counter) = freq#

       ' PRINT counter,freq#,xValue#(counter)

      counter = counter + 1
      ' freq# = freq# + (1 / ((xInterval#)*numOfPoints&) )
      freq# = freq# + (1# / ((xInterval#)*tempNumOfPoints#) )
    UNTIL counter >= numOfPoints& + 3

'Filling up the xValue#() array with the negative frequency values
    freq# = (-1) * (freq# - 2 * (1# / ((xInterval#)*tempNumOfPoints#) ) )
   DO
     xValue#(counter) = freq#
     counter = counter + 1
     xValue#(counter) = freq#
     counter = counter + 1
     freq# = freq# + (1# / ((xInterval#)*tempNumOfPoints#) )
    UNTIL counter = numOfData& +1

    xInterval# = xValue#(3) - xValue#(1)
    xAxis$ = "Frequency (Hz)"
    lowerBoundView = 3
    upperBoundView = numOfData&
    FN generateY
    FN drawData
  XELSE
    xInterval# = (1# / (numOfPoints& * (xValue#(3) - xValue#(1))))
    timeValue# = 0
    counter = 1
   DO
      xValue#(counter) = timeValue#
     counter = counter + 1
      xValue#(counter) = timeValue#
     counter = counter + 1
      timeValue# = timeValue# + xInterval#
    UNTIL counter = numOfData& + 1

    FOR counter = 1 TO numOfData&
      tValue&(counter) = INT(tempArray#(counter))
    NEXT counter
    xAxis$ = "Time (sec)"
    FN expandOut
  END IF
END FN

LOCAL FN fourierTransform
  iSign = 1
```

```
  FN fastFourierTransform
END FN

LOCAL FN inverseFourierTransform
  iSign = -1
  FN fastFourierTransform
END FN

LOCAL FN doMenu
  menuid = MENU(_menuID)                    'which menu was chosen?
  itemid = MENU(_itemID)                    'which item in the menu was chosen?
  SELECT menuid
    CASE _mFile                             'was the file menu selected?
      SELECT itemid                         'which item in the file menu?
        CASE _iOpen                         'the Open item
          FN openFile
        CASE _iConvert                      'the Convert item
          FN convert
        CASE _iSaveR                        'the Save Real item
          FN saveRealFile
        CASE _iSaveC                        'the Save Complex item
          FN saveComplexFile
        CASE _iQuit                         'the Quit item
        END
      END SELECT
    CASE _mEdit
      SELECT itemid
        CASE _iUndo
        CASE _iCut
        CASE _iPaste
        CASE _iClear
        CASE _iSelectAll
      END SELECT
    CASE _mCommands
      SELECT itemid
        CASE _iMakeReal
          FN makeReal
        CASE _iFourierTransform
          FN fourierTransform
        CASE _iInverseFourierTransform
          FN inverseFourierTransform
        CASE _iFitLongTimes
          FN fitLongTimes
        CASE _iZeroPoints
          FN zeroPoints
        CASE _iAddPortion
          FN addPortion
```

```
      CASE _iSelectRegions
       FN selectRegions
      CASE _iZoom
       FN zoomIn
      CASE _iExpand
       FN expandOut
       CASE _iFitShortTimes
        FN fitShortTimes
    END SELECT
  END SELECT
  MENU
END FN

LOCAL FN initialize
  MENU _mFile, 0, _enable, "File"                'create file menu
  'an open item to open a data file
  MENU _mFile, _iOpen, _enable, "Open.../O"
  'an item to convert a data file
  MENU _mFile, _iConvert, _enable, "Convert.../K"
  'an item to save a real data file
  MENU _mFile, _iSaveR, _disable, "Save.../S"
  'an item to save a complex data file
  MENU _mFile, _iSaveC,_disable,"Save Complex..."
  'need a way to quit the program
  MENU _mFile, _iQuit, _enable,"Quit/Q"
  MENU _mEdit, 0, _disable, "Edit"               'create edit menu
  MENU _mEdit, _iUndo, _disable, "Undo/Z"        'an undo item
  MENU _mEdit, 2, _disable, ";"                  'a separator
  MENU _mEdit, _iCut, _disable, "Cut/X"          'a cut item
  MENU _mEdit, _iCopy, _disable, "Copy/C"        'a copy item
  MENU _mEdit, _iPaste, _disable, "Paste/V"      'a paste item
  MENU _mEdit, _iClear, _disable, "Clear"        'a clear item
  MENU _mEdit, 7, _disable, ";"                  'a separator
  MENU _mEdit, _iSelectAll, _disable, "Select All/A"
  'create a Commands menu
  MENU _mCommands, 0, _enable, "Commands"
  MENU _mCommands, _iMakeReal, _disable, "Delete Imaginary Points/D"
  MENU _mCommands, _iFourierTransform, _disable, "Fourier Transform/F"
  MENU _mCommands, _iInverseFourierTransform, _disable, "Inverse Fourier
Transform/I"
  MENU _mCommands, _iFitLongTimes, _disable, "Fit Ending Tail/T"
  MENU _mCommands, _iZeroPoints, _disable, "Zero A Spectrum Portion/Z"
  MENU _mCommands, _iAddPortion, _disable, "Append New Values"
  MENU _mCommands, _iSelectRegions, _disable, "Select Regions"
  MENU _mCommands, _iZoom, _disable, "Zoom In"
  MENU _mCommands, _iExpand, _disable, "Expand Out"
  MENU _mCommands, _iFitShortTimes, _disable, "Approximate Short Times"
```

```
  baseYCoordinate = 15
  windowOpen = _no
  plotFlag = 0
  regionsSelected = _no
  pi# = (ATN(1) << 2)
END FN

'------------------------------ Main --------------------------------
FN initialize                       'put up menus and set up vars
ON MENU FN doMenu                          'routine to handle menu selection
ON DIALOG FN doDialog               'routine to handle window update events

DO                                  'round and round until the program ends
  HANDLEEVENTS                            'if event happens call a routine
UNTIL programEnds                         'if programEnds = true then loop ends
END                                 'program ends
```

CHAPTER 5

EXAFS Studies on Cytochrome $P450_{11\beta}$

5.1. Background and Significance

X-ray absorption spectroscopy (XAFS) has played a major role in characterizing cytochrome P450 systems. Extended x-ray absorption fine structure (EXAFS) spectroscopy was one of the techniques that helped to confirm that the proximal axial ligand of cytochrome P450 enzymes was a sulfur [1]; it even revealed that this sulfur was a thiolate [2]. X-ray absorption near edge spectroscopy (XANES) and EXAFS has also given support for porphyrin cation radicals and short iron-oxygen bonds in compounds I and II of horseradish peroxidase [3, 4]; these reports helped implicate the presence of an oxenoid species in the P450 catalytic cycle (see section **1.1** of this thesis). In addition, recently XANES has shown that axial thiolate ligation to heme proteins affects the electronic properties of the iron [5], consistent with it role in facilitating the breaking the O-O bond in oxygen [6].

EXAFS has also been used as a tool in the partial mapping of the active site of $P450_{scc}$. Joardar [7] used a sulfoxide analog of 22(*R*)-hydroxycholesterol - having the sulfur replace the C-22 atom and a sulfoxide oxygen in place for the 22(*R*) hydroxy group - to determine heme iron to substrate distances. Such distances are obtained by examining the modulations of the X-ray absorption by the central iron, caused by surrounding atoms. This effect is more sensitive for larger neighbors; therefore the sulfur containing substrate analog used in Joardar's studies [7] enabled the relatively rare incident of second shell ligand characterization.

The principle behind the EXAFS phenomenon is that of the photoelectric effect. When metal atoms are exposed to X-rays of a particular energy range, the absorption of the x-ray photon gives rise to the ejection of an inner shell electron. This electron then propagates outward as a spherical wave (a photoelectron), with a corresponding de Brogli wavelength. Surrounding atoms are then able to backscatter this wave toward the central atom (see **Figure 5.1**). This backscattered wave alters the electron energy levels of the central atom, which in turn affects its absorption coefficient, relative to that of the same atom in an isolated state. As the absorption (or fluorescence) is measured over a range of energies, modulations in the absorption coefficient arise due to the changing photoelectron wavelength.

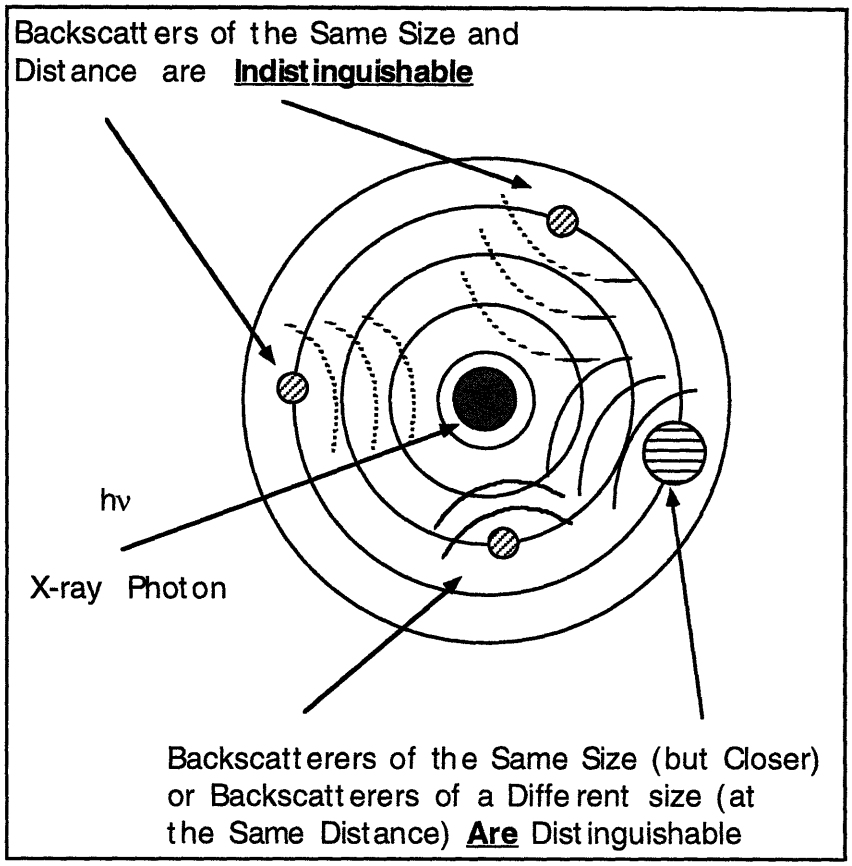

Figure 5.1: A pictorial description of the origin of EXAFS phenomenon which is caused by the ejection from the central atom and the backscattering back from surrounding ligands, of photoelectrons.

The absorption modulation can be used to determine the distance between the central and backscattering atom. By converting the post edge (see **Figure 5.2**) absorption (or fluorescence) curve from energy space to momentum space (k-space), more easily defined periodicities and beat patterns become apparent. Fourier transforming the k-space data into distance space (r-space), gives a curve which resembles the radial distribution function of ligands around the absorbing atom.

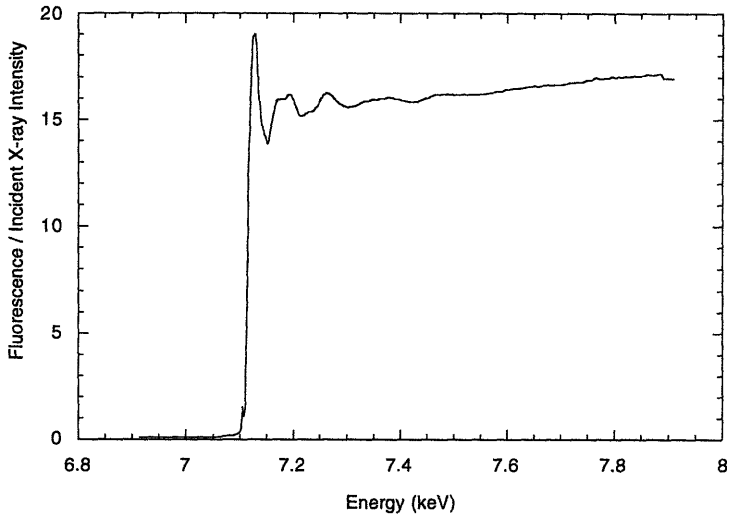

Figure 5.2: Fluorescence EXAFS of tetraphenylporphine iron (III) chloride.

Ligand distances cannot be directly read off of the r-space EXAFS data. A variety of ligand and absorber properties must be factored in before definitive distance assignments can be made. These are: the phase changes (of the photoelectron wave) caused by the central absorber and the individual backscatterers, the atomic (static and thermal) disorder in the system, and the electron mean free path. As a result, geometric assignments are usually performed by simulating the k-space data, while varying the all of the possible parameters. The r-space data (although not an accurate representation of the distances) reliably separates the EXAFS modulations from atoms of different coordination shells. Taking advantage of this, the spectroscopist uses this representation of the data to "window" on certain shells, back transforming them into k-space - where each shell is individually fitted.

The existence of numerous factors, influencing the EXAFS, would seem to give rise to ambiguous ligand distances. This problem can be addressed by incorporating theoretically derived values for these parameters or by incorporating information from (structurally characterized) model compound EXAFS data. In principle either approach could be used, but there is a strong preference for empirically derived values. This has to do with extensive approximations that were

made with early versions of these tables [8] and with the problem of background removal.

All EXAFS spectra have backgrounds with some degree of non-linearity. These primarily arise from the effects of the absorbing atom being imbedded in a molecule (apart from near-neighbor backscattering) and from detector non-linearities. Apart from the intrinsic background from the sample and the detection system, the amplitude of the EXAFS modulations are dependent on the geometry of the experiment. When EXAFS is measured for model compounds, one need not bother with the absorption of X-rays from the intervening air between detectors and the sample. Unfortunately suitable model compounds are not always available; the use of theoretical values, in such cases, is preferable to using data from inappropriate models. However, this adds to the level of noted experimental detail and increases the data processing time while fitting the data.

The basic geometry of heme system of cytochrome P450 proteins has previously been worked out with EXAFS and x-ray crystallography. However, fine adjustments to heme structure and cysteine coordination, caused by the binding of specific substrates or inhibitors, remains a largely unexplored area. Among individual P450 proteins, particular compounds can bind in the active site of the enzyme and enable the system (in the presence of reducing equivalents and electron transfer proteins) to reduce oxygen without oxidizing an organic substrate; such compounds are called pseudosubstrates (see **section 1.1** of this thesis).

Differences in the polarity of the active sites (caused by mutations or the binding of pseudosubstrates) has been proposed for causing P450-dependent futile oxygen reduction [9-12]. The x-ray crystal structure of one of these mutants has been determined [9]. If small differences in iron coordination were at play, these may not be apparent from an x-ray crystal structure. EXAFS, however, is ideally suited for measuring small distances; although backscattering effects are normally limited to a maximum distance of 4.0 Å, small distances can often be measured to within 0.02 Å [13].

Early EXAFS studies on $P450_{cam}$ demonstrated a difference in iron coordination between high and low spin versions of the enzyme [2]. Such

differences presumably exist in other P450 enzymes. This chapter describes EXAFS experiments on bovine $P450_{11\beta}$ - either bound with 11-deoxycorticosterone (high spin form) or with the relatively specific inhibitor metyrapone (low spin form). The goal of these studies is to determine the differences in iron coordination between $P450_{11\beta}$-DOC and $P450_{11\beta}$-metyrapone.

5.2 Materials and Methods

5.2.1. Materials

5.2.1.1. Model Compounds and Sample Holders

Two heme model compounds - (protoporphyrin IX)-iron (III) bis (1-methylimidazole) and iron(III) tris (N,N-diethyldithiocarbamate) - were made according to published procedures. (Tetraphenylporphine)-iron (III) chloride and metyrapone was purchased from Aldrich Chemical Co. Aluminum-iron sample holders were made by the MIT chemistry department machine shop according to the specifications shown in **Figure 5.3**. All heme model compounds were dissolved/dispersed in benzene (at concentrations of approximately 10 mM) and frozen as glasses in liquid nitrogen.

5.2.1.2. Sample Preparation and Characterization

Cytochrome $P450_{11\beta}$ was purified as described in **section 3.4.4** of this thesis. $P450_{11\beta}$, with bound 11-deoxycorticosterone had the uv-vis absorption and EPR spectra shown in **Figures 3.4** and **5.4**, respectively. This sample was concentrated (using ultrafiltration against an Amicon YM30 membrane) to the point of creating a suspension. The protein slurry was then placed in an EXAFS sample holder and frozen in liquid nitrogen. The integrity of the $P450_{11\beta}$ protein was confirmed by EPR spectroscopy.

Cytochrome $P450_{11\beta}$, with bound metyrapone was prepared by combining a 10-fold excess (with respect to cytochrome heme) of metyrapone with deoxycorticosterone-bound $P450_{11\beta}$ and incubated at room temperature for 1 hour.

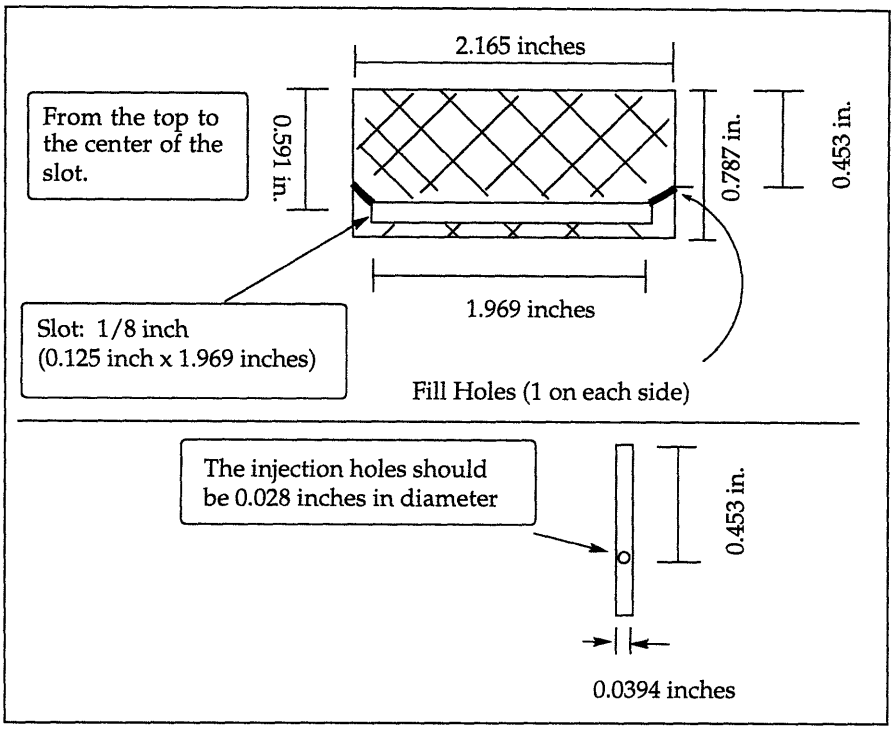

Figure 5.3: Design for EXAFS sample holders. The slot in the middle of the aluminum object is a bored out hole. This opening can be covered with (x-ray transparent) mylar tape; the injection holes on the side then allow one to enter the sample.

An aliquot of this sample was monitored by uv-vis absorption spectroscopy; measurement of a growing peak at 420 nm was taken as an indication that metyrapone was displacing deoxycorticosterone in the active site of the protein. When the 420 nm (low spin) signal stopped increasing, the sample was immediately subjected to ultrafiltration (at 5 °C) as described above. The uv-vis absorption spectrum of the unconcentrated sample is shown in **Figure 5.5** .

5.2.2. Methods

5.2.2.1. EPR and UV-VIS Spectroscopy

EPR spectra were acquired on the MIT Chemistry Department's Brüker ER series X-band CW spectrometer (at 9.44 GHz), using a commercial liquid helium circulating Oxford cryostat. Uv-vis absorption spectra were acquired on a Hewlett Packard diode array spectrophotometer.

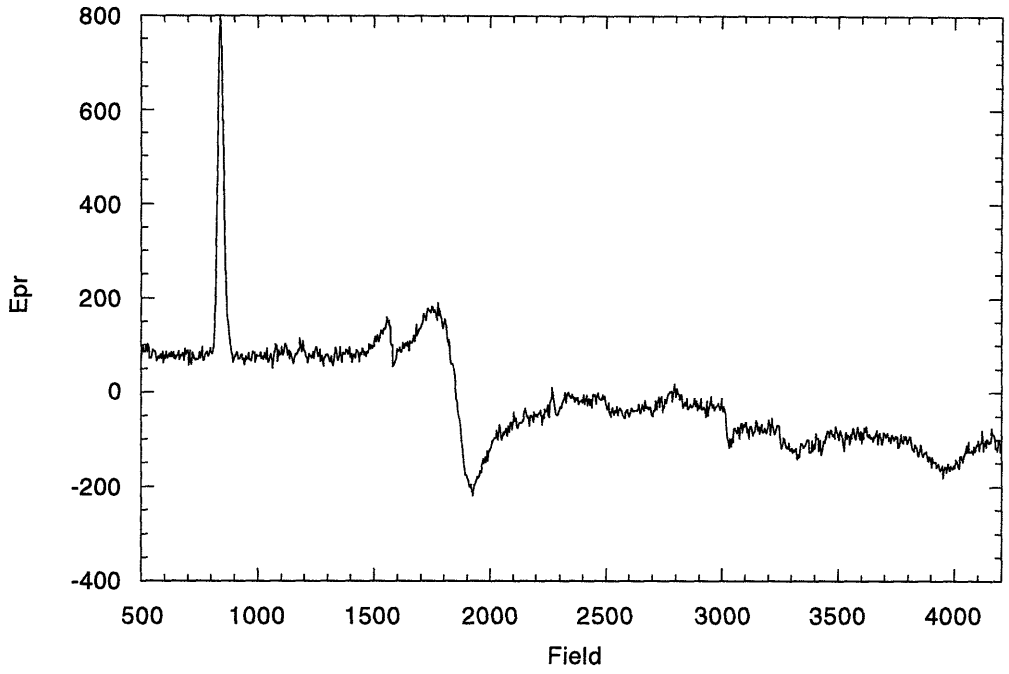

Figure 5.4: EPR spectrum of $P450_{11\beta}$, with bound 11-deoxycorticosterone. The spectrum was taken at 10 K at a microwave frequency of 9.44 GHz.

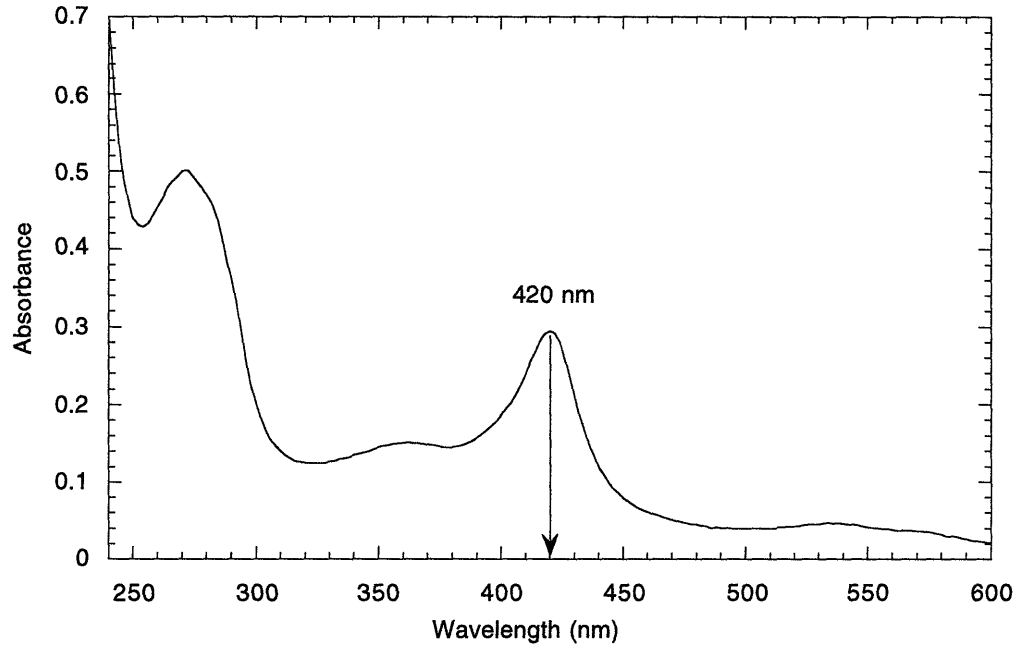

Figure 5.5: The uv-vis absorption spectrum of purified $P450_{11\beta}$, bound with metyrapone.

5.2.2.2. EXAFS Data Acquisition

X-ray absorption spectra were collect at beamline X9B of the National Synchrotron Light Source (Brookhaven National Laboratories). The X-rays were tuned with a Si(111) double crystal monochrometer. Throughout the data acquisition, samples were kept at 20 K with the use of a closed-cycle refrigerated displex. The sample was placed at a 45° angle from the incident x-rays. Incident intensities were measured using a nitrogen gas ionization chamber detector. Fluorescence data was measured perpendicular to the incident beam, using an enery-resolving Canberra 13-element germanium detector . Data were recorded at the following energy resolutions (relative to the 7.113 keV edge): 10 eV steps from -200 eV to -25 eV, a 1.0 eV steps from -25 eV to +25 eV, 2.0 eV steps from +25 eV to +150 eV, 3.0 eV steps from +150 eV to +400 eV, and 6.0 eV steps from +400 eV to 800 eV. The duration that monochrometer remained at an individual energy value was approximately scaled to the beam current in the electron ring; a dwell time of 1.5 second (per energy step) for a beam current of 200 mA was used as the standard.

5.2.2.3. Data Acquisition For Determination of Detector Dead Times

Saturation data for the 13-element detector was acquired while maintaining the monochrometer at 7.2 keV (a nominal energy above the edge). Once the beam was centered on the sample, the vertical shutter aperture was varied from 0.0 mm to 2.0 mm in size, in increments of 0.05 mm while acquiring fluorescence counts for 1.0 second at each step. The total internal counts for each of the detectors was also measured for each of these steps in incident intensity. Although the detectors' fluorescence counts were found to saturate at high incident intensities, the total internal counts (for each element of the detector; see **Figure 5.6**) responded linearly at all times. As a result, the total internal counts were taken as a measure of total impingement of photons on the detector.

5.2.2.4. Software Utilized

Curve fitting for detector dead times was performed using Kaleidagraph 3.0 (for the Macintosh). Formatting the EXAFS data and correcting the measured fluorescence counts (as dictated by the detector dead times) was performed by Microsoft Excel 5.0, running tailored programs written in Visual Basic For Applications.

5.3. Results and Discussion

5.3.1. Determination of Fluorescence Detector Dead Times

Data from the energy resolving 13-element fluorescence detector (see **Figure 5.6**) deviates from linearity at high photon count rates. However, the total internal counts (for each of the 13 sub detectors; i.e. ic_x, where x is the element number) was found to remain linear at all incident intensities examined. The fact that the internal count measurement did not saturate provided an internal gauge of the total photon impingement on each of the 13 elements of the detector.

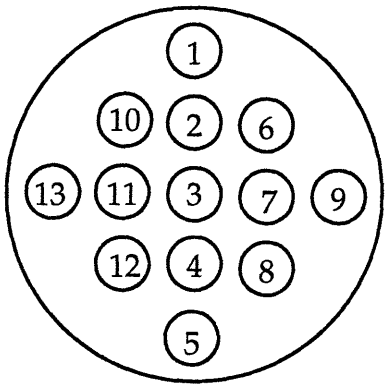

Figure 5.6: The circular array of the 13 individual detectors in the Canberra fluorescence detector. During data acquisition, the face of this array was centered toward the sample - making detector 3 receive the most photons.

By correlating the energy-windowed fluorescence counts for each detector element (i.e. ge_x, where x is the element number), detector element dead times were obtained. This was performed by plotting ge_x versus icr_x (i.e., the internal count rate of element x) and fitting this to the function given in equation (1) below:

$$ge_{measured_x} = \beta \bullet icr_x \bullet e^{-icr_x \bullet \tau_x} \quad (1)$$

where β is the slope of the curve at icr=0 and τ_x is the fitted dead time for detector x. This equation was fitted to fluorescence data acquired for both $P450_{11\beta}$-deoxycorticosterone and $P450_{11\beta}$-metyrapone, when measured at an x-ray beam energy of 7.2 keV at a series of different intensities. The dead times for each element, from each series, were pair-wise averaged as shown in **Table 5.1**. These averaged dead times were used in the correction of measured fluorescence counts.

Detector Element	$P450_{11\beta}$ (DOC) τ (μsec)	R Value	$P450_{11\beta}$ (MET) τ (μsec)	R Value	Average Dead Time τ (μsec)
1	0.2516	0.997	1.7772	0.999	1.0144
2	2.6644	0.998	2.0388	0.999	2.3516
3	0.6348	0.999	1.4068	0.999	1.0208
4	5.5034	1.000	2.0950	0.999	3.7992
5	3.6781	1.000	2.0427	0.999	2.8604
6	2.2497	0.999	2.2380	1.000	2.2439
7	4.3293	0.999	2.9062	0.998	3.6178
8	3.1591	1.000	2.1979	0.999	2.6785
9	1.0334	0.999	2.5695	0.999	1.8015
10	4.5182	0.999	1.9646	0.999	3.2414
11	1.5557	0.999	1.2339	0.999	1.3948
12	3.9911	0.999	1.9089	0.999	2.9500
13	2.4113	0.999	2.1276	0.999	2.2694

Table 5.1: Tabulation of dead times for each of the elements of the Canberra fluorescence detector.

Correction of the fluorescence counts was based on the notion that if the dead times were all zero, then the ge_x *vs.* icr_x relations would all be straight lines, passing through the origin. The expected counts, in such a situation would follow the trend in equation (2).

$$ge_{expected_x} = \beta \bullet icr_x \qquad (2)$$

Making the corrected equal to the expected counts, results in:

$$ge_{corrected_x} = ge_{measured_x} \Big/ e^{-icr_x \bullet \tau_x} \qquad (3)$$

Since every measured fluorescence counts (for each detector element) had a companion icr that was also stored (for each scan), the counts for each data point was augmented by using equation (3).

5.3.2. Summing Up the Individual Scans

In the inspection of the fluorescence *vs.* energy EXAFS spectra for the individual detectors (i.e. ge_x/I_o *vs.* Energy), it was found that the 13 different spectra had noticeably different backgrounds. These backgrounds were found to be endemic to the individual detectors of the Canberra unit. As a result, the summation of data was performed by adding up the scans from the same detector for each of the scans (see **Figures 5.7** through **5.19**) , producing 13 final summed spectra for each sample. Before these 13 spectra can be combined to form the final EXAFS spectrum for the sample, the individual backgrounds from each must be removed. Only afterwards should these 13 data sets be combined. Fitting the post edge region to a polynomial spline background of the 13 summed spectra for $P450_{11\beta}$-deoxycorticosterone and $P450_{11\beta}$-metyrapone has not yet been performed. As a result, the analysis of $P450_{11\beta}$-deoxycorticosterone and $P450_{11\beta}$-metyrapone samples is incomplete.

This individuality of detector background was not found in the scans of the heme model compounds, which were at least one order of magnitude more concentrated that the $P450_{11\beta}$ samples. As a result, the summed data for the model

compounds were performed by adding the individual ge_x, producing a final ge_{sum}/I_o *vs.* energy plots (see **Figures 5.2, 5.20** , and **5.21**).

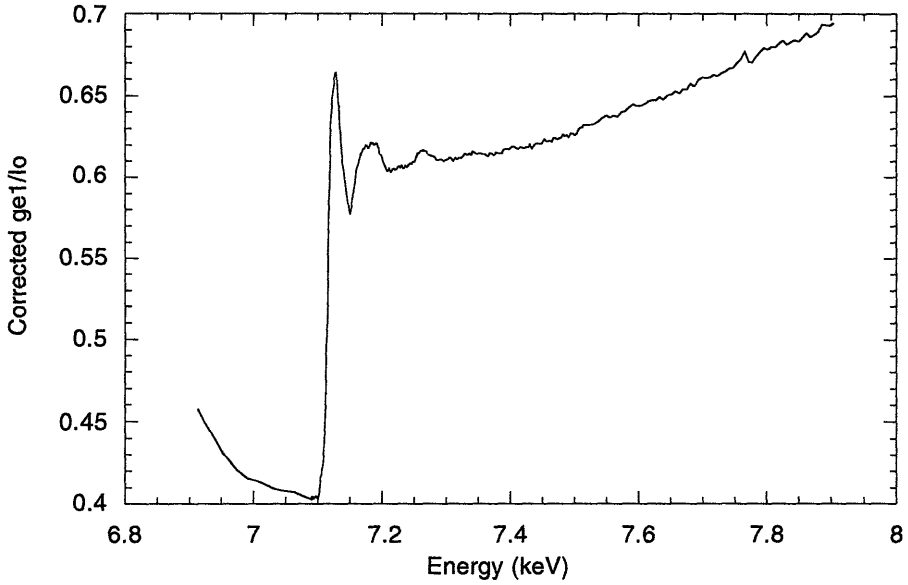

Figure 5.7: 75 Summed $P450_{11\beta}$-metyrapone EXAFS spectra from ge_1.

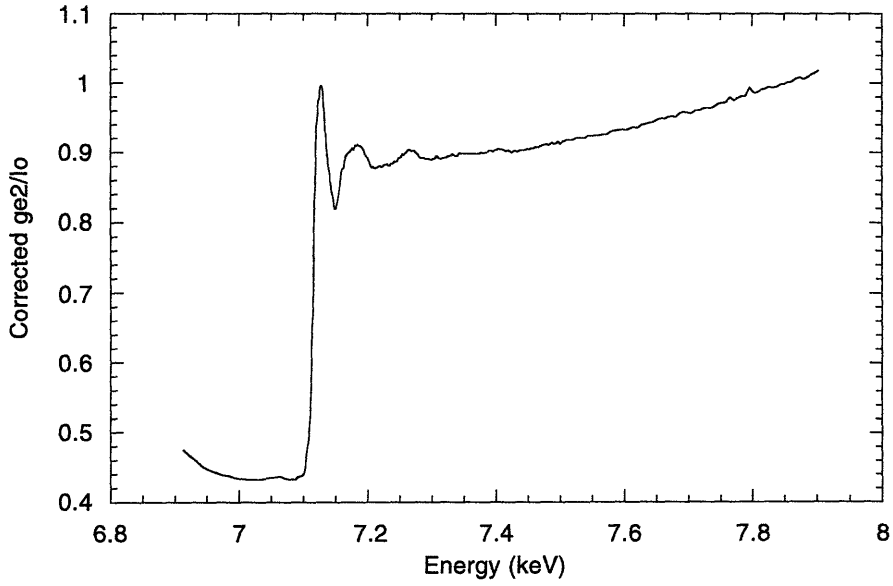

Figure 5.8: 75 Summed $P450_{11\beta}$-metyrapone EXAFS spectra from ge_2.

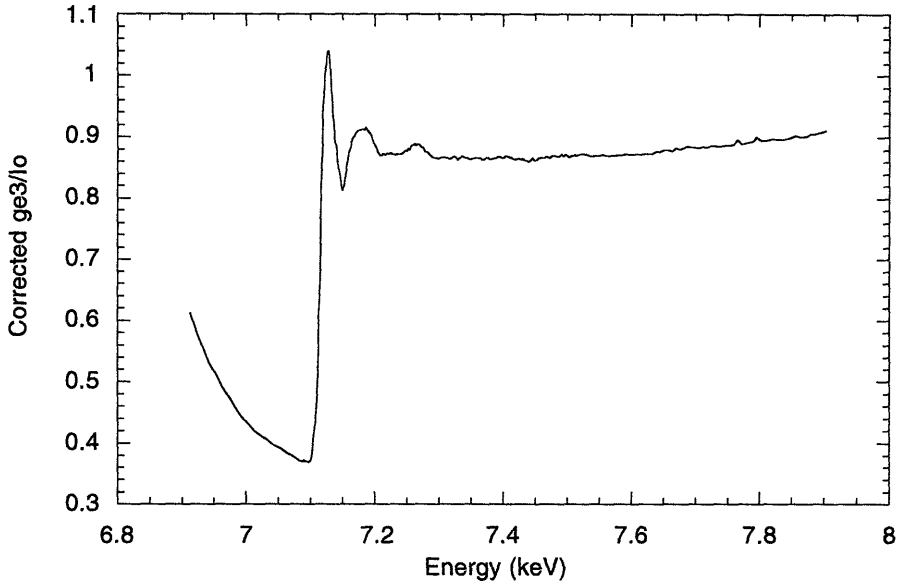

Figure 5.9: 75 Summed $P450_{11\beta}$-metyrapone EXAFS spectra from ge_3.

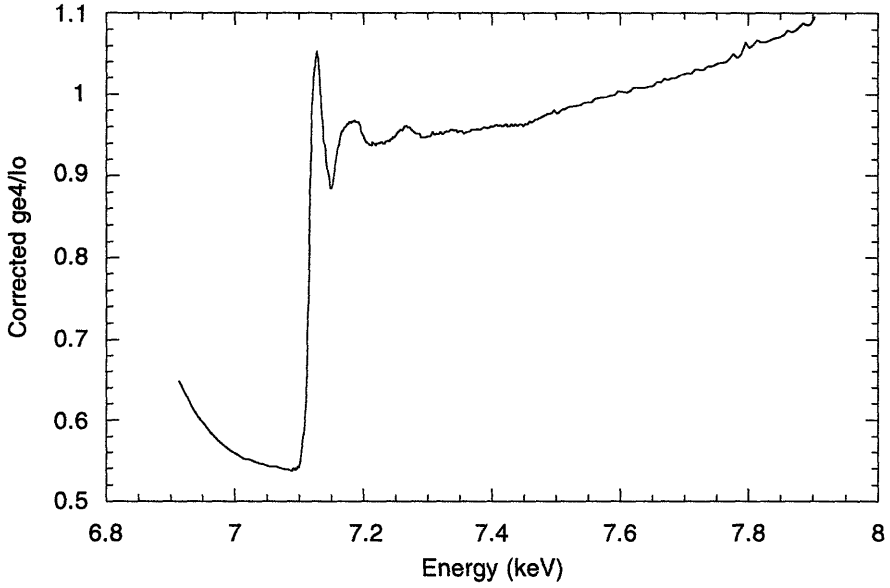

Figure 5.10: 75 Summed $P450_{11\beta}$-metyrapone EXAFS spectra from ge_4.

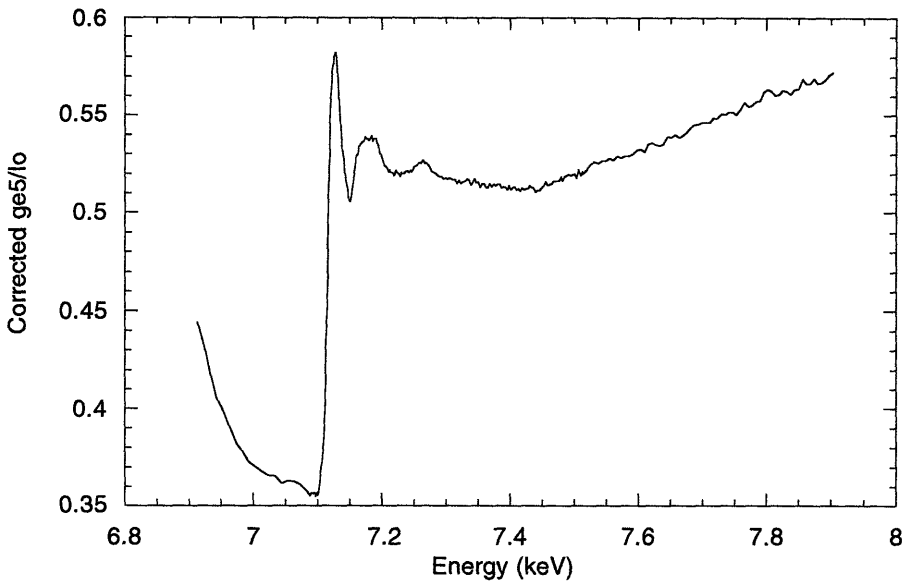

Figure 5.11: 75 Summed $P450_{11\beta}$-metyrapone EXAFS spectra from ge_5.

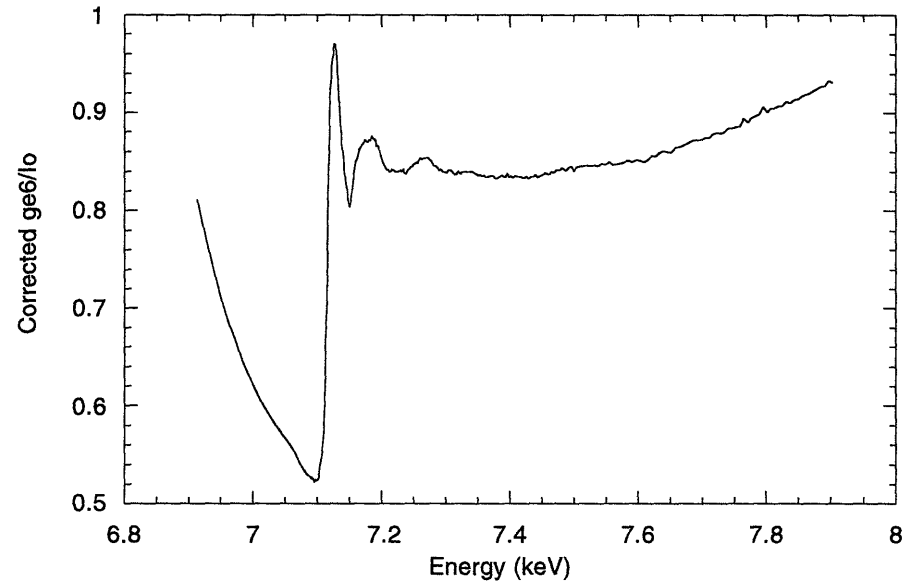

Figure 5.12: 75 Summed $P450_{11\beta}$-metyrapone EXAFS spectra from ge_6.

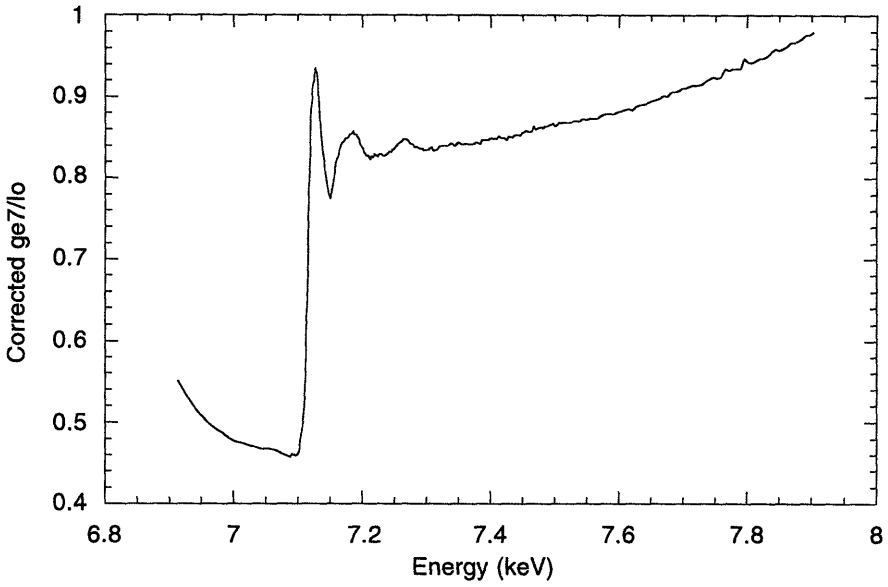

Figure 5.13: 75 Summed $P450_{11\beta}$-metyrapone EXAFS spectra from ge_7.

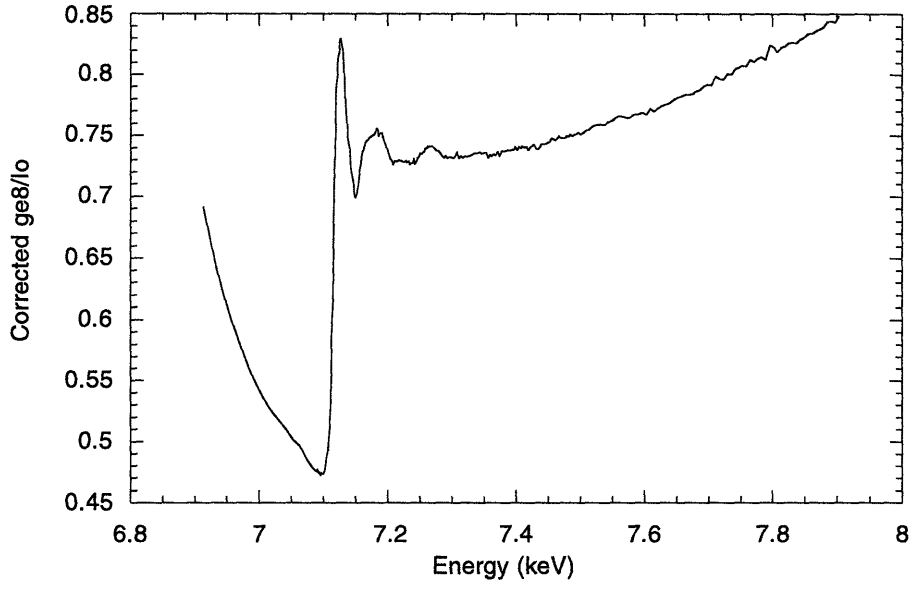

Figure 5.14: 75 Summed $P450_{11\beta}$-metyrapone EXAFS spectra from ge_8.

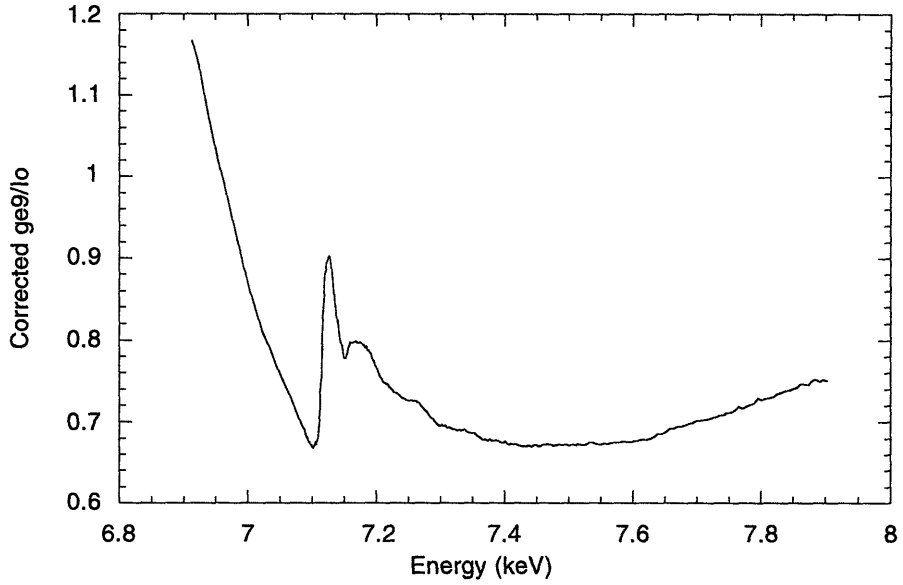

Figure 5.15: 75 Summed $P450_{11\beta}$-metyrapone EXAFS spectra from ge_9.

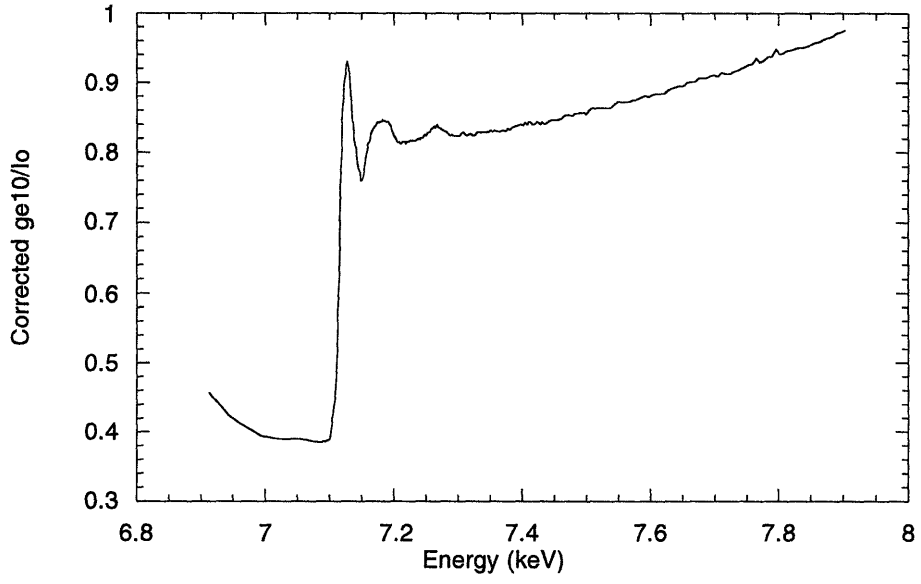

Figure 5.16: 75 Summed $P450_{11\beta}$-metyrapone EXAFS spectra from ge_{10}.

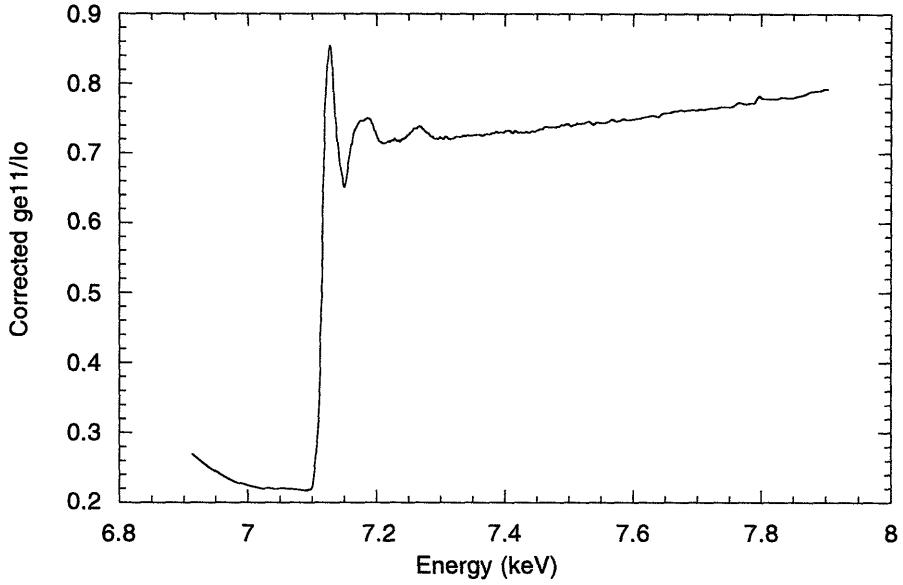

Figure 5.17: 75 Summed $P450_{11\beta}$-metyrapone EXAFS spectra from ge_{11}.

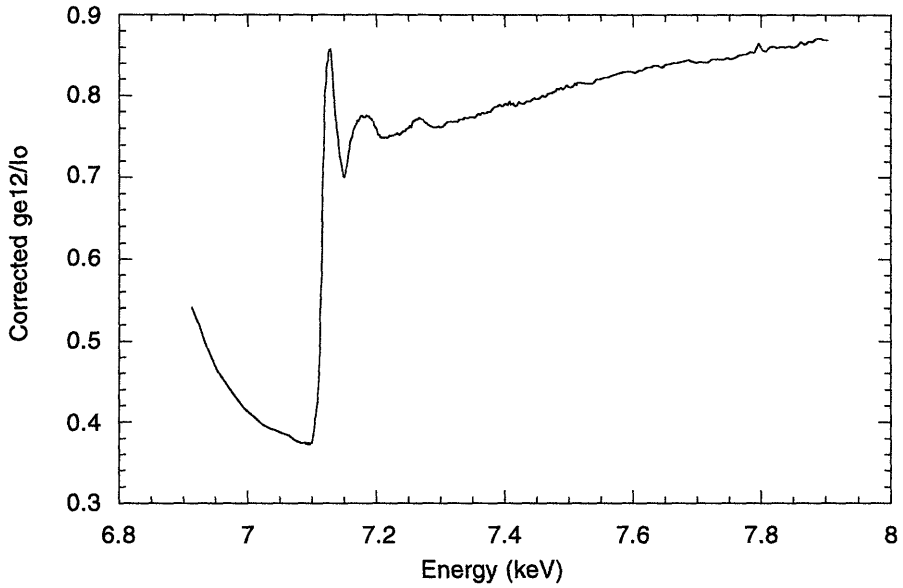

Figure 5.18: 75 Summed $P450_{11\beta}$-metyrapone EXAFS spectra from ge_{12}.

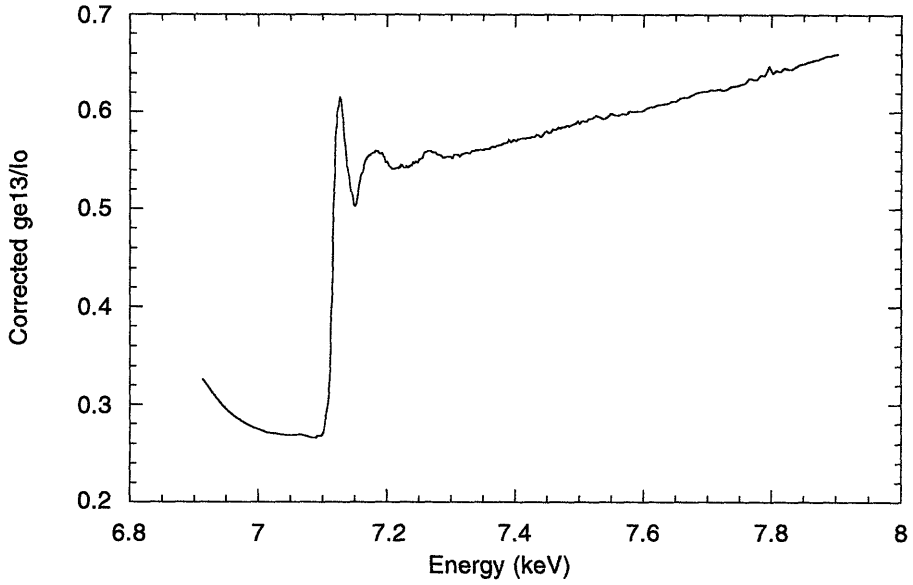

Figure 5.19: 75 Summed $P450_{11\beta}$-metyrapone EXAFS spectra from ge_{13}.

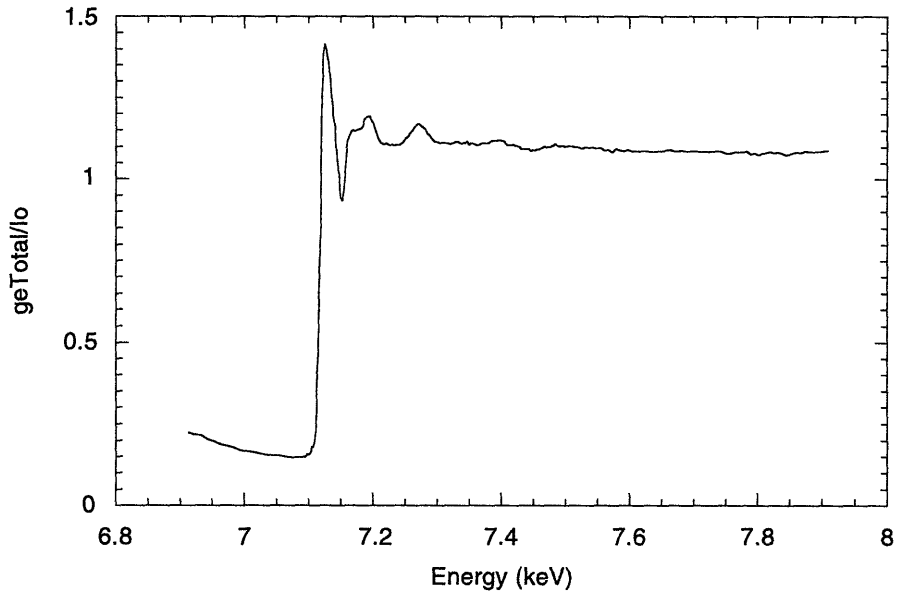

Figure 5.20: Summed EXAFS of heme bis (imidazole).

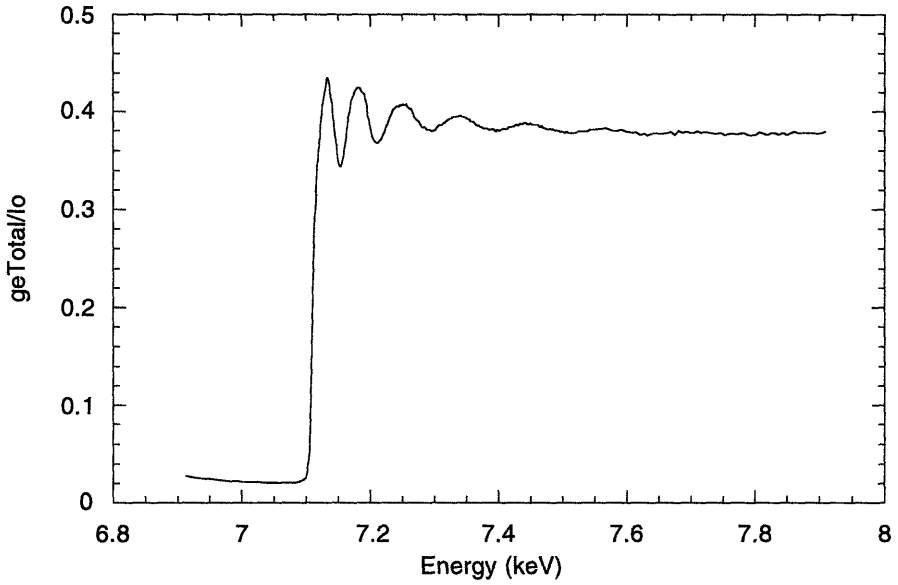

Figure 5.21: Summed EXAFS of Fe^{3+} tris (N,N-diethyldithiocarbamate).

Preliminary analysis of the summed model compound data has been performed (data not shown). After removing the pre-edge region of the spectra, the energy-space data were converted to k-space. Fourier transforming the k-space data to r-space gave a radial distribution function. Analysis beyond this point was not performed. Nevertheless, it was found that the radial distribution for each of the model compounds had a low distance peak corresponding to approximately 1.6 Å.

This low distance peak appears identical to the troublesome 1.6 Å peak that Joardar could not explain in his EXAFS data of $P450_{scc}$ - bound with either 22(*R*)-aminocholesterol or 20(*S*),22(*R*)-thiacholesterol-S-oxide [7]. When measuring the EXAFS of the same model compounds described in this chapter, Joardar used a gas ionization Lytle detector [14] rather than the Canberra unit used for his protein samples. One result of this was that the 1.6 Å peak did not appear in the scans for the model compounds, leaving Joardar to believe that this low distance peak was a property of the protein samples. The EXAFS measured on the model compounds for the work described in this chapter was acquired using the Canberra detector. Therefore, it appears that the ~1.6 Å peak is an artifact of detector background.

The creation of an artificial peak, resulting from a particular detector, illustrates an important point. One of the major uses of model compounds is to eliminate (as much as possible) the problems associated with systematic errors in data acquisition. Model compound EXAFS data in this laboratory has, in the past, been acquired exclusively using gas ionization or scintillation detectors. The reason behind this decision was based on the fact that these detectors did not saturate easily and EXAFS could be acquired at high count rates. However, because these detectors are not energy-resolving, an N-1 filter (i.e. a filter made of an element 1 atomic number less than the absorbing species of the experiment) was placed between the sample and the fluorescence detector. Although more photons were counted, the quality of spectra were not as high as when an energy-resolving detector is used. This is most probably because the N-1 filter was absorbing both fluorescence photons as well as background photons. Nevertheless, the attention paid to acquiring a large number of counts ignores that the value to optimize is the number of *effective* counts. In most cases, the number of effective counts for concentrated compounds is similar or higher when measured with the Canberra unit, as compared to the Lytle detector.

The systematic error of the sample self-absorption of fluorescence photons can also be taken into account by measuring EXAFS of model compounds on the same detector as the unknown sample. However, in order for this to be done properly, the model compound should be of similar concentration (and preferably in the same solvent) as that of the unknown. This was not the case for the model compounds used in the experiments described in this chapter.

5.4.3. The Next Steps in Data Analysis

Having summed up the EXAFS data for the model compounds, a full analysis of this data may now proceed. This work is will be performed in the near future. Previous analyses in this laboratory have utilized programs based on the algorithms described by Teo [15]. These programs require the use of VAX computers and offer very little flexibility in the way data is handled; spectra that were acquired under different detector gains can only be properly weighted (in the final sum) in a file by

file manner. When hundreds of files are being dealt with, this offers a large chance for human error in the data analysis. In addition, the algorithms used in these programs utilize the plane wave approximation of x-rays, which is now considered (in the general field of EXAFS) to introduce unnecessary approximations. The current standard is to utilize spherical wave formulations of x-rays. Many software packages are now available that implement this.

Future analysis of the EXAFS data described in this chapter will rely on the programs developed by the University of Washington - the famous UWXAFS package [16]. This package is continually updated and runs on either UNIX, MS DOS, or Macintosh systems. It uses the most current versions of accepted data analysis algorithms and is designed to facilitate the incorporation of theoretical parameters when needed. It also uses common (ASCII) file formats. All of its components are executed by first writing out a script. This enables long procedures to be executed in an unattended fashion. The combination of these features should aid in the completion of the $P450_{11\beta}$ EXAFS analysis started in this chapter. The final result will offer a significant contribution of our limited knowledge of this neglected but important enzyme.

References

1. Cramer, S.P., Dawson, J.H., Hodgson, K.O., and Hager, L.P., *Studies on the Ferric Forms of Cytochrome P-450 and Chloroperoxidase by Extended X-ray Absorption Fine Structure. Characterization of the Fe-N and Fe-S Distances.* Journal of the American Chemical Society, 1978. **100**: p. 7282-7290.
2. Hahn, J.E., Hodgson, K.O., Andersson, L.A., and Dawson, J.H., *Endogenous Cysteine Ligation in Ferric and Ferrous Cytochrome P-450. Direct Evidence From X-ray Absorption Spectroscopy.* Journal of Biological Chemistry, 1982. **257**: p. 10934-10941.
3. Penner-Hahn, J.E., McMurray, T.J., Renner, M., Latos-Grazynsky, L., Eble, K.S., Davis, I.M., Balch, A.L., Groves, J.T., Dawson, J.H., and Hodgson, K.O., *X-ray Absorption Spectrosopic Studies of High Valent Iron Porphyrins.* J. Biol. Chem., 1983. **258**(21): p. 12761-12764.
4. Penner-Hahn, J.E., Eble, K.S., McMurry, T.J., Renner, M., Balch, A.L., Groves, J.T., Dawson, J.H., and Hodgson, K.O., *Structural Characterization of Horseradish Peroxidase Using EXAFS Spectroscopy. Evidence for Fe=O Ligation in Compounds I and II.* J. Am. Chem. Soc., 1986. **108**: p. 7819-7825.
5. Liu, H.I., Sono, M., Kadkhodayan, S., Hager, L.P., Hedman, B., Hodgson, K.O., and Dawson, J.H., *X-ray Absorption Near Edge Studies of Cytochrome P450cam, chloroperoxidase, and myoglobin: Direct evidence for the electron releasing character of a cysteine thiolate proximal ligand.* Journal of Biological Chemistry, 1995. **270**(18): p. 10544-10550.
6. Dawson, J.H., *Probing structure-function relations in heme-containing oxygenases and peroxidases.* Science, 1988. **240**(4851): p. 433-439.
7. Joardar, S., *Mapping the Active Sites of Steroidogenic Cytochromes P-450*, in *Chemistry*. 1993, M.I.T.: Cambridge. p. 197.
8. Teo, B.-K. and Lee, P.A., *Ab Initio Calculations of Amplitude and Phase Functionis for Extended X-ray Absorption Fine Structure Spectroscopy.* J. Am. Chem. Soc., 1979. **101**: p. 2815-2832.
9. Raag, R., Martinis, S.A., Sligar, S.G., and Poulos, T.L., *Crystal structure of the cytochrome P-450CAM active site mutant Thr252Ala.* Biochemistry, 1991. **30**(48): p. 11420-11429.
10. Di Primo, C., Hui Bon Hoa, G., Deprez, E., Douzou, P., and Sligar, S.G., *Conformational dynamics of cytochrome P-450cam as monitored by photoacoustic calorimetry.* Biochemistry, 1993. **32**(14): p. 3671-3676.
11. Loida, P.J. and Sligar, S.G., *Molecular Recognition in Cytochrome P-450: Mechanism for the Control of Uncoupling Reactions.* Biochemistry, 1993. **32**(43): p. 11530-11538.
12. Paulsen, M.D., Filipovic, D., Sligar, S.G., and Ornstein, R.L., *Controlling the regiospecificity and coupling of cytochrome P450cam: T185F mutant increases coupling and abolishes 3-hydroxynorcamphor product.* Protein Sci, 1993. **2**(3): p. 357-365.
13. Bertagnolli, H. and Ertel, T.S., *S-ray Absorption Spectroscopy of Amorphous Solids, Liquids, and Catalytic and Biochemical Systems - Capabilities and Limitations.* Angew. Chem. Int. Ed. Engl., 1994. **33**: p. 44-66.
14. Stern, E.A. and Heald, S.M., Rev. Sci. Instrum., 1979. **50**: p. 1579-1582.
15. Teo, B.K., *EXAFS: Basic Principles and Data Analysis.* Inorganic Chemistry Concepts. Vol. 9. 1986, Berlin: Springer-Verlag. 349.
16. Stern, E.A., Newville, M., Ravel, B., Yacoby, Y., and Haskel, d., *The UWXAFS Analysis Package: Philosophy and Details.* Physica B, 1995. **208 & 209**: p. 117-120.